NOTE TO USERS

CURVED CONCRETE SLAB-ON-STEEL I-GIRDER BRIDGES

BY

Joseph Wassef, P. Eng.
B.Sc., Ain Shams University, Egypt

A Thesis
Presented to Ryerson University
In partial fulfillment of the
Requirement for the degree of
Master of Applied Science
In the program of
Civil Engineering
Toronto, Ontario, Canada, 2004

I hereby declare that I am the sole author of this thesis.

I authorize Ryerson to lend this document to other institutions or individuals for the purpose of scholarly research.

Joseph Wassef

I further authorize Ryerson University to reproduce the document by photocopying or by other means, in total or part, at the request of other institutions or individuals for the purpose of scholarly research.

Joseph Wassef

BORROWERS' PAGE

Ryerson University requires the signatures of all persons using or photocopying this thesis.

Please sign below, and give address and date.

Student Name	Signature	Date

CURVED CONCRETE SLAB-ON-STEEL I-GIRDER BRIDGES

Joseph Wassef, P. Eng.
Master of Applied Science, Department of Civil Engineering
Ryerson University, Toronto, Ontario, Canada, 2004

ABSTRACT

A parametric study was conducted, using the finite-element method, to study the load distribution characteristics of curved composite I-girder bridges under truck loading. The influence of several geometric parameters on the moment, and deflection distribution factors, as well as warping stresses in straight and curved composite I-girder bridges was examined. For straight bridges, the moment distribution factors were correlated with those specified in the Canadian Highway Bridge Design Code of 2000, CHBDC. Also, the magnitudes of warping stresses in the steel bottom flanges were correlated with the specified limits in bridge codes. The results showed that the CHBDC moment distribution factors significantly overestimate the structural response of straight bridges considered in this study. It was also observed that the curvature limitation specified in the CHBDC to treat a curved bridge of low curvature as a straight one underestimate the structural response.

ACKNOWLEDGEMENTS

The author wishes to express his deep appreciation to his advisor Dr. K. Sennah at Ryerson University, for his constant support and valuable supervision during the development of this research. Dr. Sennah devoted his time and effort to make this study a success. His most helpful guidance is greatly appreciated. The author also appreciates the financial support from the Natural Science and Engineering Research Council of Canada, NSERC. Moreover, the author is very grateful to his wife and daughters for their great support and encouragement during the course of this study.

TO MY FAMILY

TABLE OF CONTENTS

NOTATIONS

A	bridge width
[D]	constitutive matrix or elasticity matrix
E	modulus of Elasticity
[K]	the global stiffness matrix
[k`]	the element stiffness matrix
L	centre line span of a simply supported bridge
n	number of design lanes
N	number of girders
[P]	applied loads vector at the nodes
R	radius of curvature of the centre span of the curved bridge
R_L	multi-lane factor
[U]	displacement vector at the nodes
[u`]	the vector of virtual displacement
W_c	deck width
W_e	width of design lane
W_E	the external virtual work
W_I	the internal virtual work
α	the generalized coordinates
φ	displacement function
υ	the internal displacement vector of the element
[B]	the strain-displacement matrix.

$[\varepsilon(x,y)]$	the stain matrix
$[\sigma(x,y)]$	the stress matrix
Φ	Rotation (degree of freedom)
$(\sigma_{E1})_{DL}$	mid-span stress in bottom flange fibres at point 1 of exterior girder, for the dead load case, obtained from finite-element analysis
$(\sigma_{E3})_{DL}$	mid-span stress in bottom flange fibres at point 3 of exterior girder, for the dead load case, obtained from finite-element analysis
$(\Delta_{E2})_{DL}$	mid-span deflection in bottom flange fibres at point 2 of exterior girder, for the dead load case, obtained from finite-element analysis
$(\sigma_{E1})_{FL}$	mid-span stress in bottom flange fibres at point 1 of exterior girder, for the full lane loading case, obtained from finite-element analysis
$(\sigma_{E1})_{PL}$	mid-span stress in bottom flange fibres at point 1 of exterior girder, for the partial lane loading case, obtained from finite-element analysis
$(\sigma_{E3})_{FL}$	mid-span stress in bottom flange fibres at point 3 of exterior girder, for the full lane loading case, obtained from finite-element analysis
$(\sigma_{E3})_{PL}$	mid-span stress in bottom flange fibres at point 3 of exterior girder, for the partial lane loading case, obtained from finite-element analysis
$(\Delta_{E2})_{FL}$	mid-span deflection in bottom flange fibres at point 2 of exterior girder, for the full lane loading case, obtained from finite-element analysis
$(\Delta_{E2})_{PL}$	mid-span deflection in bottom flange fibres at point 2 of exterior girder, for the partial lane loading case, obtained from finite-element analysis
$(\sigma_{E1})_{Fat}$	mid-span stress in bottom flange fibres at point 1 of exterior girder, for the fatigue case, obtained from finite-element analysis

$(\sigma_{E3})_{Fat}$ mid-span stress in bottom flange fibres at point 3 of exterior girder, for the fatigue case, obtained from finite-element analysis

$(\Delta_{E2})_{Fat}$ mid-span deflection in bottom flange fibres at point 2 of exterior girder, for the fatigue case, obtained from finite-element analysis

$(\sigma_{M1})_{DL}$ mid-span stress in bottom flange fibres at point 1 of middle girder, for the dead load case, obtained from finite-element analysis

$(\sigma_{M3})_{DL}$ mid-span stress in bottom flange fibres at point 3 of middle girder, for the dead load case, obtained from finite-element analysis

$(\Delta_{M2})_{DL}$ mid-span deflection in bottom flange fibres at point 2 of middle girder, for the dead load case, obtained from finite-element analysis

$(\sigma_{M1})_{FL}$ mid-span stress in bottom flange fibres at point 1 of middle girder, for the full lane loading case, obtained from finite-element analysis

$(\sigma_{M3})_{FL}$ mid-span stress in bottom flange fibres at point 3 of middle girder, for the full lane loading case, obtained from finite-element analysis

$(\Delta_{M2})_{FL}$ mid-span deflection in bottom flange fibres at point 2 of middle girder, for the full lane loading case, obtained from finite-element

$(\sigma_{M1})_{Fat}$ mid-span stress in bottom flange fibres at point 1 of middle girder, for the fatigue case, obtained from finite-element analysis

$(\sigma_{M3})_{Fat}$ mid-span stress in bottom flange fibres at point 3 of middle girder, for the fatigue case, obtained from finite-element analysis

$(\Delta_{M2})_{Fat}$ mid-span deflection in bottom flange fibres at point 2 of middle girder, for the fatigue case, obtained from finite-element analysis

$(\sigma_{I1})_{DL}$ mid-span stress in bottom flange fibres at point 1 of interior girder, for the dead load case, obtained from finite-element analysis

$(\sigma_{I3})_{DL}$ mid-span stress in bottom flange fibres at point 3 of interior girder, for the dead load case, obtained from finite-element analysis

$(\Delta_{I2})_{DL}$ mid-span deflection in bottom flange fibres at point 2 of interior girder, for the dead load case, obtained from finite-element analysis

$(\sigma_{I1})_{FL}$ mid-span stress in bottom flange fibres at point 1 of interior girder, for the full lane loading case, obtained from finite-element analysis

$(\sigma_{I1})_{PL}$ mid-span stress in bottom flange fibres at point 1 of interior girder, for the partial lane loading case, obtained from finite-element analysis

$(\sigma_{I3})_{FL}$ mid-span stress in bottom flange fibres at point 3 of interior girder, for the full lane loading case, obtained from finite-element analysis

$(\sigma_{I3})_{PL}$ mid-span stress in bottom flange fibres at point 3 of interior girder, for the partial lane loading case, obtained from finite-element analysis

$(\Delta_{I2})_{FL}$ mid-span deflection in bottom flange fibres at point 2 of interior girder, for the full lane loading case, obtained from finite-element analysis

$(\Delta_{I2})_{PL}$ mid-span deflection in bottom flange fibres at point 2 of interior girder, for the partial lane loading case, obtained from finite-element analysis

$(\sigma_{I1})_{Fat}$ mid-span stress in bottom flange fibres at point 1 of interior girder, for the fatigue case, obtained from finite-element analysis

$(\sigma_{I3})_{Fat}$ mid-span stress in bottom flange fibres at point 3 of interior girder, for the fatigue case, obtained from finite-element analysis

$(\Delta_{I2})_{Fat}$ mid-span deflection in bottom flange fibres at point 2 of interior girder, for the fatigue case, obtained from finite-element analysis

$(\sigma_{simple})_{DL}$ mid-span stress in bottom flange fibres, for a straight simply supported girder subject to dead load

$(\Delta_{simple})_{DL}$ mid-span deflection in bottom flange fibres, for a straight simply supported girder subject to dead load

$(\sigma_{simple})_{truck}$ mid-span stress in bottom flange fibres, for a straight simply supported girder subject to CHBDC truck loading

$(\Delta_{simple})_{truck}$ mid-span deflection in bottom flange fibres, for a straight simply supported girder subject to CHBDC truck loading

$(\sigma_E)_{DL}$ the bigger mid-span stresses of points 1 and 3 of exterior girder for the dead load case

$(\sigma_M)_{DL}$ the bigger mid-span stresses of points 1 and 3 of middle girders for the dead load case

$(\sigma_I)_{DL}$ the bigger mid-span stresses of points 1 and 3 of interior girder for the dead load case

$(\sigma_E)_{FL}$ the bigger mid-span stresses of points 1 and 3 of exterior girder for the full load case

$(\sigma_E)_{PL}$ the bigger mid-span stresses of points 1 and 3 of exterior girder for the partial load case

$(\sigma_M)_{FL}$ the bigger mid-span stresses of points 1 and 3 of middle girders for the full load case

$(\sigma_I)_{FL}$	the bigger mid-span stresses of points 1 and 3 of interior girder for the full load case
$(\sigma_I)_{PL}$	the bigger mid-span stresses of points 1 and 3 of interior girder for the partial load case
$(\sigma_E)_{Fat}$	the bigger mid-span stresses of points 1 and 3 of exterior girder, for the fatigue load case
$(\sigma_M)_{Fat}$	the bigger mid-span stresses of points 1 and 3 of middle girders, for the fatigue load case
$(\sigma_I)_{Fat}$	the bigger mid-span stresses of points 1 and 3 of interior girder, for the fatigue load case
$(MDF)_{DL\ ext}$	the moment distribution factor of exterior girder for dead load case
$(MDF)_{FL\ ext}$	the moment distribution factor of exterior girder for full load case
$(MDF)_{PL\ ext}$	the moment distribution factor of exterior girder for partial load case
$(MDF)_{Fat.ext}$	the moment distribution factor of exterior girder for fatigue case
$(MDF)_{DL\ mid}$	the moment distribution factor of middle girder for dead load case
$(MDF)_{FL\ mid}$	the moment distribution factor of middle girder for full load case
$(MDF)_{Fat.mid}$	the moment distribution factor of middle girder for fatigue case
$(MDF)_{DL\ int}$	the moment distribution factor of interior girder for dead load case
$(MDF)_{FL\ int}$	the moment distribution factor of interior girder for full load case
$(MDF)_{PL\ int}$	the moment distribution factor of interior girder for partial load case
$(MDF)_{Fat.int}$	the moment distribution factor of interior girder for fatigue case
$(DDF)_{DL\ ext}$	the deflection distribution factor of exterior girder for dead load case
$(DDF)_{FL\ ext}$	the deflection distribution factor of exterior girder for full load case

$(DDF)_{PL\ ext}$ the deflection distribution factor of exterior girder for partial load case

$(DDF)_{Fat.ext}$ the deflection distribution factor of exterior girder for fatigue case

$(DDF)_{DL\ mid}$ the deflection distribution factor of middle girder for dead load case

$(DDF)_{FL\ mid}$ the deflection distribution factor of middle girder for full load case

$(DDF)_{Fat.mid}$ the deflection distribution factor of middle girder for fatigue case

$(DDF)_{DL\ int}$ the deflection distribution factor of interior girder for dead load case

$(DDF)_{FL\ int}$ the deflection distribution factor of interior girder for full load case

$(DDF)_{PL\ int}$ the deflection distribution factor of interior girder for partial load case

$(DDF)_{Fat.int}$ the deflection distribution factor of interior girder for fatigue case

$(WBR)_{DL\ ext}$ the warping bending stress ratio of exterior girder for dead load case

$(WBR)_{FL\ ext}$ the warping-to-bending stress ratio of exterior girder for full load case

$(WBR)_{PL\ ext}$ the warping-to-bending stress ratio of exterior girder for partial load case

$(WBR)_{Fat.ext}$ the warping-to-bending stress ratio of exterior girder for fatigue case

$(WBR)_{DL\ mid}$ the warping-to-bending stress ratio of middle girder for dead load case

$(WBR)_{FL\ mid}$ the warping-to-bending stress ratio of middle girder for full load case

$(WBR)_{Fat.mid}$ the warping-to-bending stress ratio of middle girder for fatigue case

$(WBR)_{DL\ int}$ the warping-to-bending stress ratio of interior girder for dead load case

$(WBR)_{FL\ int}$ the warping-to-bending stress ratio of interior girder for full load case

$(WBR)_{PL\ int}$ the warping-to-bending stress ratio of interior girder for partial load case

$(WBR)_{Fat.int}$ the warping-to-bending stress ratio of interior girder for fatigue case

LIST OF TABLES

LIST OF FIGURES

Figure | Page

CHAPTER I
INTRODUCTION

1.1. General

In structural design, it is necessary to obtain an appropriate geometric shape for the structure so that it can safely and economically carry the loads imposed on it. Nowadays, horizontally curved bridges became an important component in urban bridges, especially where tight geometric restrictions are encountered. Curved bridges allow for smooth traffic flow and create a painless directional transition at interchanges. This directly results in fewer traffic jams, less air pollution due to idle-car emissions, and less road rage. Due to its increasing use in modern highways, the impact of curved bridges, both socially and economically, is cause for the intense research, which has been performed in previous years. Increasing complex interchanges and the desire to conform to existing terrain have made curved steel I-girder bridges the preferred choice because of its simplicity of fabrication and construction, fast speed of erection and excellent serviceability performance. These bridges are mostly located on and off ramps and characterized by complex vertical and horizontal geometries.

Generally, bridges can be constructed entirely from reinforced concrete, pre-stressed concrete, steel, or composite concrete deck-steel girders. These bridges may be comprised of a concrete slab deck or steel deck on concrete or steel box girders or I-girders. In the case of curved steel plate girders, as shown in Figure 1.1, there are two fabrication methods that are usually employed. The first method involves cutting curved

flanges from straight plates to the required curvature and then welding them on the mechanically bent plates or webs, which are curved. The second method involves prefabrication of straight webs followed by either cold bending or heat curving in which a straight girder is curved to the stipulated radius by applying heat to the edges of the flanges to achieve the required curvature. This actual curving of girders has allowed more aesthetically pleasing structures than straight girders used as chords in forming a curved alignment. Figure 1.2 shows a typical cross-section of a four-girder bridge. It consists of concrete deck slab supported over steel I-girders. Cross-bracings as well as top and bottom chords are used at equal intervals between bridge support lines to stabilize the girders during construction and enhance its structural integrity.

1.2. The Problem

Although horizontally curved steel bridges constitute roughly one third (Zureick and Naqib 1999) of all steel bridges, the structural behavior is still not well understood. Based on the literature review, the investigation of the load distribution characteristics of such bridges is needed. Currently, the Canadian Highway Bridge Design Code (CHBDC, 2000) recognizes plan curvature as a factor affecting the structural behaviour of bridges. The North American Codes of Practice (AASHTO-LRFD, 2004; AASHTO, 1996) specify load distribution factor equations for the design of straight composite I-girder bridges and provide a geometrically defined criterion when horizontally curved bridges may be treated as straight bridges. In both cases, there is no practical design method in the form

of expressions for moment and deflection distribution factor for composite concrete-steel I-girder bridges with significant curved alignment.

The AASHTO Guide Specifications for Horizontally Curved Bridges, (Guide, 2003), recommend few numerical and analytical methods for the analysis of such bridges. Among them is the finite-element method. In practice, detailed finite-element method (FEM) is frequently employed for accurate results. Unfortunately, most engineers are not familiar with FEM procedure. The FEM procedure is quite time consuming, especially in preliminary design when girder dimensions are not known. Simplified formulas are desired to predict accurate live load distribution for curved bridges. Therefore, to meet the practical requirements arising during the design process, a simple design method is needed for curved composite I-girder bridges in the form of load distribution factors for bending stresses, warping stresses and girder deflection to fill the gaps found in bridge codes.

1.3 Objectives

The objectives of this study are:

1. To identify the key parameters that influence the lateral distribution of loads in curved composite concrete deck-over steel I-girder bridges.
2. To provide database that can be used to develop simplified design method for curved composite I-girder bridges in the form of load distribution factors for bending stresses, warping stresses and girder deflection.

1.4 Scope

The scope of this study includes the following:

1. A literature review of the research work, and codes of practice pertained to the load distribution of straight and curved I-girder bridges.
2. A practical-design-oriented parametric study, using the commercially available finite-element "SAP2000" software on 144 curved and 48 straight composite I-girder bridge prototypes subjected to the CHBDC truck loading as well as dead load.
3. Correlation between the data generated for the straight bridges and the moment distribution factor values specified in the Canadian Highway Bridge Design Code of 2000.
4. Preparation of database that can be used to develop empirical formulas for moment and deflection distribution factors for straight and curved steel I-girder bridges when subjected to the CHBDC truck loading as well as dead load.
5. Examining the warping-to-bending stress ratio for the curved bridges considered in this study due to different loading conditions.

1.5 Contents and Layout of this Study

Chapter I demonstrates the problem which led to this research and the objective of it. Chapter II contains the literature review on straight and curved bridges pertained to the topic of the thesis. Chapter III describes the finite-element method and "SAP2000" software used in the parametric study. Also, chapter III presents the methodology to

obtain the moment and deflection distribution factors as well as the warping-to-bending stress ratio. Chapter IV presents the results of the parametric study performed on the prototype bridges. Chapter V gives a summery of this research, the conclusion reached, and recommendations for further research.

CHAPTER II

LITERATURE REVIEW

2.1 Concept of Lateral Load Distribution Factor

Bridges are subjected to dead load and truck loading. The calculation of dead load, in the case of straight bridges, is simple. The deck slab, wearing surface, and curbs or traffic barriers can be considered to be distributed evenly among girders. Since curbs or traffic barriers are constructed after the concrete deck is cured, for better accuracy, these dead loads can also be considered as live load. For sure, this approach is not valid in the case of horizontally curved bridges due to the torsion effects resulting from curvature.

To calculate the live load carried by each girder in the case of a straight bridge, lateral load distribution factor is a key issue. For simplicity, a straight single girder and multi-girder bridge are used herein to introduce the concept of lateral load distribution factor. Figure 2.1a shows the free body diagram of a straight single girder under live load P. Considering η (x) the influence line of a certain section of the girder, then the internal force at this section can be calculated as $F = P \times \eta(x)$. This is a simple two-dimensional problem since both the load and the girder deformation is in the plane of *xoz*. However, for multi-girder straight bridge subject to live load P, as shown in Figure 2.1b, the mechanism is totally different. Lateral rigidity makes the live load P to distribute in the lateral direction (y direction) as well as in the longitudinal direction (x direction). Therefore, the live load on the bridge is shared among the girders. Each girder is

subjected to different magnitude of the live load. The live load position and structural deformation are three-dimensional and consequently three-dimension approach is required to solve the internal forces of the structure. The common characteristic of three-dimension approach is that the internal forces and deformation at any point of the structure can be solved directly.

Alternatively, the internal forces can be calculated using the influence surface, just like using the influence line to determine the internal forces in a single girder. Considering $\eta(x,y)$ the influence surface of a certain section of the structure under live load, the response of the structure is then $F=P \times \eta (x,y)$. Since the live loads on the bridge are multiple concentrated wheel loads, which can move both longitudinally and transversely, using influence surface to determine the maximum internal forces will be tedious and complicated. Therefore, the influence surface method is not widely used in practice.

A frequently used method is to convert the complex three-dimensional problem (Figure 2.1b) into a simple two-dimensional problem (Figure 2.1a). The principle of this method is to convert the two-variable influence surface function $\eta (x,y)$ into the product of two single-variable functions, that is, $\eta (x,y) = \eta (x) \times \eta (y)$. The internal force at the section is then

$$F = P \times \eta (x,y) = P \times \eta (x) \times \eta (y) \qquad (2.1)$$

Where $\eta (x)$ is the longitudinal influence line of that section for a single girder (Figure 2.1a), $\eta (y)$ is the live load distributed to one certain girder when a unit load moves

transversely across the bridge. η *(y)* is referred to as the ***transverse influence line*** for that girder and $P \times \eta$ *(y)* is the load distributed to that girder when live load P is at point *a(x, y)* (Figure 2.1b). Therefore, the internal forces at a certain section for a specific girder can be determined using the longitudinal and transverse influence lines, which simplifies the three-dimensional problem.

In reality, actual truck loads are multiple wheel loads moving on the bridge. Figure 2.2a shows a multi-girder bridge subjected to truck loads. The rear, middle and front axle loads of the truck are *P1, P2* and *P3,* respectively. To determine the maximum response at point *k* of girder No. 3, for instance, the transverse influence line of girder No. 3, and the worst loading position to determine the maximum magnitude of each axle load distributed to girder No. 3 are first obtained. Secondly, the maximum response at section *k* of girder No. 3 using the longitudinal single girder influence line at section k is determined. Obviously, if the positions of the truck wheels on the bridge are fixed, the load distributed to girder No. 3 is fixed. In practice, the product of a factor g and the axle load expresses this fixed value. Therefore, the loads distributed to girder No. 3 of the rear, middle, and front truck axle loads can be expressed as gP1, gP2, and gP3, respectively, as shown in Figure 2.2b. The factor g is referred to as lateral load distribution factor. It shows that the maximum load distributed to one certain girder (here is girder No. 3) is a fraction of each axle load (usually less than one).

It should be noted, that it is an approximate approach to convert the three-dimensional problem into a two-dimensional problem, since the paths of the load being

distributed to the adjacent girders are complex. The concentrated load at one girder would no longer be concentrated load at the same longitudinal position after being distributed to the adjacent girders. However, theoretical and experimental research (Yoo, 1990) showed that the error was relatively small for lateral load distribution. Moreover, the actual truck load on the bridge is not one single concentrated load, but several wheel loads distributed at different longitudinal positions. Therefore, the error would be even smaller for truck loading.

Obviously, the distribution factor g for each girder is different within the same bridge. It also varies with the variation of truck configuration, truck longitudinal location on the bridge, and the bridge lateral rigidity. The effect of truck longitudinal location is insignificant and usually the distribution factor at girder maximum response location is used for design. The bridge lateral rigidity is related to the relative stiffness of the girders and the deck. The load distribution between girders is poor for transversely flexible bridges and is even for transversely stiff bridges. Figure 2.3 shows how the bridge girders in a cross section may deflect when subjected to applied load P. In this Figure, EI_T is the bridge transverse or lateral rigidity. Figure 2.3a shows the deformation of the bridge structure when the bridge transverse rigidity EI_T is zero and the middle girder is subjected to load P. Since the load can only transfer to the middle girder, the distribution factor g for the middle girder is one and for other girders is zero. However, when the bridge transverse rigidity is infinity and the same load P is applied at the middle girder position, every girder has the same deflection and the same magnitude of the load. Therefore, the distribution factor g for every girder is $1/N$, where N is the number of girders. For a five-

girder bridge shown in Figure 2.3c, the distribution factor g is 0.2. For concrete, reinforced concrete, and steel girder bridges, the transverse rigidity is between zero and infinity. When the middle girder is subjected to a load P, as shown in Figure 2.3b, the distribution factor for each girder is between $1/N$ and one. To determine the exact magnitude of the live load distributed to each girder is the key issue in bridge analysis and has been studied by many researchers.

With the development of high speed and capacity computers, they can be used to accurately analyze the structures under dead and live loads. One way to estimate the maximum moment and shear response in individual bridge girder would be to model the entire bridge in three dimensions using the finite element method (FEM) or other analytical methods and determine the moment and shear in individual member. The loading is varied, both in longitudinal and transverse positions, to find the worst loading positions. For bridges with very complex configurations, this method might be the only way to determine the accurate maximum moment and shear under live load for each girder. However, for many types of bridges, this process could be very cumbersome and unnecessary. Distribution factors and empirical methods are still the main methods used in design of modern bridges in North America. Empirical formulas were obtained by analyzing many bridge systems. The procedure used in the development of curved girder distribution factors followed the same technique employed in determining the straight girder load distribution equations. To analysis of a curved system is more complicated than that of a straight one. For this reason, available literature for both straight bridges and curved bridges are reviewed in the following sections.

2.2 Review of Previous Research on Load Distribution

2.2.1 Review of Study on Distribution Factors for Straight Bridges

Based on the level of bridge lateral rigidity, different methodologies are employed in practice, including lever rule, eccentric compression method, hinged joint method, fixed joint method, orthotropic plate analogy, AASHTO Standard and AASHTO-LRFD methods.

2.2.1.1 Lever Rule Method (Yao 1990)

The lever rule is one of the most frequently used methods for calculation distribution factors. This method assumes that the deck between the girders acts as a simply supported beam or cantilever beam, as shown in Figure 2.4. In this case, the load on each girder shall be taken as the reaction of the wheel loads. The lever rule method is very accurate for two girder bridges. The lever rule method can also be used for shear distribution near support, since the load would pass to the pier or abutment mostly through the adjacent two girders. When the bridge transverse stiffness is relatively flexible, lever rule can also give very good results. However, the results usually would be slightly conservative for the interior girders and unconservative for the exterior girders.

2.2.1.2 Eccentric Compression Method (Yao 1990)

This method can be applied to "Narrow Bridge" with adequate diaphragms along bridge span. "Narrow Bridge" is defined as that the ratio of bridge width, B, to span length, L, is less than or equal to 0.5 satisfying the ratios of bridge longitudinal rigidity

per unit length, D_y, to transverse rigidity per unit width, D_y, is greater than 0.48. The deflection of a narrow bridge with adequate diaphragms under truck load is similar to that of an eccentric compression member, as shown in Figure 2.5.

From the theory of mechanics, when the girder k is subjected to a load P, the load distributed to girder i is:

$$R_{ik} = \left(\frac{I_i}{\sum_{i=1}^{n} I_i} + \frac{a_i a_k I_i}{\sum_{i=1}^{n} a_i^2 I_i} \right) * P \qquad (2.2)$$

Where I_i is the moment of inertia of girder No. i; a_i and a_k are the distances from bridge centerline to girder No. i and k respectively. Therefore, the transverse influence line can be obtained from Equation 2.2 when load P is equal to one. If all the girders have the same cross section or the same moment of inertia, the control values of the transverse influence line for girder No. 1 are simplified as (note that $a_1 = a_5$):

$$\eta_{11} = \left(\frac{1}{N} + \frac{a_1^2}{\sum_{i=1}^{n} a_i^2} \right) \qquad (2.3a)$$

$$\eta_{15} = \left(\frac{1}{N} - \frac{a_1^2}{\sum_{i=1}^{n} a_i^2} \right) \qquad (2.3b)$$

Where N is the number of girders. Once the two control values η_{11} and η_{15} are determined, the transverse influence line for girder No 1 is determined. The distribution factor can then be obtained by arranging the trucks transversely on the bridge to get the worst situation.

Note that in the above procedure, the girder torque is ignored. When considering the girder torque, Equations 2.3a and b become:

$$\eta_{11} = \left(\frac{1}{N} + \beta \frac{a_1^2}{\sum_{i=1}^{n} a_i^2} \right) \tag{2.4a}$$

$$\eta_{15} = \left(\frac{1}{N} - \beta \frac{a_1^2}{\sum_{i=1}^{n} a_i^2} \right) \tag{2.4b}$$

where

$$\beta = \frac{1}{1 + \dfrac{GL^2 \sum_{i=1}^{n} J_i}{12E \sum_{i=1}^{n} a_i^2 I_i}} < 1 \tag{2.5}$$

and G is modulus of elasticity in shear or modulus of rigidity; E is modulus of elasticity i; L is the bridge span length; J_i is the torsional inertia of girder No. i.

2.2.1.3 Hinged Joint Method (Yao 1990)

2.2.1.3.1 Hinged Joint Method for Slab Bridges

This method can be used for slab bridges with pre-cast members connected by tongue-and-groove joint. The deflection of a slab bridge under concentrated wheel load is shown in Figure 2.6a. Figure 2.6b shows the general internal forces occurred at the tongue and groove joint, which are vertical shear g(x), transverse moment m(x), longitudinal shear $t(x)$, and normal force $n(x)$. Longitudinal shear $t(x)$ and normal force

$n(x)$ are relatively small compared with vertical shear $g(x)$ when the bridge is subjected to truck load. Since the joint is relatively short in configuration and very flexible in resisting moment, the transverse moment $m(x)$ as well as the longitudinal shear $t(x)$ and normal force $n(x)$ can be neglected in analysis. Therefore, the joint can be simplified as a hinge, assuming only vertical shear force $g(x)$ exists, as shown in Figure 2.6c.

To convert the three-dimensional problem into a two-dimensional problem, the ratio of the deflection, moment, shear, and applied load, in any two strips or girders must be equal to a constant, that is,

$$\frac{w_1(x)}{w_2(x)} = \frac{M_1(x)}{M_2(x)} = \frac{Q_1(x)}{Q_2(x)} = \frac{P_1(x)}{P_2(x)} = C \tag{2.6}$$

Sinusoidal load is assumed to meet this requirement and the sinusoidal load is in the form of

$$P(x) = P_0 \sin \frac{\pi x}{L} \tag{2.7}$$

The free body diagram of a slab strip under sinusoidal load is shown in Figure 2.7.

The error of the sinusoidal load assumption is very small since along the bridge span there will be many wheel loads. To obtain the distribution factor, the girder transverse influence line must be obtained first. For a bridge with n strips, an indeterminate problem of n-1 order is to be solved to obtain the influence line. For convenience, transverse influence line control values for bridges with 3 to 10 slab strips are tabulated and the tables can be found in *Bridge Engineering* (Yao, 1990). After the transverse influence

line is obtained, trucks can then be arranged transversely across the bridge to find the worst situation and the maximum distribution factors.

2.2.1.3.2 Hinged Joint Method for T-Shaped Girder Bridge

The hinged joint method can also be used for small span concrete T-shaped girder bridges without intermediate diaphragms. Figures 2.8a and 2.8b show the free body diagrams of unit length section at bridge middle span of the hinged T-shaped girder bridge under unit sinusoidal load. Different from slab bridges, the deflection of the T-shaped girder flanges must be considered, as shown in Figures 2.8c and 2.8d. When the cantilever length is within 0.80 m and the span length is greater than 10 m, the tables found in *Bridge Engineering* (Yao, 1990) for calculating transverse influence line values for hinged slab bridges can also be used for hinged girder bridges. For better accuracy, detailed calculation is required for bridges beyond this range.

2.2.1.4 Fixed Joint Girder method (Yao 1990)

When the lateral connection between girders is stiffer, the joint can be considered as a fixed joint. In addition to shear force at the joint, moment must be considered, as shown in Figure 2.9. For an n-girder bridge, a $2(n\text{-}1)$ order of indeterminate problem is to be solved to obtain the shear and moment at each joint. However, only shearing force g_i is considered for calculating distribution factor. Once g_i is known, the same procedure as in hinged joint method can be followed to obtain the transverse influence line as well as the distribution factors.

2.2.1.5 Orthotropic Plate Analogy (Guyon-Massonnet or G-M Method) (Yao 1990)

For concrete bridges with continuous slab and intermediate diaphragms and with the bridge width to span length ratio B/L greater than 0.5, grillage system may be used to simulate the bridge system. Or, the bridge may be analogized to a rectangular thin plate, which is called orthotropic plate analogy or Guyon-Massonnet (G-M) method (Yao 1990). Orthotropic plate is referred to as a plate with the elastic properties different in x and y directions. Figure 2.10a shows the longitudinal and transverse configuration of a bridge structure. In this case, the girder spacing is considered as S, girder moment of inertia and torsional inertia are I_x and I_{Tx}, respectively, diaphragm spacing is S_c, and diaphragm moment of inertia and torsional inertia are I_y and I_{Ty} respectively. For very small values of S and S_c compared to the bridge width and span length, and for fully composite action, we can distribute girder moment of inertia and torsional inertia I_x and I_{Tx} to the distance S and distribute diaphragm moment of inertia and torsional inertia I_y and I_{Ty} to the distance S_c. Thus, the real grid system (Figure 2.10a) is analogized to an imaginary plate (Figure 2.10b). In Figure 2.10b, the thickness in the x direction is shown in dashed line, which indicates that, the equivalent thickness in the x and y direction are different for the analogized plate. The moment of inertia and torsional inertia per unit width in the x and y directions for the analogized plate are considered as follows:

$$J_x = \frac{I_x}{S}, J_{Tx} = \frac{I_{Tx}}{S}, J_y = \frac{I_y}{S_c}, J_{Ty} = \frac{I_{Ty}}{S_c} \tag{2.8}$$

For beam and slab concrete bridges and prestressed concrete bridges, Poisson's ratio v can be neglected for simplicity. In that case, the bridge can be analogized to an orthotropic plate with rigidity per unit width $E_x J_x$, $G_x J_{Tx}$, $E_x J_y$, and $G_x J_{Ty}$. The analogized

orthotropic (in configuration) plate differential equilibrium with $E_x=E_y=E$ and $\nu_x=\nu_y=\nu$ *is:*

$$EJ_x \frac{\partial^4 w}{\partial x^4} + G(J_{Tx} + J_{Ty}) \frac{\partial^4 w}{\partial x^2 \partial y^2} + EJ_y \frac{\partial^4 w}{\partial y^4} = p(x,y) \tag{2.9}$$

Let $D_x = EJ_x$, $D_y = EJ_y$ and $H = G(J_{Tx} + J_{Ty})/ 2E$, Equation 2.9 becomes:

$$D_x \frac{\partial^4 w}{\partial x^4} + 2H \frac{\partial^4 w}{\partial x^2 \partial y^2} + D_y \frac{\partial^4 w}{\partial y^4} = p(x,y) \tag{2.10}$$

which is identical to the differential equation for orthotropic plate (in material elastic properties). This means that analogized orthotropic (in configuration) plate can be solved the same way as orthotropic (in material properties) plate, except that that the stiffness constants contained in the equations are different.

The internal forces can be obtained by solving this equation for displacement w under applied load. Directly solving the partial differential equation is difficult. For convenience, Guyon and Massonnet had developed solution charts, which can be found in *Bridge Engineering* (Yao 1990) and can be used to easily obtain the transverse influence line. Once the transverse influence line is obtained, the distribution factors can be obtained by arranging the trucks transversely on the bridge.

2.2.1.6 AASHTO Methods

Compared with the theoretical methods mentioned above, AASHTO empirical methods are more convenient to use. AASHTO defines the distribution factor as the ratio of the moment (or shear) obtained from the bridge system to the moment (or shear) obtained from a single girder loaded by one truck wheel line (*AASHTO Standard* 1996)

or the axle loads (*AASHTO-LRFD* 2004). It should be noted that AASHTO Standard Specifications and AASHTO LRFD Specifications define the live load differently. The live load in the Standard specifications consists of an HS 20 truck or a lane load. While, the live load in the LRFD specifications consists of an HS 20 truck in conjunction with a lane load. Since both trucks have a 1.8 m axle (gauge) width, it is assumed that the difference in the live load configuration does not affect the lateral load distribution.

2.2.1.6.1 AASHTO Standard Method (1996)

AASHTO Standard specifications (1996) adopted the simplified formulas for distribution factors based on the work done in the 1940s by Newmark (1948). The formulas are in the format of *S/D*, where *S* is the girder spacing in feet and *D* is a constant based on the bridge type. This method is applicable to straight and right (i.e. nonskewed) bridges only. It was proved to be accurate when girder spacing was near 1.8m and span length was about 18 m (Zokaie, 2000). For relatively meduim or long bridges, these formulas would lose accuracy.

2.2.1.6.2 AASHTO LRFD Method

During the past 20 years or so, structural design has been moving toward a more rational and probability-based design procedure referred to as Load and Resistance Factor Design, (LRFD). AASHTO LRFD Specifications have become more and more attractive for bridge engineers because of its incentive permitting the better and more economical use of materials. The rationality of LRFD and its many advantages over the allowable stress design methods, ASD, are indicative that the design philosophy will relegate ASD

to the background in the next few years (Salmon and Johnson, 1996). AASHTO LRFD (1998) adopted the research results of the National Cooperative Highway Research Program (NCHRP) 12-26 project, which was entitled "Distribution of Live Loads on Highway Bridges" and initiated in 1985. More parameters, such as girder spacing, bridge length, slab thickness, girder longitudinal stiffness, and skew effect are considered in the developed formulas. The research results were first adopted by AASHTO Standards in 1994 and were then officially adopted by AASHTO-LRFD in 1998. The AASHTO-LRFD formulas, evaluated by Shahawy and Huang (2001), showed good agreement with test results for bridges with two or more design lanes loaded, provided that girder spacing and deck overhang did not exceed 2.4 m and 0.9 m, respectively. Outside of these ranges, the error could be as much as up to 30%. For one design lane loaded, the relative error was less than 10% for interior girders and could be as high as 100% and as low as –30% for exterior girders. Shahawy and Huang (2001) presented modification factors for the AASHTO LRFD formulas and the results of the modified formulas showed good agreement with the test results.

2.2.1.7 Other Studies

Besides the AASHTO formulas, numerous papers have been published for load distribution factors since 1950. They are invaluable for further studies. Kostem and DeCastro (1977) showed that the contribution of diaphragms to lateral load distribution was marginal regardless of the loading pattern. Hayes et al. (1986) developed a program, SALOD, to evaluate the lateral load distribution of simple-span bridges in flexure. Span length was found to be an important parameter in calculating the distribution factor.

Bakht and Moses (1988) presented a procedure to calculate the constant *D* in the AASHTO load distribution formula (*S/D*). Tarshini and Frederick (1992), using FEM, studied the effect of various parameters on wheel load distribution for I-girder highway bridges and found that composite and non composite construction showed a negligible effect; the effect of the most common types of channel diaphragm and cross bracing between beams had negligible effect.

2.2.2 Review of Study on Distribution Factors for Curved Bridges

Many articles on curved bridges have been published in the literature as listed by McManus et al. (1969), discussed by Ketchek (1969) and Pandit et al. (1970), and recently stated by Zureick and Naqib (1999). However, valuable studies related to the analysis and design of horizontally curved bridges began only in 1969 when the Federal Highway Administration (FHWA) of the United States formed the Consortium of University Research Teams (CURT). This team consisted of Carnegie Mellon University, University of Pennsylvania, University of Rhode Island, and Syracuse University, whose research efforts, along with those at University of Maryland, resulted in the initial development of working Stress Design (WSD) or Allowable Stress Design (ASD) criteria and tentative design specifications. The American Society of Civil Engineers (ASCE) and the AASHTO Task Committee (1977) compiled the results of most of the research efforts prior to 1976 and presented a set of recommendations pertaining to the design of curved I-girder bridges. The CURT research activity was followed by the development of Load Factor Design (LFD) criteria (Stegmann and Galambos 1976, Galambos 1978) adopted by AASHTO to go along with the ASD criteria. These provisions appeared in the first

Guide (1980) as well as the Guide (1993). Studies on curved bridges will be concluded in the following lines such as Heins and Siminou's study (1970), AASHTO Guide and its Commentary methods, AASHTO with V-load modification method, Heins and Jin's method (1984), Brockenbrough's study (1986); Yoo and Littrell's study (1986), Davidson, Keller and Yoo's study (1996), Schelling, Namini, Fu's study (1989), Sennah, Eissa, and Lee's Study (2000) and Zhang's study (2002).

2.2.2.1 Heins and Siminou's Study (1970)

Heins and Siminou presented a series of simplified equations, which permit evaluation of internal forces and deformation in a single, two, and three-span curved girder system. These forces can then be utilized to estimate preliminary section properties, which are necessary in utilizing various computer programs. These studies, resulting in design equations, have the following limitations:

1. Girder spacing may be 2.1, 2.4, 2.7or 3 m.
2. Individual girder span lengths varied from 15 to 30m.
3. The girders of the system must have a constant curvature and are limited to radii of 30 to 180 m.
4. The number of girders in the system may be 4, 6 or 8.
5. Only two-and three-span continuous bridges were examined, with all interior end spans of equal length.

The main reason why the Heins-Siminou's result is too conservative is that the entire deck in the three-dimensional model was not included and the bridge centerline length in equations was used rather than the individual actual girder length.

2.2.2.2 AASHTO Methods

2.2.2.2.1 AASHTO Guide Commentary Method

The Commentary of the AASHTO Guide Specifications for Highway Bridges of 1993, (Guide, 1993), which adopted the research results of Heins and Siminou (1970), gives the distribution factors for bending moment as:

$$g = \frac{S}{5.5}\left[(\bar{N}+3)\frac{L}{4R}+0.7\right] \qquad (2.11)$$

where

S = girder spacing in ft (7 ft $\leq$ S $\leq$12 ft),

$\bar{N} = \frac{R}{100}$ (R > 100 ft),

L = span length in ft, and

R = radius of curvature in ft (R > 100ft).

It should be noted that Equation 2.11 is analogous to AASHTO Standard equation S/D. This equation is intended to present the outside exterior girder moment distribution and would be increasingly conservative for other girders across the bridge. This method was omitted from the current version of the AASHTO Guide (Guide, 2004)

2.2.2.2.2 AASHTO Guide Method

The equation specified in the AASHTO Guide Specifications for Horizontally Curved Bridges (1993) takes into account the effect of lateral bracing, connecting the bottom flanges of the girders. For both ASD and LRFD, the distribution factors, in terms of the resulting maximum live load (normal stress component + warping stress component) bottom flange stress in the girder, can be calculated as:

For outside exterior girder:

$$g_{ebf} = \frac{3.0 - 0.06\,(L)}{S^{3/2}} \left[\frac{L}{R}\right] + 0.9 \quad \text{for all bays with bottom lateral bracing} \qquad (2.12)$$

$$g_{ebf} = \frac{3.0 - 0.06\,(L)}{S^{3/2}} \left[\frac{L}{R}\right] + 0.95 \quad \text{or bottom lateral bracing in every other bay} \qquad (2.13)$$

For inside exterior girder:

$$g_{ibf} = g_{ebf}\left[-0.366 \times \left[\frac{L}{R}\right] + 0.944\right] \text{ for all bays with bottom lateral bracing} \qquad (2.14)$$

$$g_{ibf} = g_{ebf}\left[-0.473 \times \left[\frac{L}{R}\right] + 0.934\right] \text{ for bottom lateral bracing in every other bay} \qquad (2.15)$$

where, in equations 2.12 through 2.15, L is the outside exterior girder span length in feet, S is the girder spacing in feet, and R is the radius of curvature of the outside exterior girder in feet. The maximum live load flange stress is obtained by multiplying the distribution factor with the maximum stress based on grid analysis.

2.2.2.2.3 AASHTO with V-Load Modification Method

To equilibrate the torsional couple on the cross bracing, vertical shear forces (V) are developed at each end of the cross bracing as a result of cross-frame rigidity and fixity (Figure 2.11). These shear forces then react on the girders resulting in a set of self-equilibrating girder shears. The net effect of the shears is to shift the total load on the curved bridge toward the outside girder. These girder shears, which are applied as the external loads to the equivalent straight structure to account for the curvature, are known as the V- loads. Application of the external V-loads ensures that the internal forces in the

straight structure be nearly the same as those that exist in the curved structure under applied vertical loads. In the V-Load analysis of a system, the bending moments caused by the applied vertical loads at the cross bracings in each isolated developed straight girder are first determined by applying the loads to straight girders. These vertical-bending moments will hereafter be referred to as primary moments. The corresponding V-load moments, which are caused by the V-load and are referred to as secondary moment, are then determined by applying the V- loads in the proper directions to the straight girders at the cross bracings. The final moment in the curved girder are then obtained by simply summing the respective straight-girder primary and secondary moments.

The V-load is calculated by (Grubb, 1984):

$$V = \sum M_p/(C \times K) \qquad (2.16)$$

Where

$\sum M_p$ = summation of the primary moments in each girder at a particular cross bracing,

C =coefficient depending on the number of girder in the system (see Table 2.1),

$K = (R \times D)/S_d$, R and S_d are for the outside girder

Where R = radius of curvature in feet,

S_d = diaphragm spacing, and

D = girder spacing.

The distribution factor can then be calculated as:

$$g_B = \frac{S}{5.5} \times \frac{\text{primary + secondary moment}}{\text{primary moment}} \qquad (2.17)$$

This method is referred to as the AASHTO with modified V-load Method. The results were proved to agree with those from the FEM analysis (Brockenbrough 1986) for exterior girder and to be conservative for the interior girders.

2.2.2.3 Heins and Jin's Method (1984)

Heins and Jin (1984) studied the effect of cross bracing spacing on curved bridge distribution factors and found the following relationship:

$$g = \frac{S}{5.5}\left[0.0083\frac{Sc}{S}\frac{L^2}{R} + 1.0\right] \qquad (2.18)$$

Where S_c is the cross bracing spacing in feet.

This factor differs from the traditional factor in that it includes the effect of the warping stresses. With warping included, the cross bracing is important and the relationship in Equation 2.18 shows good agreement with Brockenbrough's Study.

2.2.2.4 Brockenbrough's study (1986)

Brockenbrough (1986) studied the effects of various parameters on load distribution for only four girder-curved bridges using FEM. He found that (1) the central angle per span including the combined effect of curvature and span length has larger effect; (2) girder spacing has larger effect; (3) cross bracing spacing has negligible effect; and (4) girder stiffness has relatively small effect on distribution factor. Brockenbrough also provided charts depicting the variation of the distribution factors with the variation of the parameters. These findings and the charts are valuable to examine load distribution factors in curved bridges. However, the charts are inconvenient to use in practice

2.2.2.5 Yoo and Littrell's Study (1986)

The response of a system of horizontally curved girders connected by a slab and cross-bracings was evaluated (Yoo and Littrell, 1985), using the finite-element method, for dead and line loads. In investigating the effects of radius, length, and number of braced intervals on curved system, empirical design equations were developed to predict the ratio of: (1) Maximum bending stress; (2) Maximum warping stress; (3) Maximum deck deflection for a curved bridge to corresponding parameters of a straight bridge of equal length. It was observed that maximum bending stress and maximum deck deflections stabilized with minimal bracing but warping stresses were sensitive to the number of braced intervals. Therefore, an equation based on a combination of dead and live loads was chosen to limit allowable bracing spacing.

2.2.2.6 Davidson, Keller, and Yoo's Study (1996)

Davidson et al. (1996) used the finite-element method to create detailed models of horizontally curved steel I-girder bridges connected by cross-bracings. In investigating the effects of different parameters on curved system, it was concluded that span length, radius of curvature, flange width, and cross-bracing spacing have the greatest effect on the warping-to-bending stress ratio. Based on this information, a regression analysis was performed to predict the effect of these parameters on the warping-to-bending stress ratio. An equation was developed from this regression analysis and proposed for preliminary cross-frame spacing design as follows:

$$S_{max} = L \left[- \ln \left(\frac{Rb_f}{2000L^2} \right) \right]^{-1.52} \qquad (2.19)$$

where S_{max} is the maximum bracing spacing in m, L is the span length in m, R is the radius of curvature in m, and b_f is the flange width in mm.

2.2.2.7 Schelling, Namini, Fu's Study (1989)

The moment distribution factors for dead load at construction phase, considering the significance of the spacing of cross-bracing and the presence of horizontal bracings connecting the steel flanges, were obtained (Schelling et al, 1989) for two-girder, four, and six girders. Imperial equations were developed to determine the stresses in the lateral bracing system due to construction loads. The drawback of these equations is that it can be used in conjunction with the results given by the two-dimensional grid analysis method. Also, the range of bridge spans considered in this study (36 m to 90) in not practical for slab-on-steel I-girder bridges.

2.2.2.8 Sennah, Eissa, and Lee's Study (2000)

In investigating the effect of different parameters on composite concrete deck-steel I-girder bridges when shoring is not used at construction phase, Sennah et al. (2000) constructed a finite-element model capable of capturing the response after pouring, and before hardening of, the concrete deck slab. It was concluded that span length, radius of curvature, number of girders, and girder spacing have significant effect on the longitudinal bending moments carried by each steel girder. Empirical expressions were proposed for computing the moment distribution factors carried by outer, central, and inner steel girders due to construction loads.

2.2.2.9 Zhang's study (2002)

The load distribution factors for curved steel I girder bridges were studied by Zhang, 2002, using the finite-element method, when subjected to AASHTO truck loading. The parameters considered in the study were:

Radius of curvature: 45 to 450 m;

Girder spacing: 1.8 to 5.0 m;

Span length: 15 to 70 m;

Slab thickness: 170 to 300 mm;

Longitudinal stiffness: 32122 to 72226 cm^4;

Torsional inertia: 772 to 3850 cm^4;

Number of girders: 3 to 7;

Distance from centre of exterior girder and inside edge of traffic barrier: 0.3 to 1.5 m;

Cross frame spacing: 2 to 7 m;

Ratio of girder stiffness to overall bridge stiffness: 0.1492 to 0.3882.

The study showed that radius of curvature, girder spacing, and distance from centre of exterior girder and inside edge of traffic barrier, number of girders or ratio of girder stiffness to overall bridge stiffness had significant effect on the load distribution. Span length, slab thickness, and longitudinal stiffness had slight effect. Effect of cross-bracing spacing and girder torsional inertia could be neglected. Simplified formulas for positive moment, negative moment, and shear distribution factors for inside and outside exterior girders due to one-lane loading and multiple-lane loading were developed. It was found that the distribution factors of outside exterior girder positive moment obtained

from AASHTO *Guide Commentary* method (1993) for multiple-lane loading were less conservative compared with the results of FEM analysis. However, the results obtained from AASHTO *Guide Commentary* were too conservative for other cases. AASHTO-LRFD formulas for straight bridges led to either larger or smaller results when used for curved bridges. The Heins and Jin's formula was too conservative for all cases. The proposed formulas are recommended for preliminary design of curved steel I-girder bridges. Since the formulas were calibrated by limited amount of real bridges, the formulas would be most accurate when applied to bridges with similar restraints. For bridges beyond these application ranges or special cases, detailed analysis is recommended for more accurate results.

2.3 Review of Linear Elastic Behaviour of Curved I- Girder System

The behavior of thin-walled members of open cross-section under flexure and torsion has been established for a long time and has been reviewed in many books on elementary mechanics. A recent comprehensive presentation of the basic theory of thin-walled beams, including flexure, torsion, distortion, and stress distribution, can be found in "*Analysis and Design of Curved Steel Bridges*" (Nakai and Yoo, 1988). In curved bridge, the curvature makes the cross bracings (or diaphragms) the primary members to resist torsional loads, which are of importance for curved bridge stability. Correspondingly, cross bracings introduce restoring torques to the girders and therefore cause nonuniform torsions in the girders. The torsions are resisted in part by St.-Venant torsion and in part by warping torsion. The warping causes *lateral bending moment* of the top and bottom flanges. The product of the lateral flange moment and lever arm of the

couple (less than girder depth) is often referred to as bimoment (in the unit of force x length^2). This bimoment causes twisting of the curved girders about their longitudinal axes. For compression flange, the axial flange force tends to accentuate curvature while the lateral flange bending moment tends to reduce it. However, the net effect is always to increase curvature of the compression flange. For tension flange, the axial force tends to reduce the curvature and the lateral flange bending moment tends to increase it. The net effect can be either to increase or decrease the curvature of the tension flange, depending on flange stress and stiffness.

Two approximate methods: AASHTO *Guide* (1993) and V-load method presented below, can be used to estimate the flange lateral bending moment, M_{LAT}

1) AASHTO Guide (1993) method

$$M_{LAT} = M_S \times DF_B \times DF_{Bi} \times \left[\frac{(0.35\,L - 15)}{0.108L - 1.68} \times \frac{L}{DR} \right] \Big/ D' \qquad (2.20)$$

Where Ms is the equivalent straight girder moment due to truck load, which straight girder will have a length equal to the arc length of the curved girder; DF_B is the distribution factor for bending moment; DF_{Bi} is the distribution factor for bimoment; D is the girder depth in feet; R is the radius of curvature in feet; L is the span length in feet; and D' is the arm from the centroid of girder top flange to the centroid of girder bottom flange in feet.

This equation should satisfy that the radius of curvature is greater than 30.5m.

2) V-Load Method

$$M_{LAT} = M_V \times \left[\frac{L^2_{UN}}{10\,DR} \right] \qquad (2.21)$$

Where M_V is the vertical moment of curved girder, and L_{UN} is the unbraced length. The exact solution of lateral flange moment is discussed in the following sections.

From the classic strength of material theory, St.-Venant torque, T_P, is commonly expressed in terms of the torsional rotation, Ø at any cross section as

$$T_P = GJ\frac{d\text{Ø}}{dx} \tag{2.22}$$

Where GJ is the St. Venant torsion rigidity; G is the elastic modulus in shear; x is measured along the member.

From warping theory, the warping torque, T_w, can be expressed as:

$$T_w = Vh \tag{2.23}$$

Where V is the lateral shearing force in the flanges as shown in Figure 2.12; and h is the distance from the top flange-shearing center to the bottom flange-shearing center. The equation of equilibrium for torsion of a thin-walled member is then

$$GJ\frac{d\text{Ø}}{dx} + Vh = T \tag{2.24}$$

Where T is the total torsion at the cross section.

From the elastic curve equation, lateral bending moment in the lateral direction of the upper flange in Figure 2.12 is

$$\frac{EI_y}{2}\frac{d^2y}{dx^2} = -M \tag{2.25}$$

in which the X and Y axes are chosen with positive directions as shown in Figure 2.12; M is the lateral bending moment in the flange at any section producing lateral bending in the flange ; E is the modulus of elasticity ; and I_y is the moment of inertia of the entire cross section of the beam with respect to the axis of symmetry in the web so that ½ I_y closely

approximate the value of the moment of inertia of a flange cross section. In Figure 2.12, the deflection of the flange at section *AB* is

$$y = (h/2)\,\emptyset \tag{2.26}$$

Differentiation of Equation 2.26 twice with respect to x gives

$$\frac{d^2 y}{dx^2} = \frac{h\, d^2 \emptyset}{2\, dx^2} \tag{2.27}$$

Substituting this value of d^2y/dx^2 into Equation 2.22 gives

$$\frac{EI_y\, h\, d^2 \emptyset}{4\quad dx^2} = -\,M \tag{2.28}$$

Since dM / dx = V by differentiating both sides of Equation 2.27 with respect to x we obtain

$$\frac{EI_y\ hd^3 \emptyset}{4\quad dx^3} = -\,V \tag{2.29}$$

Substituting the value of V in Equation 2.29 into Equation 2.24, which then becomes

$$JG\frac{d\emptyset}{dx} - \frac{EI_y\, h^2\ d^3 \emptyset}{4\quad dx^3} = T \tag{2.30}$$

Let $I_w = EI_y h^2\ /4$, the warping torque can be written as

$$T_w = -\,EI_w \frac{d^3 \emptyset}{dx^3} \tag{2.31}$$

And Equation 2.30 can be rewritten as

$$EI_w \frac{d^4 \emptyset}{dx^4} - GJ\frac{d^2 \emptyset}{dx^2} = t \tag{2.32}$$

Where t is the distributed torque applied to the member; and EI_w is warping rigidity. Equation 2.32 along with two boundary conditions at each end can be used to describe the behavior of a thin-walled member subject to torsion. The boundary conditions at each end may be the rotation Ø and warping dØ/dx.

2.4 Review of Methods of Analysis for Curved System

In the literature, six major methodologies have been applied in curved bridge analysis as shown in the following subsections.

2.4.1 The V-Load method (Grubb 1984)

The V-Load method is a simplified approximate analysis method for curved open girder bridges. It can be considered as a two-step process. First, equivalent straight girders with span lengths equal to the arc lengths instead of the individual curved girders are used so that the applied vertical loads are assumed to induce only longitudinal girder stresses. Next, self-equilibrating external vertical shear forces (acting on diaphragm location) are applied to the straight structure so that the resulting internal forces are the same as those that exist in the curved structure subjected to only vertical load (refer to Figure 2.11). Thus, in the V-Load development, the curvature forces on the equivalent straight structure are treated as externally applied load. These loads are dependent on the radius of curvature, the bridge width, and diaphragm spacing (refer to Equation 2.16). The V-load method was found suitable for approximate analysis of composite sections, variable radius of curvature, and skewed supports. The effects of bracing in the plane of the bottom flange are not considered. The dead load results obtained from the V-load method were proved to be very close to those obtained from the FEM analysis. For live

load, the lateral load distribution factor used in the V-load analysis has a significant influence on the results.

2.4.2 Finite Strip Method (FSM)

This approach divides the curved bridge into many narrow strips in the circumferential direction that are supported in their radial direction. Bending, membrane action, warping, and distortional effect, are considered in the analysis. This method has been successfully used to analyze composite curved box/plate girders with complete and incomplete interaction using curved strip elements for the concrete slab and steel girder and spring elements for the shear connectors (Arizumi al et. 1982). Since only one single variable in the circumferential direction is considered in the function, the analysis requires smaller number of unknowns and provides some simplicity and economy over FEM. It is difficult to apply this method for continuous bridges with diaphragms since it lacks flexibility and versatility

2.4.3 Finite Difference Method

In this method, a grid is superimposed on the structure and the governing differential equations are replaced by algebraic difference equations that are solved for each grid point. This method was used in dynamic analysis for curved bridges with large deflections and small rotations (Tene al et. 1975; Sheinman 1982).

2.4.4 Analytical Solution to Differential Equations

An analytical solution to the Governing Differential Equations (GDE) is obtained in the method. The solution is usually a closed form or a convergent series solution, such as a Fourier series. This method was used in studying curved bridge dynamic response (Culver 1969; Montalvao e Silva and Urgueira 1988).

2.4.5 Slope Deflection Method

The partial differential equations are established in terms of slope-deflection equations, and the solution is assumed to be a Fourier series. The analysis includes the effects of curvature, nonuniform torsion, and diaphragms. The COBRA (Curved Orthotropic Bridge Analysis) program (Bell and Heins 1969), developed at the University of Maryland, is based on analytical techniques of the slop-deflection Fourier series and is recommended by the current AASHTO *Guide* Specifications of 1993 to study composite or noncomposite girder-slab action. This method was proved by experiment to be an accurate analytical method of curved orthotropic deck bridge systems (Heins and Bell 1972).

2.4.6 Finite Element Method (FEM)

This numerical method discretizes the structure into small divisions, or elements, where each element is defined by a specified number of nodes. The behavior of each element, and ultimately the structure, is assumed to be a function of its nodal quantities (displacements), which serve as the primary unknowns in the formula. This is one of the most general and accurate methods to use, since it does not put any limitation on the geometry, loads, or boundary conditions. This method can be applied to any shape of girders

for static or dynamic analysis. Also, the structure's response can always be improved by refining the mesh. Two major categories of the finite element models can be classified: approximate and refined methods. Approximate methods require a minimal modeling effort on part of the designer, and therefore, are adequate for preliminary analysis and design purpose. Plane grid and space frame are the most frequently used approximate methods. Refined methods, on the other hand, are somewhat more elaborate, computationally intensive, and time-consuming terms of modeling. Refined methods usually are used for final or detailed analysis. Three-dimensional plate/shell is the most frequently used element.

2.4.6.1 Plane-Grid or Grillage Approach

This method models the structure as an assemblage of one-dimensional grid members with four degrees of freedom (DOF) at each node. In a curved steel I-grid bridge system, the two translational displacements in the plane of curvature of the bridge and the rotational displacement about the axis perpendicular to the plane of curvature are small compared to the out-of plane displacements and thus may be neglected. This is the basic assumption of grillage method, which assumes four DOF at each node, including a warping degree of freedom. The CURVBRG computer program (Mondkar and Powell 1974), developed by University of California at Berkeley, and the CUGAR2 computer programs (Lavelle at el. 1971; Lavelle and Lasks 1975a,b), developed at the University of Rhode Island, were proved to be very accurate in analyzing curved bridges and are recommended by the current *Guide* Specifications. Plane grid model is considered the most appropriate approach for practical analysis of open girder bridges. A major advantage of plane grid analysis is that shear and moment values of girders are directly obtained and integration of

stresses is not needed. When loads are applied between nodal points, the simple beam theory can be used to distribute wheel loads to adjacent nodes. With a plane grid idealization, the computer running time is reasonably short and only moderate effort is required for modeling. The disadvantages are: a) the method is nonrigorous and does not exactly converge to the exact solution of the mathematical model; b) obtaining good solutions requires some experience with the grillage method; and c) the assignment of the cross section properties requires some discretion.

2.4.6.2 Space–Frame Approach

This method idealized the curved members as three-dimensional straight members, while the diaphragms and lateral bracing are assumed as truss members that can carry only axial loads. The Three-Dimensional Analysis program (Brennan and Mandel 1973) developed at Syracuse University is recommended for this type of analysis by the current *Guide* Specifications.

2.4.6.3 Three-Dimensional plate/shell Approach

The STACRB (Shore and Wilson 1973) computer program developed at the University of Pennsylvania is characterized by a fully compatible three-dimensional flat plate circular element. A lot of different elements and shape functions have been studied since then, including using segmental and quadrilateral element for plate bending, annular conforming and fully compatible four-noded segment element for thin plates, horizontally curved three-noded isoparametric beam element, three-dimensional beam element with axial and transverse displacements or arbitrary polynomial order, and so on. General finite

element packages, such as ABAQUS, ADINA, ALGOR, SAP, ANASYS and MSC/NASTRAN are also frequently used for curved bridges. The high-speed and capacity computer allows three-dimensional modeling to be possible. The bridge deck is usually modeled as shell element, including membrane and bending effects. Girder flanges are usually modeled as beam elements to include axial and bending strains in two directions and torsional effects. Girder web can be modeled as shell element to account for the bending stiffness. Rigid beams are usually used to connect the deck slab to girder flange and simulate the composite action with slab. Cross bracings and wind bracings can be modeled as hinged bar element.

Three-dimensional plate/shell models can consider unusual geometry and complex configuration and can get the most accurate results. The disadvantages are: a) since most of the programs do not allow loads to be placed at any point on the elements, equivalent nodal loads must be calculated with care and the mesh must be fine enough to minimize errors that may arise because of load approximations; b) since the programs report stresses and strains other than shear and moment values, calculation of shear and moment values from the stresses must be carefully performed through integration over the beam section, and c) integration of stresses at node points is normally less accurate and may lead to inaccurate results.

CHAPTER III

FINITE-ELEMENT ANALYSIS

3.1 General

The Canadian Highway Bridge Design Code (CHBDC 2000) permits the use of six different refined methods of analysis for short and medium span bridges. The finite element method is one of the methods recognized by the CHBDC. It is also considered to be the most powerful, and versatile of all the six permitted methods. The most important advantages of the finite element method include:

1- It permits the combination of various structural elements such as plates, beams, and shells.

2- It is able to analyze structures having arbitrary geometries with any material variations .

Therefore, the finite-element method is very suitable for the analysis of curved composite I-girder bridges. Because of recent development in computers, it is now possible to model a bridge in a very realistic manner and to provide a full description of its structural response within the elastic and post-plastic stages of loading, using the finite-element method.

This chapter includes descriptions of modeling the different components of the composite I-girder bridges. The finite-element model includes the reinforced concrete deck slab, top steel flanges, steel webs, bottom steel flange, and the cross-bracings as described in subsequent sections in this chapter. The finite-element program, SAP2000,

was used throughout this study to examine the structural behaviour. A general description of this program is presented later in this chapter. This chapter also explains the procedure to conduct an extensive parametric study on selected straight and curved bridge prototypes to study their load distribution characteristics.

The simple presence of curvature in curved girders causes nonuniform torsion and consequently, lateral bending moment (warping or biomoment) in the flanges of the girder must be considered, which greatly complicates the analysis and design of the structure. Torque can be neglected in straight girders, whereas it plays an important part in curved bridge stability. At the end of this chapter, the methodology to obtain the warping-to-bending stress ratio for the bridges considered in this study is presented.

3.2 Finite-Element Approach

The finite-element method is a numerical method for solving problems in engineering and mathematical physics. In structural problems, the solution is typically concerned with determining stresses and displacements and will yield approximate values of the unknowns at discrete number of points in a continuum. This numerical method of analysis starts by discretizing a model. Discretization is the process where a body is divided into an equivalent system of smaller bodies or sub-regions (elements) interconnected at points (nodes) common to two or more elements and/or boundary lines and/or surfaces. These sub-regions can be in the form of line elements, planar two-dimensional triangular, quadrilateral shaped elements, or three-dimensional solid shaped elements. An equation is then formulated combining all the elements to obtain a solution for one whole body. Using a displacement formulation, the stiffness matrix of each element is derived and the global

stiffness matrix of the entire structure can be formulated by the direct stiffness method. This global stiffness matrix, along with the given displacement boundary conditions and applied loads, is then solved, thus that the displacements and stresses for the entire system are determined. The global stiffness matrix represents the nodal force-displacement relationships and is expressed in a matrix equation form as follows:

$$[P] = [K][U] \tag{3.1}$$

where:

[P] = nodal load vector;

[K] = the global stiffness matrix;

[U] = the nodal displacement vector;

The steps for deriving the above equation can be summarized in the following basic relationships:

(a) $$\upsilon(x, y) = [\Phi(x, y)][\alpha] \tag{3.2}$$

where:

υ= the internal displacement vector of the element.

Φ= the displacement function.

α= the generalized coordinates.

(b) $$[U] = [A][\alpha] \quad \text{then, } [\alpha] = [A]^{-1}[U] \tag{3.3}$$

where [A] is the transformation matrix from local to global coordinates,

(c) $$[\varepsilon(x, y)] = [B(x, y)][\alpha] = [B(x, y)][A]^{-1}[U] \tag{3.4}$$

where:

[B(x,y)]= the strain-displacement matrix.

[ε(x,y)]= the strain matrix.

(d) $$[\sigma(x,y)] = [D][\varepsilon(x,y)] = [D][B(x,y)][A]^{-1}[U] \quad (3.5)$$

where; [D] is the constitutive matrix or the elasticity matrix. From the principle of minimization of the local potential energy for the total external work equal to 1/2 $[U]^T[P]$, then

(e) (i) $$W_E = [u']^T [P]$$

(ii) $$W_I = \int_{vol.} [\bar{\varepsilon}]^T [\sigma] = [u']^T [A]^{-1} [k'][A]^{-1} [U] \quad (3.6)$$

where:

W_E = the external virtual work;

W_I = the internal virtual work;

[u'] = the vector of virtual displacement;

[k'] = the element stiffness matrix.

where $$[k'] = \int_{vol.} [B(x,y)]^T [D][B(x,y)] \quad (3.7)$$

(f) From the principle of virtual work, $W_E = W_I$. By taking one element of virtual nodal

$$[P] = [K][U] \quad (3.8)$$

displacement vector [u'] equal to unity successfully, the solution becomes:

(g) The solution of the resulting system of equations yields the values of nodal displacement [U] and the internal forces for each element can be obtained from equation (3.4).

3.4 SAP2000 Computer Program

SAP2000 (Wilson, and Habibullah, 1999) is a structural analysis program that employs the finite-element method and has a range of capabilities depending on the version used. SAP2000 is also capable of analyzing structures in static and/or dynamic modes. Its finite-element library consists of six elements.

1- Three-dimensional FRAME element.

2- Three-dimensional SHELL element

3- Two-dimensional PLANE element

4- Two-dimensional SOLID element

5- Three-dimensional SOLID element

6- Three- dimensional NLLINK element

In addition, subsets of these elements with varying degrees of freedom are available in the form of truss, frame, membrane, beam, strain, gap, and hook elements.

3.5 CHBDC Specifications For Truck Loading

The critical live load for the design of highway bridges in Canada consists of a specified truck and lane load. The live load specified in the new Canadian Highway Bridge Design Code (CHBDC, 2000) was utilized in this study. Figure 3.1 shows a view of CL-W truck loading as well as the CL-W lane load. The CL-W truck is an idealized five-axle truck. The number "W" indicates the gross load of the CL-W truck in KN. Wheel and axle loads are shown in terms of W, and are also shown specifically for CL-625 truck. The CL-W lane load consists of CL-W truck, with each axle load reduced to 80% of the value, superimposed within a uniformly distributed load of 9 KN/m, that is

3.0 m wide. Three different CHBDC truck loading configurations were considered, namely: Level 1, Level 2, and Level 3 truck, Figure 3.2 shows the configurations of each of these load levels. The Level 1: truck was used for bridges with span of 15 m, while Level 2 : truck was considered in case of 25-m-span bridges. Level 3: truck was applied to bridges of 35-m span. In studying the moment and deflection distributions, the loading on the bridge prototype was applied in such a way to produce maximum mid-span longitudinal stresses.

3.6 Loading Conditions

Considerations were given to the effects of highway truck loads and bridge dead loads on the distribution of loads among girders. CHBDC specifies both the CL-625 truck load and CL-625 lane loading in bridge design, whichever gives the greatest design values. A sensitivity study on this regard showed that the CL-625 truck- load provides the design bending moment for a single girder of 15, 25 or 35 m span. As a result, the CL-625 lane loading was not considered in this study. The design of bridge superstructure based on the CHBDC is characterized by three limit states, namely: (i) the ultimate limit state, (i) the serviceability limit state, and (iii) the fatigue limit state. As such, loading conditions considered herein include dead load case and truck loading case for each of the three limit states of design. According to CHBDC, for the fatigue limit state, the traffic load shall be one truck, placed at centre of one travelled lane. Since the bridge configurations considered in this study include one-lane, two-lane, three-lane and four-lane bridges, four different sets of loading cases were considered in this study. Figures 3.3, 3.4, 3.5 and 3.6 show schematic diagrams of the loading cases considered for flexural

design of the exterior girder, internal girder and middle girders. It should be noted that the exterior girder here is the one far away from the centre of curvature and the internal girder is the closest girder to the centre of curvature.

As an example of the loading cases, the diagrams shown in Figure 3.8 will be explained herein. Loading case (1) was always the dead load of the structure. For the exterior girder, two truck loading cases were considered. Load case (2) included a truck load located in the outer lane far away from the centre of curvature, on which the outer wheel load was located 0.6 m from the barrier. Load case (3) included two trucks one in each lane with the outer wheel load located 0.6 m from the barrier for the first truck and 0.6 m from the outer edge of the inner lane for the second truck. Load case (4) was intended to provide the maximum load on the middle girder, which is at or very close to the centroid of the bridge cross-section. In this case one truck was considered in each lane and located as shown in Figure 3.4. Load case (5) was intended to provide the maximum moment in the internal girder. It was similar to load case (2) for the exterior girder. Load cases (6) and (7) were intended to provide the maximum moment in the girders for fatigue design. In this case, CDBHC specifies only a truck load located at the centre of the actual lane.

3.7 I-Girder Bridge Configurations

192 bridge configurations were considered for finite-element analysis in the parametric study. The span lengths (L) of the bridges were taken 15, 25, and 35 m. The spacing of the girders (S) was taken as 2, 2.5, and 3 m. The number of girders (N) was

considered as 7, 6, 5, 4, 3 for girder spacing of 2 m; 6, 5, 4, 3 for girder spacing of 2.5 m, and 5, 4, 3 for girder spacing of 3 m. The decision to choose these numbers of girders was based on the range of bridge width for number of lanes ranging from 1 to 4 as specified in the CHBDC (see table 3.1). For 15-m-span bridges, the span-to-radius of curvature ratio (L/R) was taken 0, 0.1, 0.2, and 0.3. While for 25-m-span bridges, it was taken as 0, 0.1, 0.3, and 0.5. For 35m span bridges, L/R was considered as 0, 0.1, 0.4, and 0.7. The overhang slab length was taken half of the girder spacing. The thickness of the deck slab was taken as 225 mm. The width of the deck (W_c) was taken equal to the bridge width minus 1 m to allow for two parapets of 0.50 m thickness on each side of the bridge. The depth of the girder webs was taken 1/20 of the centre line span and their thickness was 16mm. The width of the bottom and top steel flanges were taken 300 mm, with 20 mm thickness. Figure 3.7 shows details of the typical steel girder cross-section dimensions used in this study.

According to CHBDC, deck widths, ranging between 10 and 13.5 m, should be designed for both 2 and 3 design lane configurations. Table 3.1 shows details of bridge cross-section dimensions and the associated number of design lanes per the CHBDC specifications. Figures 3.7 shows typical cross-section of the composite I-girder bridge with exterior girder far away from the centre of curvature and internal girder, the closest to the center of curvature. X-type bracings with top and bottom chords were considered at equal intervals between the support lines and were made of single angles (L150x150x25mm) of 0.0075 m^2 cross–sectional area. They were typically spaced at intervals based on equation 2.19, developed by Davidson et al. (1996). It should be noted

that this equation was developed to limit the warping-to-bending stress ratio to 0.25 in case of noncomposite steel girders subjected to construction loads. Figure 3.8 shows typical plan of a straight bridge with transverse bracings and a curved bridge with radial bracings. The shear connecters were considered of M22 studs.

The study was based on the following assumptions:

1. the reinforced concrete slab deck had complete composite action with the top steel flange of the girders (100% shear interaction);
2. the bridges were simply-supported;
3. all materials were elastic and homogenous;
4. the effect of road superelevation, and curbs were ignored;
5. bridges had constant radii of curvature between support lines.

The modulus of elasticity of concrete material was taken 28 GPa with Poisson's ratio of 0.20 while they were 200 GPa and 0.30, respectively, for steel material.

3.8 Finite-Element Modeling of Composite I-Girder Bridges

3.8.1 Geometric Modeling

A three-dimensional finite-element model was used to analyze all composite bridges included. The structure was divided into a concrete deck slab, steel top flanges, steel webs, steel bottom flange and cross bracing. Concrete slab bridges, upper flanges, lower flanges and webs were modeled using four-node shell elements with six degrees of freedom at each node. Cross bracings with top and bottom chords were modeled as frame elements, pinned at both ends. Based on previous work on finite element modeling, four vertical elements were used in each web, four elements between webs were used

horizontally for the concrete slab; two elements were used horizontally for the overhang slab; and for the upper and lower steel flanges. 72 elements in the longitudinal direction were considered. One row of shell elements of 0.000774 m thickness was considered to simulate composite action between the deck and upper flange. Figure 3.9 shows a finite element discretization of a four-girder cross-section. Figure 3.10a shows view of the SAP2000 finite-element model of a curved bridge with the concrete deck slab. While Figure 3.10b shows a similar view but without the concrete deck slab.

To simulate and verify the full composite action between the deck, and upper flange, a sensitivity study on one of the bridges described in Table 3.1 was performed. A straight bridge of 35-m span, with number of girders, N, equal to 7, and girder spacing, S, equal to 2 m, was analyzed in this study. Then, a 2000 KN concentrated load per girder, was applied at the mid-span of the seven girders. The bridge was first analysed, using the finite-element method, for a case representing the M22 studs of 0.5 m spacing as frame elements and for a case representing the M22 studs as shell element with the equivalent area,(Appendix E). The results, that were verified manually using the flexural beam theory, showed the same mid-span stresses, 640,000 KN/m^2, in the bottom steel flange fibres for all girders in both modeling configurations. While the mid-span deflection of the girders when modeling the studs as frame element (0.197 m) was less than the corresponding deflection when modeling the studs as shell elements (0.235 m). However, the latter agrees with the manual calculation of deflection using the flexural beam theory.

3.8.2 Boundary Conditions

In modelling bridge support conditions, the lower nodes of the web at its two ends were restrained against translation to simulate temperature-free bridge superstructure. The most-internal support point, close to the centre of curvature, at the left end of the bridge, was restrained from moving in all directions, while the most-internal support point at the right end of the bridge was restrained from moving vertically and in the transverse direction of the bridge or normal to the chord line passing between the left and the right end of the bridge. All other support points were restrained in the vertical direction only. Samples of the resulting input files are given in Appendices A and B. The individual steps involved in creating input data files are outlined in the SAP2000 Users Manual (Wilson and Habibullah).

3.9 Calculation of the Moment Distribution Factors

In order to determine the moment distribution factor (MDF) for curved girder, the maximum flexural stresses, $(\sigma_{simple})_{truck}$, $(\sigma_{simple})_{DL}$, were calculated for a straight simply supported beam subjected to CHBDC truck loading, and dead loads, respectively. To calculate the moment of inertia of the idealized girder, the effective concrete slab width, B_e was calculated based on the following two equations specified in the CHBDC of 2000:

$$\frac{Be}{B} = 1 - \left[1 - \frac{L}{15B}\right]^3, \qquad \text{for } \frac{L}{B} \leq 15 \tag{3.9}$$

$$\frac{Be}{B} = 1, \qquad \text{for } \frac{L}{B} > 15 \tag{3.10}$$

where B is the clear spacing between girders = (S – $2b_f$) ; b_f is the steel flange width; L is the span of the girder; and S is the girder spacing.

The following flexural formula was used to calculate the flexural stress of the idealized girder due to line load truck:

$$(\sigma_{simple})_{truck} = M_{T\,(y_b)} / I_t \qquad (3.11)$$

where M_T = the mid-span moment for a straight simply supported girder subject to CHBDC truck loading.

y_b = the distance from the neutral axis to the bottom flange.

$I_{(t)}$ = the moment of transformed moment of inertia of the composite girder.

For flexure stress of the idealized girder due to dead load, the following flexural stress equation was used.

$$(\sigma_{simple})_{DL} = M_{DL\,(y_b)} / I_t \qquad (3.12)$$

where M_{DL} = the mid-span moment for a straight simply supported girder subject to dead load.

Results of these calculations are shown in Appendix C and then verified by SAP2000 software. The span of the straight simply supported girder is taken as the curved length of the bridge centreline. From the finite-element modeling, the maximum longitudinal stresses along the bottom flange for fully loaded lanes, partially loaded lanes, fatigue loading case, and dead load; were determined. Then, the moment distribution factors, MDF, were calculated from the following relationships for the exterior, interior and middle girders as follows:-

For exterior girders:

$$(MDF)_{DL\,ext} = (\sigma_E)_{DL} / (\sigma_{simple})_{DL} \qquad (3.13)$$

$$(MDF)_{FL\ ext} = (\sigma_E)_{FL} \times N/(\sigma_{simple})_{truck} \times n \quad (3.14)$$

$$(MDF)_{PL\ ext} = (\sigma_E)_{PL} \times N/(\sigma_{simple})_{truck} \times n \times R_L/R'_L \quad (3.15)$$

$$(MDF)_{Fat.ext} = (\sigma_E)_{Fat} \times N/(\sigma_{simple})_{truck} \quad (3.16)$$

For middle girders:

$$(MDF)_{DL\ mid} = (\sigma_M)_{DL} / (\sigma_{simple})_{DL} \quad (3.17)$$

$$(MDF)_{FL\ mid} = (\sigma_M)_{FL} \times N/(\sigma_{simple})_{truck} \times n \quad (3.18)$$

$$(MDF)_{Fat.mid} = (\sigma_M)_{Fat} \times N/(\sigma_{simple})_{truck} \quad (3.19)$$

For interior girders:

$$(MDF)_{DL\ int} = (\sigma_I)_{DL} / (\sigma_{simple})_{DL} \quad (3.20)$$

$$(MDF)_{FL\ int} = (\sigma_I)_{FL} \times N/(\sigma_{simple})_{truck} \times n \quad (3.21)$$

$$(MDF)_{PL\ int} = (\sigma_I)_{PL} \times N/(\sigma_{simple})_{truck} \times n \times R_L/R'_L \quad (3.22)$$

$$(MDF)_{Fat.int} = (\sigma_I)_{Fat} \times N/(\sigma_{simple})_{truck} \quad (3.23)$$

where $(\sigma_E)_{DL}$, $(\sigma_M)_{DL}$ and $(\sigma_I)_{DL}$ are the mid-span stresses which is the greater at points 1 and 3, shown in Figure 3.11, for the exterior, middle, and interior girders, respectively, for the dead load case;

$(\sigma_E)_{FL}$, $(\sigma_M)_{FL}$ and $(\sigma_I)_{FL}$ are the mid-span stresses which is the greater at points 1 and 3 for the exterior, middle, and interior girders, respectively, considering fully loaded lanes;

$(\sigma_E)_{PL}$, and $(\sigma_I)_{PL}$ are the mid-span stresses which is the greater at points 1 and 3 for the exterior, and interior girders, respectively, considering partially loaded lanes;

$(\sigma_E)_{Fat}$, $(\sigma_M)_{Fat}$ and $(\sigma_I)_{Fat}$ are the mid-span stresses which is the greater at points 1 and 3 for the exterior, middle, and interior girders, respectively, considering the fatigue loading case.

n: number of design lanes, as listed in table 3.2;

R_L : multi-lane factor based on the number of the design lanes, as shown in table 3.3;

R'_L : multi-lane factor based on the number of the loaded lanes, as shown in table 3.3;

N : number of girders.

3.10 Calculation of Deflection Distribution Factors

In order to determine the deflection distribution factor (DDF) for curved girder, the mid-span deflection, $(\Delta_{simple})_{truck}$, $(\Delta_{simple})_{DL}$, were calculated for a straight simply supported girder subjected to CHBDC truck loading, and dead loads, respectively. The span of the straight simply supported girder is taken as the curved length of the bridge centreline. The deflection values of the idealized girder due to truck loading and dead load, were calculated using SAP2000 software, and then verified by manual calculations. Results of these calculations are presented in Appendix C. From the finite-element modeling, the mid-span deflection values at the middle of the bottom flange for fully loaded lanes, partially loaded lanes, fatigue-loading case, and dead load, were determined. Then, the deflection distribution factors, (DDF), were calculated from the following relationships, for the exterior, interior and middle girders as follows:-

For exterior girders:

$$(DDF)_{DL\,ext} = (\Delta_{E2})_{DL} / (\Delta_{simple})_{DL} \qquad (3.24)$$

$$(DDF)_{FL\,ext} = (\Delta_{E2})_{FL} \times N/(\Delta_{simple})_{truck} \times n \qquad (3.25)$$

$$(DDF)_{PL\,ext} = (\Delta_{E2})_{PL} \times N/(\Delta_{simple})_{truck} \times n \times R_L / R'_L \qquad (3.26)$$

$$(DDF)_{Fat.ext} = (\Delta_{E2})_{Fat} \times N/(\Delta_{simple})_{truck} \qquad (3.27)$$

For middle girders:

$$(DDF)_{DL\ mid} = (\Delta_{M2})_{DL} / (\Delta_{simple})_{DL} \quad (3.28)$$

$$(DDF)_{FL\ mid} = (\Delta_{M2})_{FL} \times N/(\Delta_{simple})_{truck} \times n \quad (3.29)$$

$$(DDF)_{Fat.mid} = (\Delta_{M2})_{Fat} \times N/(\Delta_{simple})_{truck} \quad (3.30)$$

For interior girders:

$$(DDF)_{DL\ int} = (\Delta_{I2})_{DL} / (\Delta_{simple})_{DL} \quad (3.31)$$

$$(DDF)_{FL\ int} = (\Delta_{I2})_{FL} \times N/(\Delta_{simple})_{truck} \times n \quad (3.32)$$

$$(DDF)_{PL\ int} = (\Delta_{I2})_{PL} \times N/(\Delta_{simple})_{truck} \times n \times R_L / R'_L \quad (3.33)$$

$$(DDF)_{Fat.int} = (\Delta_{I2})_{Fat} \times N/(\Delta_{simple})_{truck} \quad (3.34)$$

Where $(\Delta_{E2})_{DL}$, $(\Delta_{M2})_{DL}$ and $(\Delta_{I2})_{DL}$ are the deflections at point 2, shown in Figure 3.11, for the exterior, middle, and interior girders, respectively, for the dead load case;

$(\Delta_{E2})_{FL}$, $(\Delta_{M2})_{FL}$ and $(\Delta_{I2})_{FL}$ are the mid-span deflections at point 2 for the exterior, middle, and interior girders, respectively, considering fully loaded lanes;

$(\Delta_{E2})_{PL}$, and $(\Delta_{I2})_{PL}$ are the mid-span deflections at point 2 for the exterior, and interior girders, respectively, considering partially loaded lanes;

$(\Delta_{E2})_{Fat}$, $(\Delta_{M2})_{Fat}$ and $(\Delta_{I2})_{Fat}$ are the mid-span deflections at point 2 for the exterior, middle, and interior girders, respectively, considering for the fatigue loading case; while.

R_L, R'_L, N, and n are as defined before

3.11 Warping to-bending stress ratio

It is well established that curved I-girders undergo a coupled lateral-bending moment in the top and bottom flanges due to curvature as shown in Figure 3.12. This lateral moment is called also: "torsional warping moment" or "bimoment", which induces

warping of the girder cross-section. The increase in longitudinal flexural stress in the flange due to this moment is called "warping stress". To examine the change in warping stress with the change in bridge configuration or loading cases, the ratio between warping stress to the average bending stress in the bottom flange is examined herein, and considered as:

$$\mathbf{WBR} = \sigma_w / \sigma_b = \sigma_1 - \sigma_3 / \sigma_3 + \sigma_1 \qquad (3.34)$$

where σ_1 and σ_3 : the corresponding mid-span stresses at points 1 and 3 shown in Figure 3.1; σ_w is the warping stress; and σ_b is the average bending stress in the bottom steel flange.

CHAPTER IV

PARAMETRIC STUDY

4.1 General

This chapter presents the results from the parametric study conducted on 192 simply supported straight and curved concrete slab-on-steel I-girder bridge prototypes, using the finite-element analysis method. The bridge prototypes were analyzed to evaluate their structural response when subjected to dead loading as well as the Canadian Highway Bridge Design truck loading, CHBDC truck. The parametric study included the investigation of the following in simply supported straight and curved slab-on-girder bridges: (i) moment distribution among composite girders; (ii) deflection distribution among composite girders and; (iii) warping distribution in steel flanges. The key parameters considered in this study included span-to-radius of curvature ratio (L/R), span length (L), number of longitudinal girders (N), girder spacing (S), number of cross-bracing intervals between the support lines and loading conditions. Based on the results generated from this parametric study, a simplified design method is proposed for this type of bridges when subjected to dead loading as well as CHBDC truck loading. Thus, the objectives of this parametric study were to:

1. Investigate the influence of major parameters affecting the straining actions of composite I-girder bridges.
2. Generate a database for the maximum longitudinal stresses developed in the bridges due to the bending moment.

4.2 Moment distribution in simply supported curved bridges

4.2.1 Effect of curvature

The results of the current parametric study revealed that curvature of the bridge is one of the most significant parameters affecting the distribution of moments between the longitudinal beams. Figures 4.1 to 4.4 show the change in the moment distribution factor for the exterior girder of two-lane four-girder bridges with the increase of the span-to-radius of curvature ratio (L/R) due to dead load, fully-loaded lanes with truck loading, partially-loaded lanes with truck loading and fatigue loading, respectively. Description of these loading configurations is shown in Figure 3.4. It can be observed that the moment distribution factor for the exterior girder increases with increase in span-to-radius of curvature ratio. For example, the moment distribution factor of 15-m-span bridge increases from 1.0 for L/R = 0 (straight bridge type) to 1.88 for L/R = 0.3. Thus, the exterior girder bending moment increases by 88% as a result of curvature. Also, it can be noticed that the rate of increase of the moment distribution factor generally increases with increase in span length. Figures 4.5 to 4.7 show similar relationships for the middle girder due to dead loading, fully-loaded lanes and fatigue loading. These relationships are similar to those for the exterior girder. Figures 4.8 to 4.11 present the relationships between moment distribution factors for the internal girder, the closest to the center of curvature, due to dead load, fully-loaded lanes with truck loading, partially-loaded lanes with truck loading and fatigue loading, respectively. For 15-m-span bridges, it can be observed that the moment distribution factors for the internal girder increase with increase in span-to-radius of curvature ratio, for dead load case (Figure 4.8), fully-loaded lane case (Figure 4.9) and fatigue loading case (Figure 4.11). However, in the case of partially-loaded lane shown in

Figure 4.10, there is no observed trend with increase in curvature; the moment distribution factor seems fluctuating around the value for straight bridges. The latter observation may not affect the design of such girder since the moment distribution factors obtained from fully-loaded lane case are always more than those obtained form the case of partially-loaded lanes. With the increase of span length from 15 m to 25 m, the trend observed is changed with the increase of curvature. It can be noticed that the moment distribution factor increases with the increase of curvature up to a certain value of L/R, after which the moment distribution factor decreases with the increase in curvature. This may be attributed to the fact that there are two parameters affecting the moment distribution factor, the former is the increase of span-to-radius of curvature ratio and the latter is the decrease of the span length of the interior girder. For low curvature, it appears that the increase in curvature dominates the decrease in span length, but with the increase in curvature, the situation is reversed.

It should be noted that the Canadian Highway Bridge Design Code of 2000 (CHBDC, 2000) states that curved bridges may be treated as straight bridges in structural design if L^2/bR is less or equal 1, where L is the curved span of bridge centre line, b is half the bridge width and R is the radius of curvature. Applying this provision to the curved bridges considered in this study, the limiting value of L/R is 0.33 in case of 15-m span, 0.20 in case of 25-m span and 0.143 in case of 35-m span. Applying these limiting values to Figures 4.1 to 4.11 shows that this specified limiting value underestimates the moment distribution factors for the external, middle and internal girders of curved system of two-lane cross-section. To provide more confidence of this finding, sensitivity study was conducted on different bridge configurations, shown in Table 4.1. This includes

considering number of girders as 3, 4, 5, and 6, number of lanes as 1, 2, 3 and 4 and span lengths as 15, 25 and 35 m. Two cases of loading were considered for the exterior girder, namely: dead load and fully-loaded lanes with truck loading. The limitations provided by other North American codes (AASHTO Guide, 2003; AASHTO-LRFD, 2004) to treat a curved bridge as a straight one in the structural design were also included in the sensitivity study. The AASHTO Guide Specifications for Horizontally Curved Bridges state that a curved bridge can be designed as a straight one if the span-to-radius of curvature ratio is less than 0.06. While, the AASHTO-LRFD Specifications state that a curved bridge can be treated as a straight one in structural design if the central angle is less than 3° for bridge cross-section made of three or four girders and 4° if the number of girders is 5 or more. Table 4.1 presents the results from this sensitivity study for the moment distribution factors of exterior girders due to dead load. While Table 4.2 shows curvature limitations by North American Codes for the moment distribution factors of exterior girders due to fully-loaded lanes with truck loading. It is evident from the results presented in these tables that the limitation specified in the AASHTO Guide of 2003 is the most applicable one to simply-supported composite concrete slab-on-steel girder bridges.

4.2.2 Effect of span length

Figures 4.12 and 4.13 show selected results for the effect of bridge span length on the moment distribution factors for the external girders of two-lane four-girder bridges due to dead load and fully-loaded lanes, respectively. It can be observed that the effect of the span length on the moment distribution factor is insignificant for straight bridges with

L/R=0. Similar behaviour was observed in the case of the middle girder of straight bridges. However, for curved bridges, the moment distribution factor of the exterior girder is observed to increase with the increase in span length as shown in Figures 4.12 and 4.13. As an example, the moment distribution factor of the exterior girder, in a two-lane four-girder bridges full-loaded with truck loading, increases from 1.75 to 2.12 when the bridge span increases from 15 to 25 m.

4.2.3 Effect of number of longitudinal girders

To study the effect of number of girders on the moment distribution factors, a bridge with 2.5-m girder spacing and 25-m span length is considered. Figures 4.14, 4.15, 4.16 and 4.17 show the effect of number of longitudinal girders on the moment distribution factors due to dead load, fully-loaded lanes, partially-loaded lanes and fatigue loading cases, respectively. Generally, in the case of dead load, there is insignificant change in the moment distribution factor with the increase in number of girders. However, in the case of fully loaded lanes and fatigue loading, it can be observed that the moment distribution factor increases with the increase of number of girders untill reaching a peak point at the number of longitudinal girders of 5. Nevertheless, in the case of partially-loaded lanes, the moment distribution factor is observed to increase with the increase in the number of girders. Figures 4.18 to 4.20 present the relationship between number of girders and moment distribution factors for the middle girder due to dead load, fully-loaded lanes and fatigue loading cases, respectively. While Figures 4.21 and 4.22 show the effect of number of girders on moment distribution factor of the internal girder due to the cases of dead load and fully-loaded lanes,

respectively. No general trend is the observed in case of the middle girder and internal girder, as compared to that of the external girder.

4.2.4 Effect of spacing of girders

Figures 4.23 to 4.25 show the effect of the spacing of longitudinal girders on the moment distribution factors for the exterior girder of two-lane curved bridges of 25-m span and number of longitudinal girders of 4 due to dead load, fully-loaded lanes and partially-loaded lanes, respectively. Generally, it can be observed that the moment distribution factor for the external girder increases with the increase in girder spacing for live load and fatigue case, while it is almost unchanged with the increase in girder spacing in case of dead load. Similar behaviour is observed in the case of middle girder (Figure 4.26) and internal girder (Figure 4.27).

4.2.5 Effect of loading conditions

To examine the effect of number of loaded lanes on the moment distribution factors of the exterior or interior girders, two loading cases were considered, namely: fully-loaded lanes with truck loading and partially-loaded lanes with truck loading, as shown in Figures 3.3 through 3.6. Figures 4.28 to 4.30 present the moment distribution factors due to fully-loaded lanes against those due to partially-loaded lanes for 15-m, 25-m and 35-m span bridges, respectively. These plotted values are for all bridges irrespective on number lanes, number of girders and girder spacing. Figures 4.31 to 4.33 show similar relationships but for the internal girder. It can be observed that the case of partially-loaded lanes sometimes provides the design value for the moment distribution factor in spite of the fact that the case

of fully-loaded lanes has almost double the live load compared to that for partially-loaded-lane case.

4.3 Deflection distribution in simply supported curved bridges

4.3.1 Effect of curvature

The results of the current parametric study revealed that the curvature of the bridge is one of the most significant parameters affecting the distribution of deflection between the longitudinal girders. Figures 4.34 through 4.44 examine the effect of curvature on the deflection distribution factors of the exterior, middle and interior girders of two-lane curved bridges of 25-m span and 2.5-m spacing for the dead, live and fatigue loading cases shown in Figure 3.4. It can be observed that deflection distribution factors for the external and middle girders increase with the increase of span-to-radius of curvature ratio. On the other hand, it can be observed that there is no general trend regarding the effect of the curvature on the deflection distribution factor for interior girders. It can be noticed that the deflection distribution factor for the interior girder increases with the increase of curvature in case of dead load and fully-loaded lanes, while in the cases of partially-loaded lanes and fatigue loading, this increase is observed to be up to a certain value of L/R, after which the deflection distribution factor decreases with the increase in curvature. This may be attributed to the fact that there are two parameters affecting the deflection distribution factor, the former is the increase of span-to-radius of curvature ratio and the latter is the decrease of the span length of the interior girder. For low curvature, it appears that the increase in curvature dominates the decrease in span length, but with increase in curvature, the situation is reversed.

It should be noted that the Canadian Highway Bridge Design Code of 2000 (CHBDC, 2000) states that curved bridges may be treated as straight bridges in structural design if L^2/bR is less or equal 1, where L is the curved span of bridge centre line, b is half the bridge width and R is the radius of curvature. Applying this provision to the curved bridges considered in this study, the limiting value of L/R is 0.33 in case of 15-m span, 0.20 in case of 25-m span and 0.143 in case of 35-m span. Applying these limiting values to Figures 4.34 to 4.44 shows that this specified limiting value underestimates the deflection distribution factors for the external, middle and internal girders of the curved system of two-lane cross-section. To provide more confidence of this finding, sensitivity study was conducted on different bridge configurations, shown in Table 4.3. This includes considering number of girders as 3, 4, 5, and 6, number of lanes as 1, 2, 3 and 4 and span lengths as 15, 25 and 35 m. Two cases of loading were considered for the exterior girder, namely: dead load and fully-loaded lanes with truck loading. The limitations provided by other North American codes (AASHTO Guide, 2003; AASHTO-LRFD, 2004) to treat a curved bridge as a straight one in the structural design were also included in the sensitivity study. The AASHTO Guide Specifications for Horizontally Curved Bridges state that a curved bridge can be designed a straight one if the span-to-radius of curvature ratio is less than 0.06. While, the AASHTO-LRFD Specifications state that a curved bridge can be treated as a straight one in structural design if the central angle is less than 3° for bridge cross-section made of three or four girders and 4° if the number of girders is 5 or more. Table 4.3 presents the results from this sensitivity study for the deflection distribution factors of exterior girders due to dead load. While Table 4.4

shows curvature limitations by North American Codes for the deflection distribution factors of exterior girders due to fully-loaded lanes with truck loading. It is evident from the results presented in there tables that the limitation specified in the AASHTO Guide of 2003 is the most applicable one to simply-supported composite concrete slab-on-steel girder bridges.

4.3.2 Effect of span length

Figures 4.45 and 4.46 show selected results for the deflection distribution factors for the external girder of a two-lane four-girder bridge with 2.5 m spacing, with different span length and degree of curvature. It can be observed that the effect of the span length on the deflection distribution factor is insignificant for straight bridges, L/R = 0. However, for curved bridges, a slight change in the deflection distribution factor is observed with increase in span length.

4.3.3 Effect of number of longitudinal girders

To study the effect of the number of girders on the deflection distribution factors, a bridge with 2.5-m girder spacing and 25-m span length is considered. Figures 4.47 to 4.50 show the effect of the number of longitudinal girders on the deflection distribution factors due to dead load, fully-loaded lanes, partially-loaded lanes and fatigue loading cases, respectively. Generally, in the case of dead load, there is an insignificant change in the deflection distribution factor with the increase in number of girders. However, in the case of fully loaded lanes and fatigue loading, it can be observed that the deflection distribution factor increases with the increase of number of girders till reaching a peak point at the number of longitudinal girders of 5. However, in the case of partially-loaded lanes, the

deflection distribution factor is observed to increase with increase in number of girders. Figures 4.51 to 4.53 present the relationship between number of girders and deflection distribution factors for the middle girder due to dead load, fully-loaded lanes and fatigue loading cases, respectively. While Figures 4.54 and 4.55 show the effect of number of girders on the deflection distribution factor of the internal girder due to the cases of dead load and fully-loaded lanes, respectively. No general trend is observed in case of the middle girder and internal girder, as compared to that of the external girder.

4.3.4 Effect of spacing of girders

Figures 4.56 through 4.60 show selected results for the effect of spacing of longitudinal girders on the deflection distribution factors for two-lane, four-girder, bridges of 25-m span. Generally, it can be observed that the deflection distribution factors for the external and internal girders increase with the increase in girder spacing for live and fatigue loading cases. On the other hand, the deflection distribution factors are almost unchanged with the increase of spacing for dead load case similar behaviour is observed in case of the middle girder.

4.3.5 Effect of loading conditions

To examine the effect of number of loaded lanes on the deflection distribution factors of the exterior or interior girders, two loading cases were considered, namely: fully-loaded lanes with truck loading and partially-loaded lanes with truck loading, as shown in Figures 3.3 through 3.6. Figures 4.61 to 4.63 present the deflection distribution factors due to fully-loaded lanes against those due to partially-loaded lanes for 15-m, 25-m and 35-m

span bridges, respectively. These plotted values are for all bridges irrespective on number lanes, number of girders and girder spacing. Figures 4.64 to 4.66 show similar relationships but for the internal girder. It can be observed that the case of partially-loaded lanes sometimes provides the design value for the deflection distribution factor in spite the fact that the case of fully-loaded lanes has almost double the live load compared to that for partially-loaded-lane case.

4.4 Warping stress distribution in simply-supported curved bridges

It is well established that curved I-girders undergo a coupled lateral-bending moment in the top and bottom flanges due to curvature as shown in Figure 3.12. This lateral moment is called also: "torsional warping moment" or "bimoment", which induces warping of the girder cross-section. The increase in longitudinal flexural stress in the bottom steel flange due to this moment is called "warping stress". To examine the change in warping stress with the change in bridge configuration or loading cases, the ratio between warping stress to the average bending stress in the bottom steel flange (WBR as calculated in equation 3.35) is examined herein. The AASHTO Guide Specifications for Horizontally Curved Bridges (Guide, 2003) states that warping-to-bending stress ratio in steel flanges of I-girder bridges should be limited to 0.5 for structural stability reason. In this parametric study, the ratio WBR was calculated for the exterior, middle and interior girder for each loading case considered herein.

Figures 4.67 to 4.70 present the ratio WBR for the exterior girder of all the curved bridges considered in this study in ascending order, for dead load, fully-loaded lanes,

partially-loaded lanes and fatigue loading cases, respectively. It should be noted that WBR should be an absolute value, however these figures show it in both negative and positive values. This is attributed to the fact that the orientation of the lateral moment in steel flanges changes with the change in truck loading cases. It can be observed that warping-to-bending stress ratio, WBR, increases with the increase in span length. Also, it increases with the increase in span-to-radius of curvature ratio. Moreover, it can be observed that the upper bound of all the recorded values of WBR for the exterior girder is 0.3, which falls within the limit provided by the AASHTO Guide of 2003. Figures 4.71 to 4.73 present the ratio WBR for the middle girders of all the curved bridges considered in this study in ascending order, for dead load, fully-loaded lanes and fatigue loading cases, respectively. Similar trend to that of the exterior girder is observed for the middle girder.

Figures 4.74 to 4.77 present the ratio WBR for the interior girders of all the curved bridges considered in this study in ascending order, for dead load, fully-loaded lanes and fatigue loading cases, respectively. It can be observed that the values of WBR are within the specified limit for all bridge types considered herein except those with span length of 35 m and span-to-radius of curvature of 0.7. This value reached 16.5 in some cases. After examining the database generated from this parametric study, it was observed that this significant increase in WBR happened for most of the loading cases with L/R = 0.7 and L = 35 m. By reviewing the assumptions and limitations of the parametric study conduced by Davidson et al. (1996) to determine the minimum number of cross-bracing intervals in curved non-composite steel-girder bridges subjected to construction loads, it was observed that the developed equation (equation 2.19 in this thesis) was based on limiting

the warping-to-bending stress ratio, WBR, of the exterior girders to 0.25 for bridge of span-to-radius of curvature ratio, L/R, of less than or equal 0.5. In this thesis, it is considered that the minimum radius of curvature is 50 m as per the Geometric Design Standards for Ontario Highways (Ministry of Transportation and communications, 1985). As such, a span-to-radius of curvature ratio of 0.7 for bridge span of 35 m is considered in this parametric study. This L/R ratio was not considered in the work conducted by Davidson et al. As a result, a new equation, in replacement of equation 2.19, should be developed to include L/R ratios more that 0.5 and those values of WBR for the composite interior girder due to dead load at service to be in the conservative side since the maximum values for WBR were observed for dead load case. To assist in developing this equation, a sensitivity study is conducted herein to determine the change in WBR with the change in number of bracing internals for 35-m span bridges with span-to-radius or curvature rations, L/R, of 0.5, 0.6 and 0.7. Table 4.5 presents the results from this study for four-girder bridges, while Table 4.6 presents similar results but for five-girder bridges.

4.5 Comparison between CHBDC load distribution equations and those obtained from the current finite-element analysis

The CHBDC moment distribution factor equations were developed for slab-on-girder bridges, including reinforced concrete girders, prestressed concrete girders and composite steel girders. These girders are assumed to be supported laterally by diaphragms at the support lines and at equal intervals between the support lines as specified in the CHBDC of 2000. The stiffness of the lateral diaphragms differs from one

bridge type to the other. In the current study, cross-bracing type with top and bottom chords is considered as lateral supports to the steel girders. These diaphragms would assist in enhancing the load distribution among girders.

To examine the empirical expression for moment distribution factors specified in CHBDC for slab-on-girder bridges, the results from the current study, using the finite-element modeling, and those specified in the CHBDC are presented against each other in a graphical format. Figures 4.78 and 4.79 show the correlation between the moment distribution factors of the exterior girder due to truck loading and fatigue loading, respectively, as specified in the CHBDC and those from the present study. Also, Figures 4.80 and 4.81 show similar correlation but for the middle girder. It can be observed that the CHBDC moment distribution equations always overestimate the structural response except for some cases for fatigue loading shown in Figure 4.79. To examine the CHBDC deflection distribution factors which are similar to those for moment, the moment and deflection distribution factors obtained from the current finite-element modeling are plotted against each other on Figures 4.82 and 4.83 for the exterior girder and Figures, 4.84 and 4.85 for the middle girder, for live and fatigue loading cases, respectively. It can be observed that the deflection distribution factors correlate very well with the moment distribution factors of this study, which proves that the deflection distribution factors specified in the CHBDC, also overestimates the structural response.

4.6 Effect of number of bracing intervals on the structural response

Based on the recommendation stated above in section 4.4 to modify equation 2.19, the number of cross-bracing intervals is expected to be increased. The Design engineer may question the effect of increasing the number of bracing intervals on the values obtained in this study for moment and deflection distribution factors. To answer this question, a sensitivity study was conducted on two-lane, five-girder bridge with span length of 25 m and span-to-radius of curvature ratio of 0.5. Three loading cases were considered herein, namely: dead load, fully-loaded lanes and partially-loaded lanes. Figure 4.86 shows the effect of increasing the number of cross-bracing intervals on the moment distribution factor of the exterior girder. It can be observed that the moment distribution factor significantly decreases with the increase of the number of bracing intervals up to 8 bracing intervals, behind which insignificant increase is observed. Figure 4.87 shows similar results but for the deflection distribution factor. It can be observed that the deflection distribution factor remains unchanged when the number of bracing intervals is more that 4. Figure 4.88 presents the change in the warping-to-bending stress ratio, WBR, with the increase in number of bracing intervals. It can be observed that the WBR significantly decreases with the increase in the number of bracing intervals up to a certain value behind which WBR remains almost unchanged.

4.7 Development of new load distribution factor equations for straight and curved composite concrete slab-on-steel I-girder bridges

The current parametric study provides a database for the moment and deflection distribution factors for both straight and curved slab-on-steel I-girder bridges. This

database can be used to develop expressions for the moment and shear distribution factors for such bridges. Artificial Neural Networks (ANN) software can be incorporated to establish a predictive model capable of accurately predicting the moment and deflection distribution factors for such bridges. It can also be extended to develop software for analysis and design of bridge superstructures. In developing the empirical expressions for the moment and deflection distribution factors or using Artificial Neural Networks application, the following comments can be considered:

1- The results presented in Figures 4.82 to 4.85 show that moment and deflection distribution factors are in very good correlation for straight bridges, L/R =0. As a result, one equation can be developed for both factors. However, this equation should be extended to other two equations for moment and deflection distribution factors for curved bridges, respectively. This is because the results presented in Figures 4.82 to 4.85 show that the deflection distribution factors are always greater than the corresponding moment distribution factors for curved bridges.

2- The database generated in this study is for the exterior, middle and interior girders. However, no available data is available for girders between the exterior and middle girders and between the middle and interior girder. Figures 4.89 and 4.90 show the moment and deflection distribution factors, respectively, for each girder in a three-lane, five-girder bridge with span length of 25 m, girder spacing of 2.5 m and span-to-radius of curvature ratio of 0.3. These figures include all the loading cases considered in this study. It can be observed that the distribution is almost linear between the exterior and interior girders for the design values that will be used to derive the empirical equations. As a result, the values of the moment and deflection

distribution factors for girders other than the exterior, middle and interior girders can be obtained by linear interpolation using the values from the developed equations.

CHAPTER V

CONCLUSIONS AND RECOMMENDATIONS

5.1 Conclusions

Numerical and Analytical studies were carried out to investigate the static response of curved composite concrete slab-on-steel I-girder bridges. A literature review was conducted in order to establish the foundation of this study. It was observed that there is a lack of information on the behaviour of such structures. It should be noted that the Canadian Highway Bridge Design Code (CHBDC, 2000) does not provide any guidance with respect to load distribution characteristics in curved slab-on-girder bridges. In this thesis, a practical-design-oriented parametric study was conducted to investigate the structural response of such bridges. The influences of several parameters on the moment, deflection and warping stress distribution in such bridges were examined with the commercially available finite-element computer program SAP2000. In the performed parametric study, the prototype bridges were subjected to Canadian Highway Bridge Design Code (CHBDC) truck and dead loading. Based on the results from the parametric study, the following conclusions are drawn:

1- Curvature is the most critical parameter that influences the design of curved girders in slab-on-girder bridges. Moment and deflection distribution factors as well as the warping-to-bending stress ratio increase with the increase in bridge curvature.

2- Span length, number of girders and girder spacing generally affect the values of the moment and deflection distribution factors.

3- Loading all bridge lanes with CHBDC truck loading does not guarantee the highest value of the moment or deflection distribution factors in curved bridges. Results show that the loading case of partially-loaded lanes sometimes provides the design value compared to the loaded case of fully-loaded lanes.

4- Warping-to-bending stress ratios of the studied curved bridges are within the recommended limit except for bridge span of 35 m and span-to-radius of curvature of 0.7. A new empirical equation for the minimum number of bracing intervals can be deduced based on the results obtained from this study to include span-to-radius of curvature ratios up to 0.7.

5- The study proved that the CHBDC moment and deflection distribution factors overestimate the structural response of interior girders by 10% and 20% at least due to truck and fatigue loading respectively and underestimate the structural response of external girders due to fatigue loading by a percentage which reaches 38% in some cases, for straight composite concrete slab-on-steel I-girder bridges. The database generated from this parametric study can be used to refine CHBDC equations.

6- The provision in the Canadian Highway Bridge Design Code of 2000 treating curved bridges as straight ones in the structural design (L^2/bR is less or equal 1) underestimates the structural response. We recommend those specified in the AASHTO-LRFD Specifications of 2004, instead. Besides, applying the distribution factors of live load to the dead load distribution, generally and using 3 equally spaced bracing intervals at least for 15m span bridges

7- can be used to develop expressions for the moment and deflection distribution factors for the curved system.

5.2 Recommendations for Future Research

It is recommended that further research efforts be directed towards the following:

1- Using the database obtained in this study, empirical expressions for bridge analysis can be deduced, and/or Neural Network software can be used to establish an integrated tool to obtain accurate distribution factors based on the developed database in this thesis.

2- The study of shear distribution factors in curved slab-on-I-girder bridges.

3- The study of load distribution in continuous curved slab-on-I-girder bridges.

4- The study of the load distribution in curved slab-on-I-girder bridges at higher load levels to include effects of concrete cracking and yielding of steel.

REFERENCES

American Association for State Highway and Transportation Officials, AASHTO. 1980 *Guide Specification for Horizontally Curved Highway Bridges*. Washington, D.C.

American Association for State Highway and Transportation Officials, AASHTO. 1993. *Guide Specification for Horizontally Curved Highway Bridges*. Washington, D.C.

American Association of State Highway and Transportation Officials, AASHTO. 1996. *Standard Specifications for Highway Bridges*. Washington, D.C.

American Association of State Highway and Transportation Officials, AASHTO. 1998. AASHTO LRFD Bridge Design Specification, 2nd edition, Washington, D.C

American Association for State Highway and Transportation Officials, AASHTO. 2003. *Guide Specification for Horizontally Curved Highway Bridges*. Washington, D.C.

American Association of State Highway and Transportation Officials, AASHTO. 2004. *AASHTO LRFD Bridge Design Specifications*. Washington. D.C.

Arizumi, Y., Oshiro, T., and Hamado, S. 1982. Finite-Strip Analysis of Curved Composite Girders with incomplete interaction. Computers & Structures, 15(6): 603-612.

Brockenbrough, R. L. 1986. *Distribution Factors for Curved I-Girder Bridges*. ASCE Journal of Structural Engineering, 112(10): 2200-2215.

Bakht, B., and Moses, F. 1988. Lateral *Distribution Factors for Highway Bridges*. Journal of Structural Engineering ASCE, 114(8): 1785-1803.

Bell, L. C., and Heins, C.P. 1969. Curved Girder Computer Manual. Report No. 30, Program Report on the Design of Curved Viaducts, University of Maryland.

Brennan, P. J., and Mandel, J. A. 1973. Users Manual-Program for Three-Dimensional Analysis of Horizontally Curved Bridges. Syracuse University Report, Research Project HPR-2(111).

Canadian Standard Association. *2000. Canadian Highway Bridge Design Code, CHBDC 2000.* Etobicoka, Ontario.

Culver, C. G. 1967. Natural Frequencies of Horizontally Curved Beams. Journal of Structural Division, ASCE, 93(2): 189-203.

Davidson, J. S., Keller, M. A., and Yoo, C. H. 1996. *Cross-frame Spacing and Parametric Effects in Horizontally Curved I-Girder Bridges.* ASCE Journal of Structural Engineering, 122(9): 1089-1096.

Galambos, T.V. 1978. *Tentative load factor design criteria for curved steel bridges.* Research Report No. 50, School of Engineering and Applied Science, Civil Engineering Department, Washington University, St. Louis.

Grubb, M.A. 1984. *Horizontally curved I-girder bridge analysis: V-load method.* Transportation Research Board Record 982, National Research Council, 26-35.

Hayes, C.O., Jr., Sessions, L.M. and Berry, A.J. 1986. *Further studies on lateral load distribution using finite element methods.* Transportation Research Record, (1072), Transportation Research Board, Washington, D.C., 6-14.

Heins, C.P., Siminou J. 1970. *Preliminary Design of Curved Bridges.* AISC Engineering Journal, 7(2), 50-61.

Heins, C. P., and Bell, L. C. 1972. *Curved Girder Bridge Analysis.* Journal of Computers and Structures, 2: 785-797.

Heins, C. P., and Jin, J. O. 1984. *Live Load Distribution on Braced Curved I-Girders.* ASCE Journal of Structural Engineering, 110(3): 523-530.

Ketchek, K.F. 1969. *Discussion of Horizontally curved girders – state of the art by McManus PF et al.* Journal of Structural Division, ASCE, 95 (ST12): 2999-3001.

Kostem, C.N. and DeCastro, E.S. 1977. *Effect of diaphragms on lateral load distribution in beam-slab bridges*, Transportation Research Record, Bridge Test, No. 645, 6-9.

Lavelle, F. H., Greig, R. A., and Wemmer, H.R. 1971. CUGAR1 –A Program to Analyze Curved Girder Bridges. University of Rhode Island, Kingston, Rhode Island.

Lavelle, F. H., and Lasks, R. J. 1975. CUGAR2 and CUGAR3 user's Manuals. CURT Final Report, Research Project HPR-2(111), University of Rhode Island.

Lavelle, F. H., and Lasks, R. J. 1975. The CUGAR2 Algorithm. CURT Final Report No. 4(L), Research Project HPR-2(111), University of Rhode Island.

McManus, P.F., Nasir, G.A. and Culver, C.G. 1969. *Horizontally curved girders – state of the art*. Journal of Structural Division. ASCE, 95(ST5): 853-870.

Ministry of Transportation and communications. 1985. *Geometric Design Standards for Ontario Highways*. Downsview, Ontario, Canada.

Modkar, D. P., and Powell, G. H. 1974. CURVBRG –A Computer Program for Analysis of Curved Open Girder Bridges. Report No. UC SESM 74-17, University of California at Berkely.

Montalvao e Silva, J. M., and Urgueira, A. 1988. Out-of-Plane Dynamic Response of Curved Beams, An Analytical Model. International Journal of Solids and Structures, 24(3): 271-284.

Nakai, H. and Yoo, C.H. 1988. *Analysis and Design of Curved Steel Bridges*, McGraw Hill Book Co., Inc., New York, N.Y.

Newmark, N.M. 1948. *Design of I-beam bridges.* Journal of Structural Engineering, ASCE, 74(ST1): 305-331.

Ontario Ministry of Transportation and Communications. 1983. *Ontario Highway Bridge Design Code, OHBDC.* Second edition, Downsview, Ontario.

Ontario Ministry of Transportation and Communications. 1992. *Ontario Highway Bridge Design Code, OHBDC.* Third edition, Downsview, Ontario.

Pandit, G.S., Ceradini, G., Garvarini, P. and Eremin, A.A. 1970. *Discussion of "Horizontally curved girders – state of the art.* Journal of Structural Division, ASCE, 96(ST2): 433-436.

Salmon, C.G., and Johnson, J.E. 1996. *Steel Structures: Design and Behavior, Emphasizing Load and Resistance Factor Design*, 4th Edition, HarperCollins College Publishers Inc., New York, N.Y.

Schelling, D., Namini, A. H., and Fu, C. C. 1989. *Construction Effects on Bracing on Curved I-Girders.* ASCE Journal of Structural Engineering, 115(9): 2145-2165.

Sennah, K., Eissa, O., and Lee, G. 2000. *Moment Distribution in Curved composite Syeel I-Girder Bridges at Construction Phase.* 3ed Structural Specialty Conference of Canadian Society for Civil Engineering.

Shahawy, M. and Huang, D. Z. 2001. *Analytical and field investigation of lateral load distribution in concrete slab-on-girder bridges.* Structural Journal, ACI, 98 (4): 590-599.

Sheinman, I. 1982. Large Deflection of Curved Beam with Shear Deformation. Journal of Engineering Mechanics Division, ASCE: 108(4): 636-647.

Shore, S., and Wilson, J. L. 1973. Users' Manual for Static analysis of Curved Bridges (STACRB). CURT Report No. T0173, Research Project HPR-2(111), Graduate Division of Civil & Environmental Engineering, University of Pennsylvania.

Stegmann, T.H., and Galambos, T.V. 1976. *Load factor design criteria for curved steel girders of open section*. Research Report 23, Civil Engineering Department, Washington University, St. Louis.

Tarshini, K.M., and Frederick, G.R. 1992. *Wheel load distribution in I-girder highway bridges*. Journal of Structural Engineering, ASCE, 118(5): 1285-1294.

Tarshini, K.M., and Frederick, G.R. 1995. *Lateral load distribution in I-girder bridges*. Computers and Structures, 54(2), Pergamon Press Inc., 351-354.

Tene, Y., Epstein, M., and Sheinman, T. 1975. Dynamics of Curved Beams involving Shear Deformation. International Journal of Solids and Structures, 11(7): 827-840.

Wilson, E. L., and Habibullah, A. 1999. *Structural Analysis Program SAP2000*, Computers & Structures.

Yao, L. 1990. *Bridge Engineering*, 1st Edition, People's Transportation Publisher, P.R. China.

Yoo, C. H., and Littrell, P. C. 1985. *Cross-Bracing Effects in Curved Stringer Bridges*. ASCE Journal of Structural Engineering, 112(9): 2127-2140.

Zhang, H. 2002. *Lateral Load Distribution for Curved Steel I-Girder Bridges*. Ph.D. Dissertation, Florida International University, Miami, Florida.

Zokaie, T. 2000. AASHTO-LRFD Live Load Distribution Specifications. Journal of Bridge Engineering, 5(2): 131-138.

Zuerick, A., Naqib, R., and Yadlosky, J. M. 1993. *Curved Steel Bridge Research Project*, Vol. 1. Interim Rep., FHWA-RD-93-129, Mclain, Va., 1-104.

Zuerick, A., Naqib, R. 1999. *Horizontally Curved Steel I-Girders State-of-the-Art Analysis Methods*. Journal of Bridge Engineering, 4 (1): 38-47.

Zureick, A., Linzell, D., Leon, R.T. and Burrell, J. 2000. *Curved steel I-girder bridges: Experimental and analytical studies*. Engineering Structures, 22(2), Elsevier Science Ltd., 180-190.

Table 2.1 Coefficient, C, for Various Multi-Girder Systems Assuming Equal Girder Spacing (Grubb, 1984)

Number of Girders	2	3	4	5	6	7	8	9	10
Coefficient C	1	1	10/9	5/4	7/5	14/9	12/7	15/8	165/81

Table 3.1 Bridge Configurations Considered in the Parametric Study

Bridge Width (m)	**Deck Width Wc (m)**	**Number of Girders**	**Spacing (m)**	**Number of Design Lanes**
6	5	3	2	1-lane
7.5	6.5	3	2.5	2-lane
9	8	3	3	2-lane
8	7	4	2	2-lane
10	9	4	2.5	2-lane
12	11	4	3	2-lane & 3-lane
10	9	5	2	2-lane
12.5	11.5	5	2.5	2-lane & 3-lane
15	14	5	3	4-lane
12	11	6	2	2-lane & 3-lane
15	14	6	2.5	4-lane
14	13	7	2	2-lane & 3-lane

Table 3.2 Number of Design Lanes

Wc	n
6.0 m or less	1
Over 6.0 m to 10.0 m incl.	2
Over 10.0 m to 13.5 m incl.	2 or 3
Over 13.5 m to 17.0 m incl.	4
Over 17.0 m to 20.5 m incl.	5
Over 20.5 m to 24.0 m incl.	6
Over 24.0 m to 27.5 m incl.	7
Over 27.5 m	8

Table 3.3 Modification Factors for Multilane Loading

Number of Loaded Design Lanes	Modification Factor
1	1.00
2	0.90
3	0.80
4	0.70
5	0.60
6 or more	0.55

Table 4.1 Curvature limitations by North American Codes for the moment distribution factors of exterior girders due to dead load

L	N	S	No. of bracing intervals	Deck width in ms (W_c)	No. of design lanes (n)	CHBDC, 2000 ($L^2/bR = 1$)			AASHTO Guide, 2003 (L/R = 0.06)			AASHTO-LRFD, 2004 ($\theta = 3°$ for N = 3 or 4, $\theta = 4°$ for N = 5 or more)		
						L/R	CHBDC $(MDF)_{straight}$	F.E. A $(MDF)_{curved}$	L/R	CHBDC $MDF)_{straight}$	F.E. A $MDF)_{curved}$	L/R	CHBDC $MDF)_{straight}$	F.E. A $MDF)_{curved}$
15	3	2	2	5	1	0.200	1.03	3.65		1.03	1.55		1.03	1.56
25			4			0.120	1.04	1.73	0.06	1.04	1.23	0.052	1.04	1.21
35			6			0.086	1.04	1.44		1.04	1.25		1.04	1.23
15	4	2.5	2	9	2	0.333	1.04	5.92		1.04	1.57		1.04	1.51
25			4			0.200	1.04	2.56	0.06	1.04	1.25	0.052	1.04	1.22
35			6			0.143	1.04	1.90		1.04	1.25		1.04	1.23
15	5	2.5	2	11.5	3	0.417	1.05	7.64		1.05	1.60		1.05	1.75
25			4			0.250	1.05	3.21	0.06	1.05	1.26	0.070	1.05	1.32
35			6			0.179	1.05	2.17		1.05	1.26		1.05	1.32
15	6	2.5	2	14	4	0.500	1.05	9.38		1.05	1.62		1.05	1.67
25			4			0.300	1.06	3.75	0.06	1.06	1.26	0.070	1.06	1.34
35			6			0.214	1.06	2.47		1.06	1.26		1.06	1.32

Table 4.2 Curvature limitations by North American Codes for the moment distribution factors of exterior girders due to fully-loaded lanes with CHBDC trucks

L	N	S	No. of bracing intervals	Deck width in ms (W_c)	No. of design lanes (n)	CHBDC, 2000 ($L^2/bR = 1$)			AASHTO Guide, 2003 (L/R = 0.06)			AASHTO-LRFD, 2004 ($\theta = 3°$ for N = 3 or 4, $\theta = 4°$ for N = 5 or more)		
						L/R	CHBDC $(MDF)_{straight}$	F.E. A $(MDF)_{curved}$	L/R	CHBDC $MDF)_{straight}$	F.E. A $MDF)_{curved}$	L/R	CHBDC $MDF)_{straight}$	F.E. A $MDF)_{curved}$
15	3	2	2	5	1	0.200	1.71	4.29		1.71	2.08		1.71	2.06
25			4			0.120	1.68	2.33	0.06	1.68	1.75	0.052	1.68	1.70
35			6			0.086	1.67	1.90		1.67	1.70		1.67	1.66
15	4	2.5	2	9	2	0.333	1.45	5.56		1.45	1.75		1.45	1.68
25			4			0.200	1.43	2.85	0.06	1.43	1.49	0.052	1.43	1.46
35			6			0.143	1.42	2.09		1.42	1.46		1.42	1.43
15	5	2.5	2	11.5	3	0.417	1.38	6.22		1.38	1.54		1.38	1.66
25			4			0.250	1.36	3.15	0.06	1.36	1.33	0.070	1.36	1.40
35			6			0.179	1.36	2.15		1.36	1.31		1.36	1.36
15	6	2.5	2	14	4	0.500	1.51	7.16		1.51	1.49		1.51	1.61
25			4			0.300	1.49	3.54	0.06	1.49	1.28	0.070	1.49	1.35
35			6			0.214	1.48	2.36		1.48	1.26		1.48	1.32

Table 4.3 Curvature limitations by North American Codes for the deflection distribution factors of exterior girders due to dead load

L	N	S	No. of bracing intervals	Deck width in ms (W_c)	No. of design lanes (n)	CHBDC, 2000 ($L^2/bR = 1$)			AASHTO Guide, 2003 ($L/R = 0.06$)			AASHTO-LRFD, 2004 ($\theta = 3°$ for N = 3 or 4, $\theta = 4°$ for N = 5 or more)		
						L/R	CHBDC $(DDF)_{straight}$	F.E. A $(DDF)_{curved}$	L/R	CHBDC $DDF)_{straight}$	F.E. A $DDF)_{curved}$	L/R	CHBDC $DDF)_{straight}$	F.E. A $DDF)_{curved}$
15	3	2	2	5	1	0.200	1.03	2.70		1.03	1.34		1.03	1.43
25			4			0.120	1.04	1.77	0.06	1.04	1.25	0.052	1.04	1.23
35			6			0.086	1.04	1.40		1.05	1.19		1.05	1.17
15	4	2.5	2	9	2	0.333	1.04	4.20		1.04	1.38		1.04	1.33
25			4			0.200	1.04	2.47	0.06	1.04	1.27	0.052	1.04	1.25
35			6			0.143	1.04	1.91		1.04	1.20		1.04	1.19
15	5	2.5	2	11.5	3	0.417	1.05	5.72		1.05	1.40		1.05	1.53
25			4			0.250	1.05	2.92	0.06	1.05	1.29	0.070	1.05	1.37
35			6			0.179	1.05	2.14		1.05	1.20		1.05	1.28
15	6	2.5	2	14	4	0.500	1.05	7.78		1.05	1.43		1.05	1.55
25			4			0.300	1.06	3.21	0.06	1.06	1.30	0.070	1.06	1.39
35			6			0.214	1.06	2.40		1.06	1.20		1.06	1.29

Table 4.4 Curvature limitations by North American Codes for the deflection distribution factors of exterior girders due to fully-loaded lanes with CHBDC trucks

L	N	S	No. of bracing intervals	Deck width in ms (W_c)	No. of design lanes (n)	CHBDC, 2000 ($L^2/bR = 1$)			AASHTO Guide, 2003 (L/R = 0.06)			AASHTO-LRFD, 2004 ($\theta = 3°$ for N = 3 or 4, $\theta = 4°$ for N = 5 or more)		
						L/R	CHBC $(DDF)_{straight}$	F.E. A $(DDF)_{curved}$	L/R	CHBC $DDF)_{straight}$	F.E. A $DDF)_{curved}$	L/R	CHBC $DDF)_{straight}$	F.E. A $DDF)_{curved}$
15	3	2	2	5	1	0.200	1.71	3.18		1.71	1.78		1.71	1.85
25			4			0.120	1.68	2.25	0.06	1.68	1.70	0.052	1.68	1.67
35			6			0.086	1.67	1.86		1.67	1.63		1.67	1.61
15	4	2.5	2	9	2	0.333	1.45	4.23		1.45	1.55		1.45	1.50
25			4			0.200	1.43	2.61	0.06	1.43	1.46	0.052	1.43	1.42
35			6			0.143	1.42	2.05		1.42	1.38		1.42	1.36
15	5	2.5	2	11.5	3	0.417	1.38	5.21		1.38	1.41		1.38	1.52
25			4			0.250	1.36	2.83	0.06	1.36	1.32	0.070	1.36	1.41
35			6			0.179	1.36	2.11		1.36	1.24		1.36	1.31
15	6	2.5	2	14	4	0.500	1.51	6.73		1.51	1.37		1.51	1.49
25			4			0.300	1.49	3.04	0.06	1.49	1.29	0.070	1.49	1.37
35			6			0.214	1.48	2.29		1.48	1.21		1.48	1.28

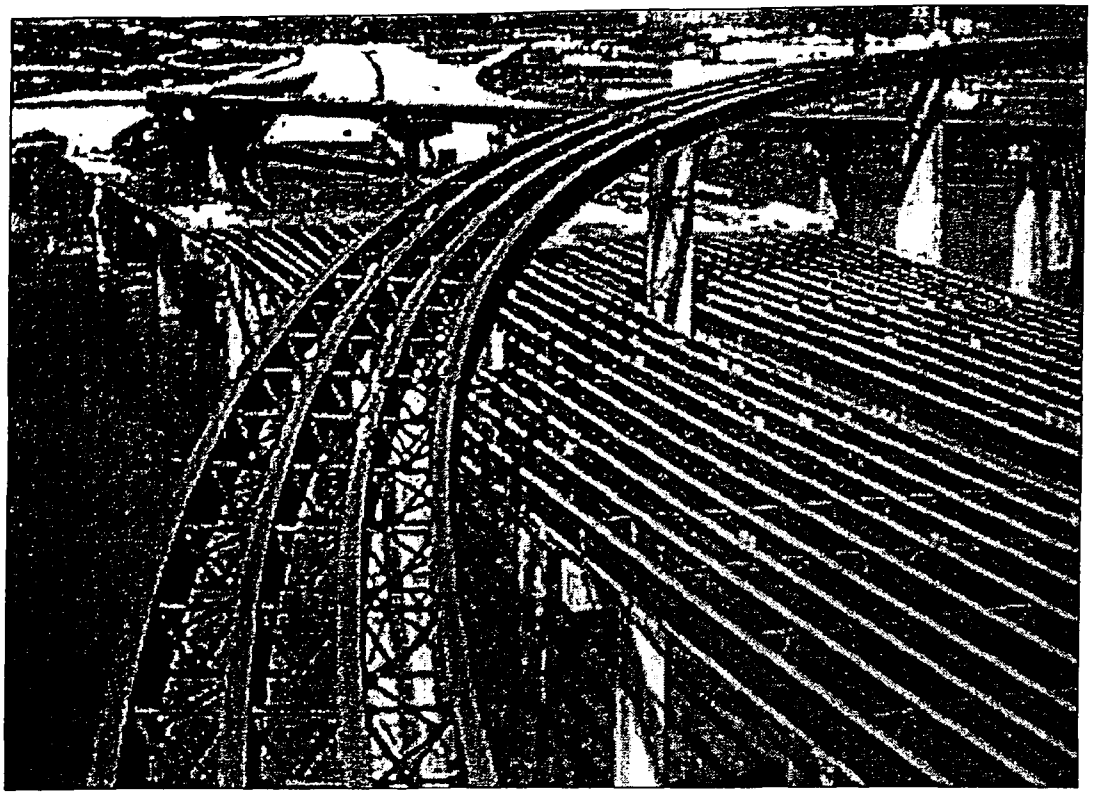

Figure 1.1 View of curved and straight steel I-girder bridges during erection

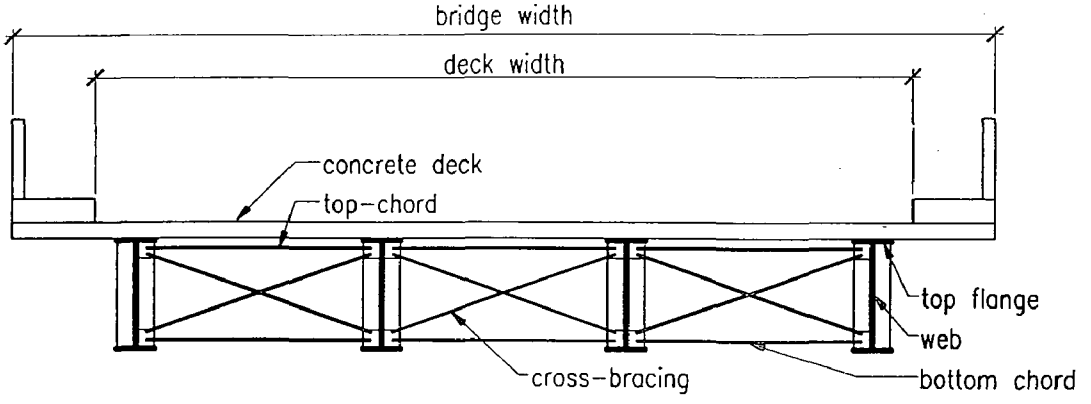

Figure 1.2 Typical I-Girder Bridge Cross-Section

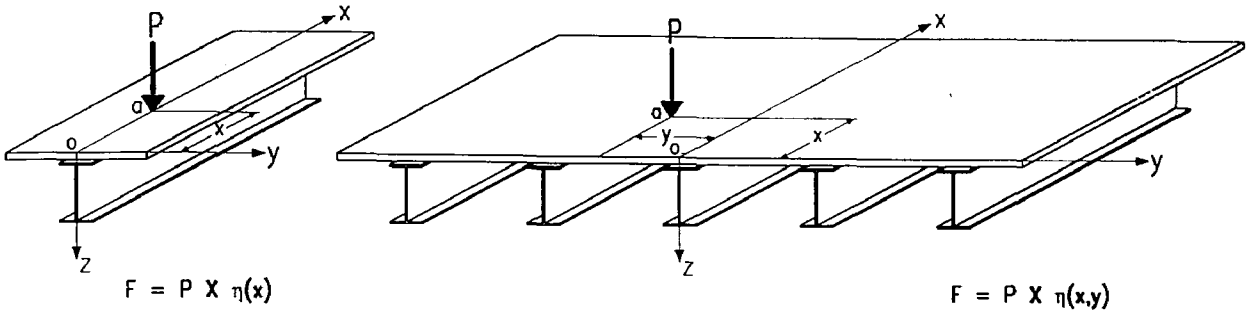

a) Single Girder b) Multi-girder bridge

Figure 2.1 Single and Multi-girder System under Concentrated Live Load P (Zhang 2002)

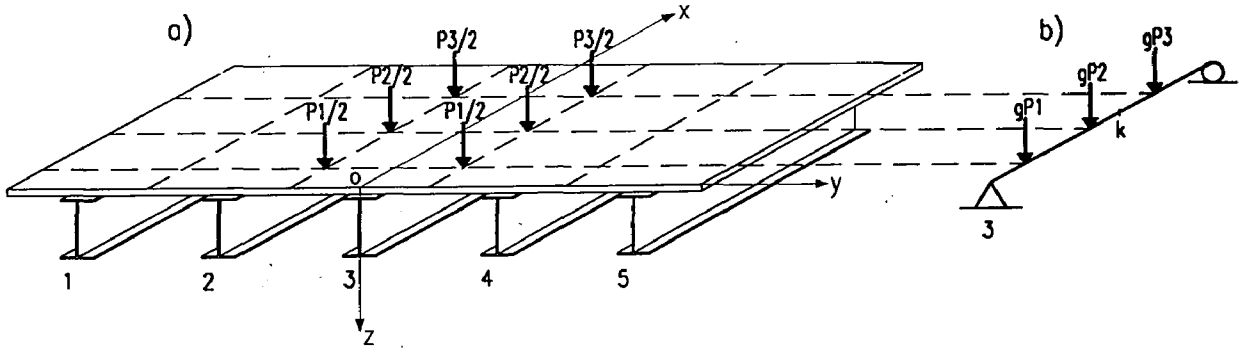

Figure 2.2 Lateral Load Distribution of Truck Axle Load (Zhang 2002)

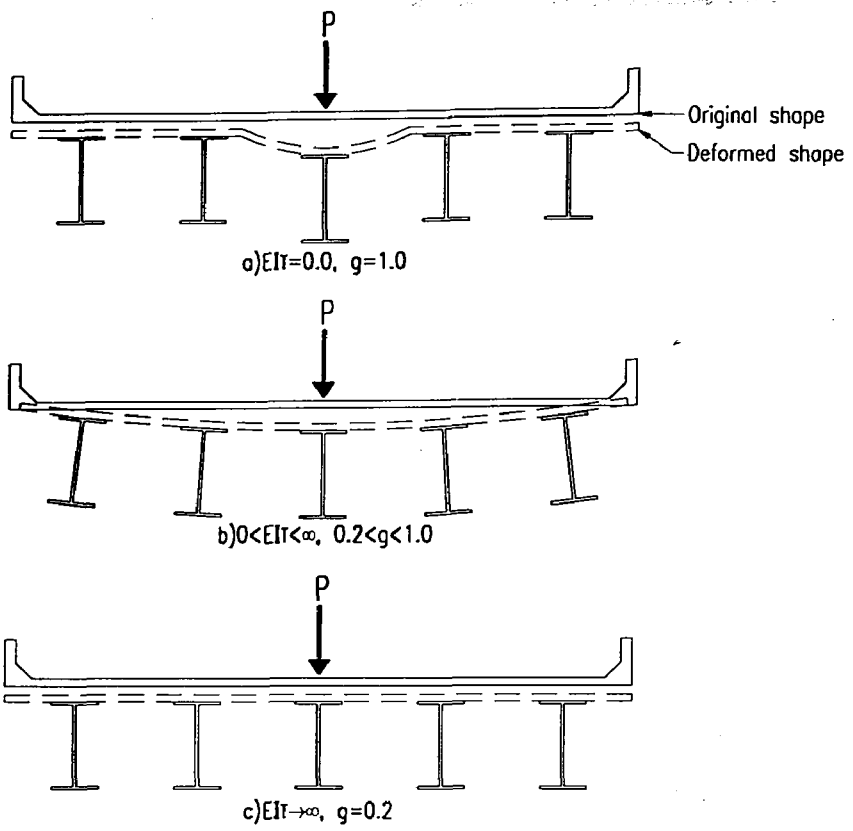

Figure 2.3 Girder Deflection with Different Transverse Stiffness (Zhang 2002)

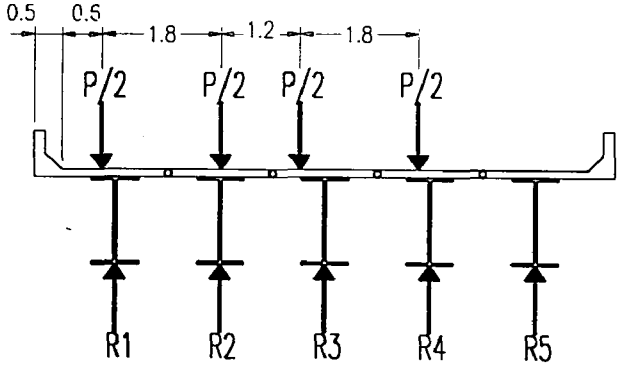

Figure 2.4 Free Body Diagram–Lever Rule Method (Zhang 2002)

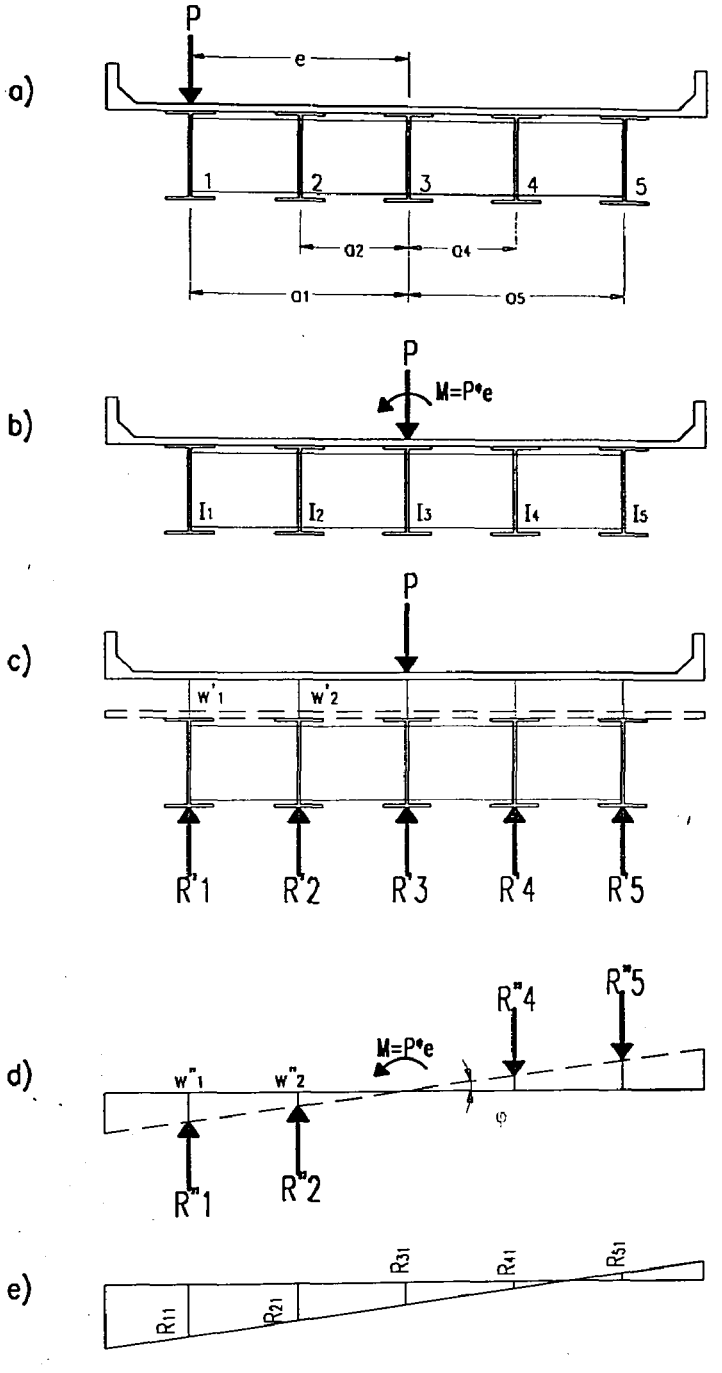

Figure 2.5 Load Distribution under Eccentric Load (Zhang 2002)

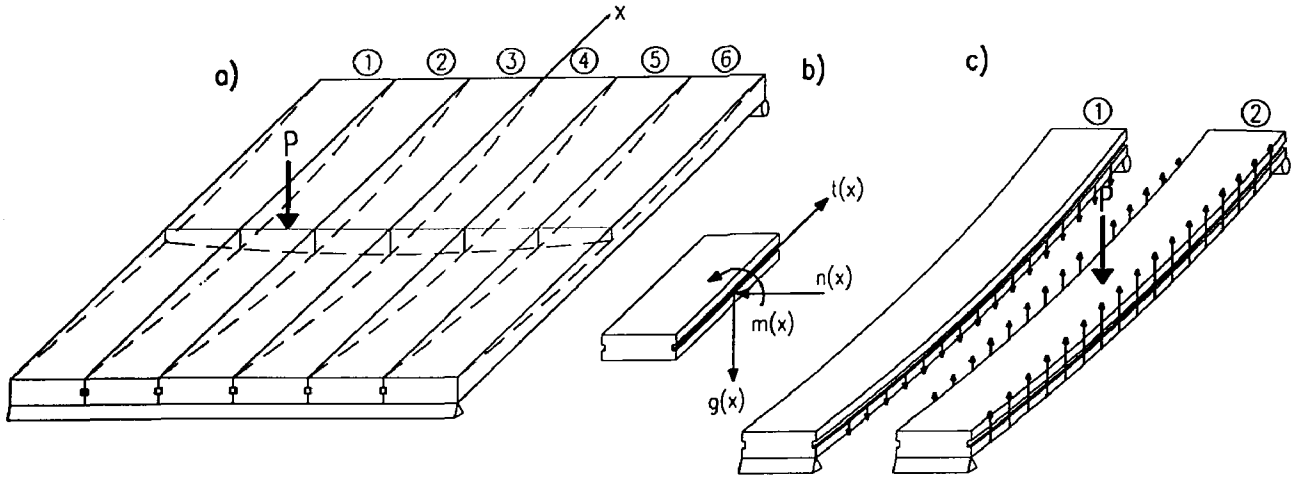

Figure 2.6 Free Body Diagram of a Hinged Slab Bridge under Concentratrated Load (Zhang 2002)

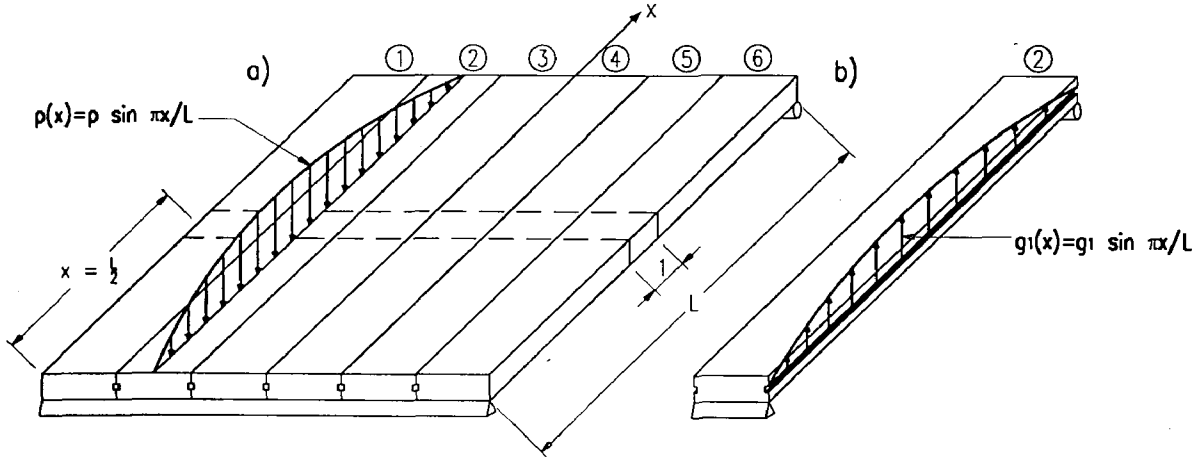

Figure 2.7 Free Body Diagram of a Hinged Slab Bridge under Sinusoidal Load (Zhang 2002)

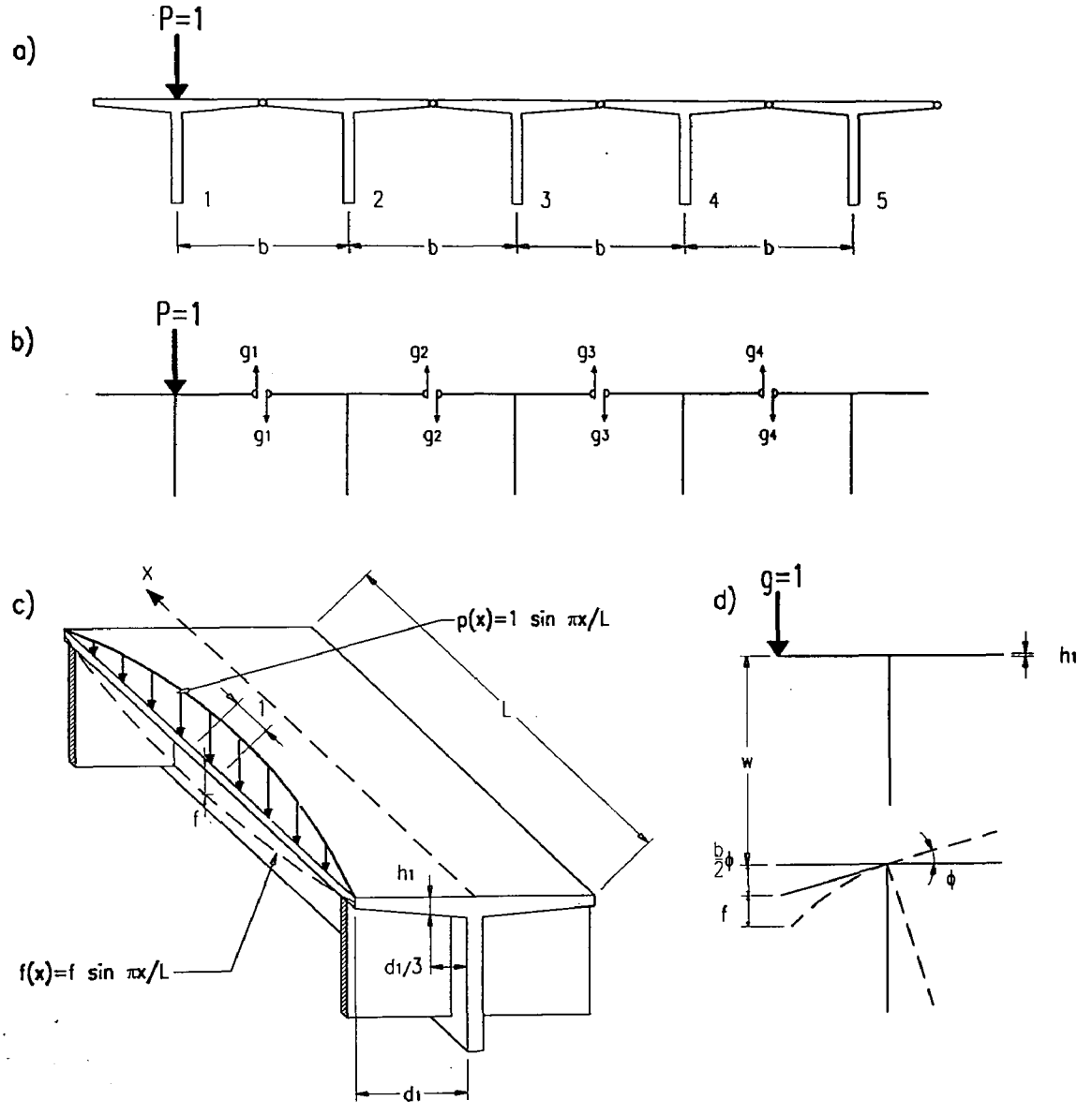

Figure 2.8 Free Body Diagram for Hinged T-shaped Girder Bridge (Zhang 2002)

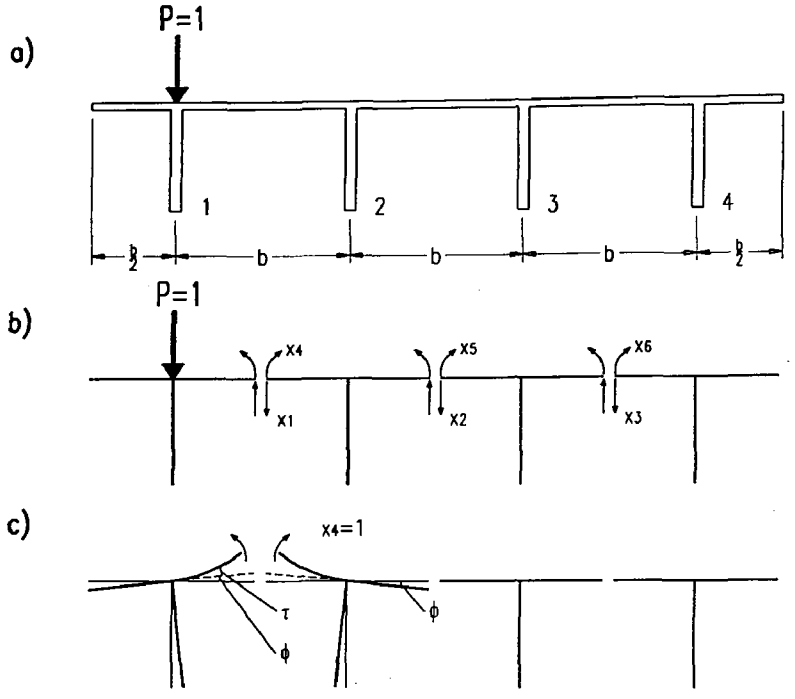

Figure 2.9 Free Body Diagram of Fixed Joint Girder Bridge (Zhang 2002)

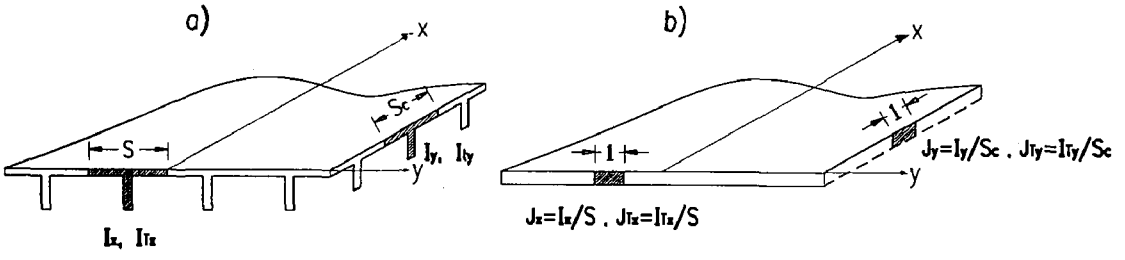

a) Real Structure

b) Analogized Equivalent Orthotropic Plate

Figure 2.10 Real Structure and Orthotropic Plate Analogy (Zhang 2002)

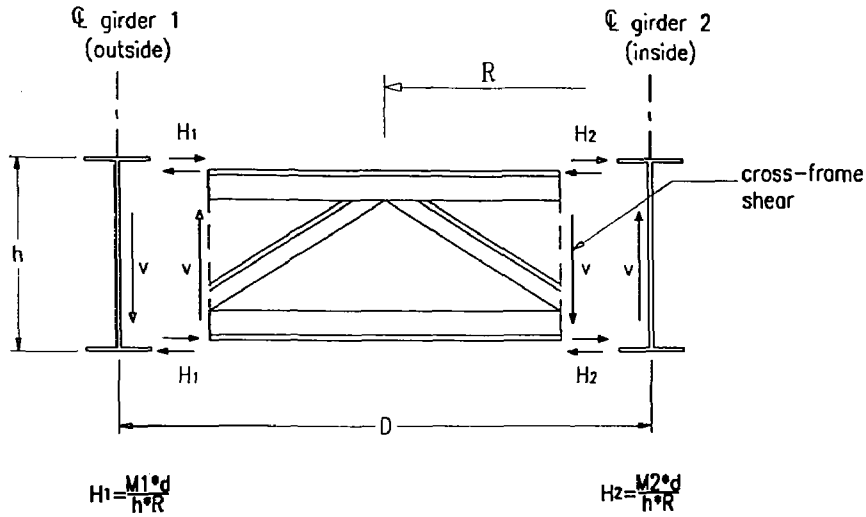

Figure 2.11 V-Load on Girder

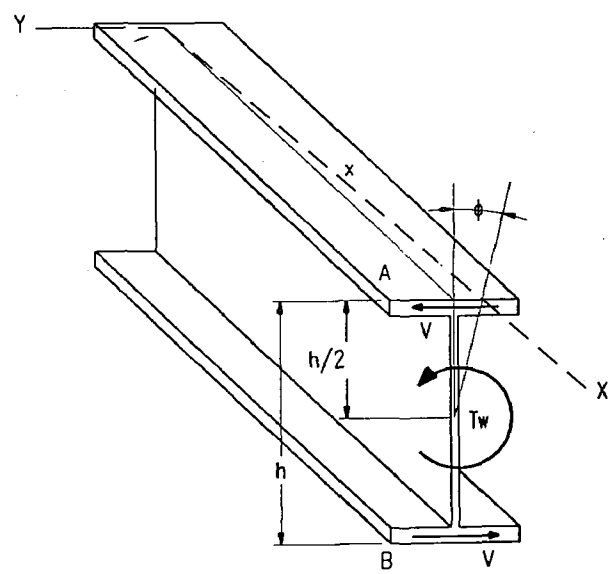

Figure 2.12 Effect of Warping Moment Applied to I-Girder

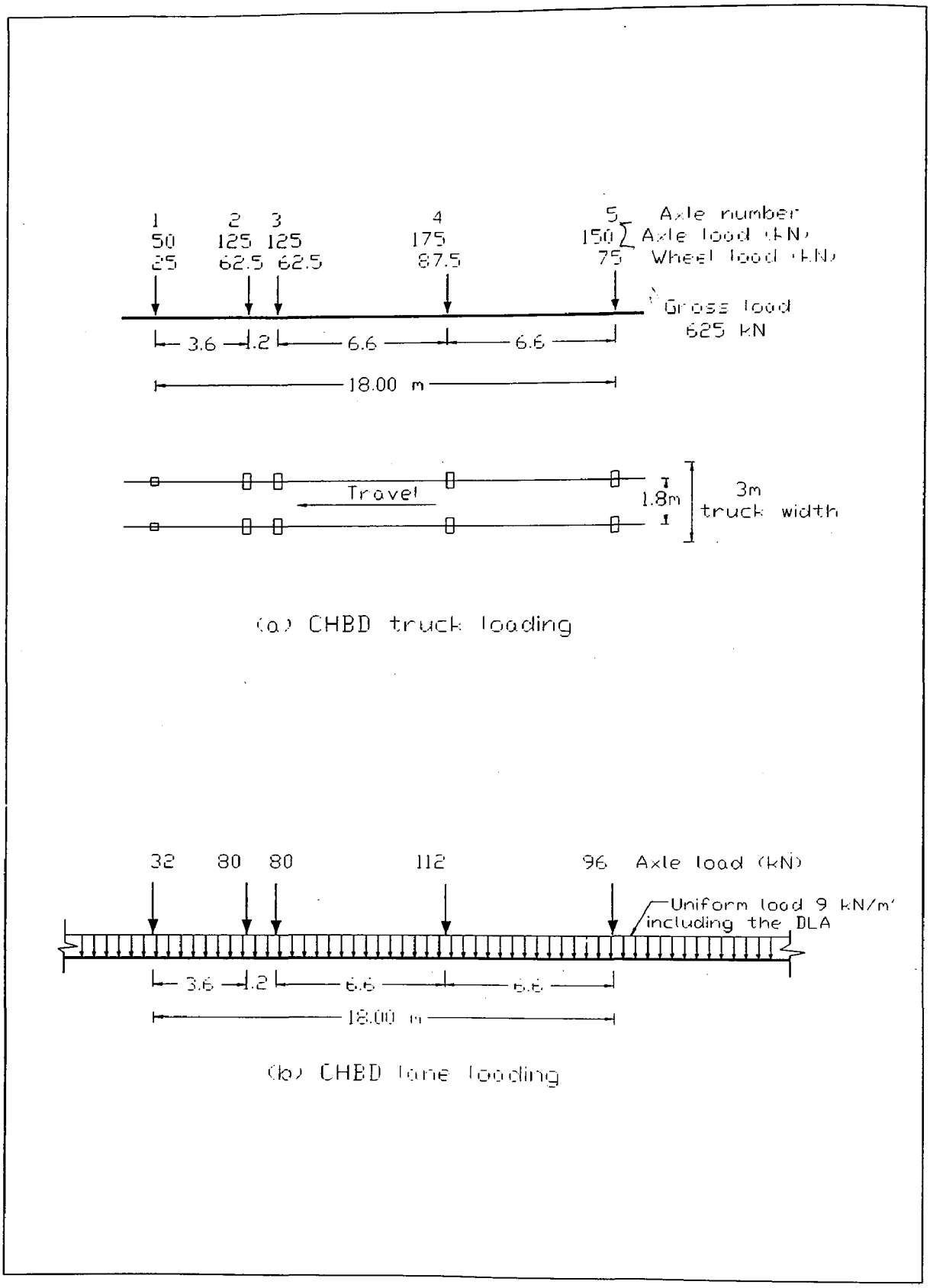

Figure 2.1 CL-W Truck Loading Configurations

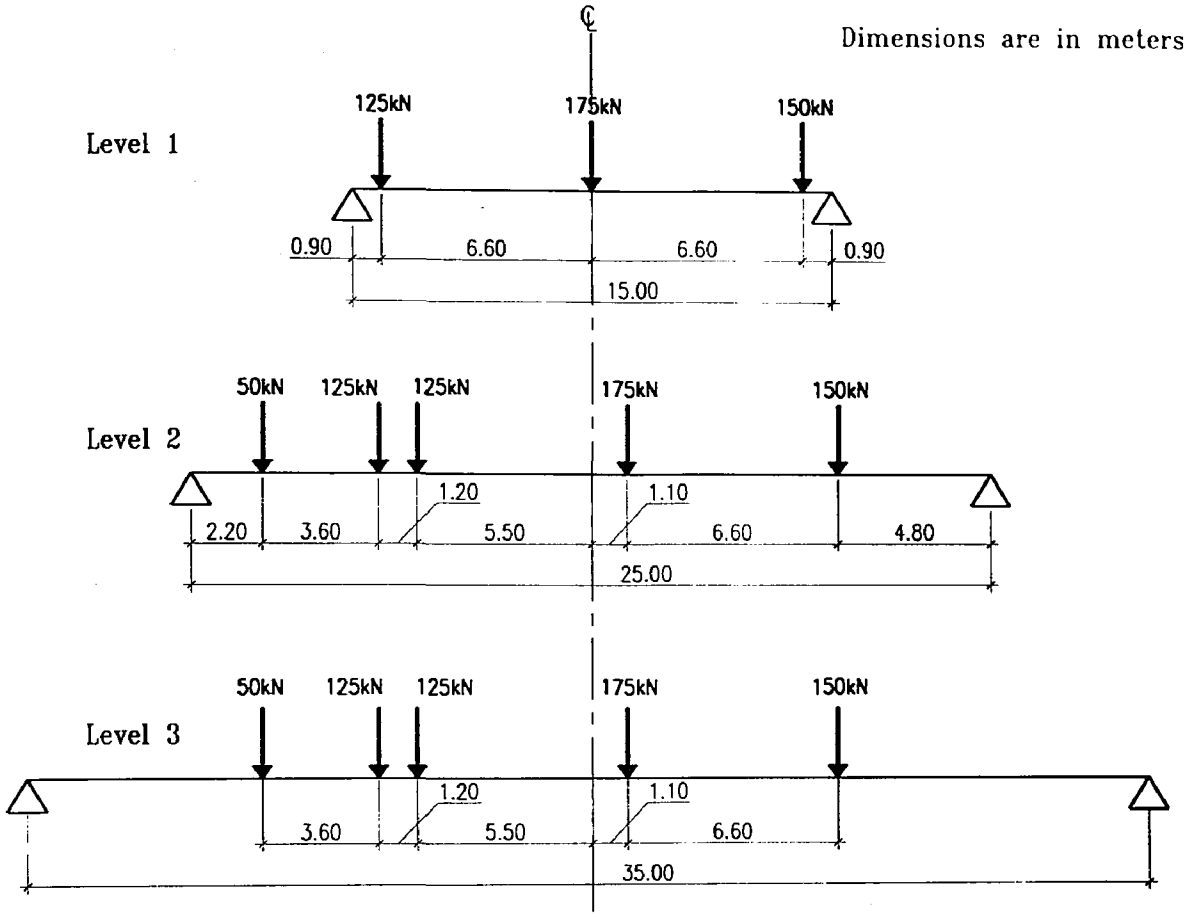

Figure 3.2 Maximum Moment Location

Case (1): Dead load

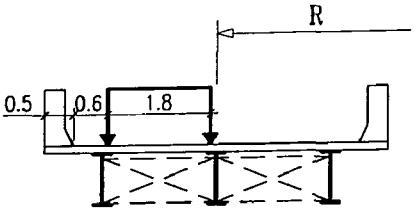

Case (2): Loading case for exterior girder

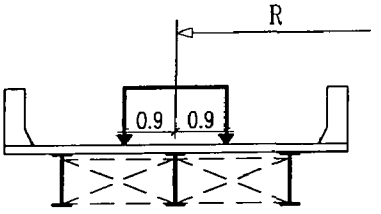

Case (3): Loading case for middle girder

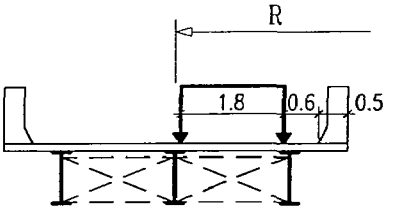

Case (4): Loading case for interior girder

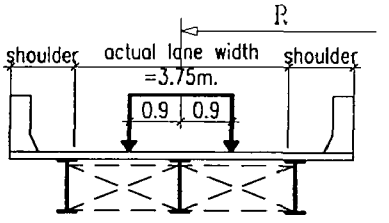

Case (5): Loading case for fatigue

Dimensions are in meters

Figure 3.3 Live loading cases for one-lane bridge

Case (1): Dead load

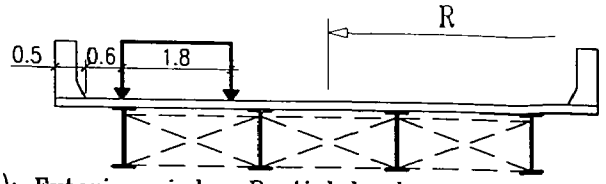

Case (2): Exterior girder–Partial load

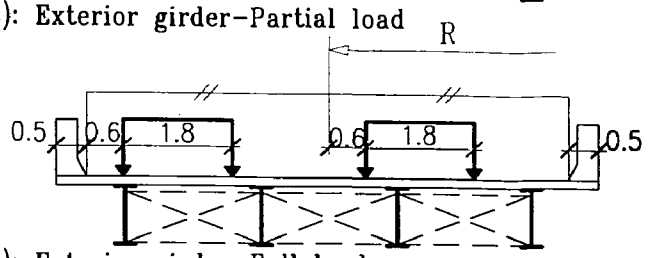

Case (3): Exterior girder–Full load

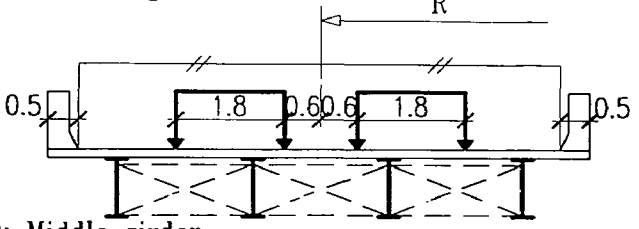

Case (4): Middle girder

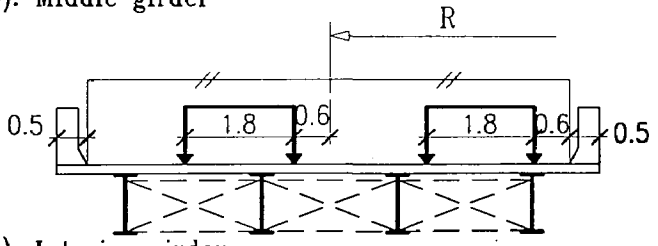

Case (5): Interior girder

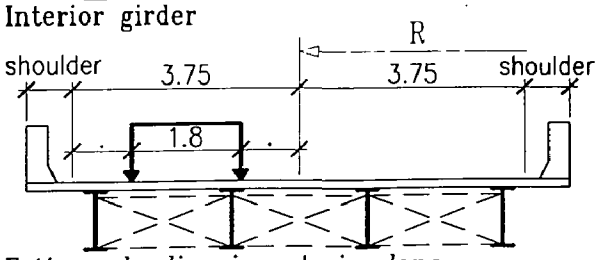

Case (6): Fatigue, loading in exterior lane

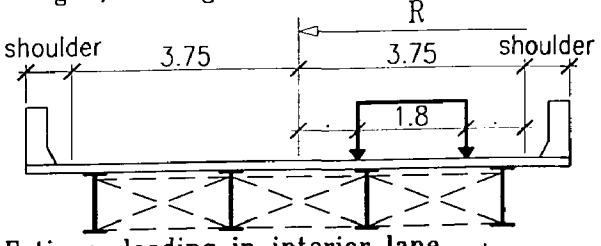

Case (7): Fatigue, loading in interior lane

Dimensions are in meters

Figure 3.4 Live loading cases for Two-lane bridge

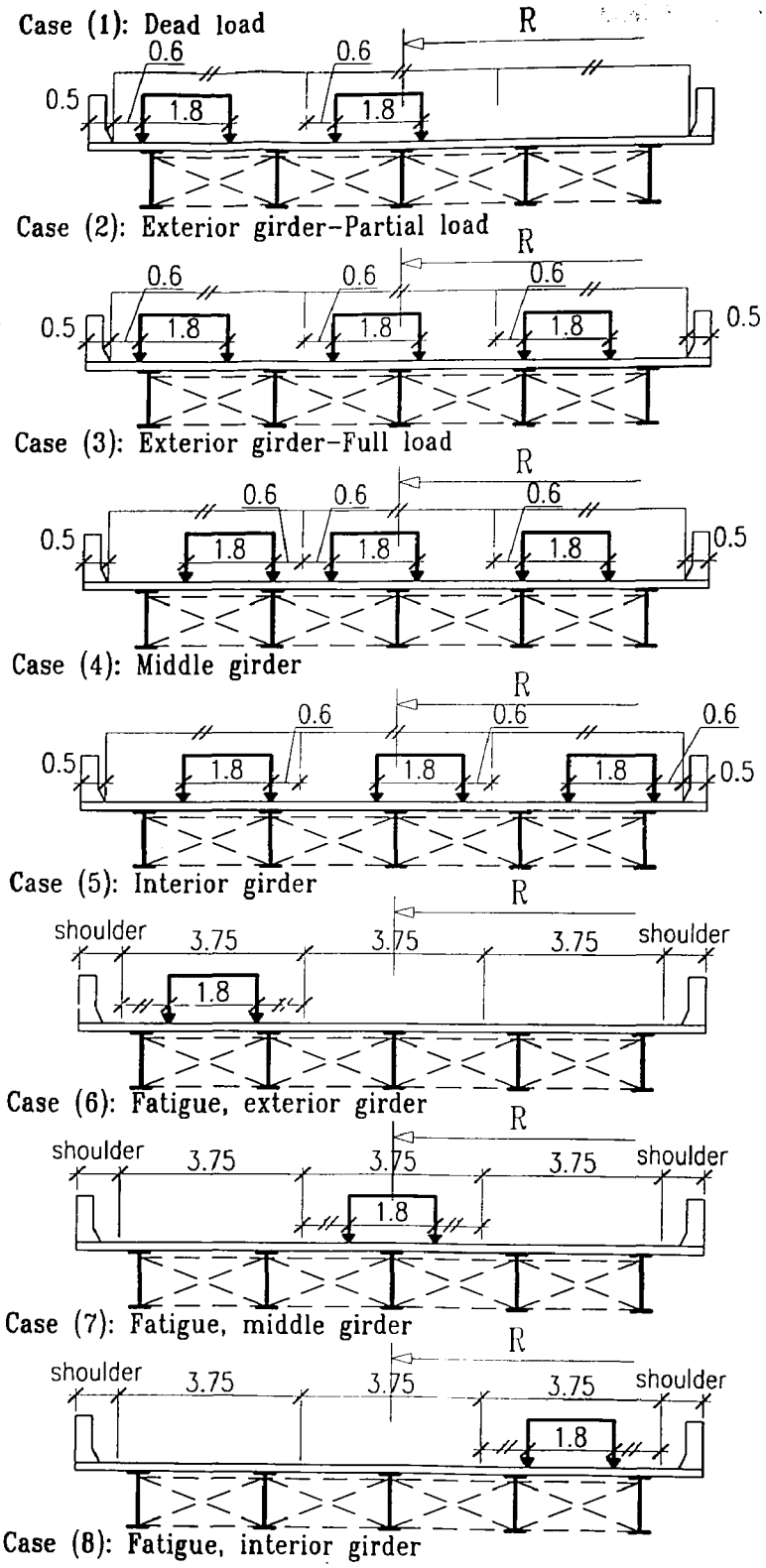

Dimensions are in meters

Figure 3.5 Live loading cases for Three–lane bridge

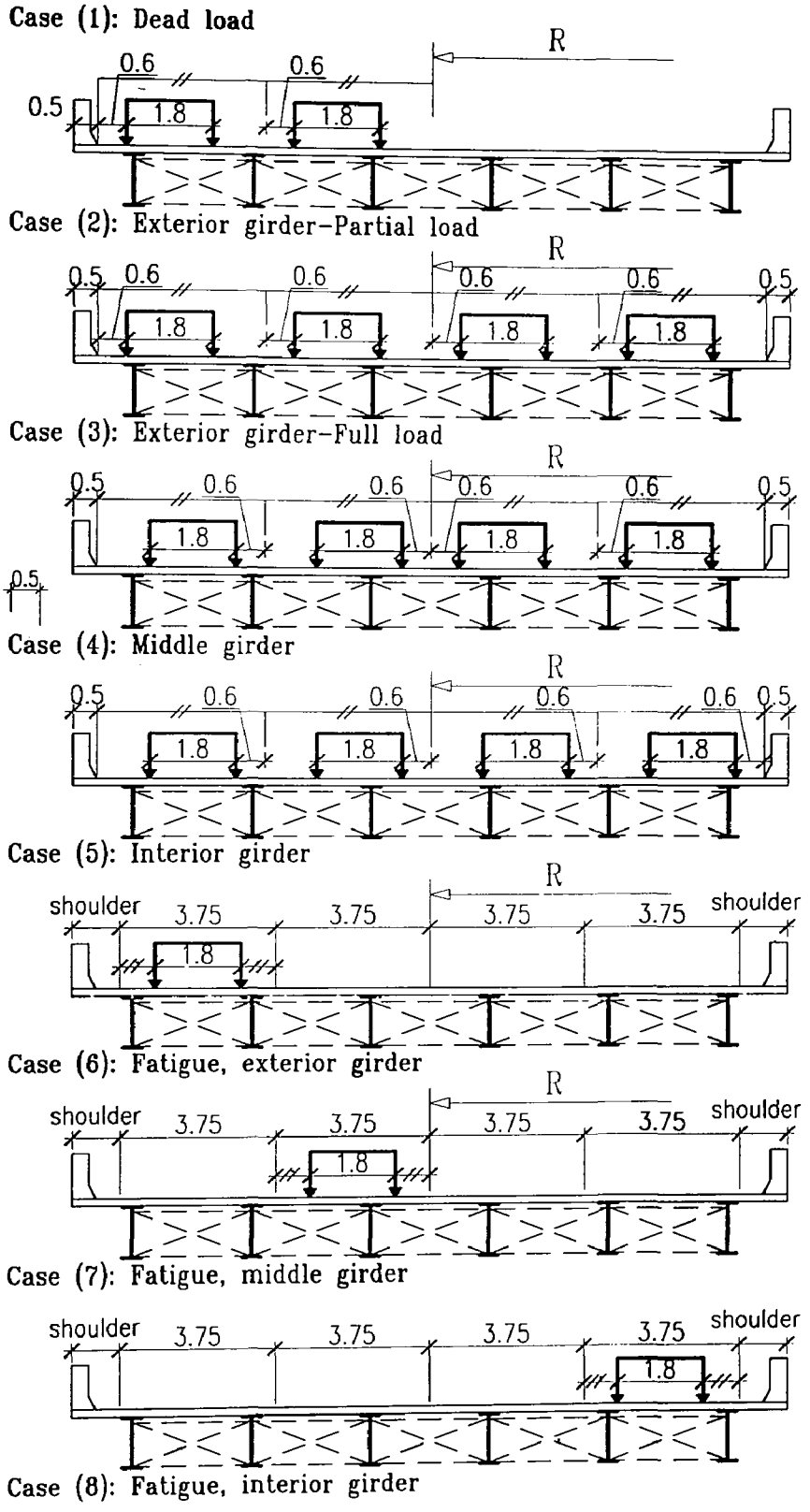

Figure 3.6 Live loading cases for four-lane bridge

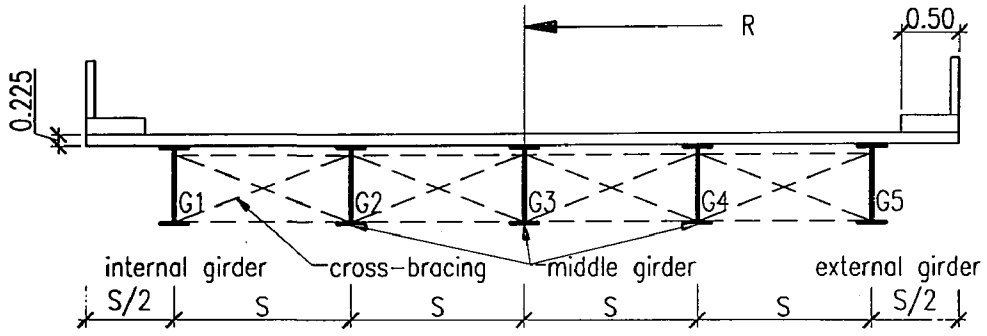

Figure 3.7 Cross-Section of a Composite I-Girder Bridge

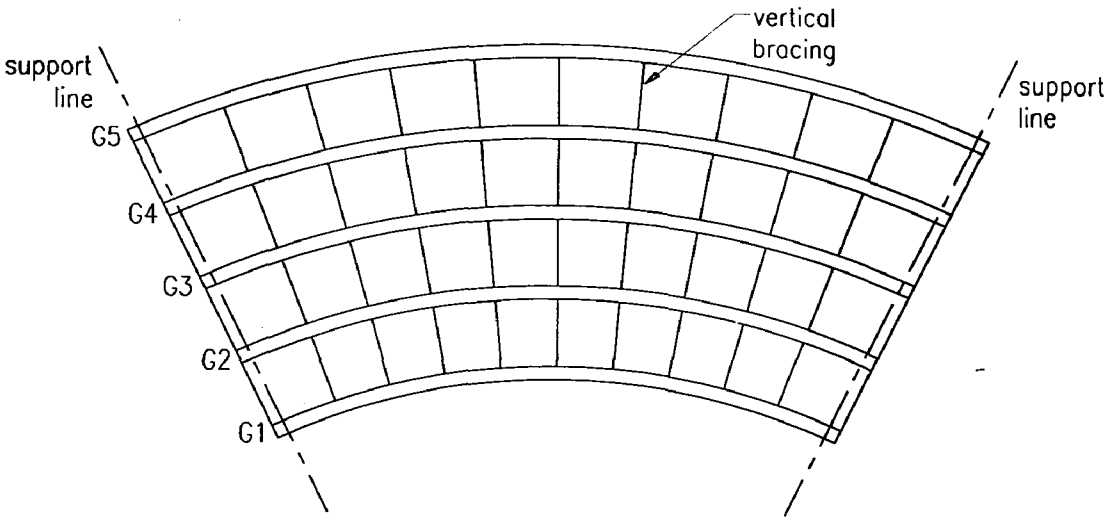

a) I-Girder with Radial Cross-Bracings

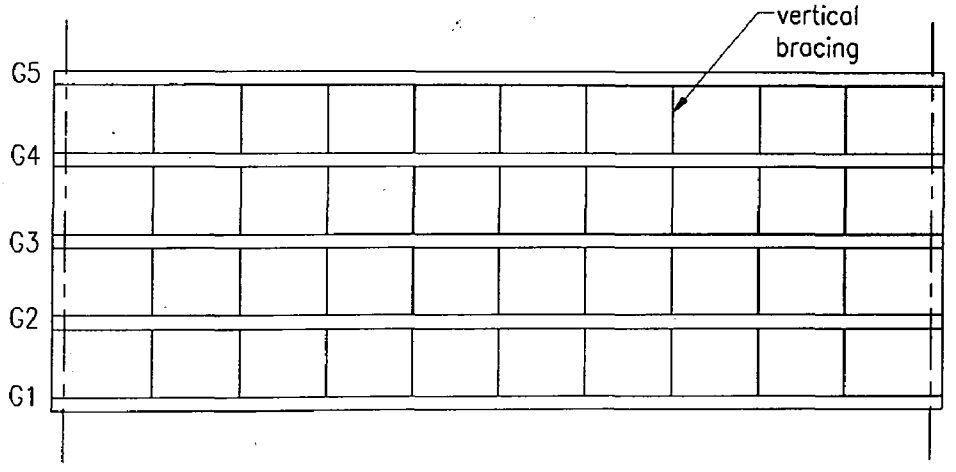

b) I-Girder with Transverse Cross-Bracings

Figure 3.8 Plan of the Steel-Girder Arrangement

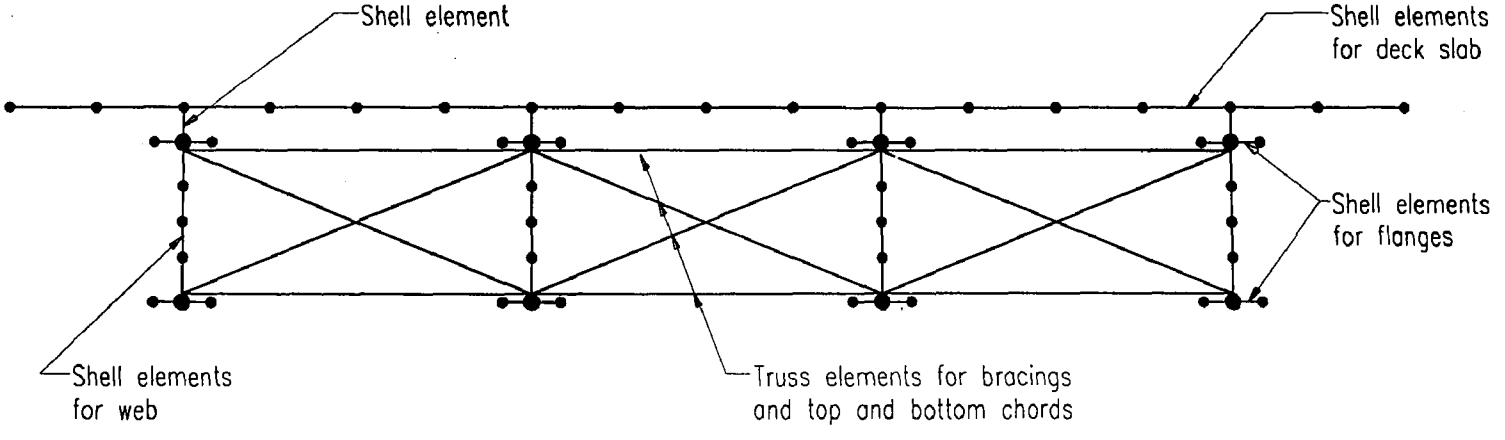

Figure 3.9 Finite element representation of bridge cross-section

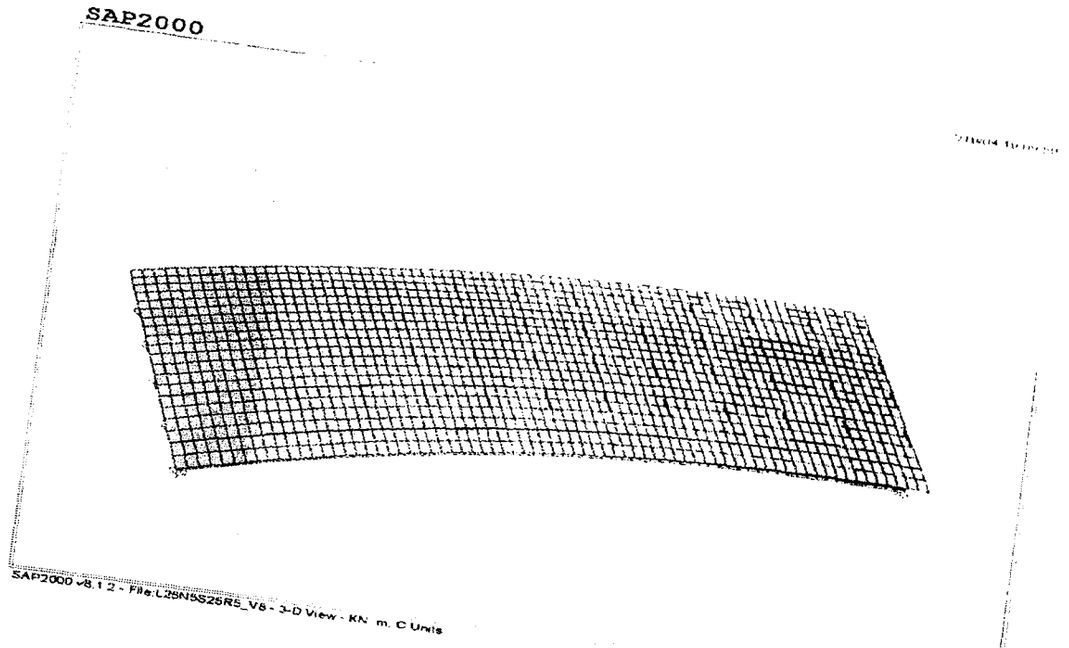

(a) View with concrete deck

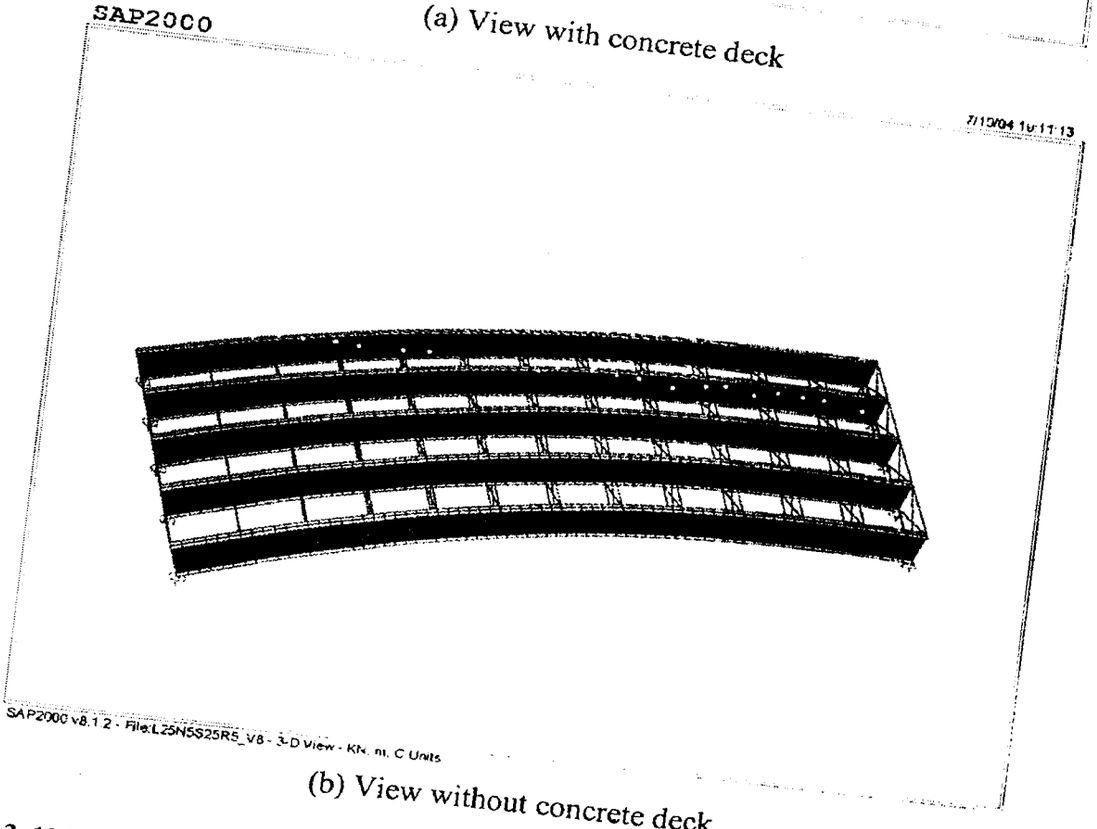

(b) View without concrete deck

Figure 3. 10 Views of SAP2000 Finite-Element Model

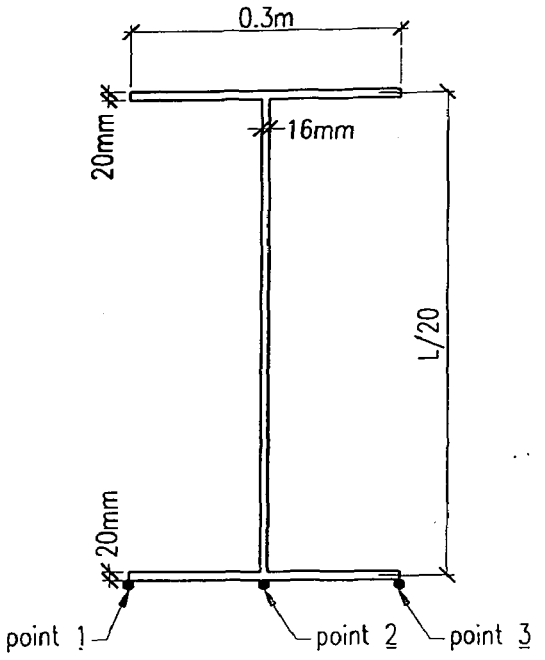

Figure 3.11 Cross-Section Dimesions of the steel girder

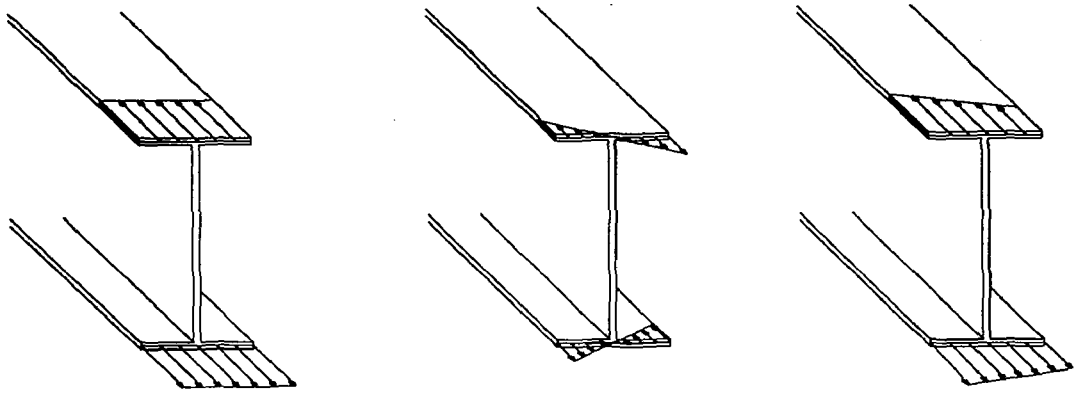

Figure 3.12 Normal Stress Distribution in Curved I-Girder Flanges

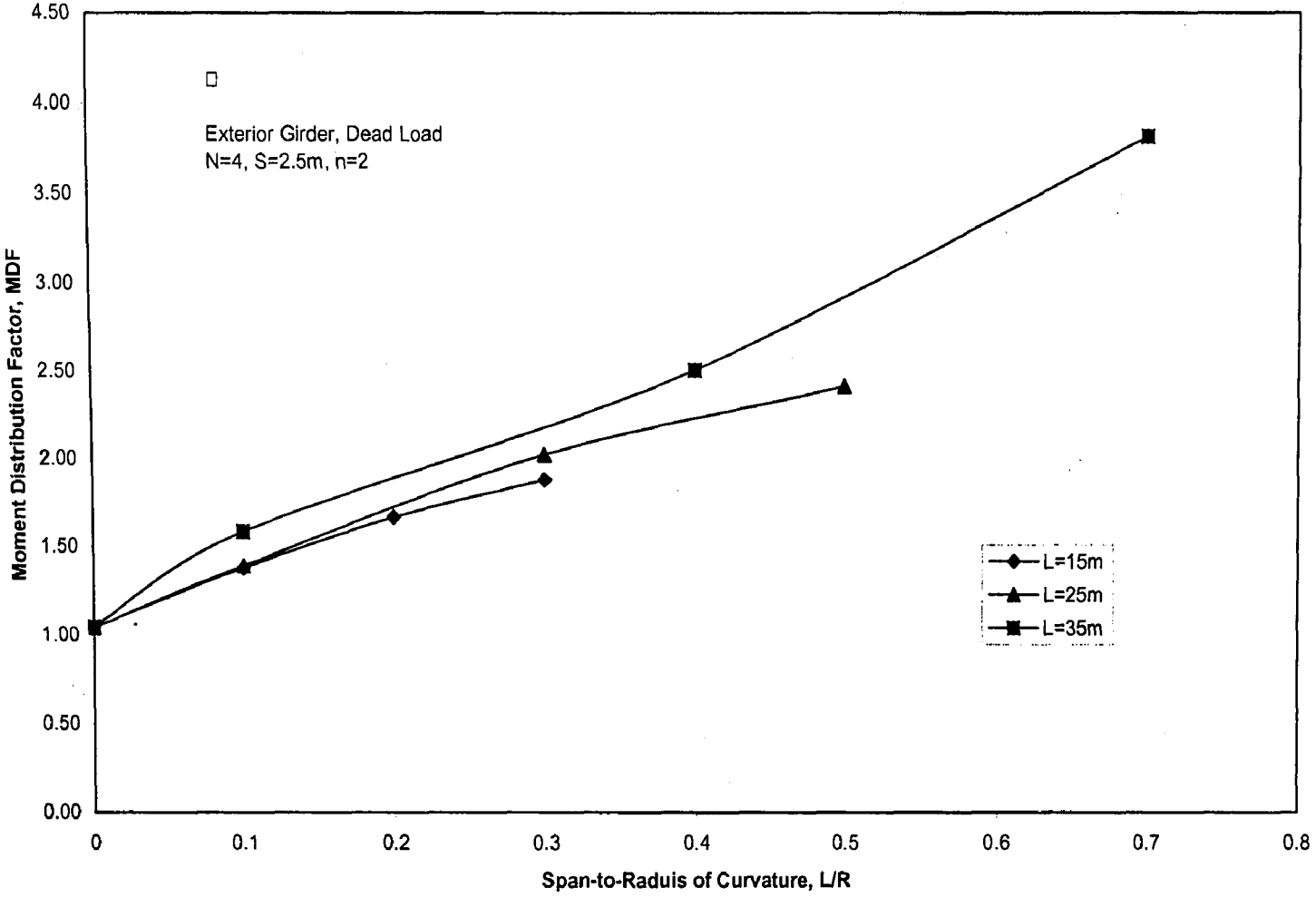

Figure 4.1 Effect of curvature on the moment distribution factor for the exterior girder due to dead load

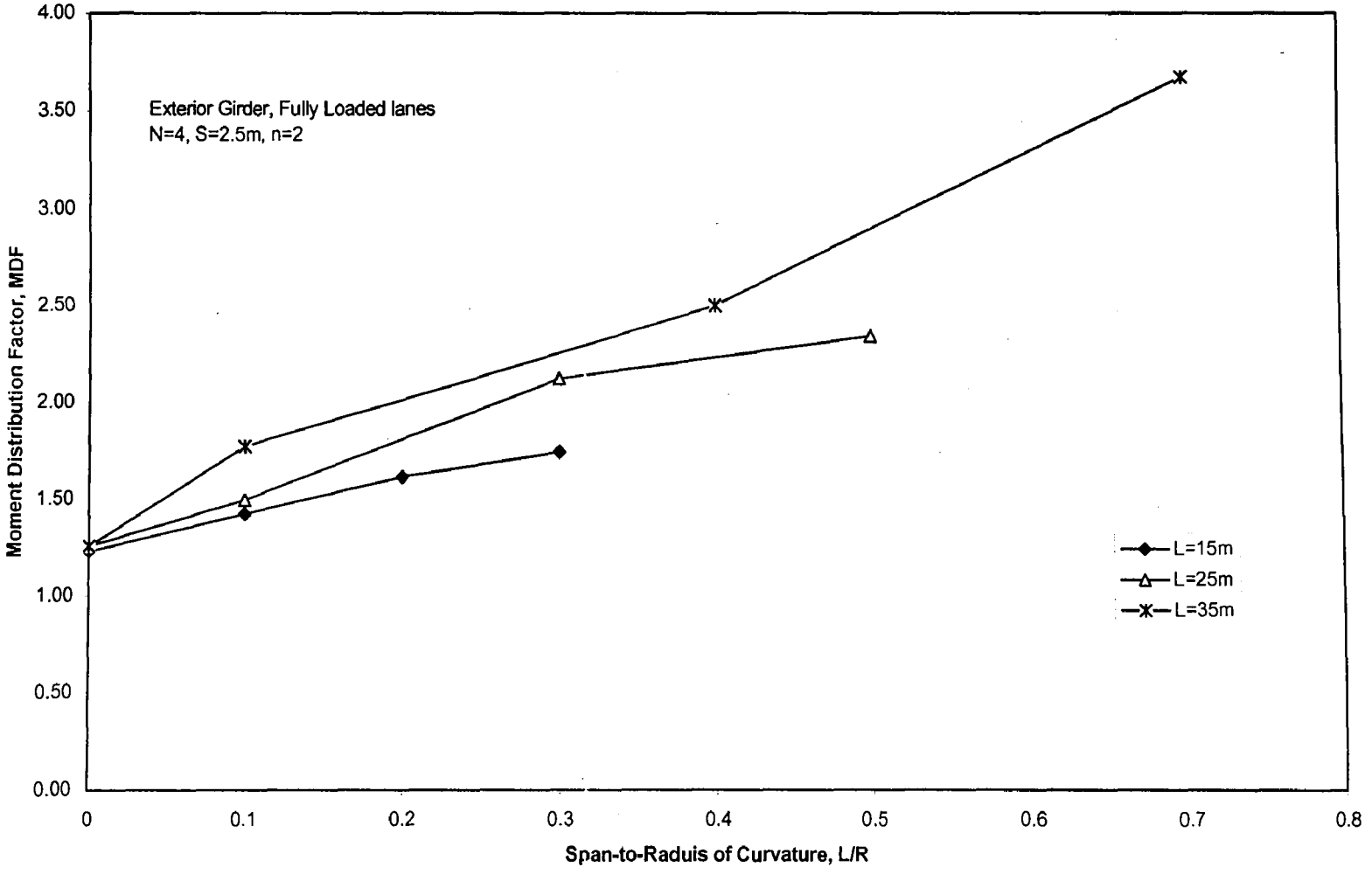

Figure 4.2 Effect of curvature on the moment distribution factor for the exterior girder due to fully loaded lanes

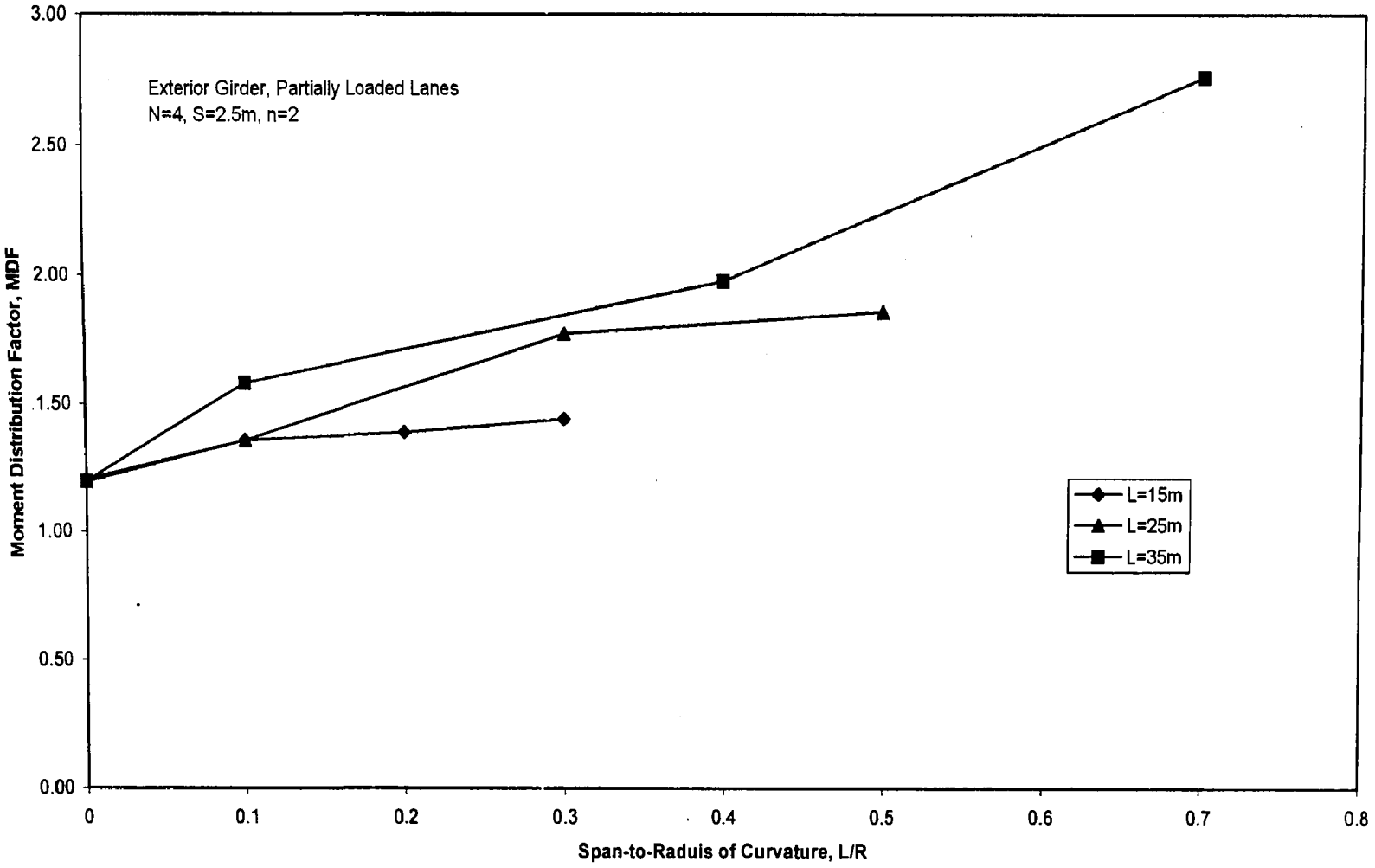

Figure 4.3 Effect of curvature on the moment distribution factor for the exterior girder due to partially loaded lanes

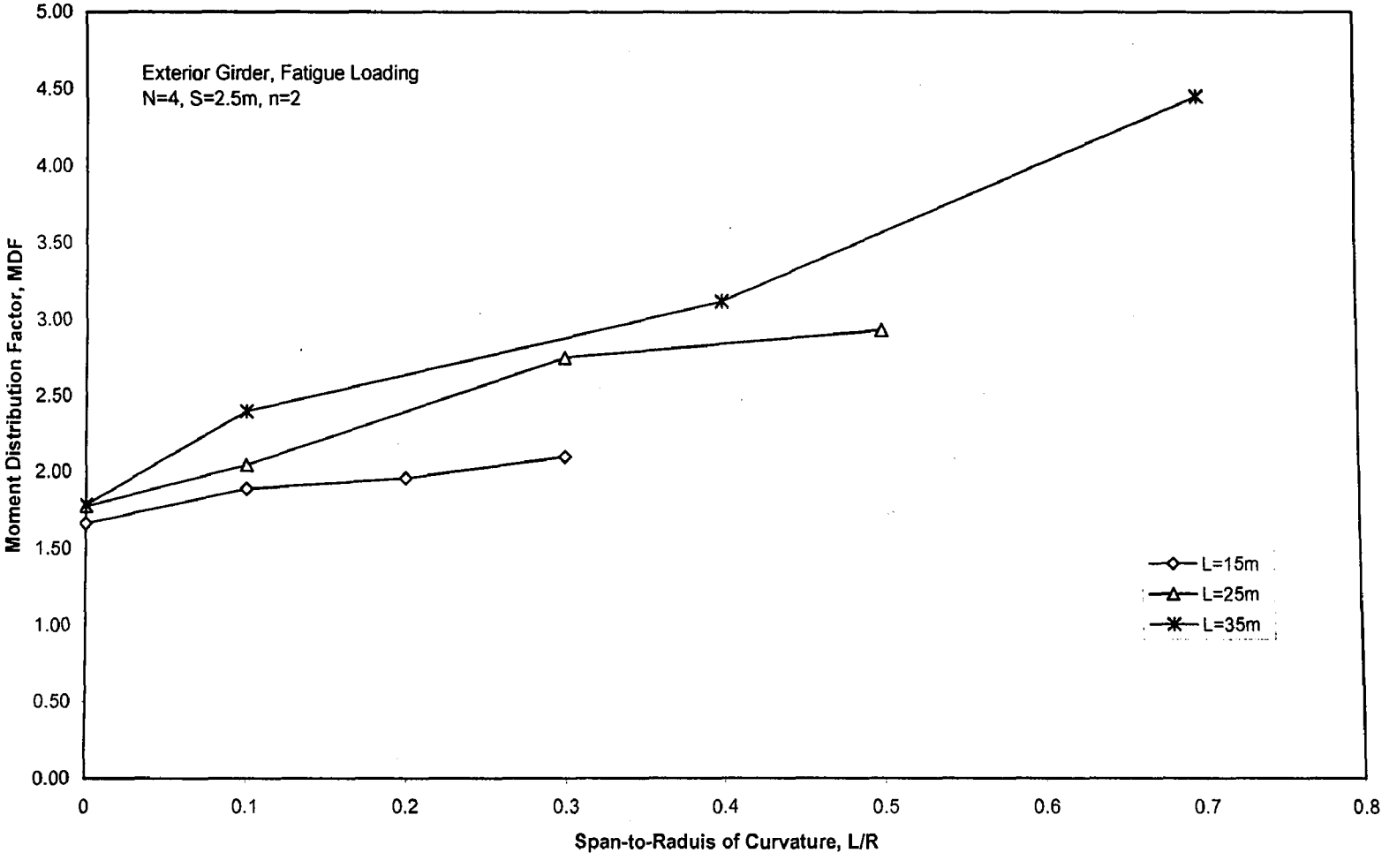

Figure 4.4 Effect of curvature on the moment distribution factor for the exterior girder due to fatigue loading

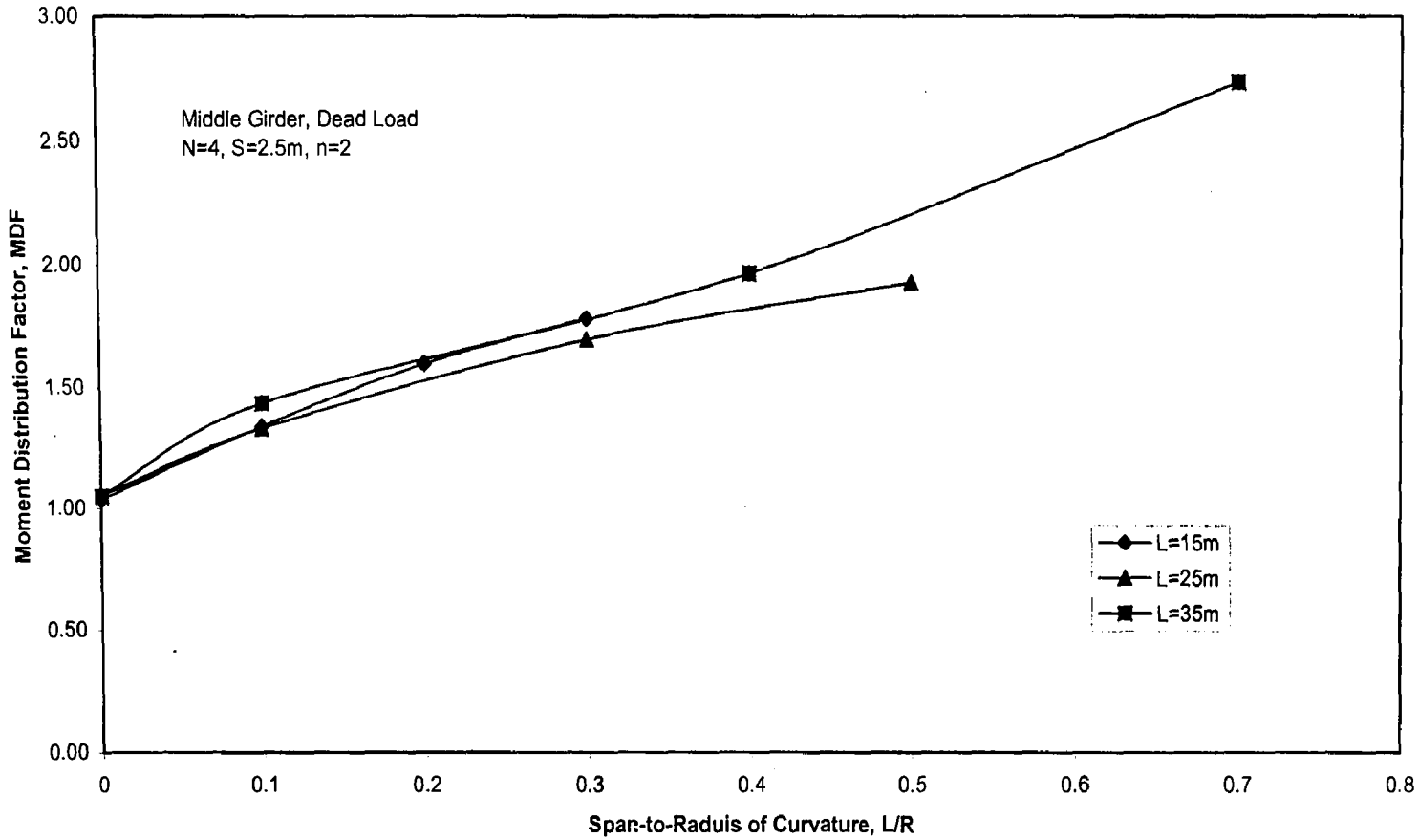

Figure 4.5 Effect of curvature on the moment distribution factor for the middle girder due to dead load

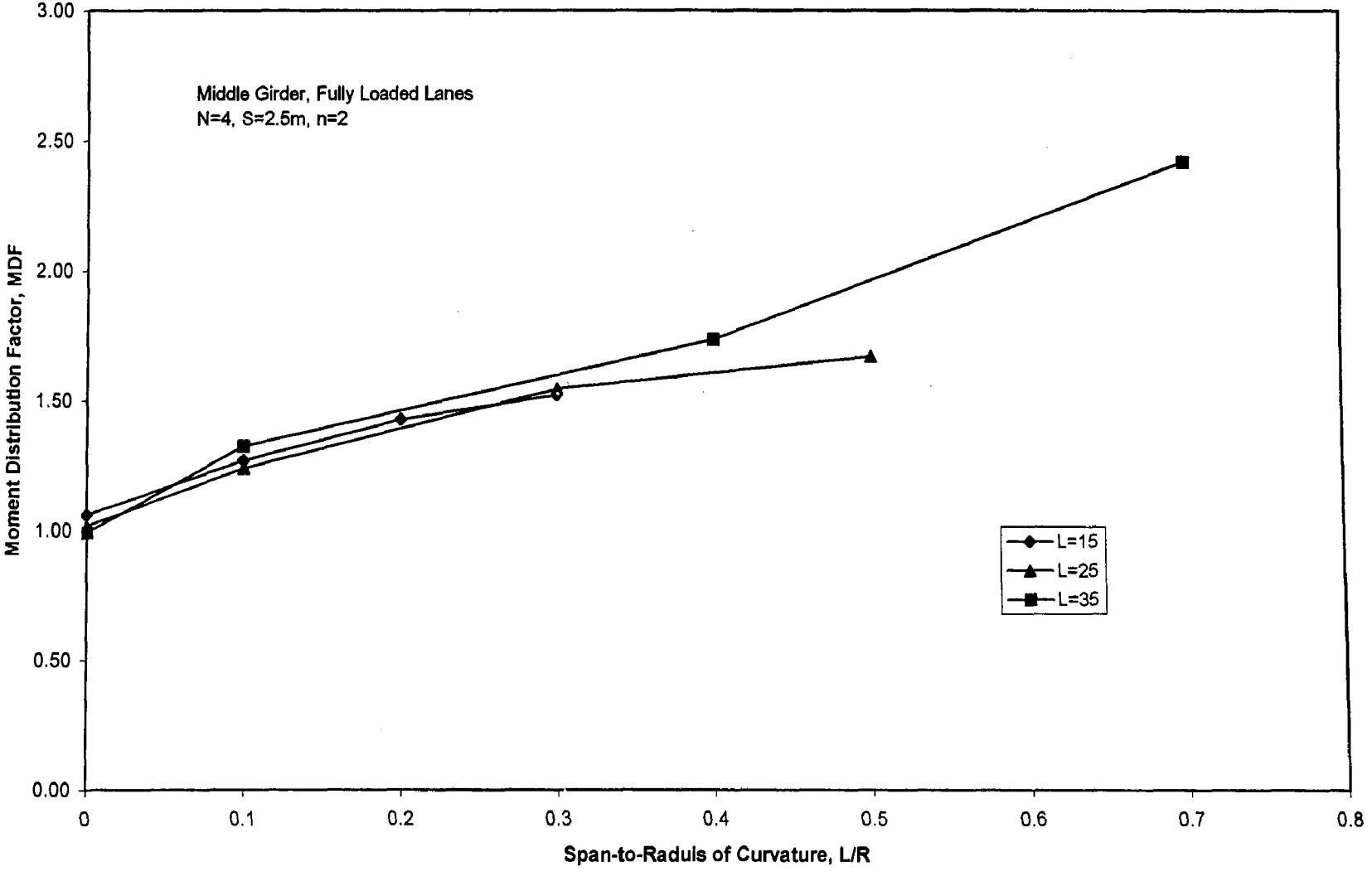

Figure 4.6 Effect of curvature on the moment distribution factor for the middle girder due to fully loaded lanes

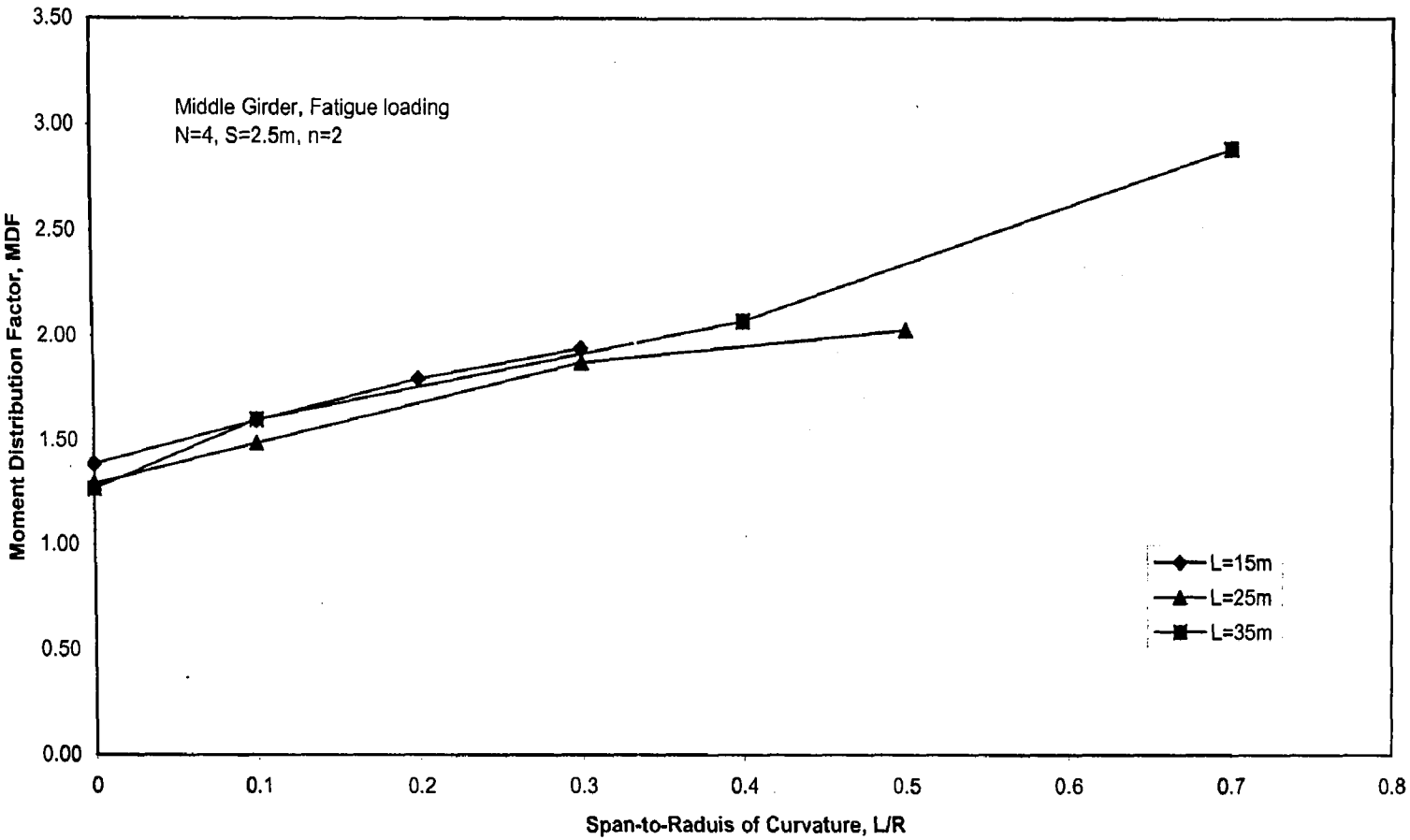

Figure 4.7 Effect of curvature on the moment distribution factor for the middle girder due to fatigue loading

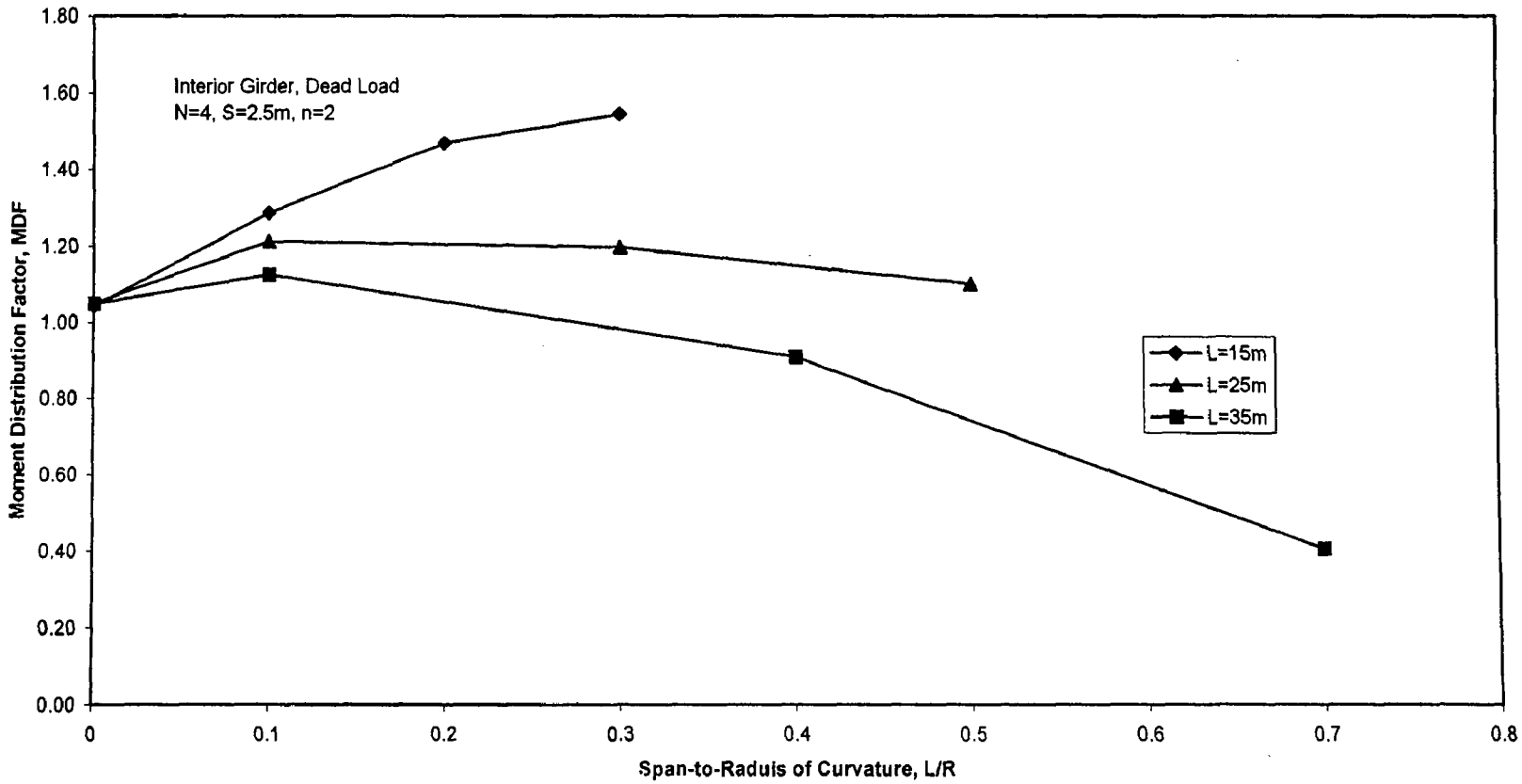

Figure 4.8 Effect of curvature on the moment distribution factor for the interior girder due to dead load

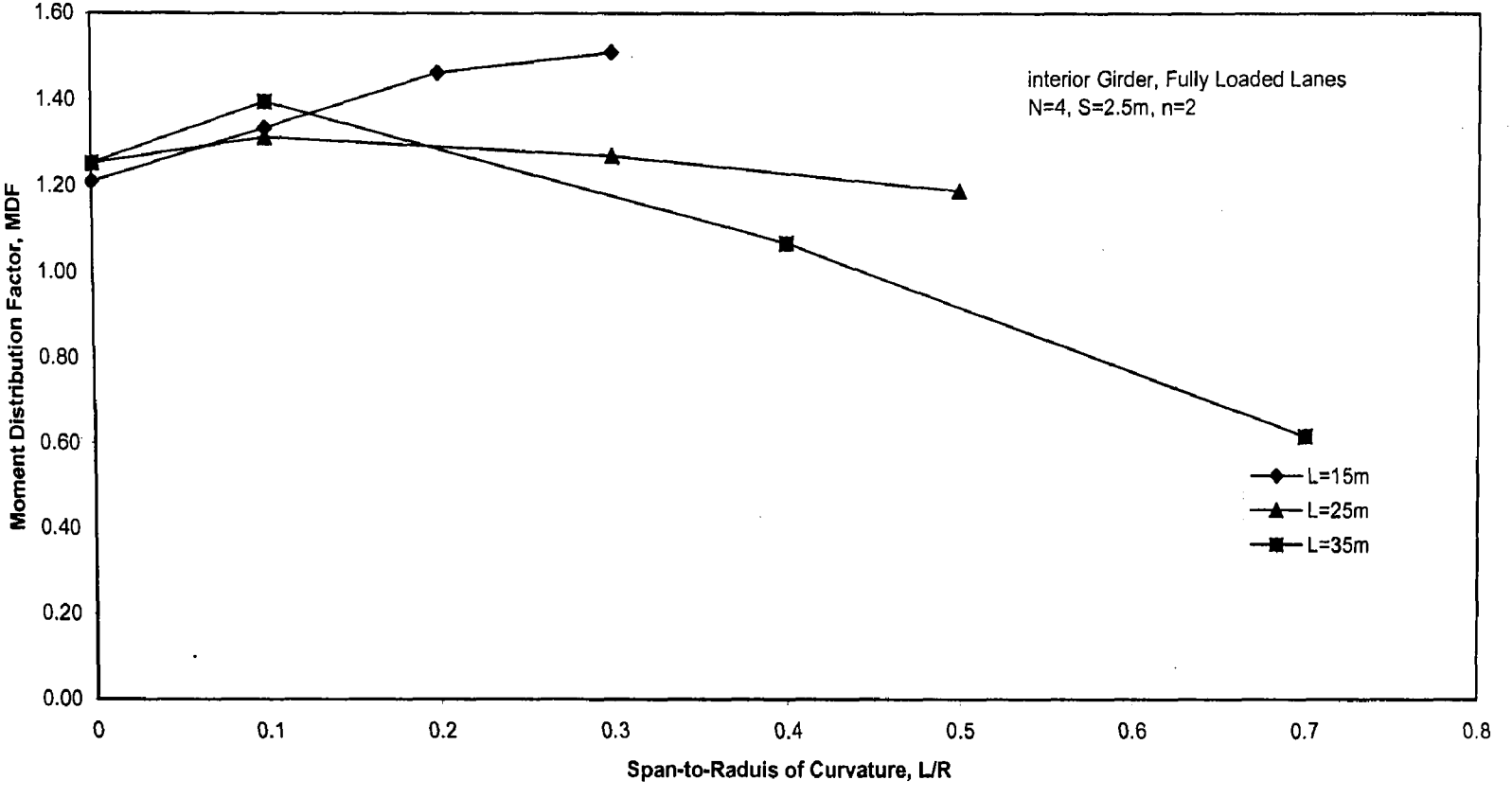

Figure 4.9 Effect of curvature on the moment distribution factor for the interior girder due to fully loaded lanes

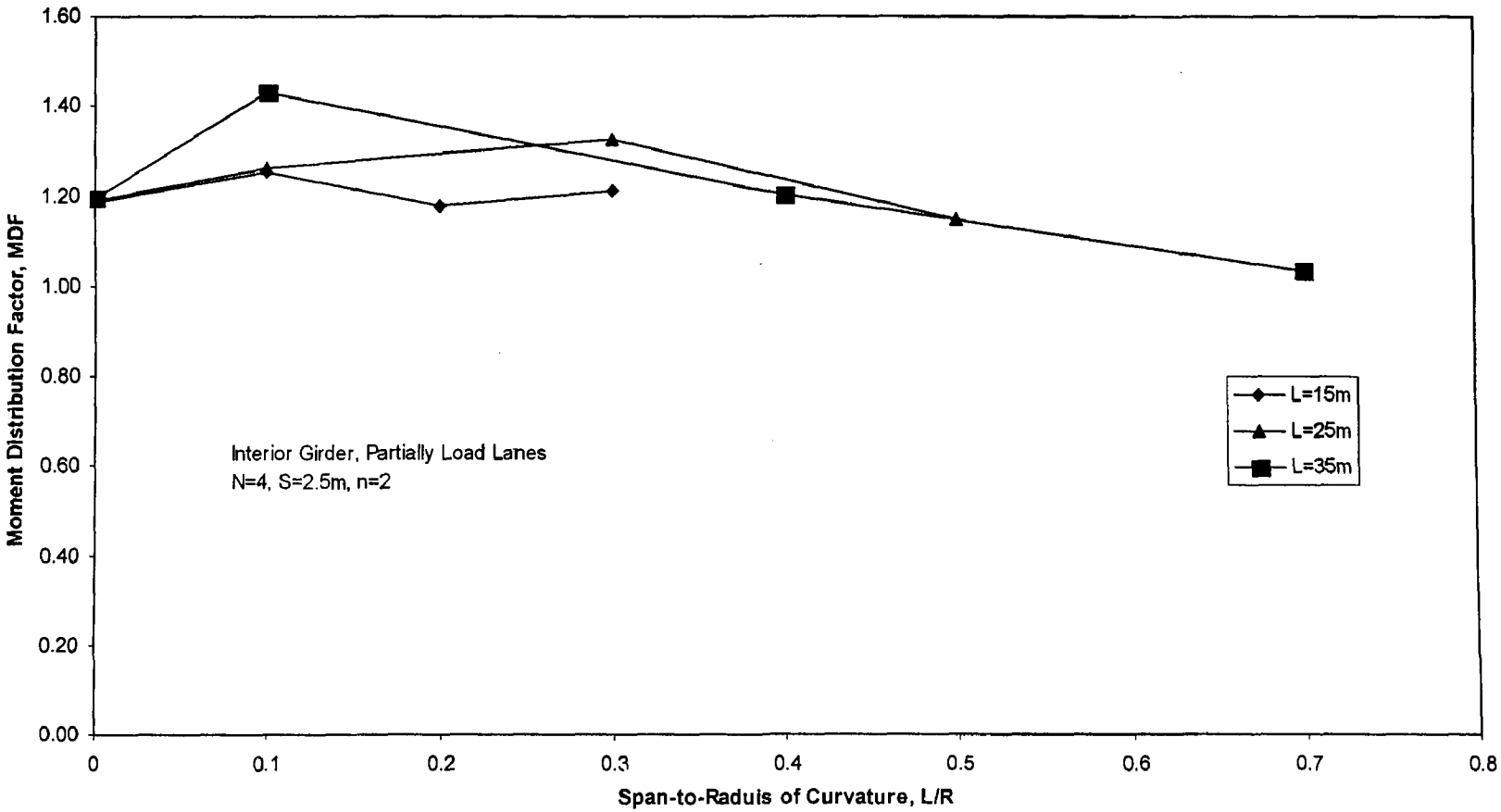

Figure 4.10 Effect of curvature on the moment distribution factor for the interior girder due to partially loaded lanes

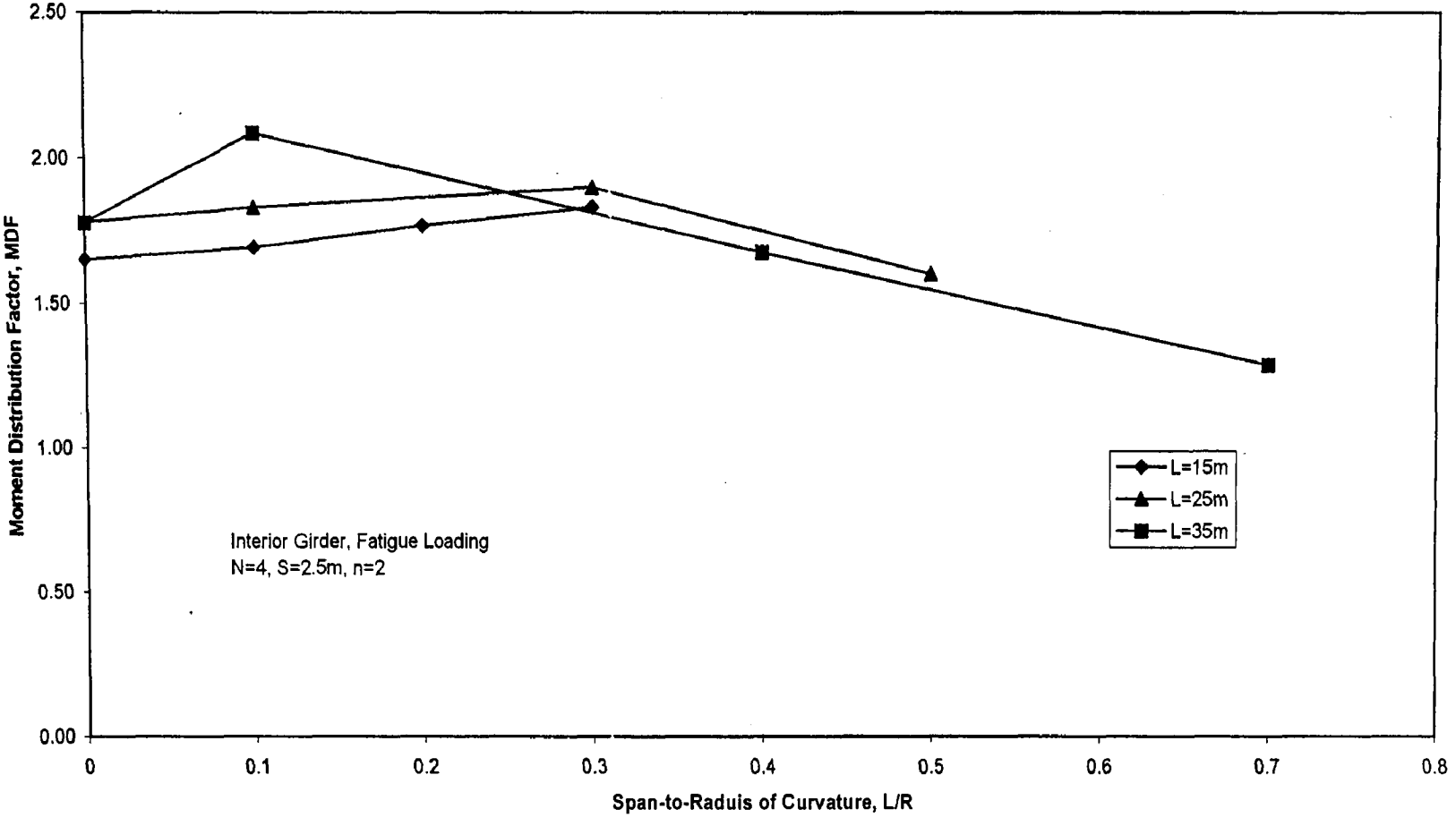

Figure 4.11 Effect of curvature on the moment distribution factor for the interior girder due to fatigue loading

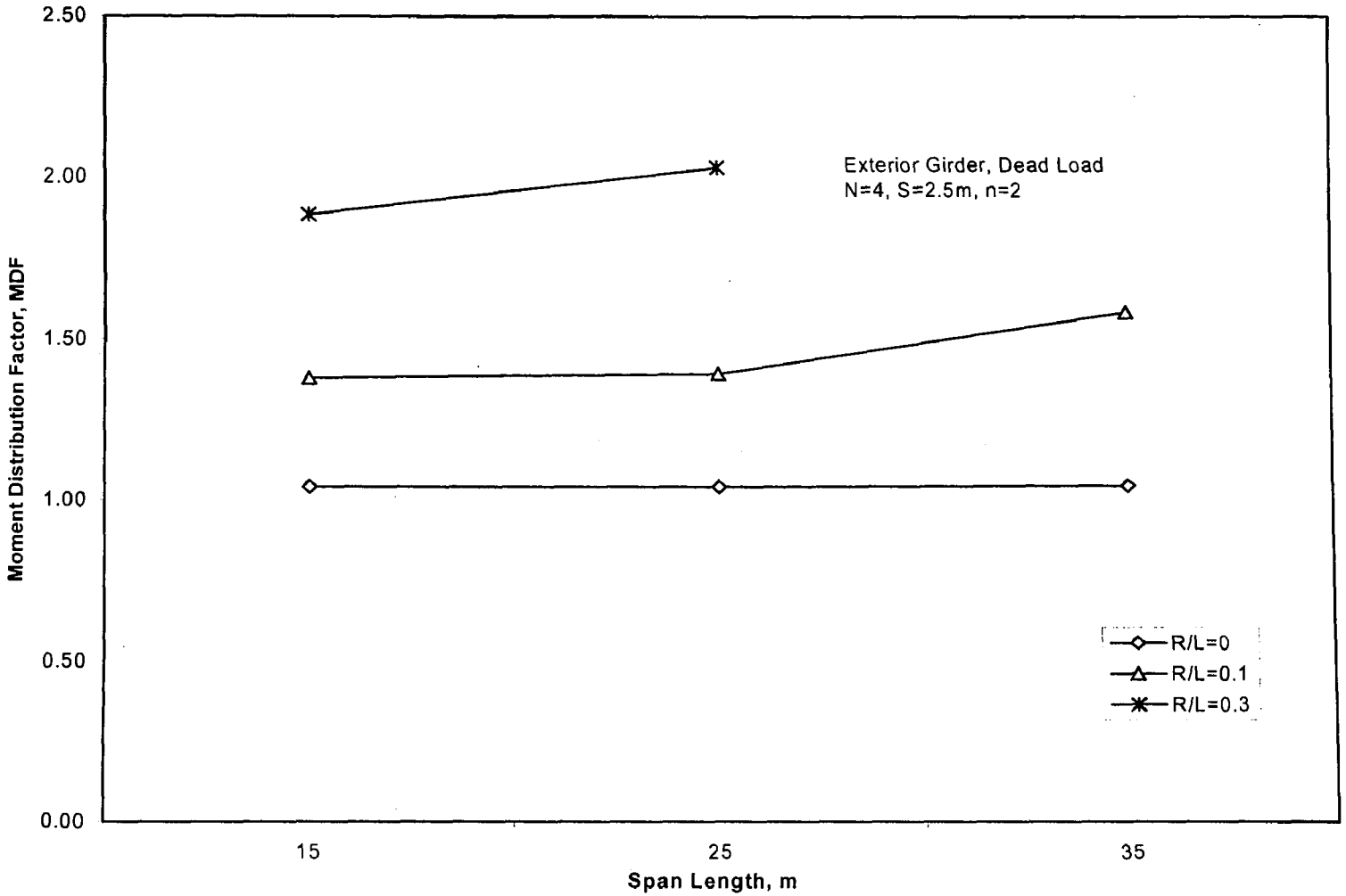

Figure 4.12 Effect of span length on the moment distribution factor for the exterior girder due to dead load

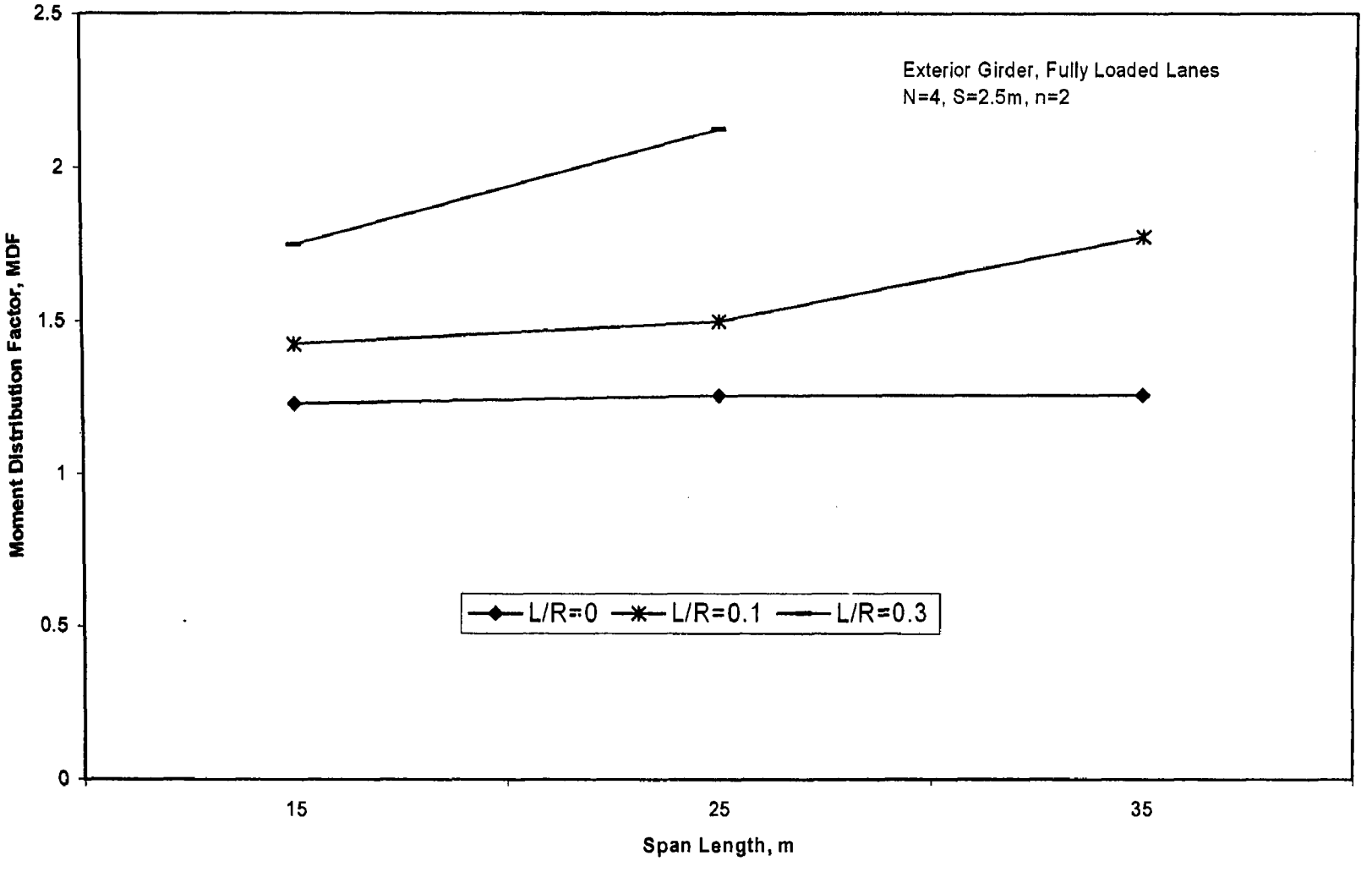

Figure 4.13 Effect of span length on the moment distribution factor for the exterior girder due to fully loaded lanes

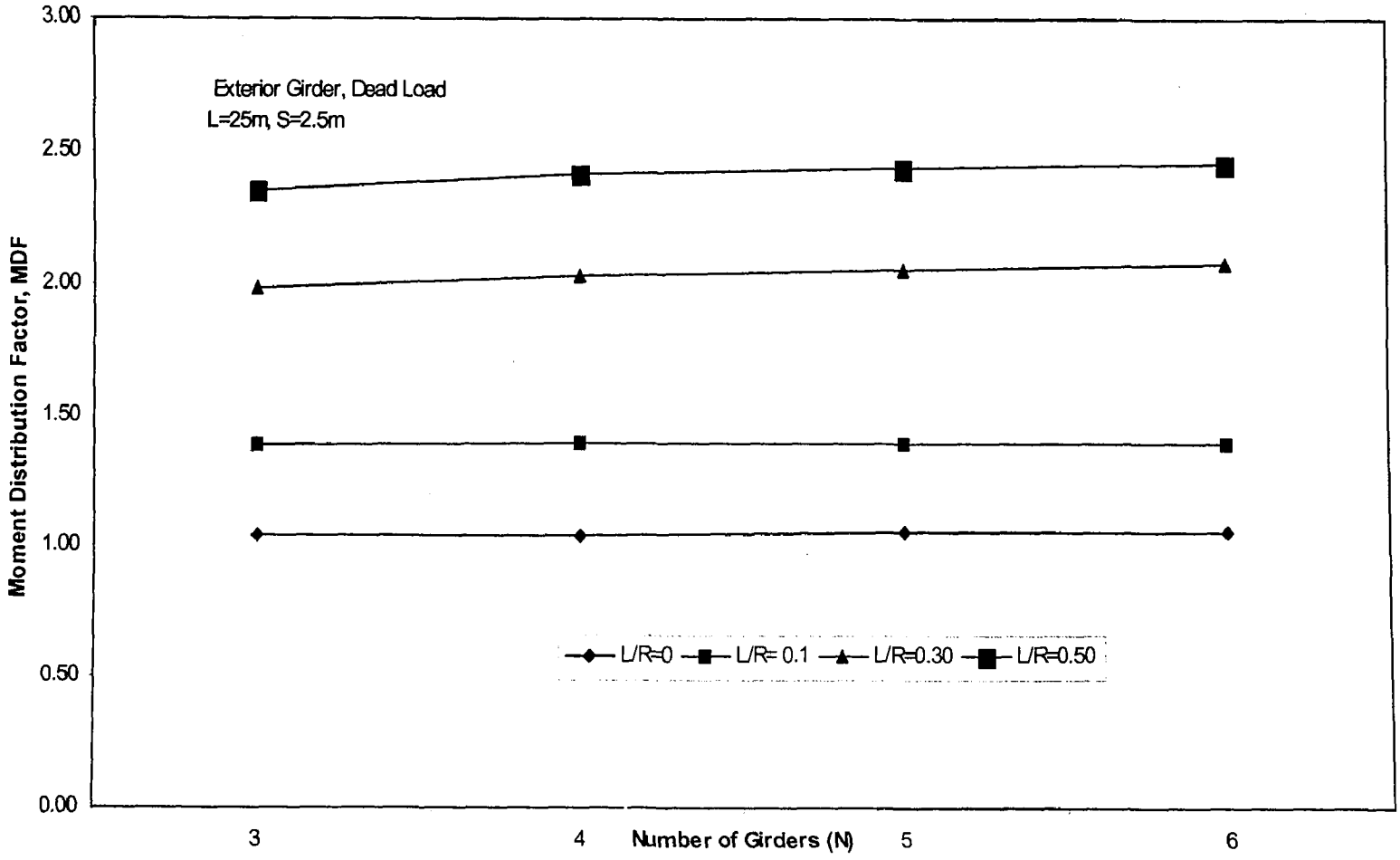

Figure 4.14 Effect of number of girders on the moment distribution factor for the exterior girder due to dead load

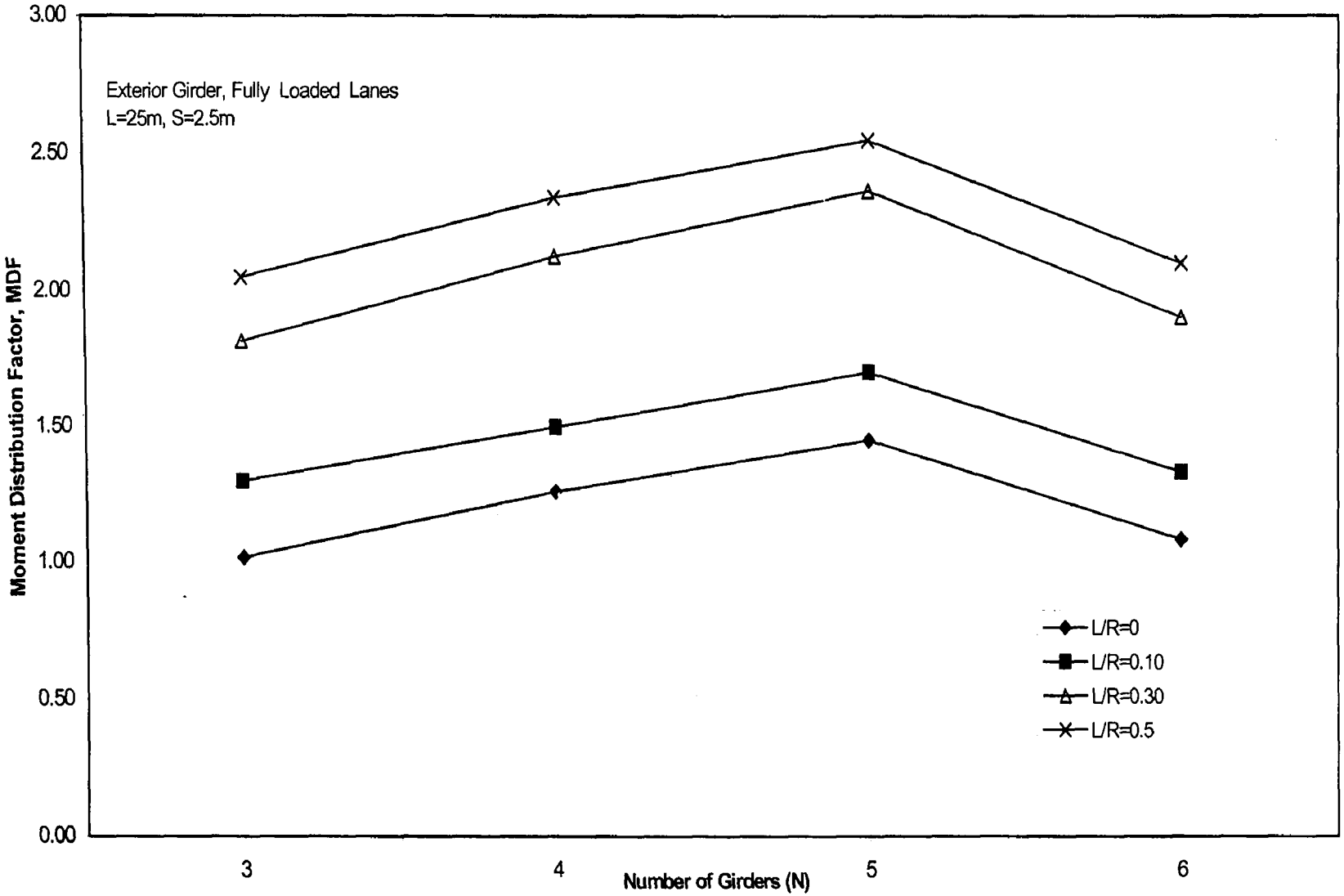

Figure 4.15 Effect of number of girders on the moment distribution factor for the exterior girder due to fully loaded lanes

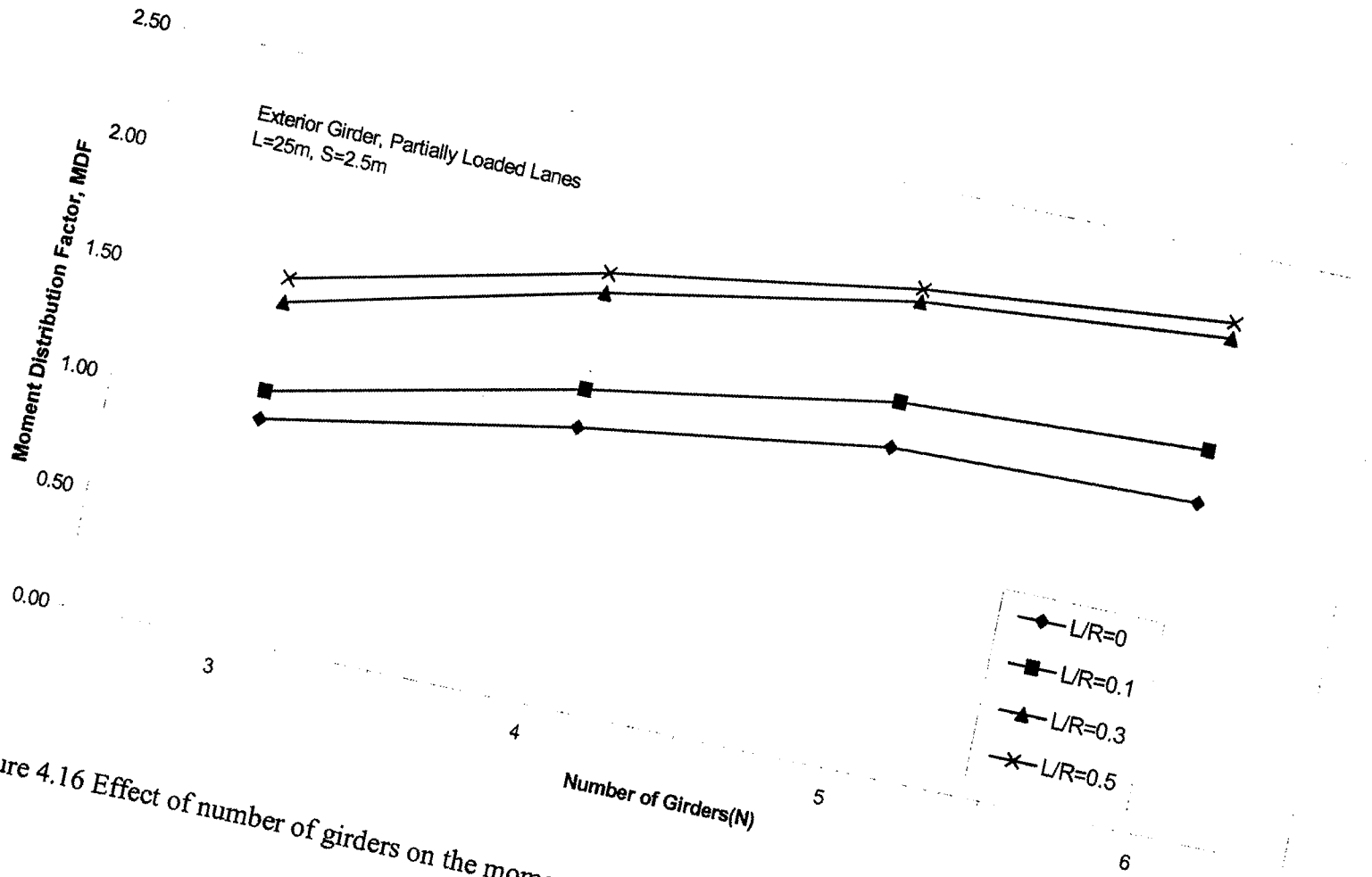

Figure 4.16 Effect of number of girders on the moment distribution factor for the exterior girder due to partially loaded lanes

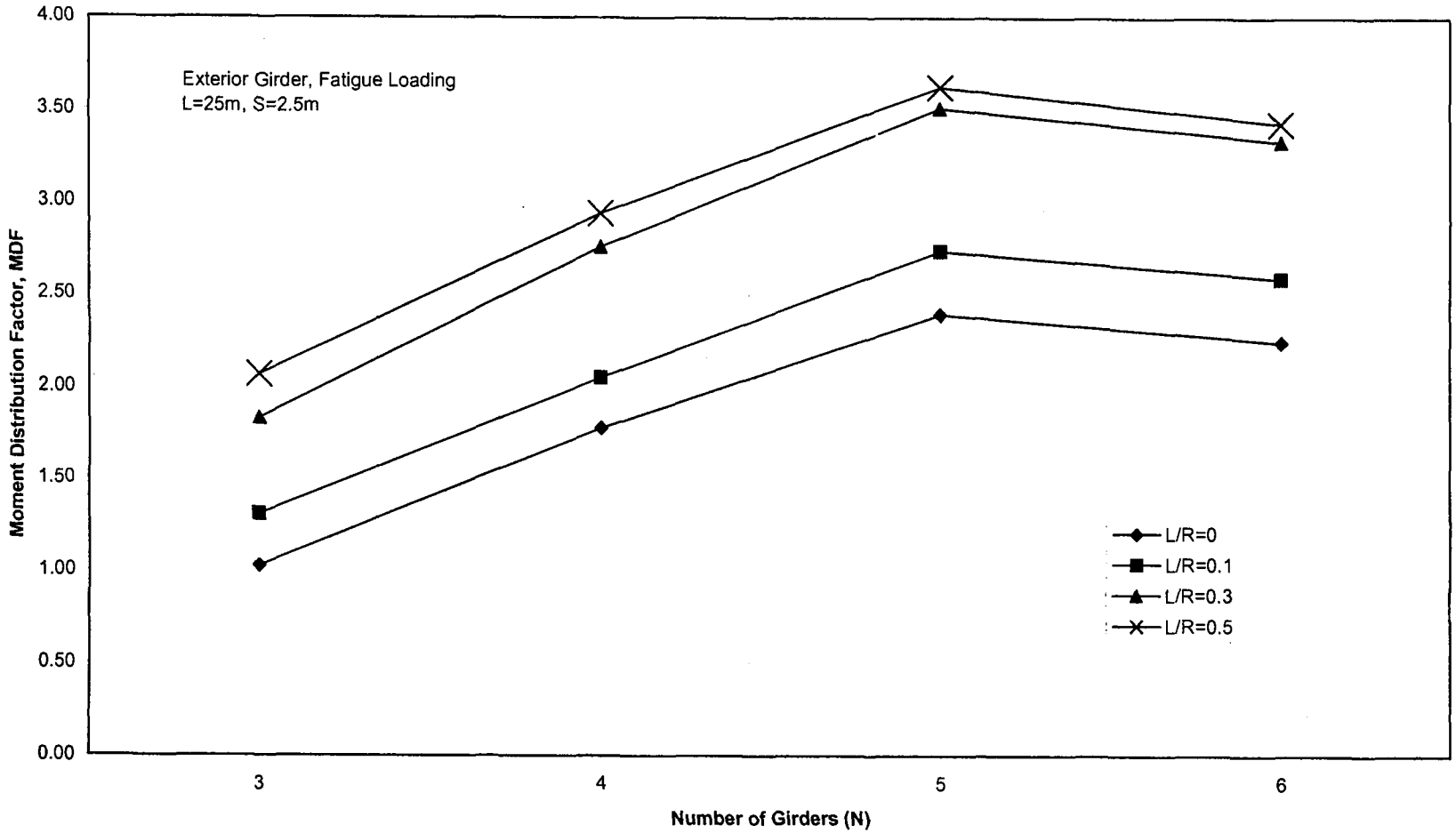

Figure 4.17 Effect of number of girders on the moment distribution factor for the exterior girder due to fatigue loading

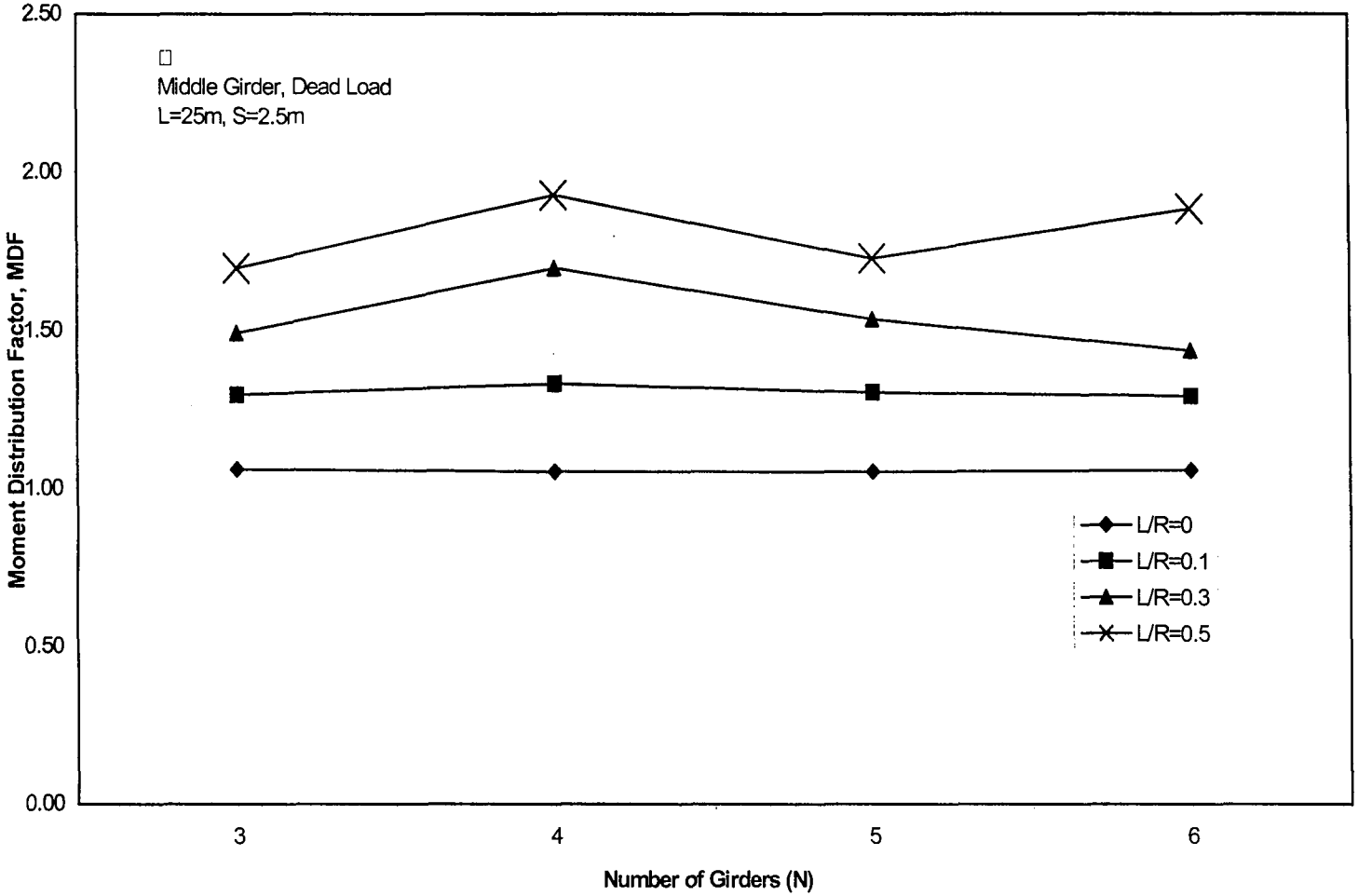

Figure 4.18 Effect of number of girders on the moment distribution factor for the middle girder due to dead load

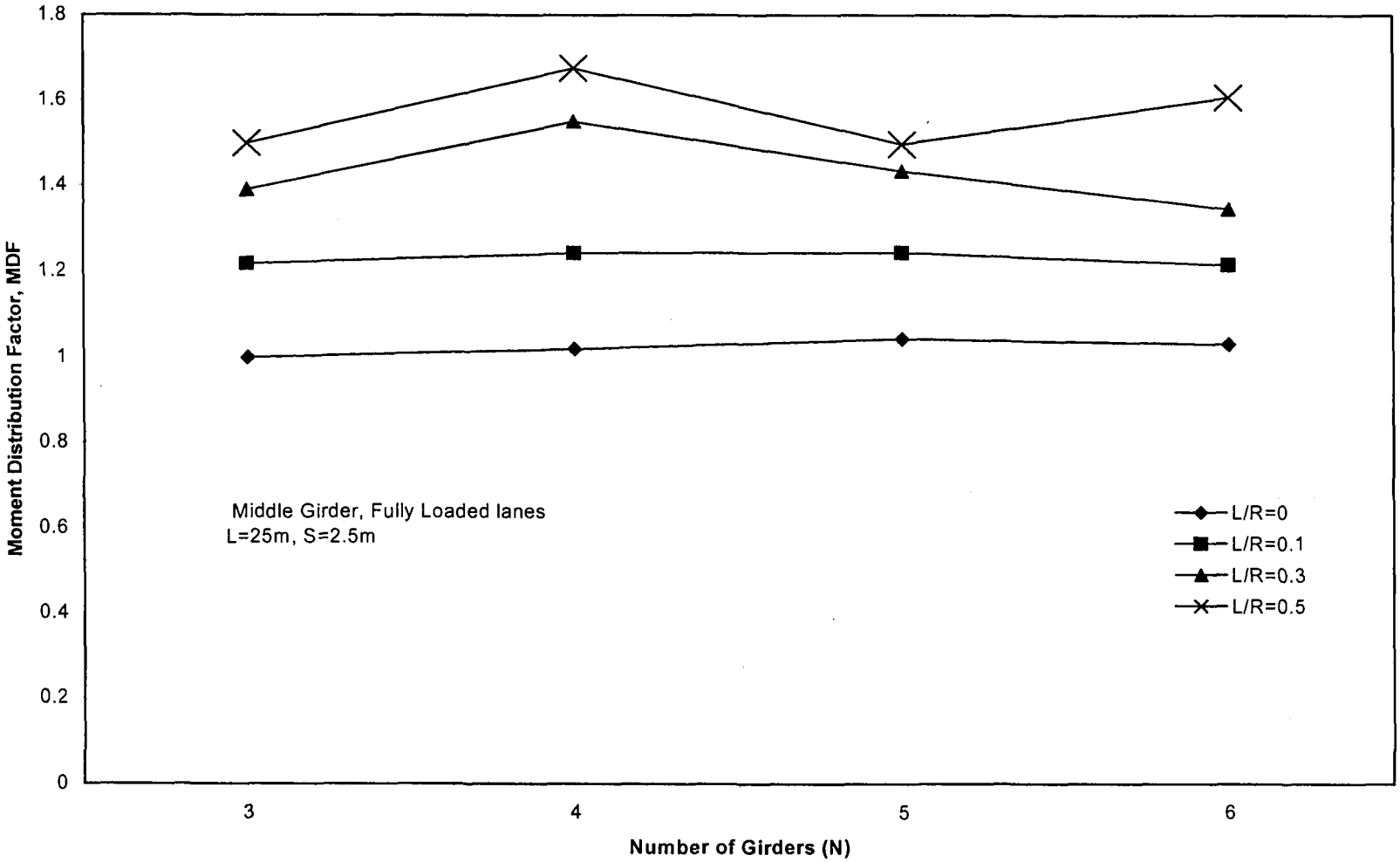

Figure 4.19 Effect of number of girders on the moment distribution factor for the middle girder due to fully loaded lanes

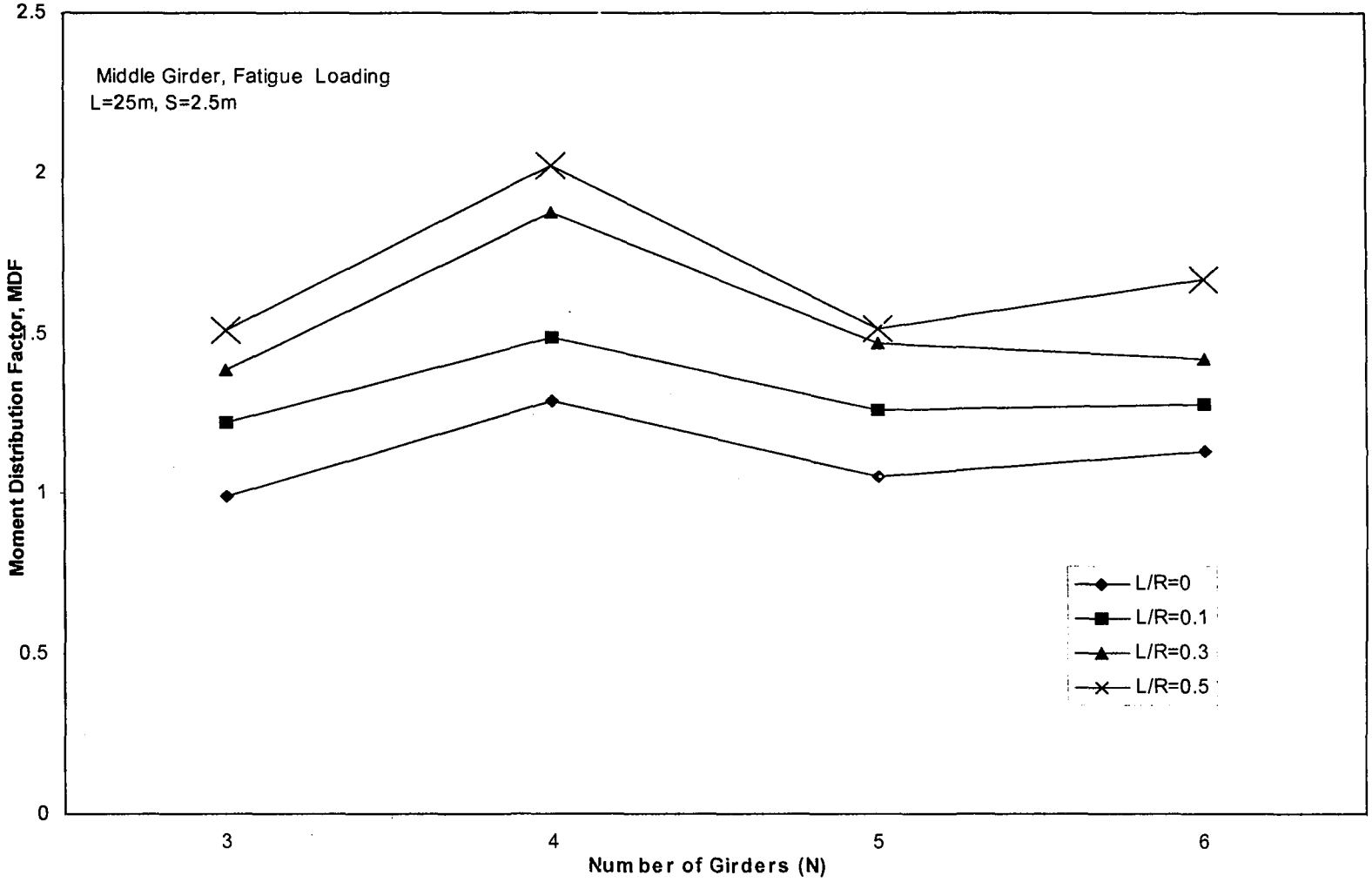

Figure 4.20 Effect of number of girders on the moment distribution factor for the middle girder due to fatigue loading

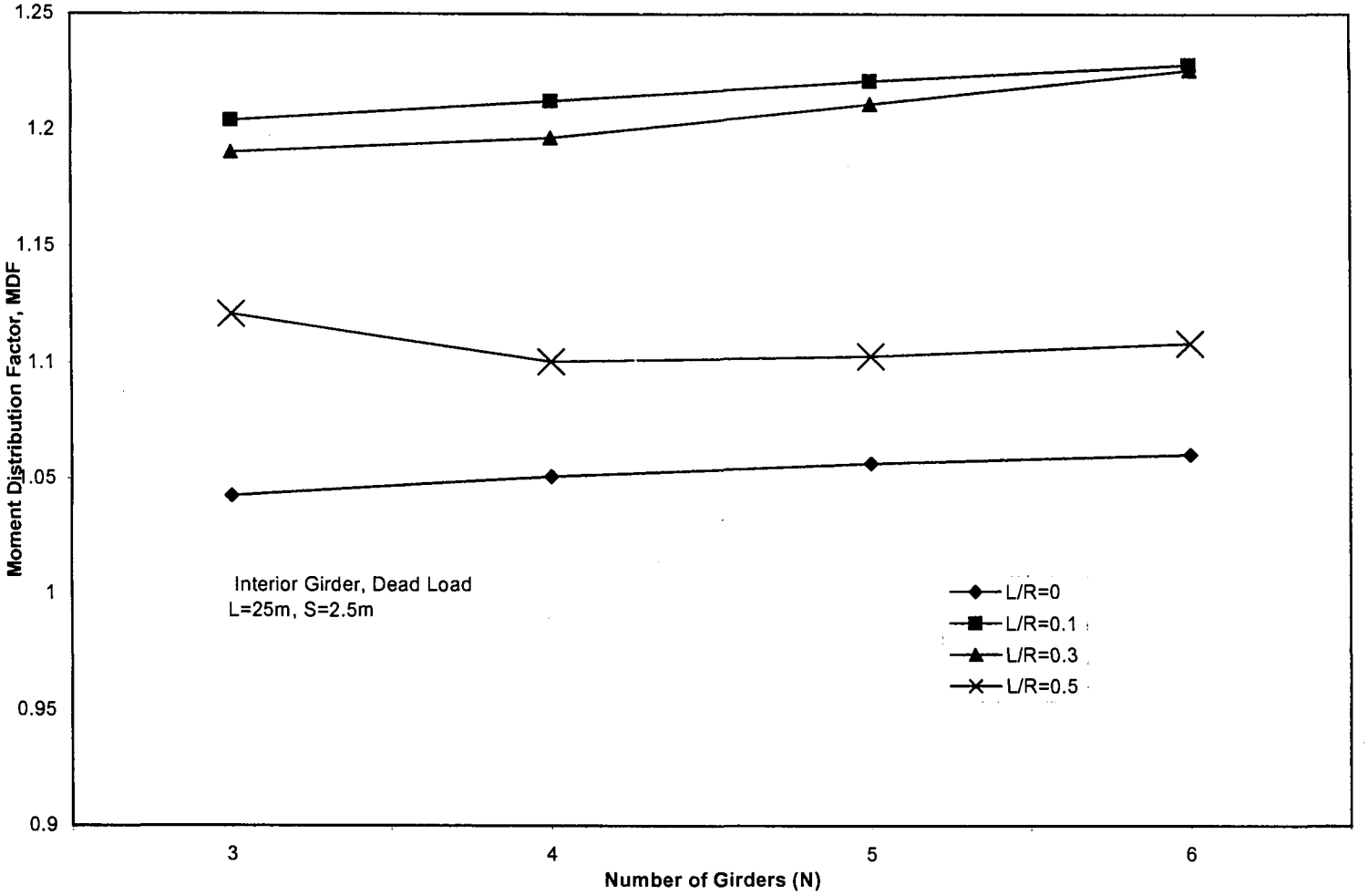

Figure 4.21 Effect of number of girders on the moment distribution factor for the interior girder due to dead load

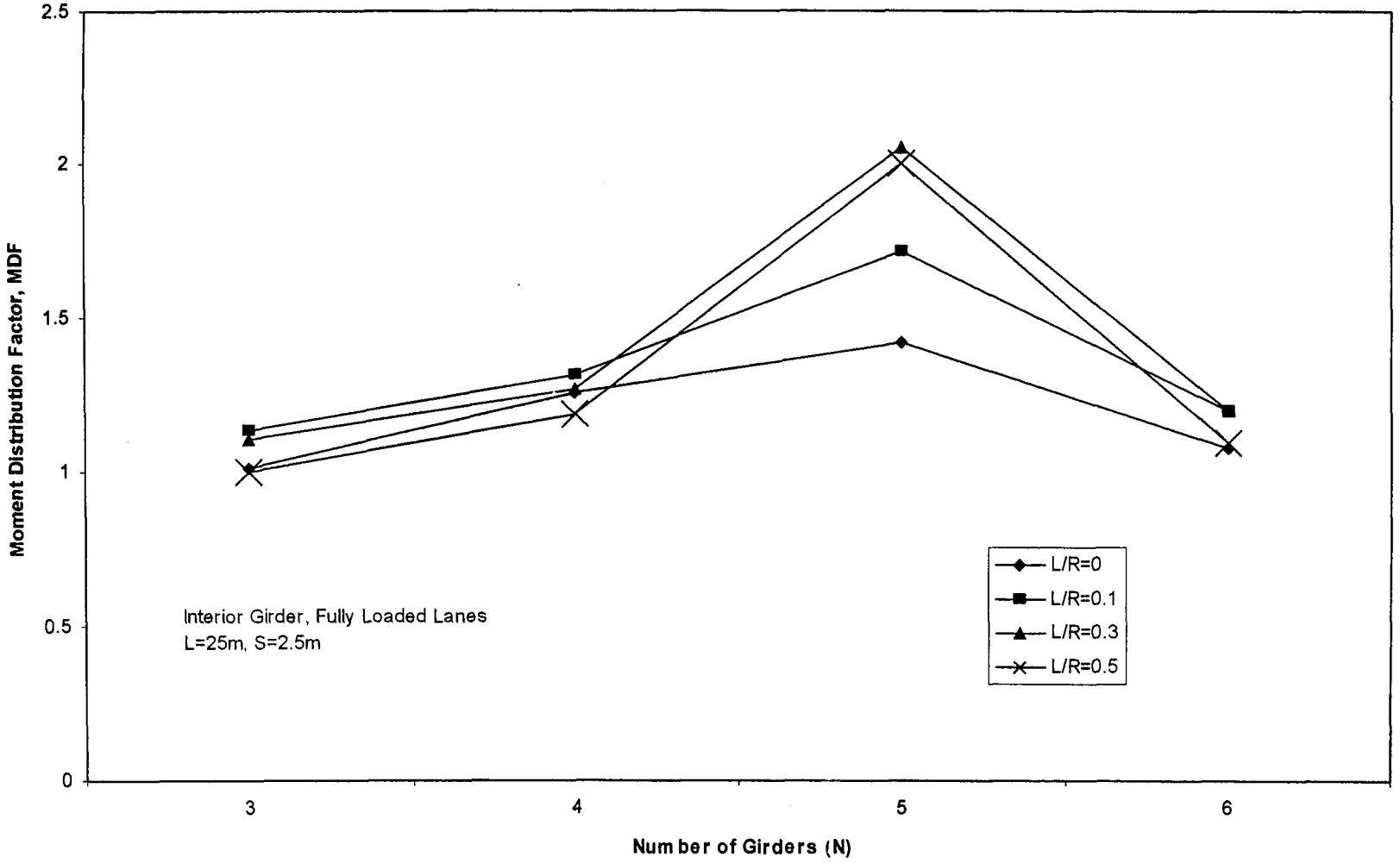

Figure 4.22 Effect of number of girders on the moment distribution factor for the interior girder due to -fully loaded lanes

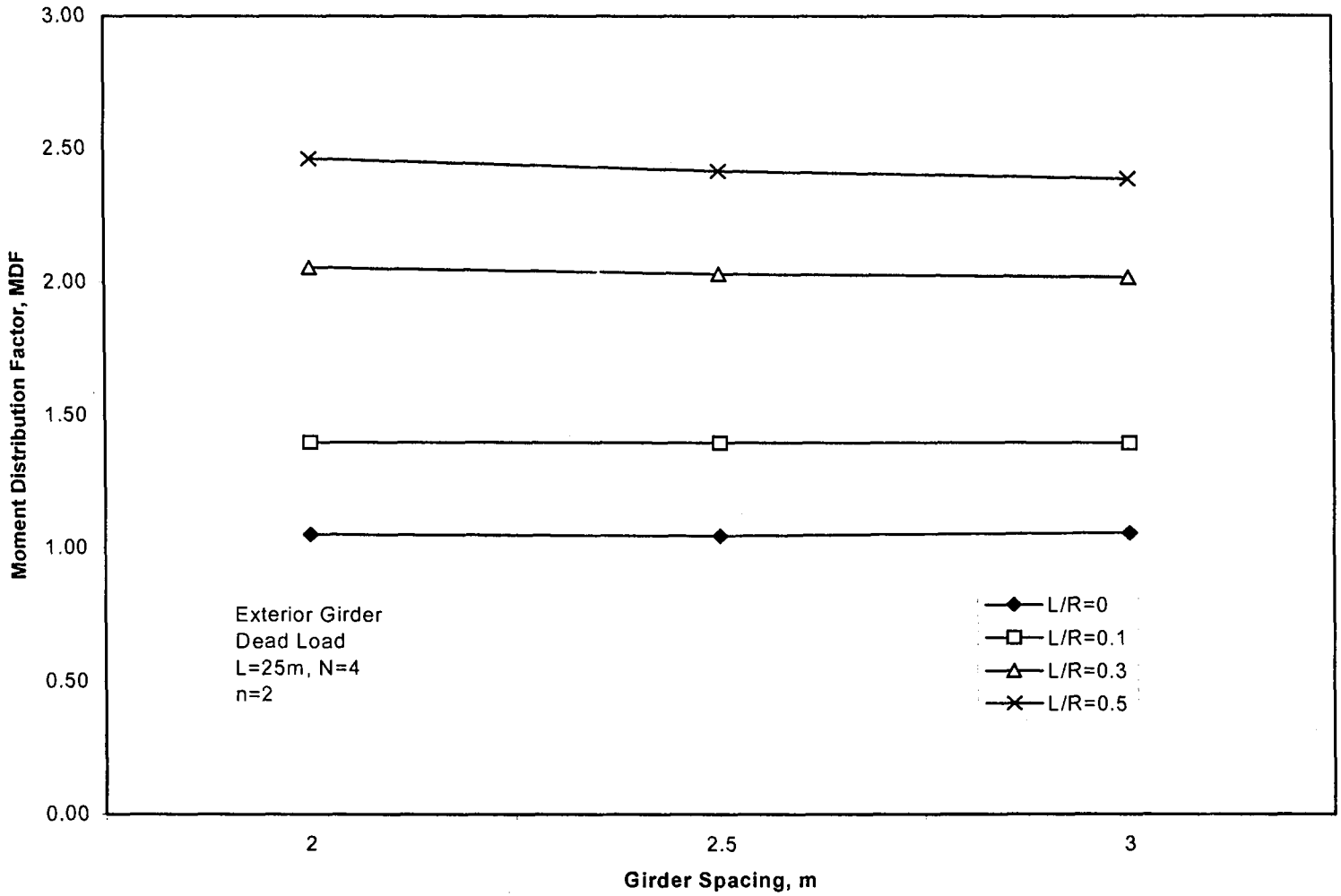

Figure 4.23 Effect of girder spacing on the moment distribution factor for the exterior girder due to dead load

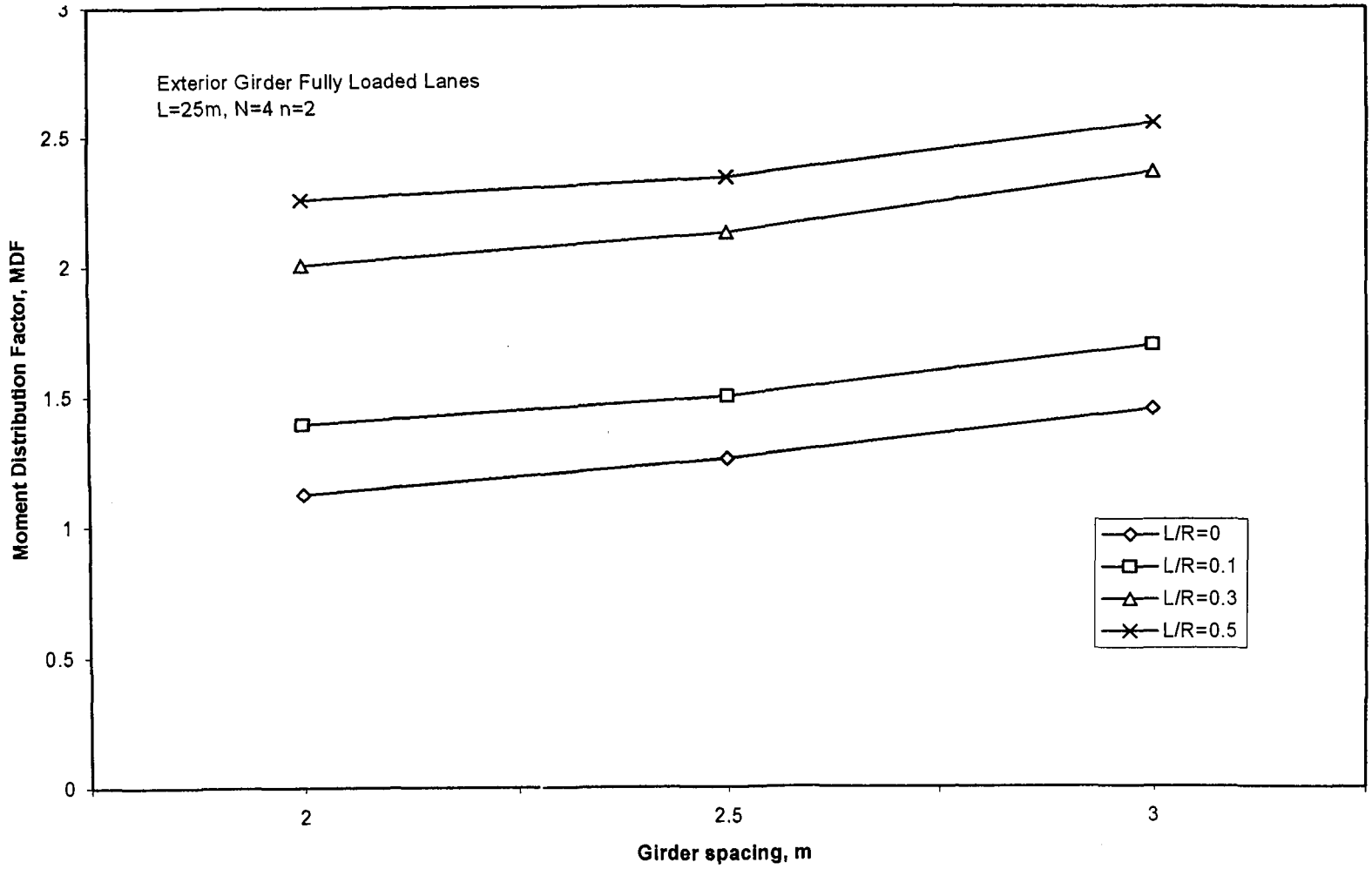

Figure 4.24 Effect of girder spacing on the moment distribution factor for the exterior girder due to fully loaded lanes

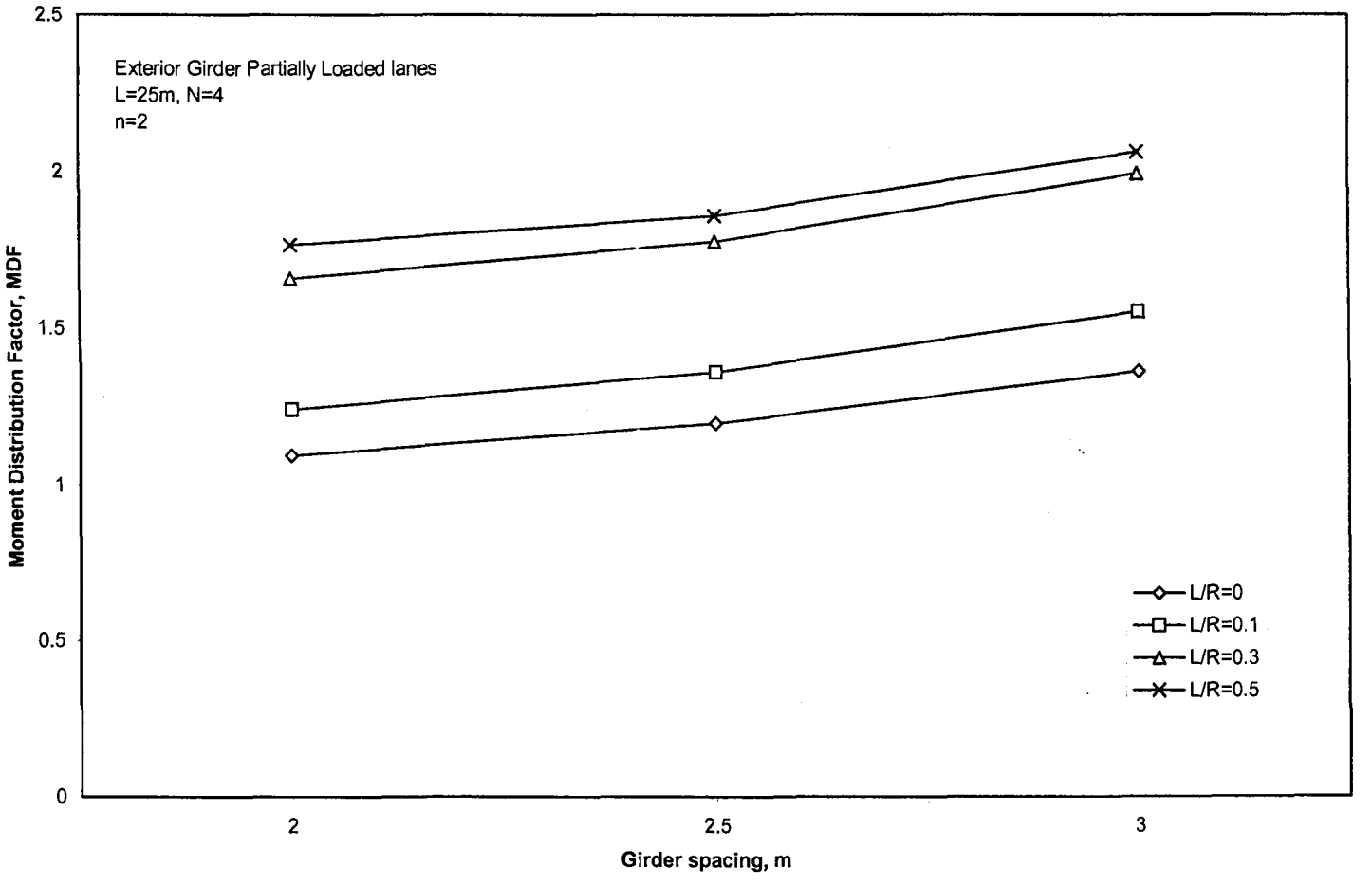

Figure 4.25 Effect of girder spacing on the moment distribution factor for the exterior girder due to partially loaded lanes

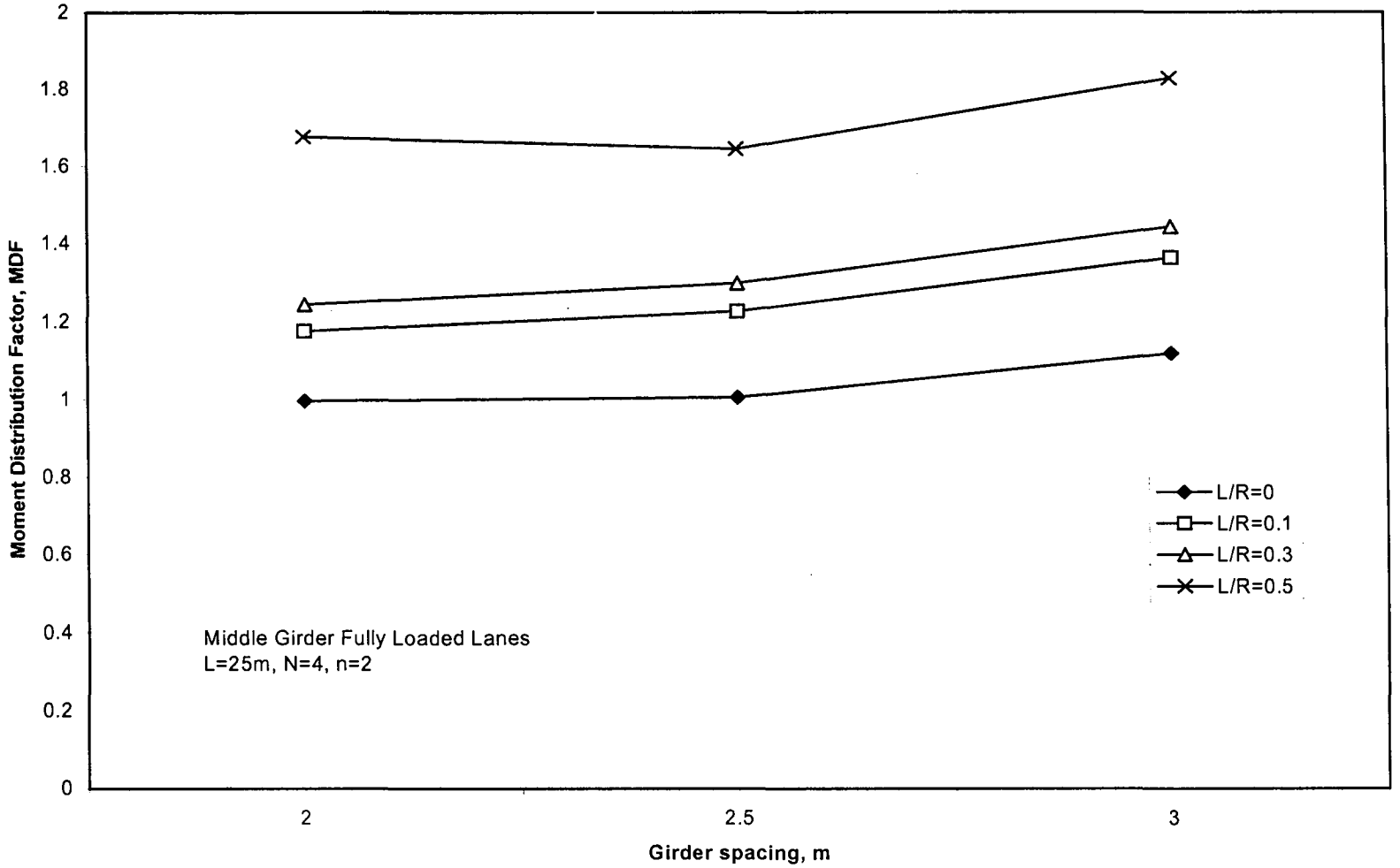

Figure 4.26 Effect of girder spacing on the moment distribution factor for the middle girder due to fully loaded lanes

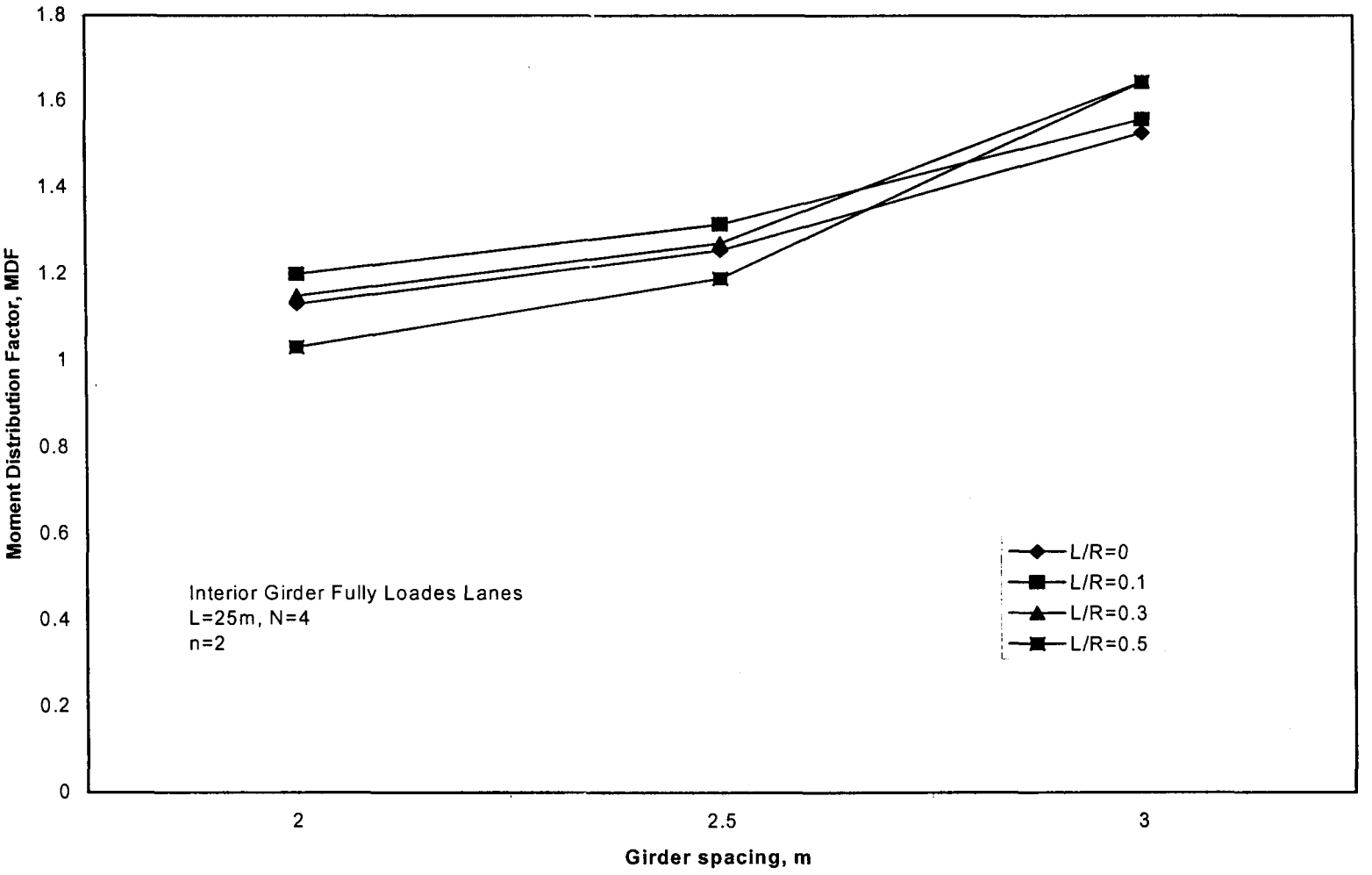

Figure 4.27 Effect of girder spacing on the moment distribution factor for the interior girder due to fully loaded lanes

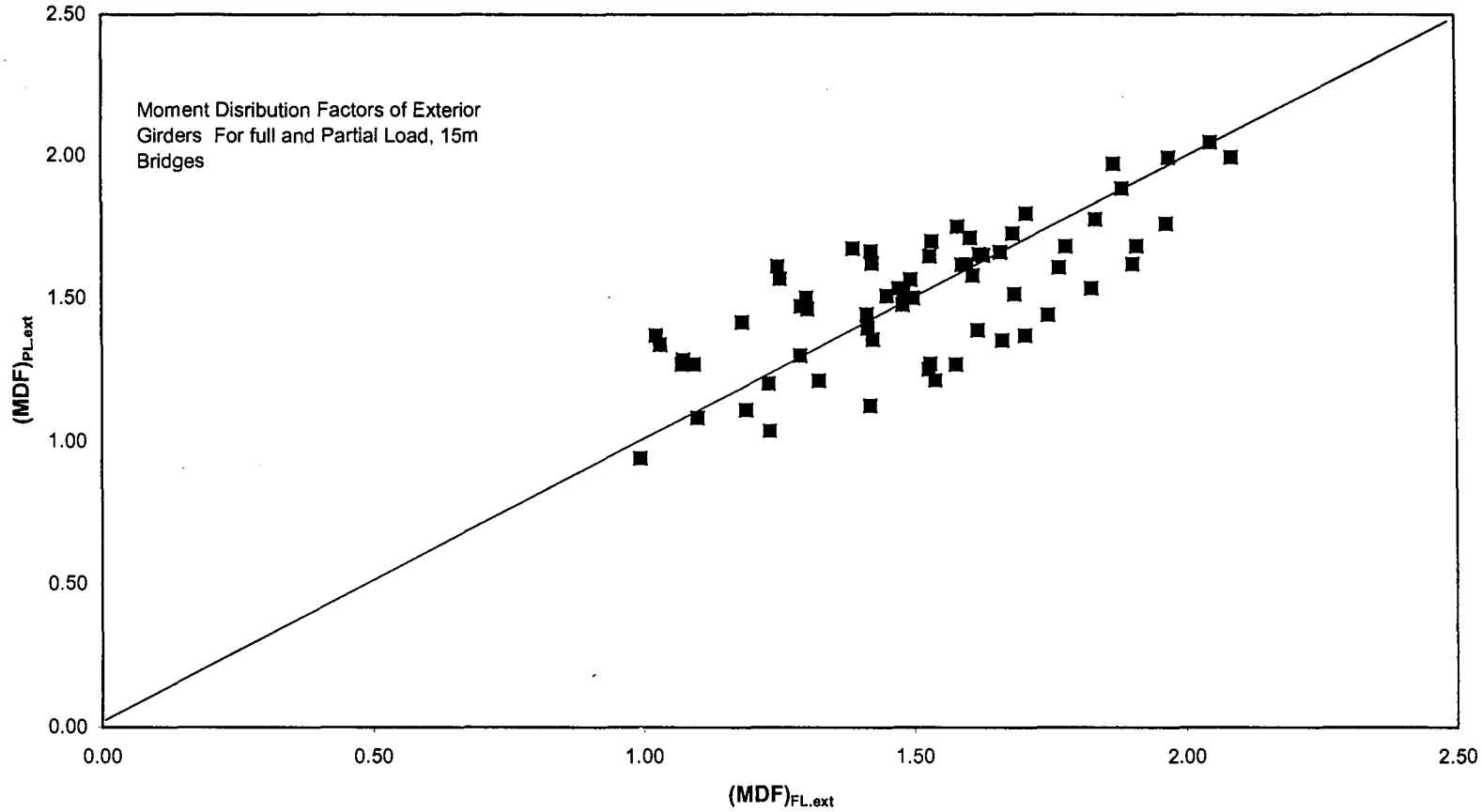

Figure 4.28 Effect of loading condition on the moment distribution factor for the exterior girder of the 15-m-span bridges

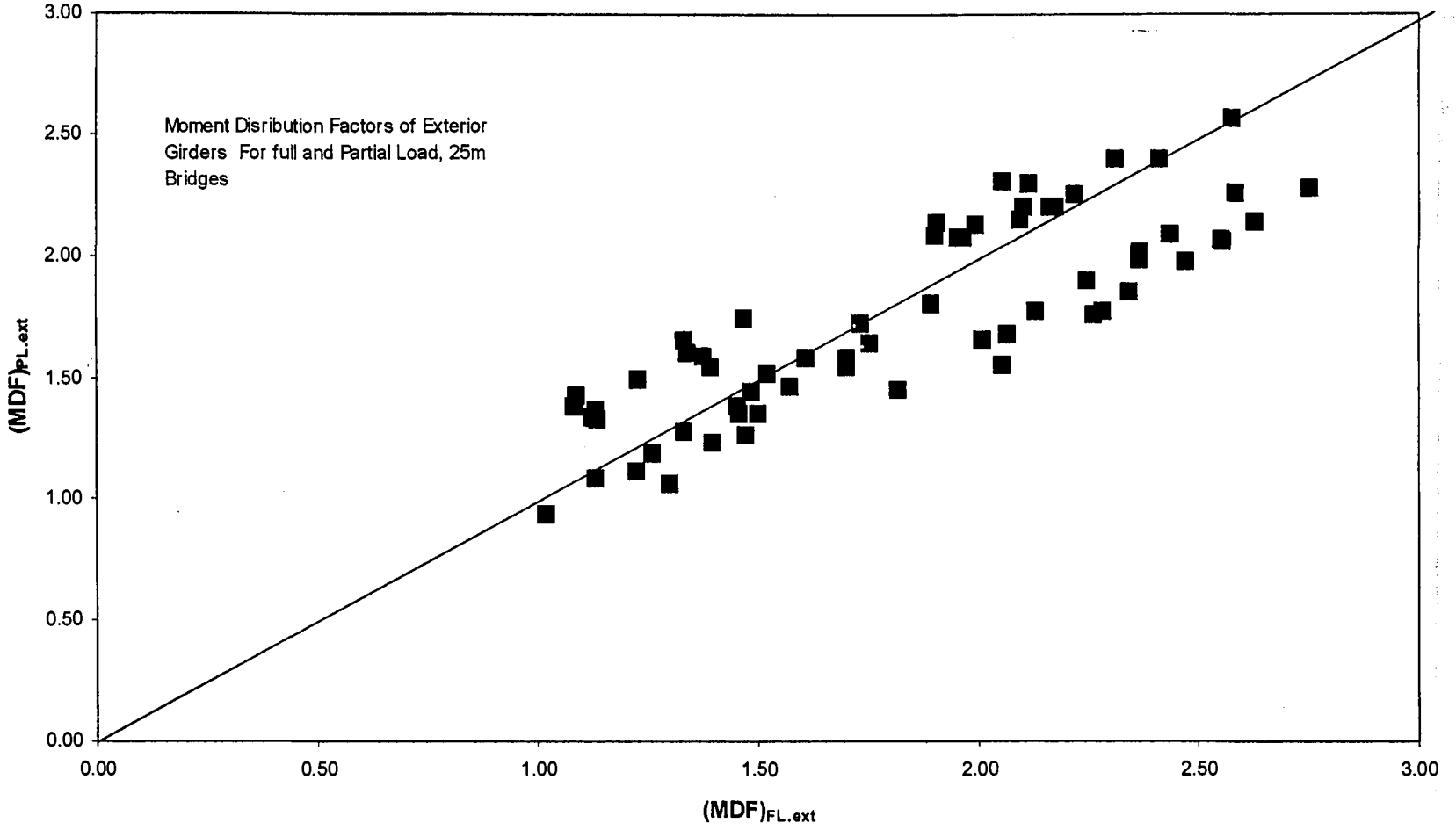

Figure 4.29Effect of loading condition on the moment distribution factor for exterior girder of the 25-m-span bridges

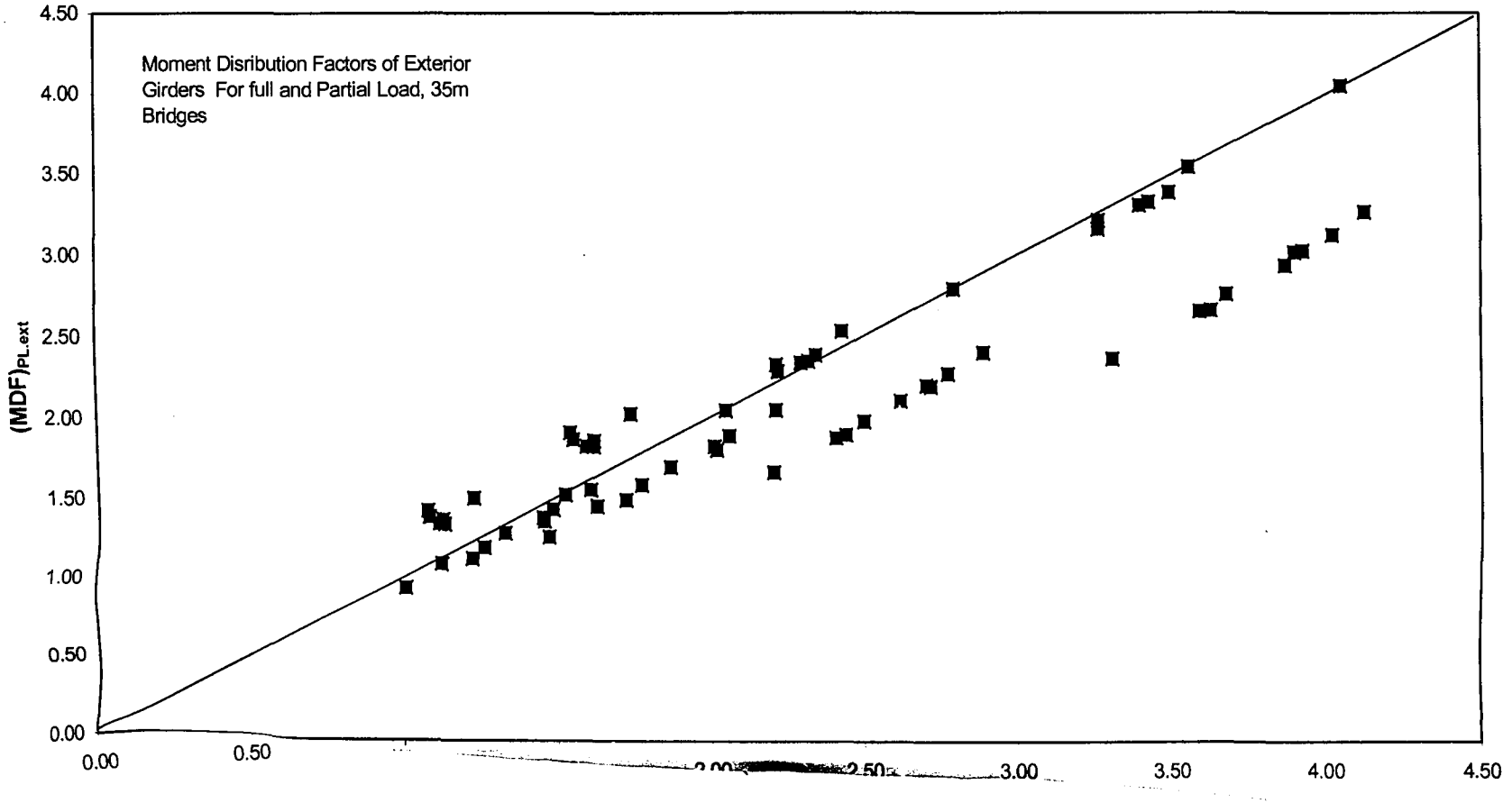

Figure 4.30 Effect of loading condition on the moment distribution factor for the exterior girder of the 35-m-span bridges

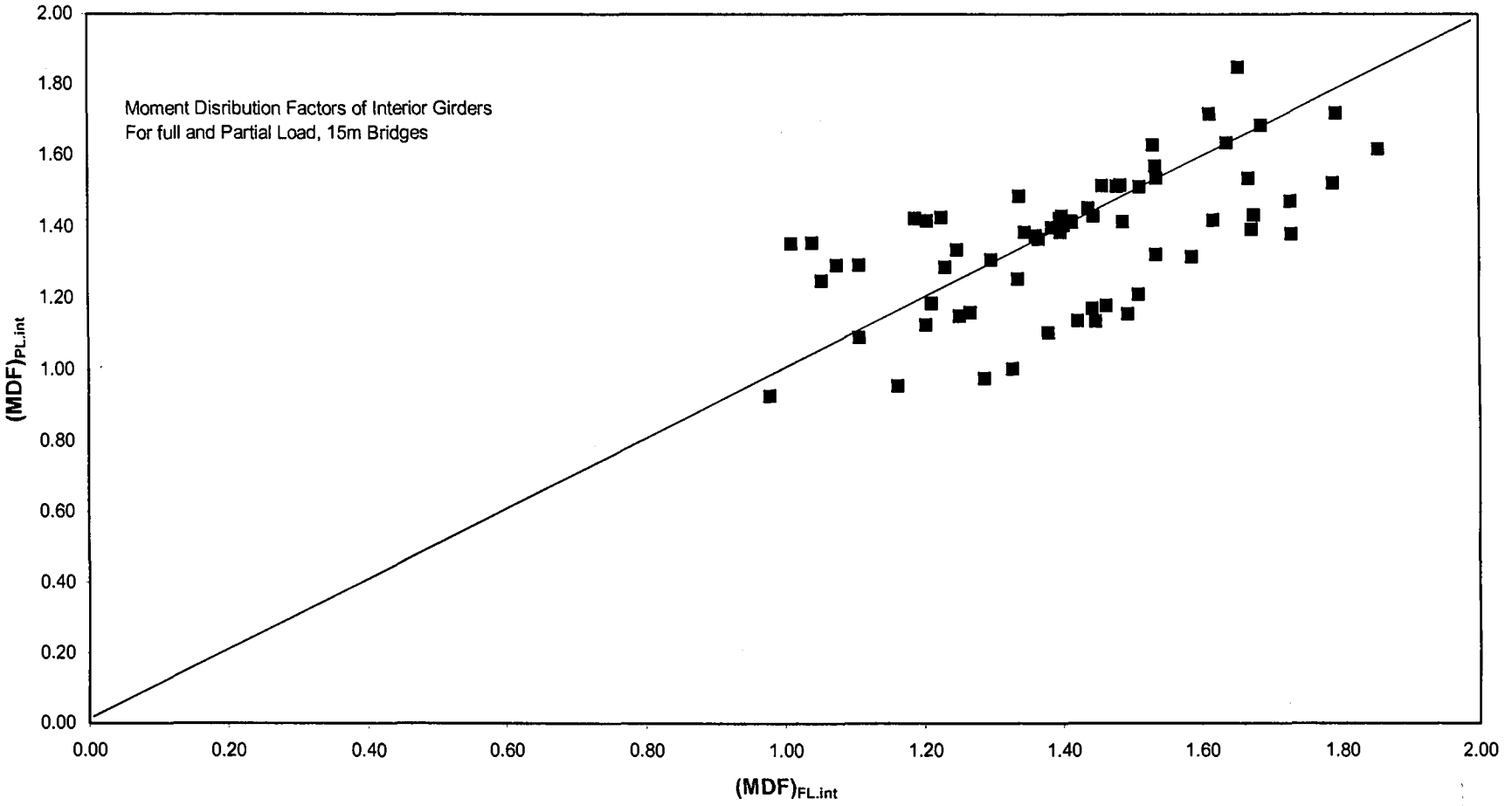

Figure 4.31 Effect of loading condition on the moment distribution factor for the interior girder of the 15-m-span bridges

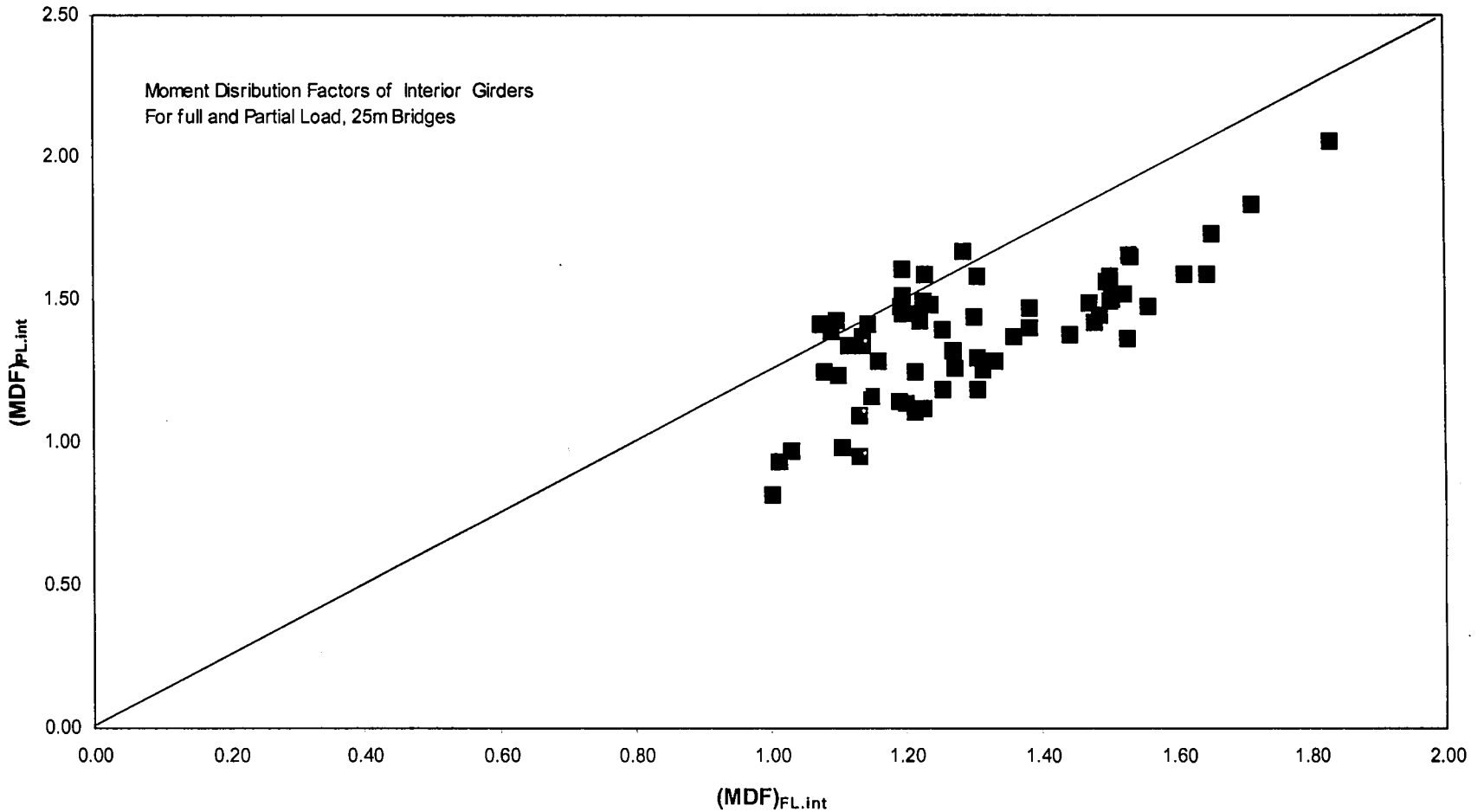

Figure 4.32 Effect of loading condition on the moment distribution factor for the interior girder of the 25-m-span bridges

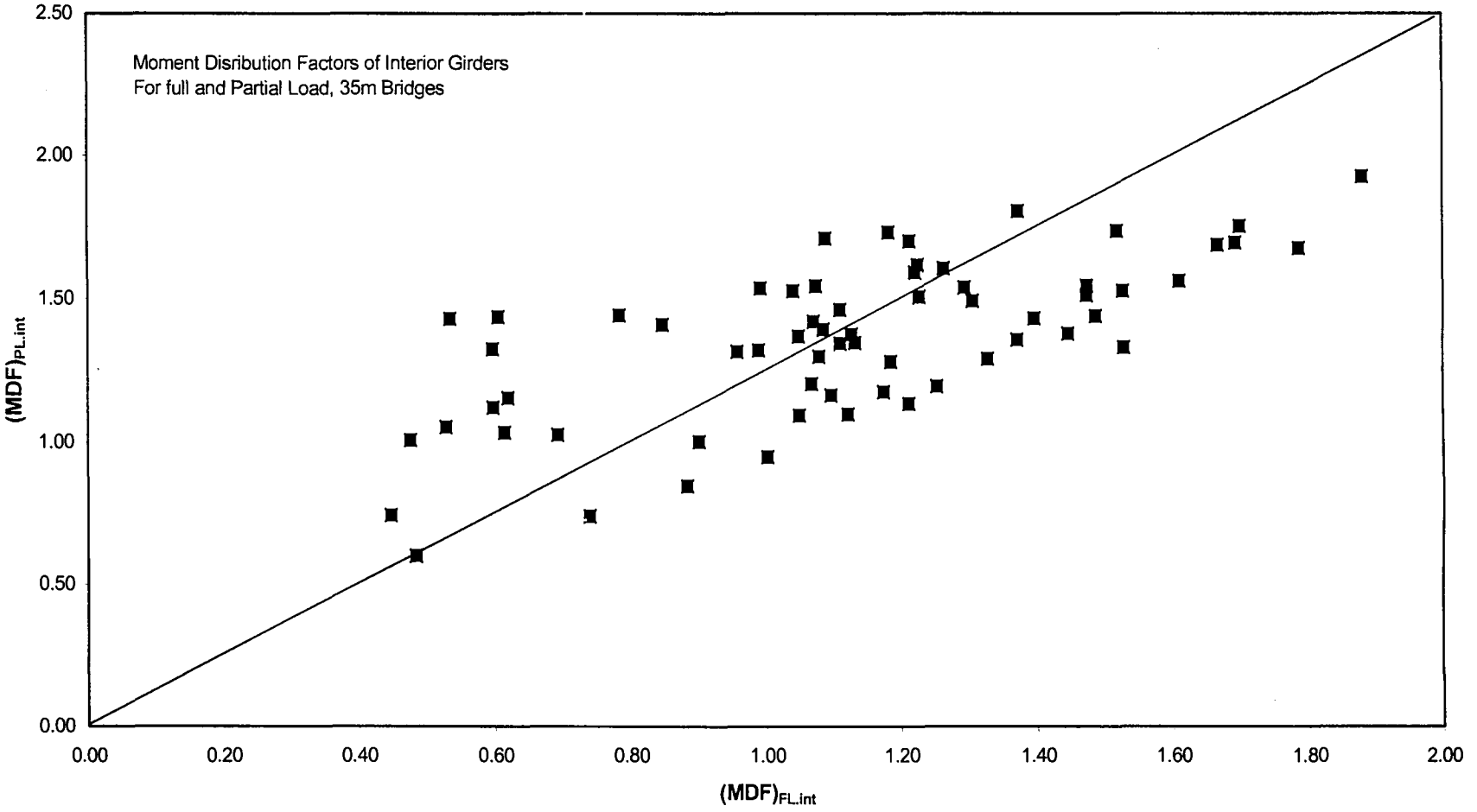

Figure 4.33 Effect of loading condition on the moment distribution factor for the interior girder of 35-m-span bridges

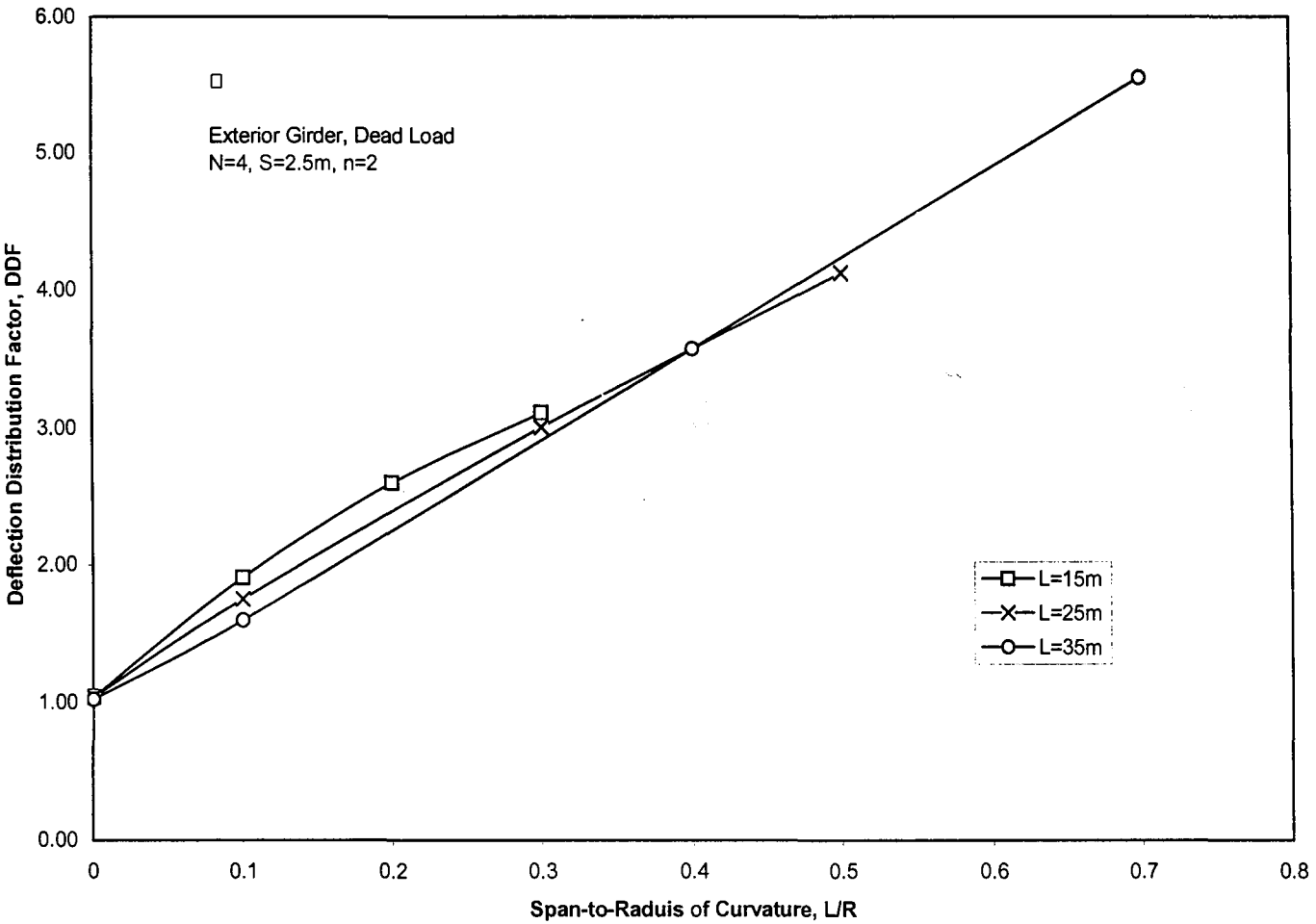

Figure 4.34 Effect of curvature on the deflection distribution factor for the exterior girder due to dead load

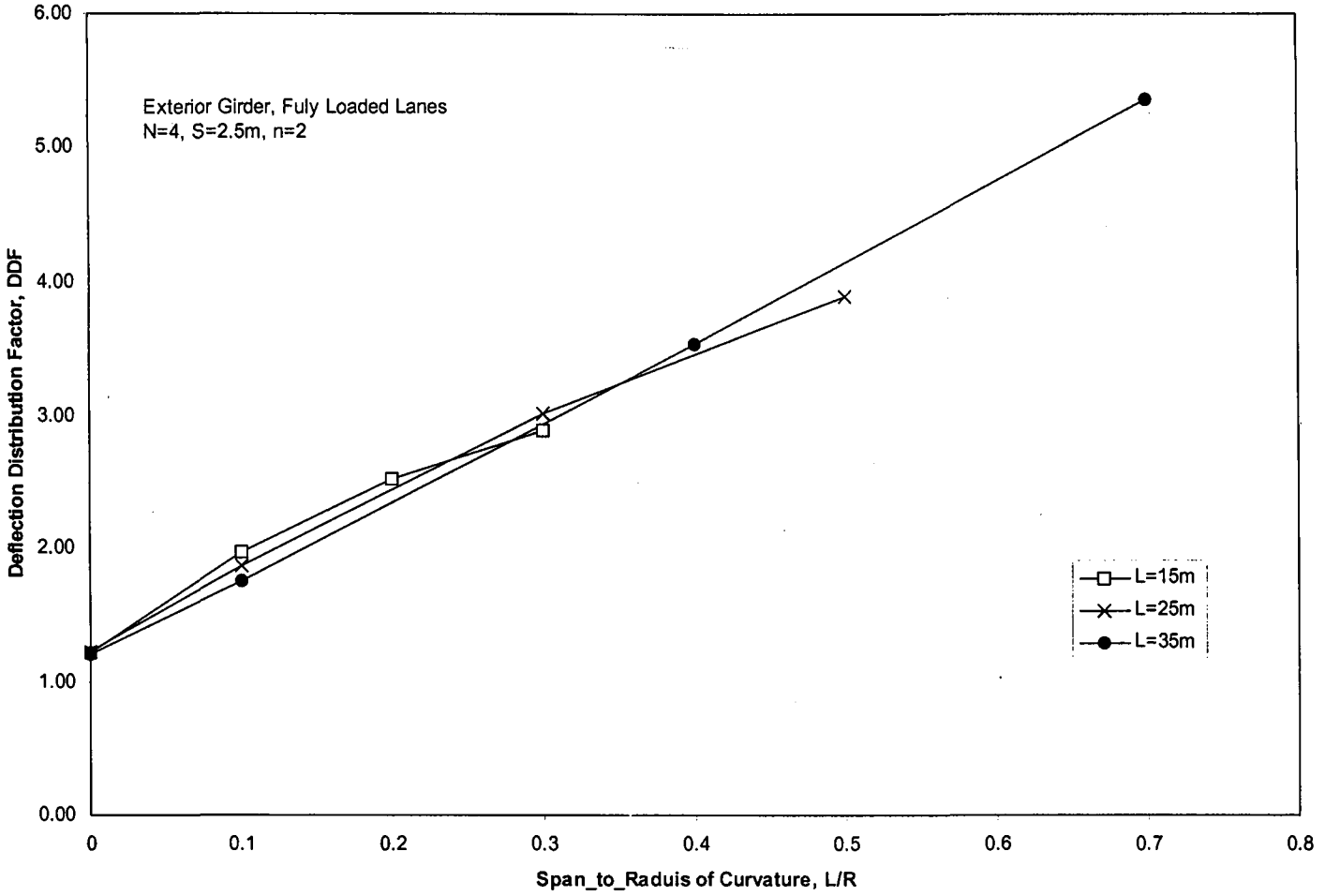

Figure 4.35 Effect of curvature on the deflection distribution factor for the exterior girder due to fully loaded lanes

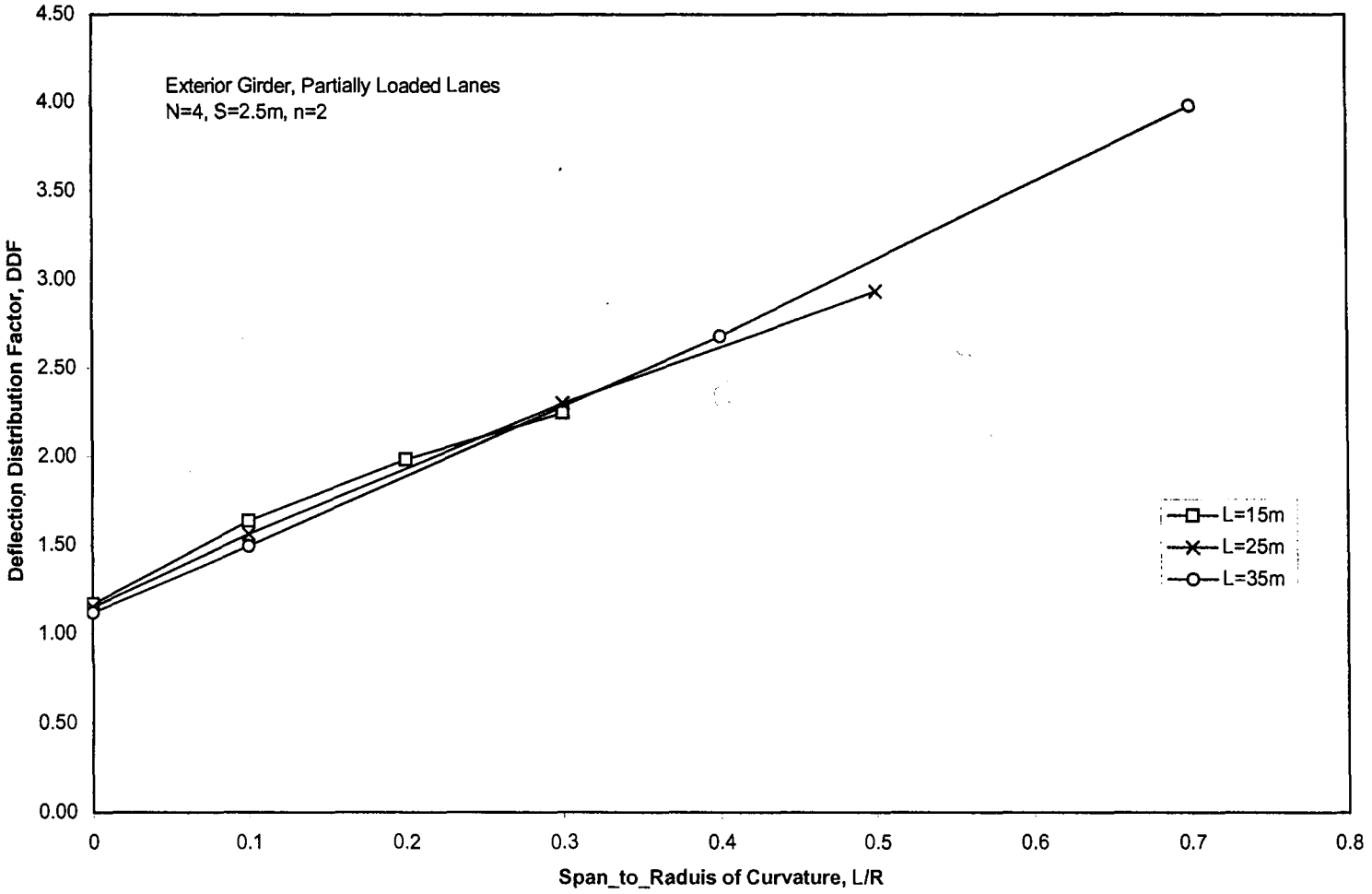

Figure 4.36 Effect of curvature on the deflection distribution factor for the exterior girder due to partially loaded lanes

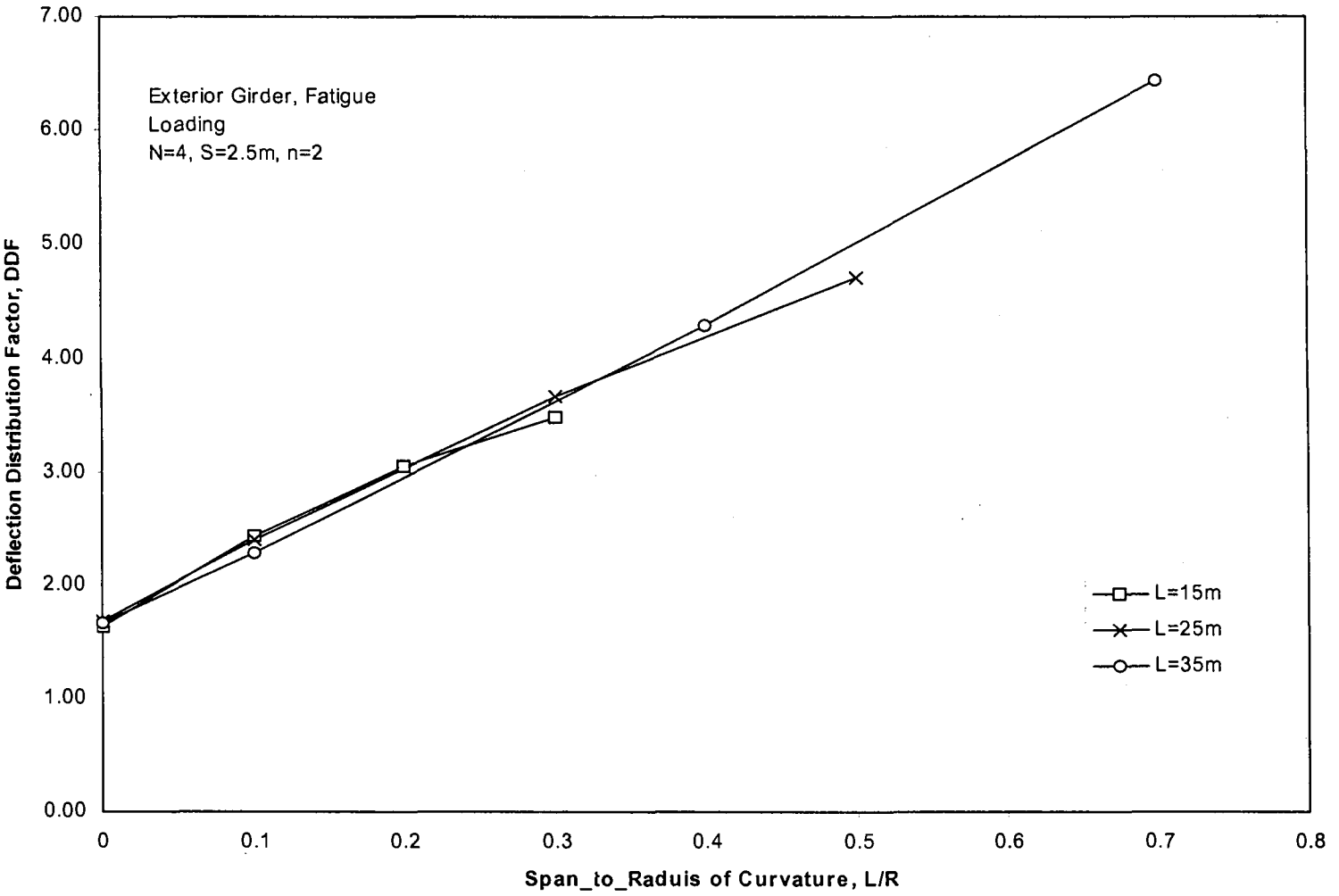

Figure 4.37 Effect of curvature on the deflection distribution factor for exterior girder due to fatigue loading

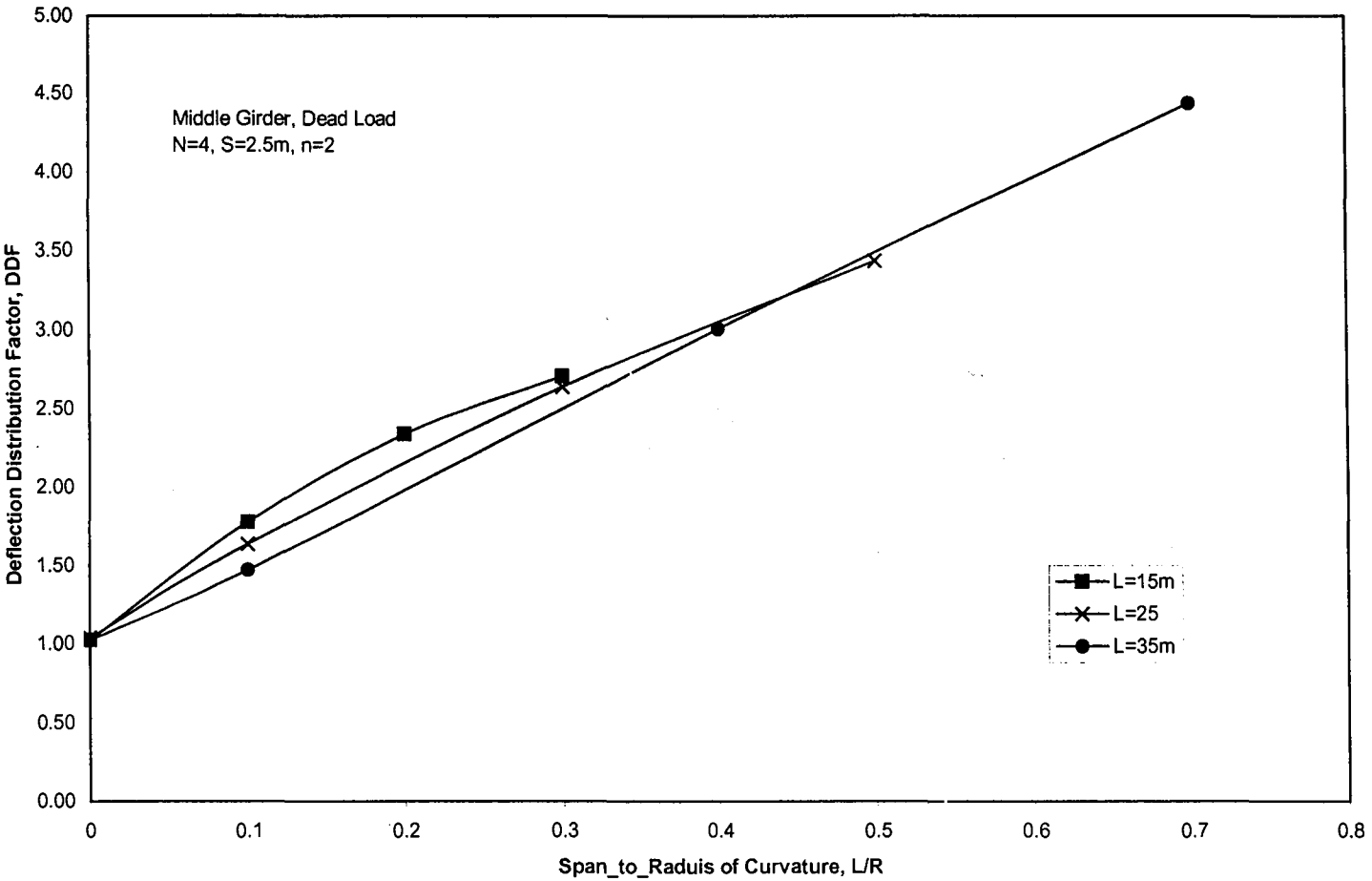

Figure 4.38 Effect of curvature on the deflection distribution factor for the middle girder due to dead load

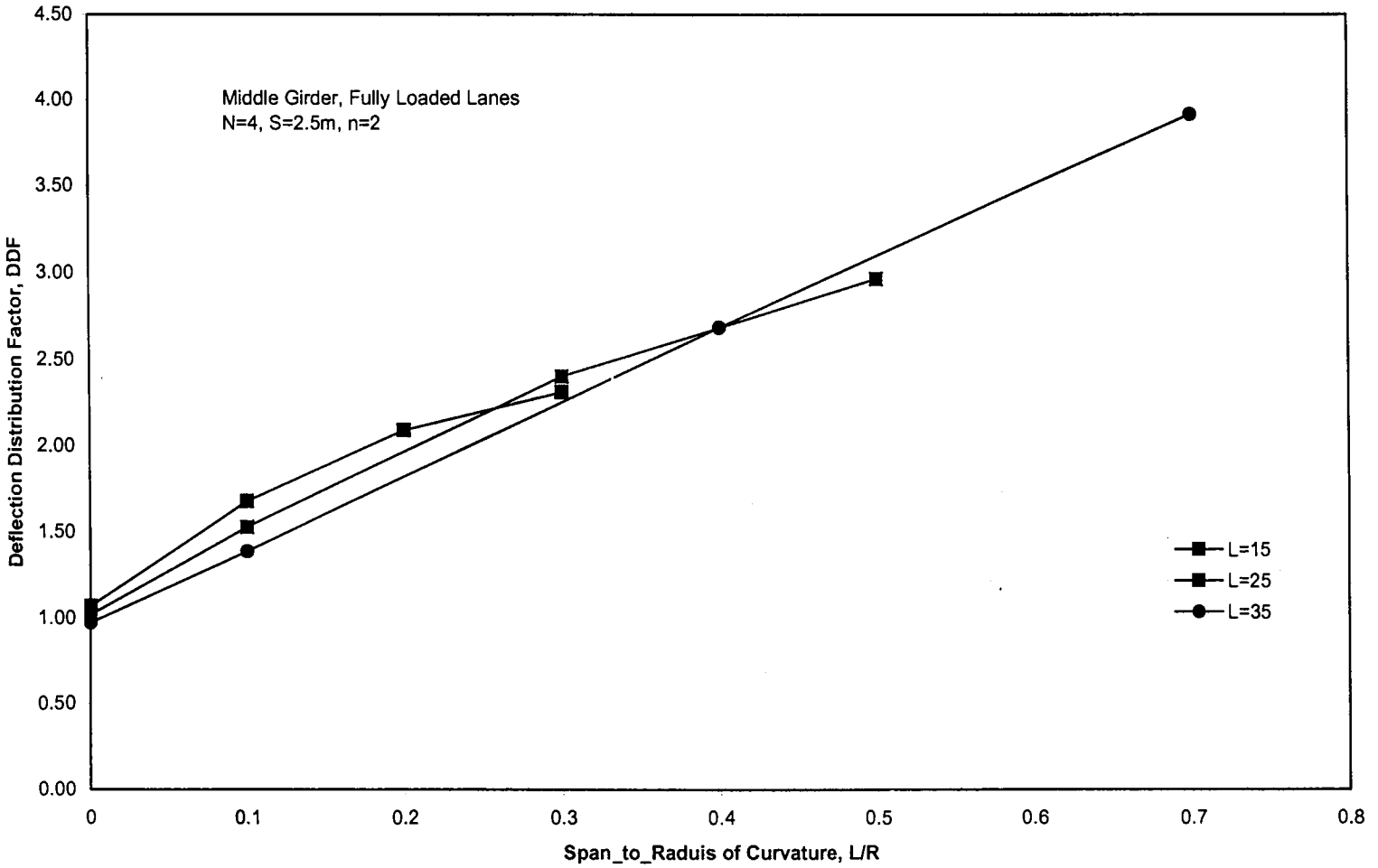

Figure 4.39 Effect of curvature on the deflection distribution factor for the middle girder due to fully loaded lanes

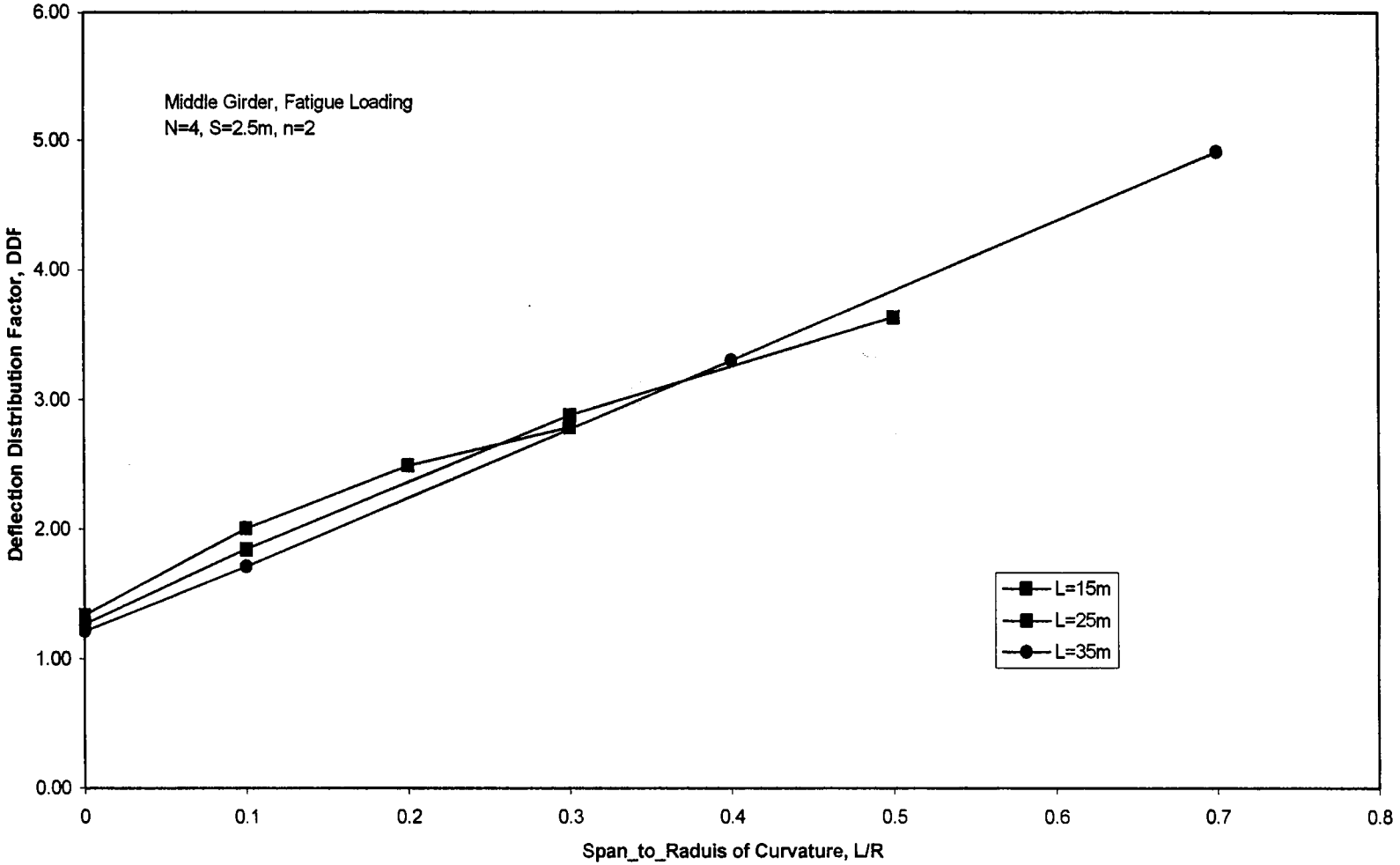

Figure 4.40 Effect of curvature on the deflection distribution factor for the middle girder due to fatigue loading

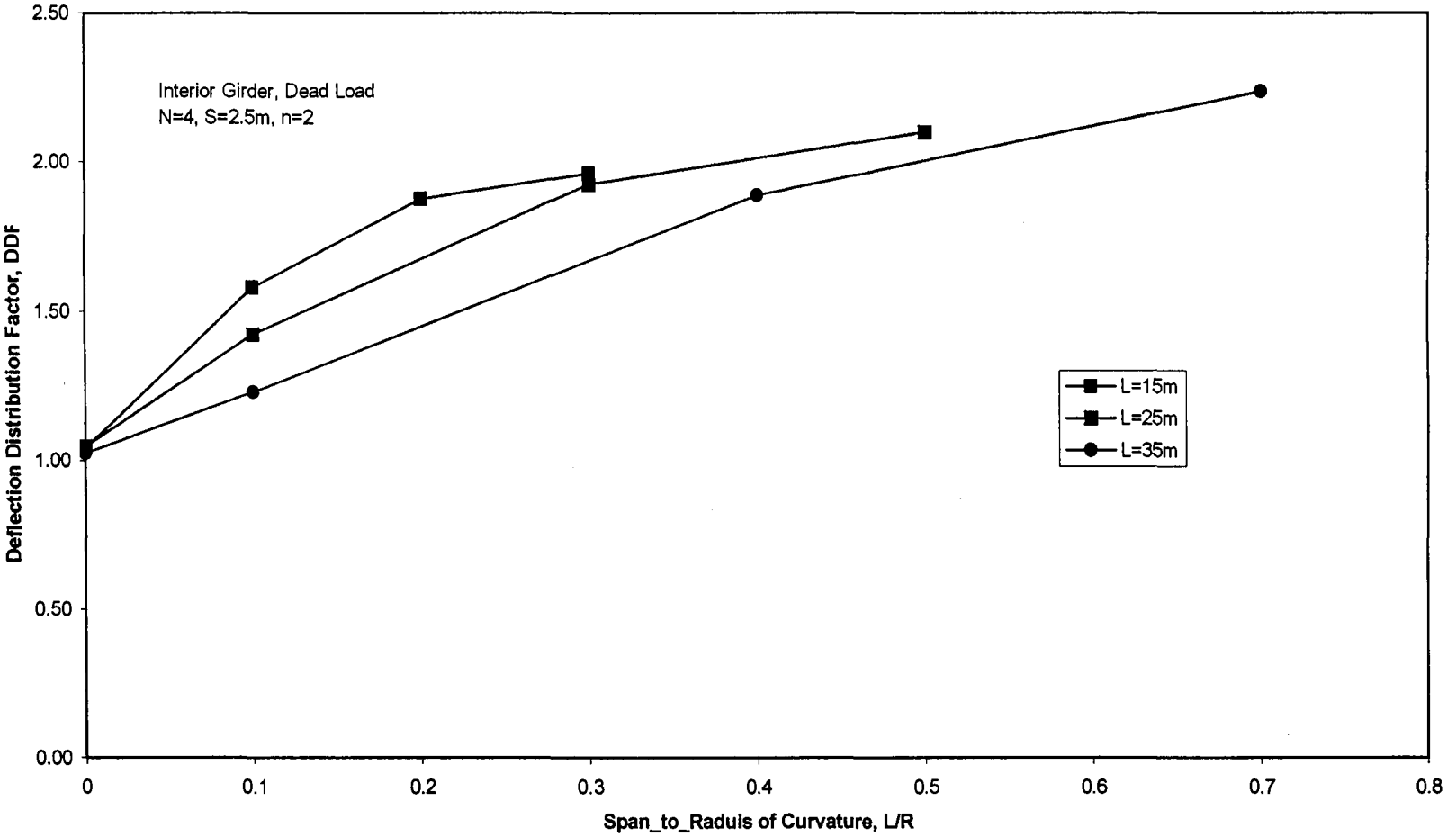

Figure 4. 41 Effect of curvature on the deflection distribution factor for the interior girder due to dead load

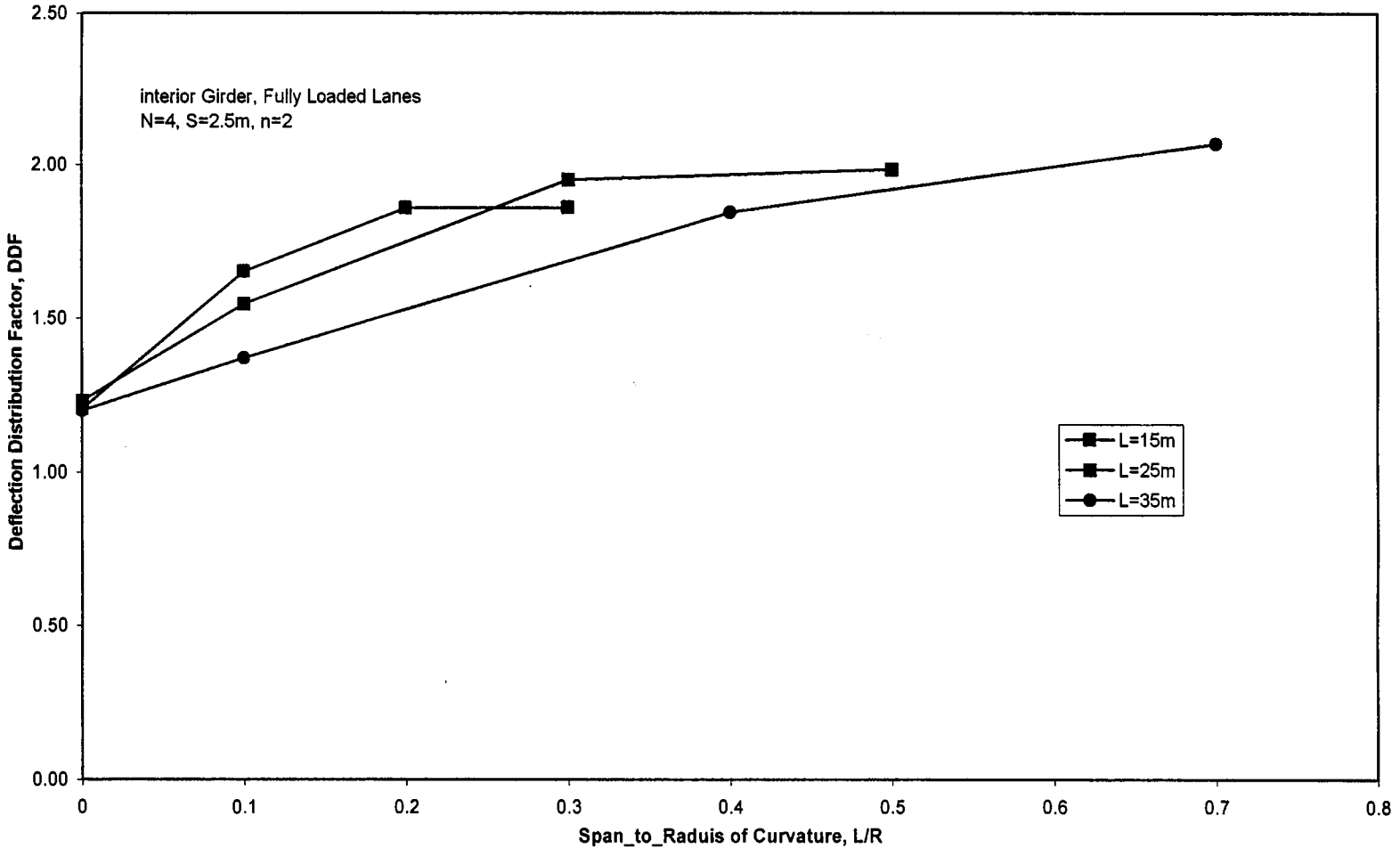

Figure 4.42 Effect of curvature on the deflection distribution factor for the interior girder due to fully loaded lanes

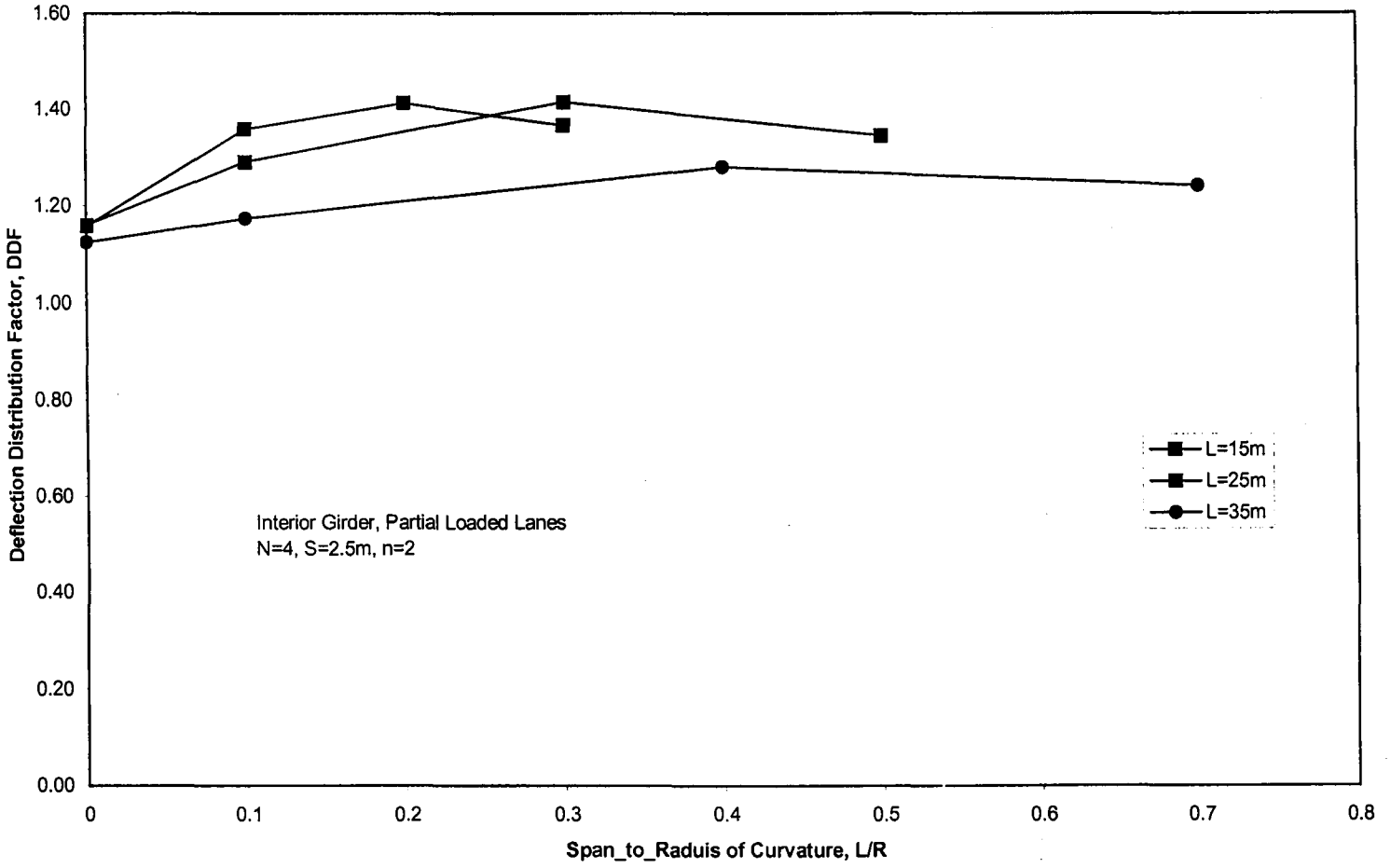

Figure 4.43 Effect of curvature on the deflection distribution factor for the interior girder due to partially loaded lanes

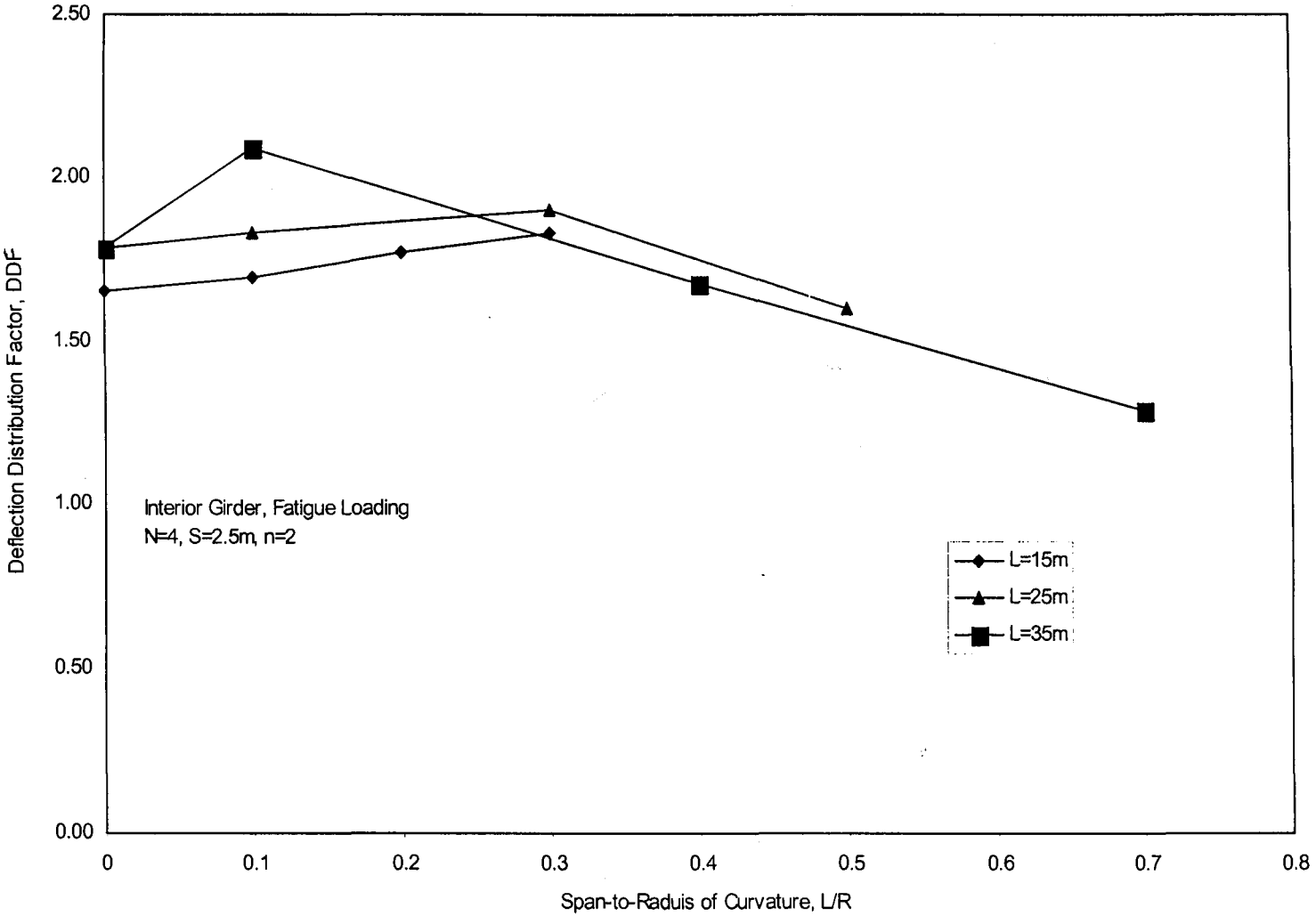

Figure 4.44 Effect of curvature on the deflection distribution factor for the interior girder due to fatigue loading

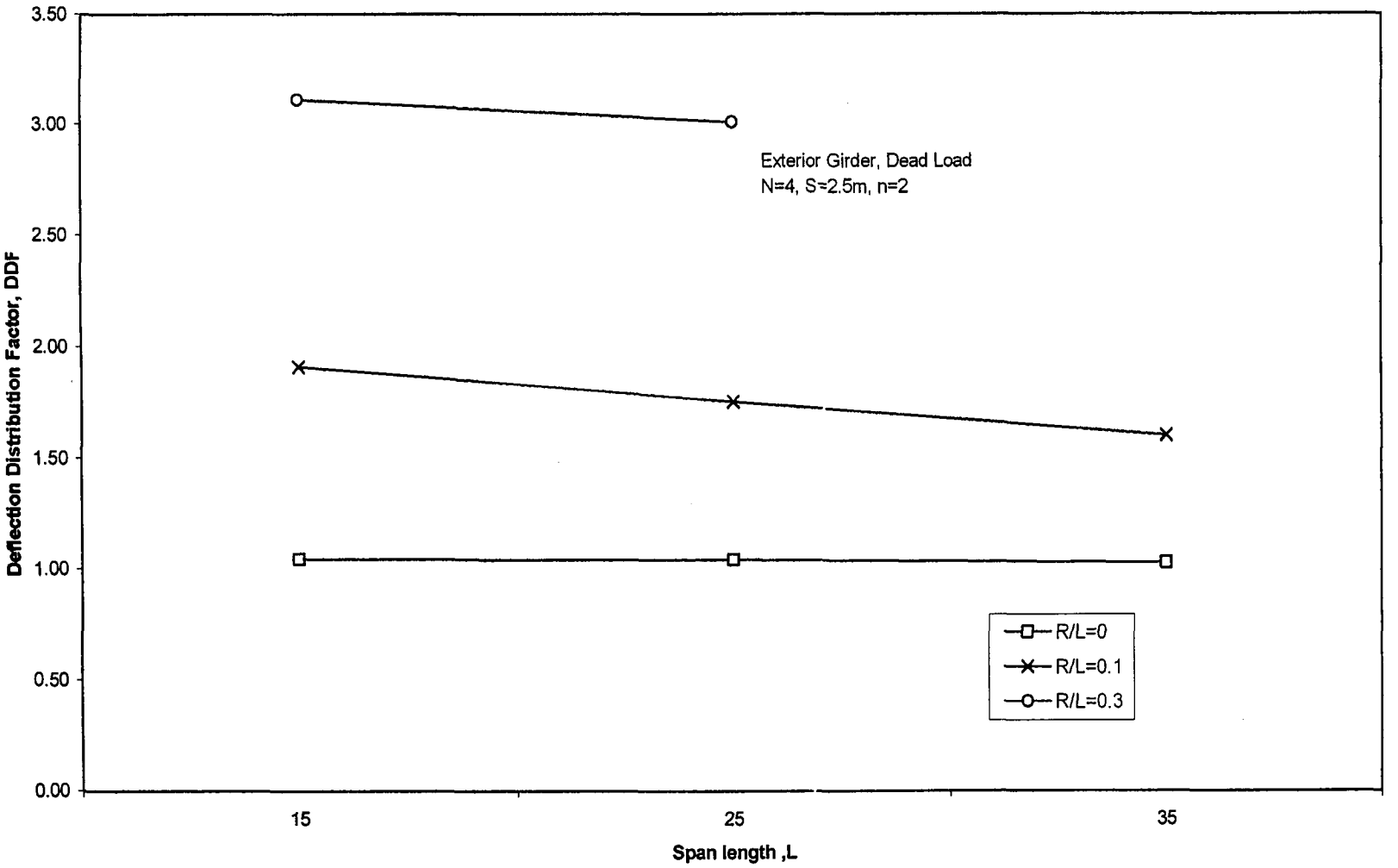

Figure 4.45 Effect of span length on the deflection distribution factor for the exterior girder due to dead load

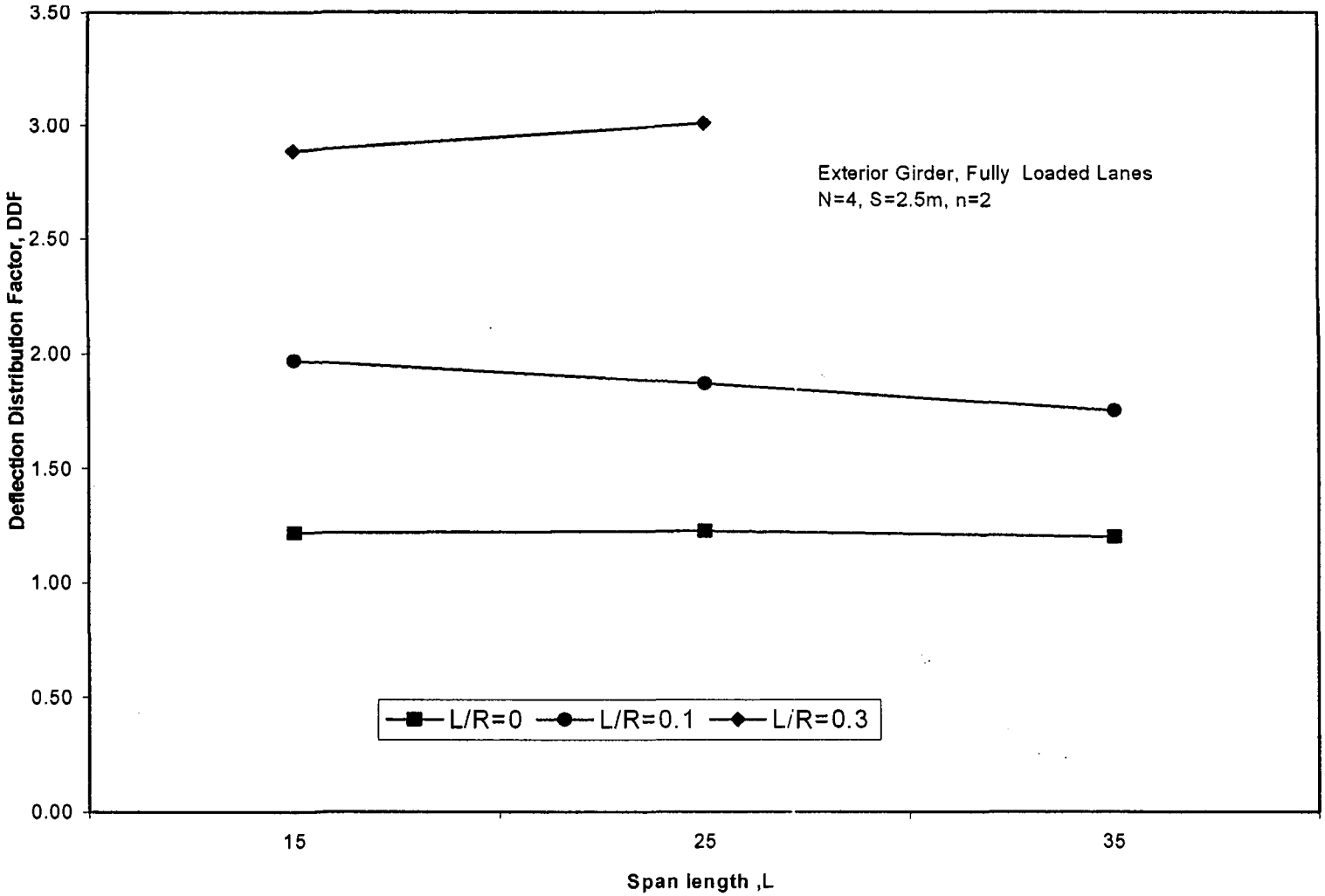

Figure 4.46 Effect of span length on the deflection distribution factor for the exterior girder due to fully loaded lanes

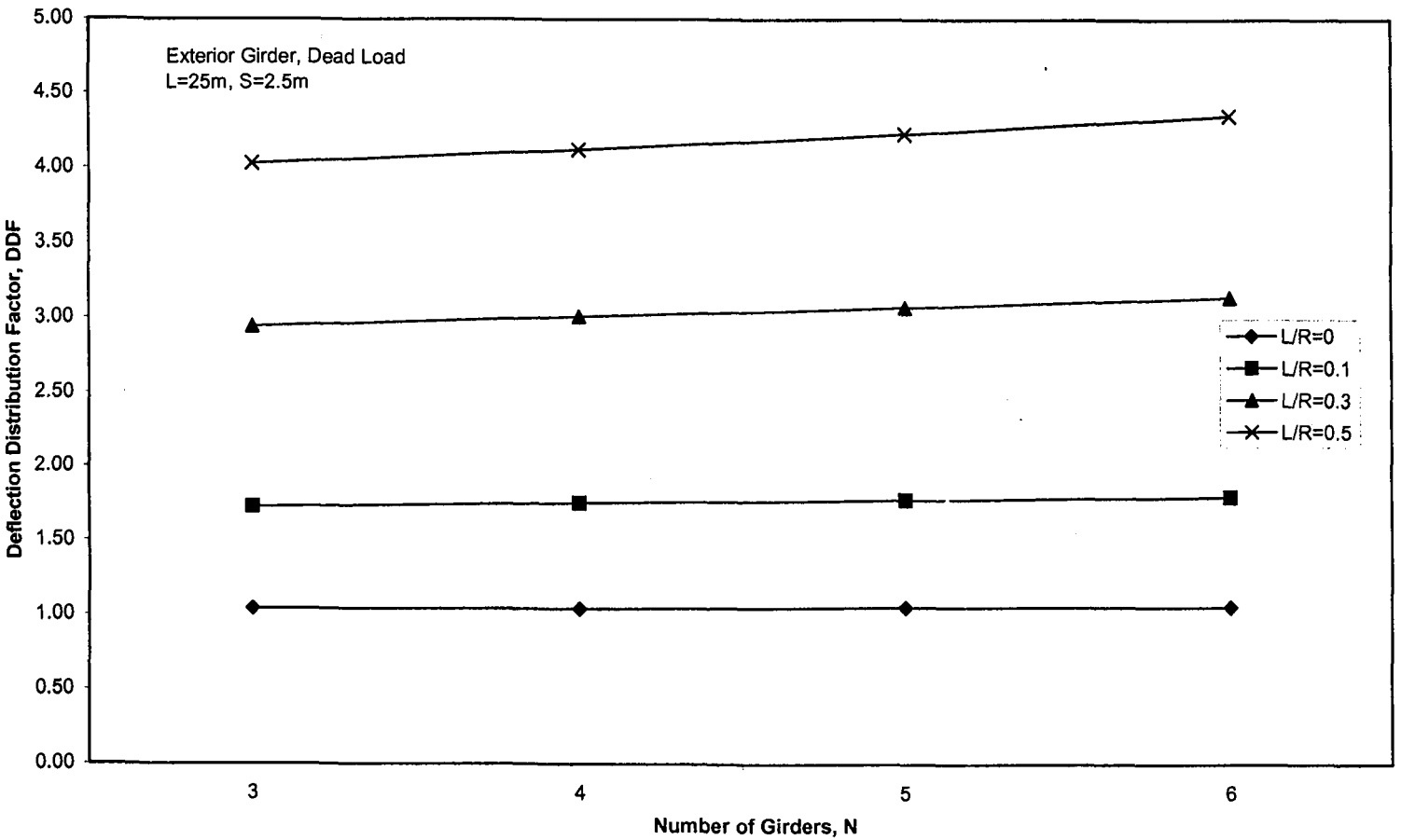

Figure 4.47 Effect of number of girders on the deflection distribution factor for the exterior girder due to dead load

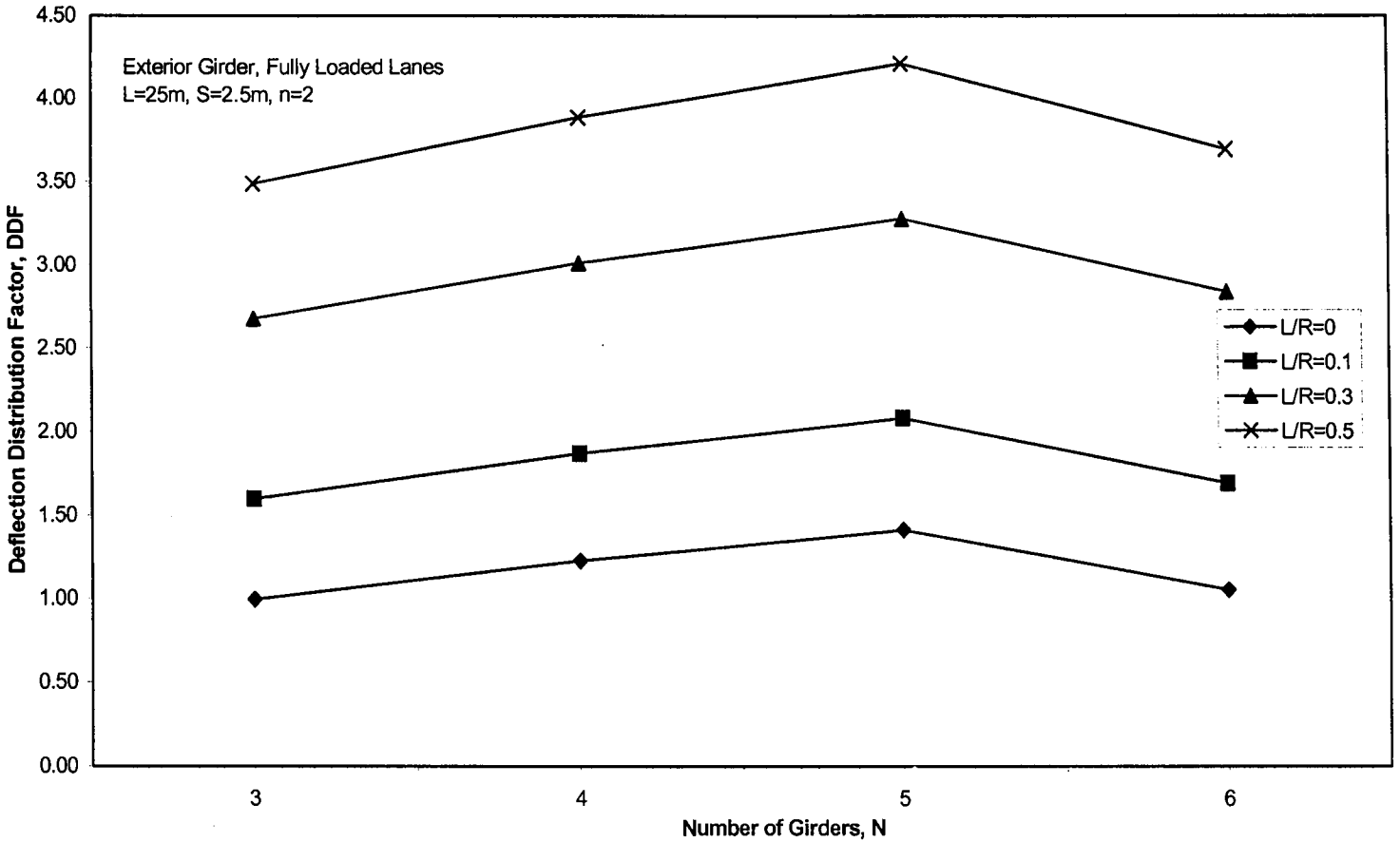

Figure 4.48 Effect of number of girders on the deflection distribution factor for the exterior girder due to fully loaded lanes

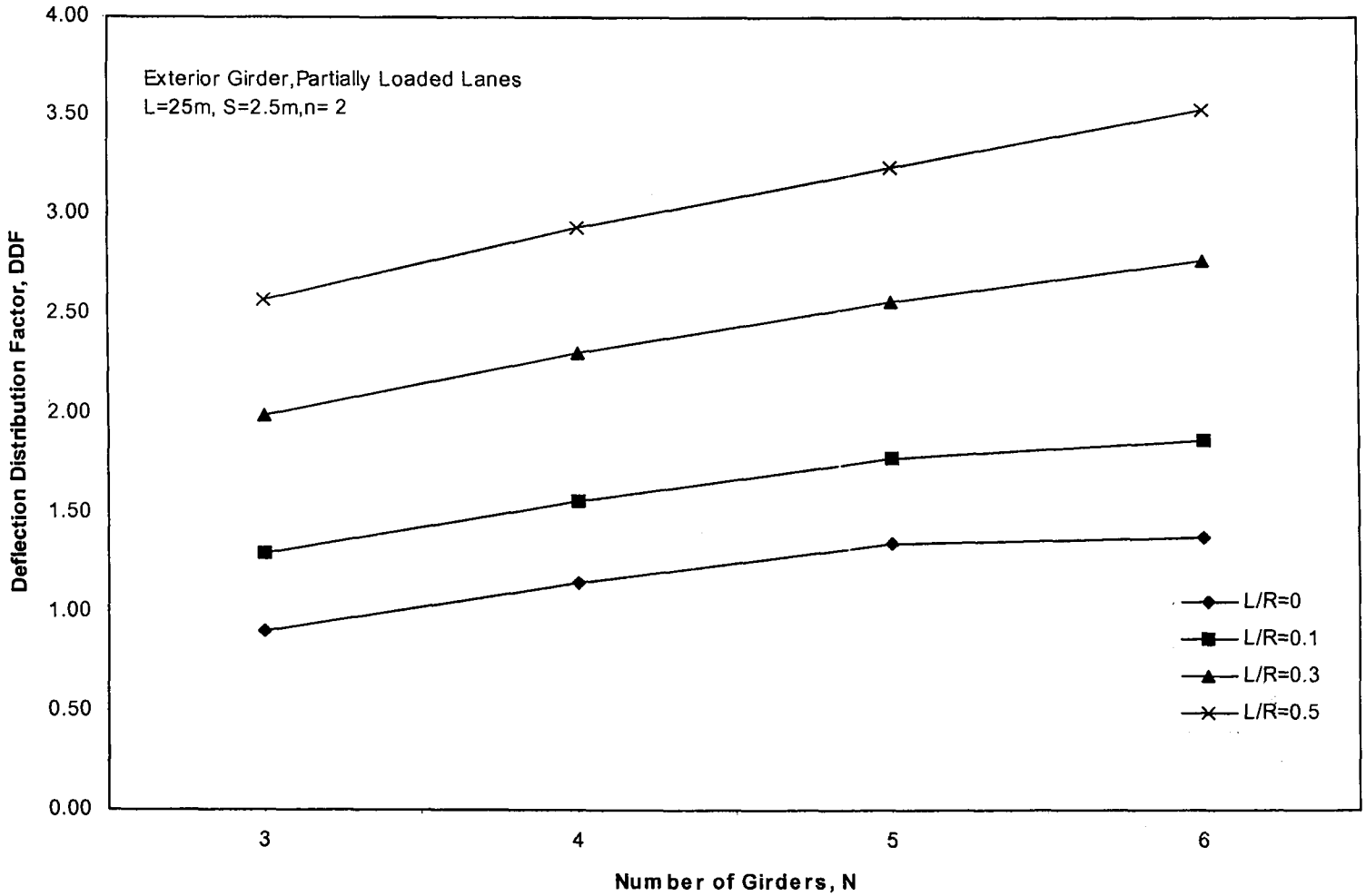

Figure 4.49 Effect of number of girders on the deflection distribution factor for the exterior girder due to partially loaded lanes

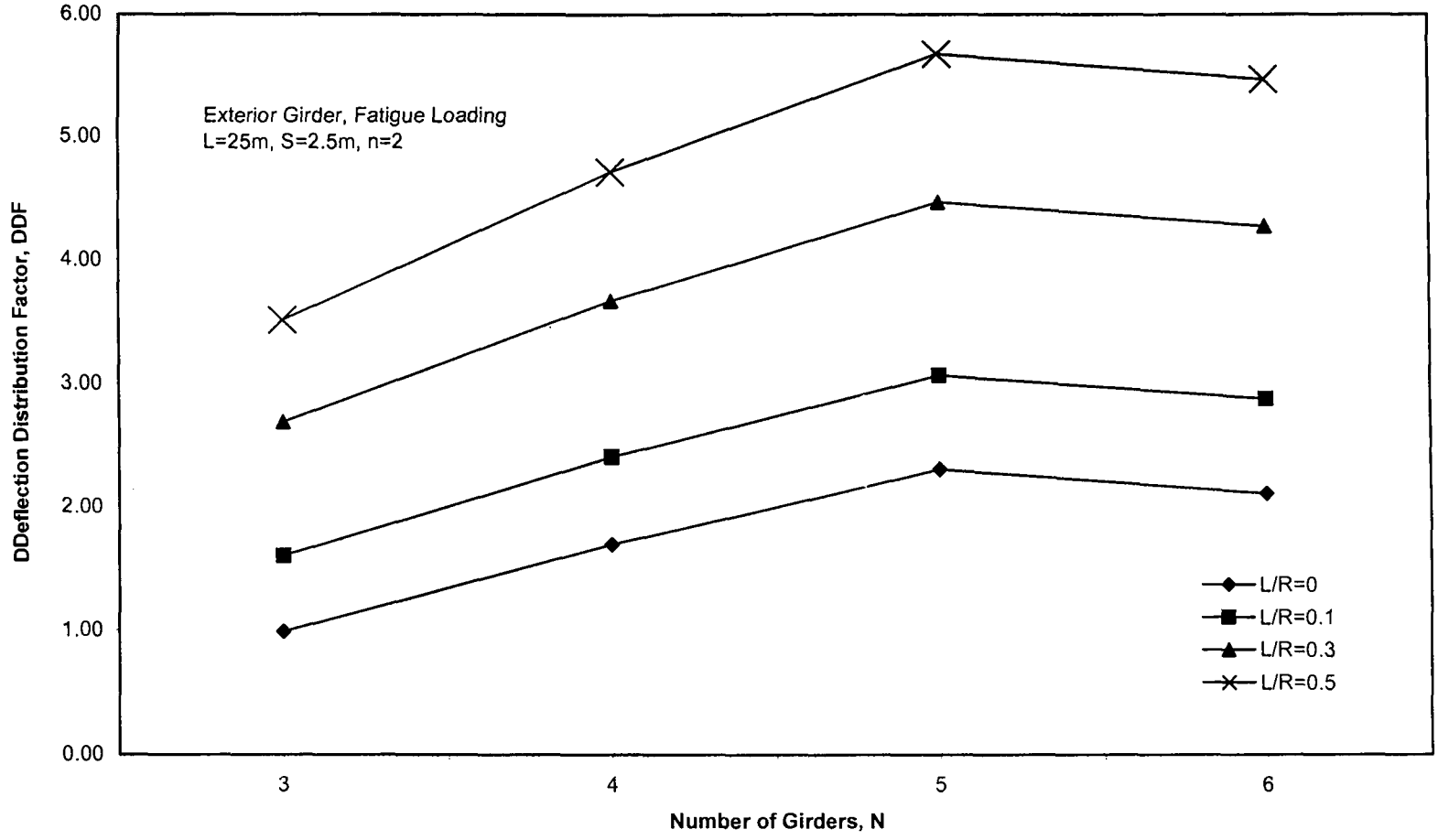

Figure 4.50 Effect of number of girders on the deflection distribution factor for the exterior girder due to fatigue loading

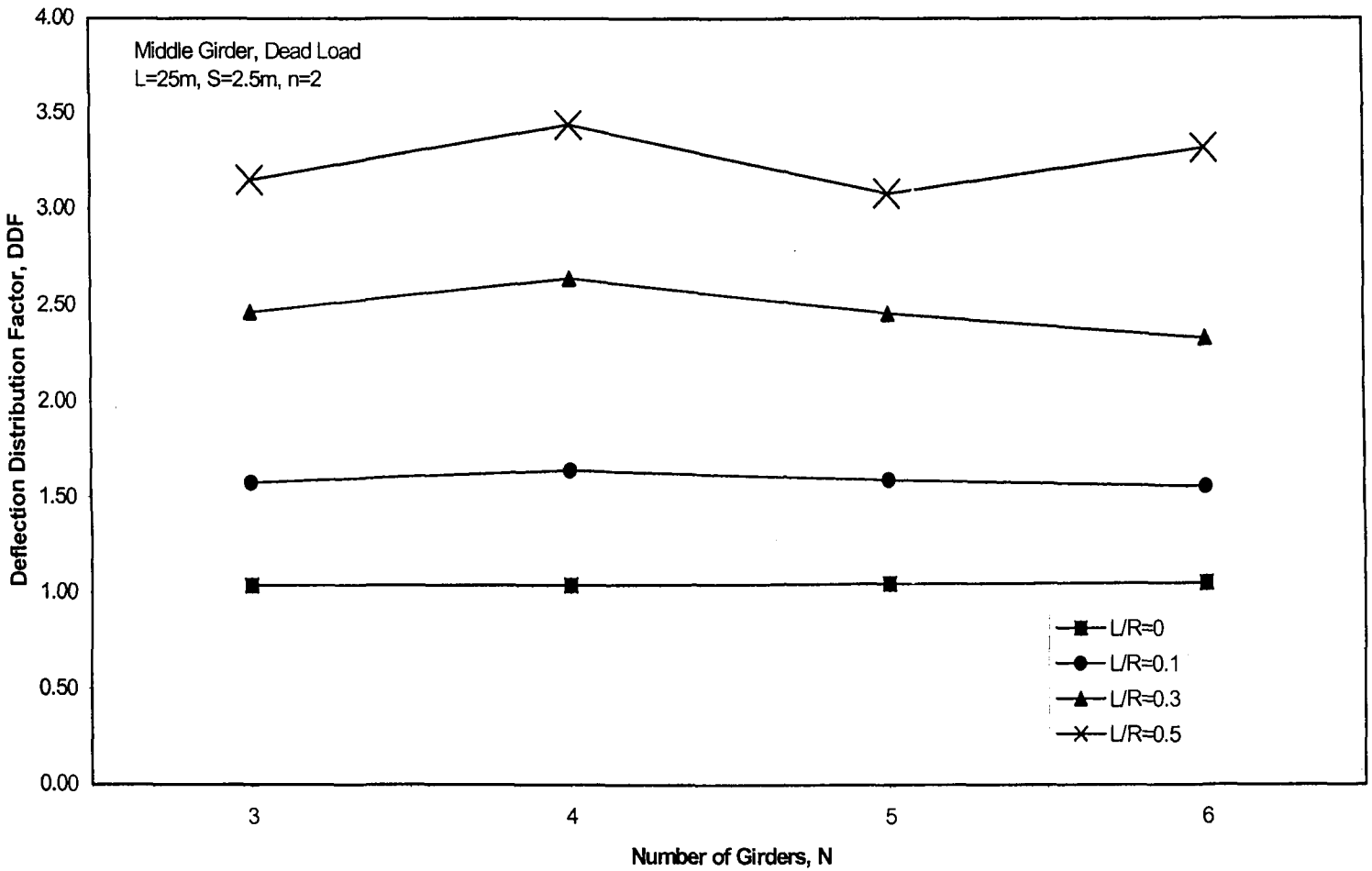

Figure 4. 51 Effect of number of girders on the deflection distribution factor for the middle girder due to dead load

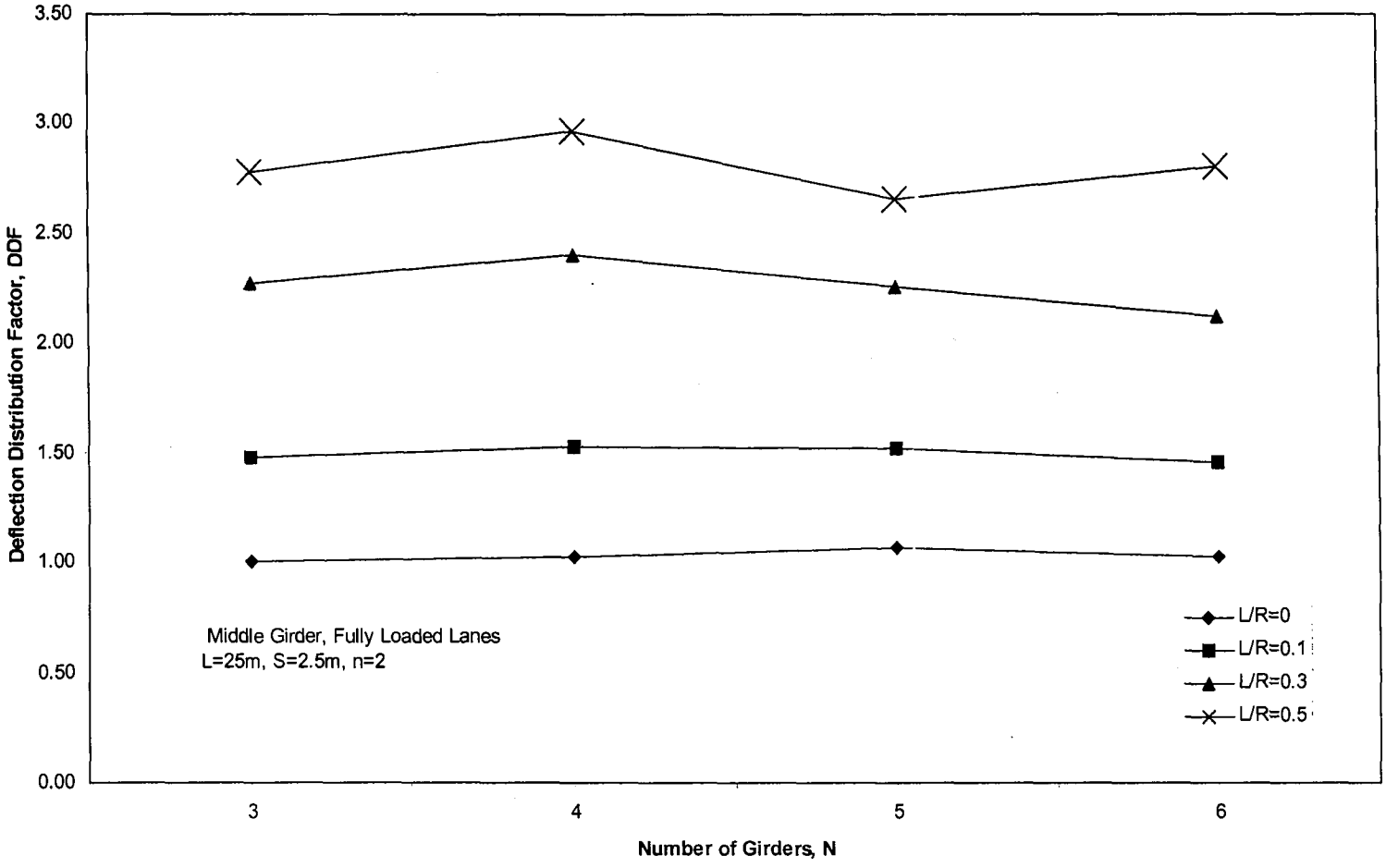

Figure 4.52 Effect of number of girders on the deflection distribution factor for the middle girder due to fully loaded lanes

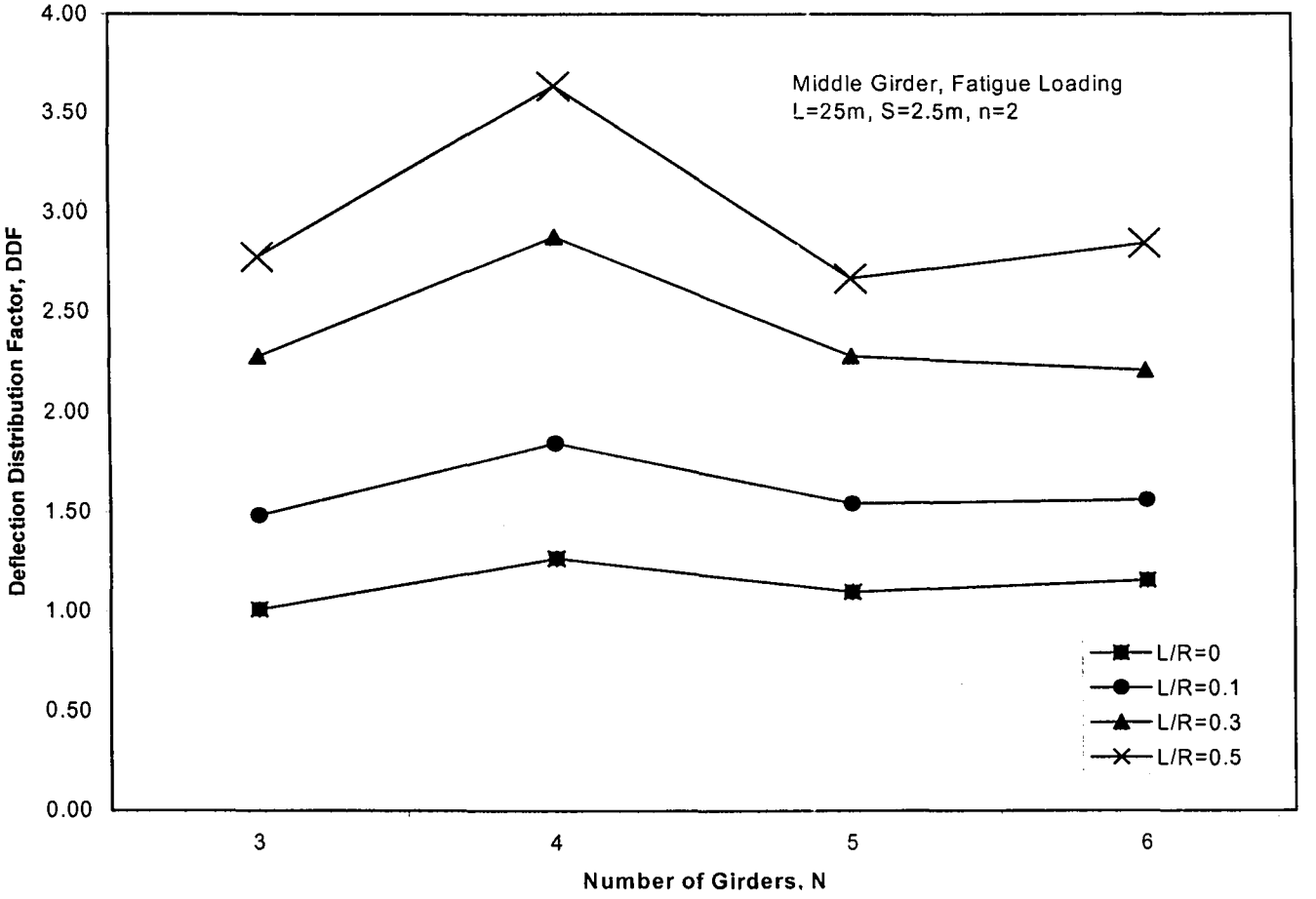

Figure 4.53 Effect of number of girders on the deflection distribution factor for the middle girder due to fatigue loading

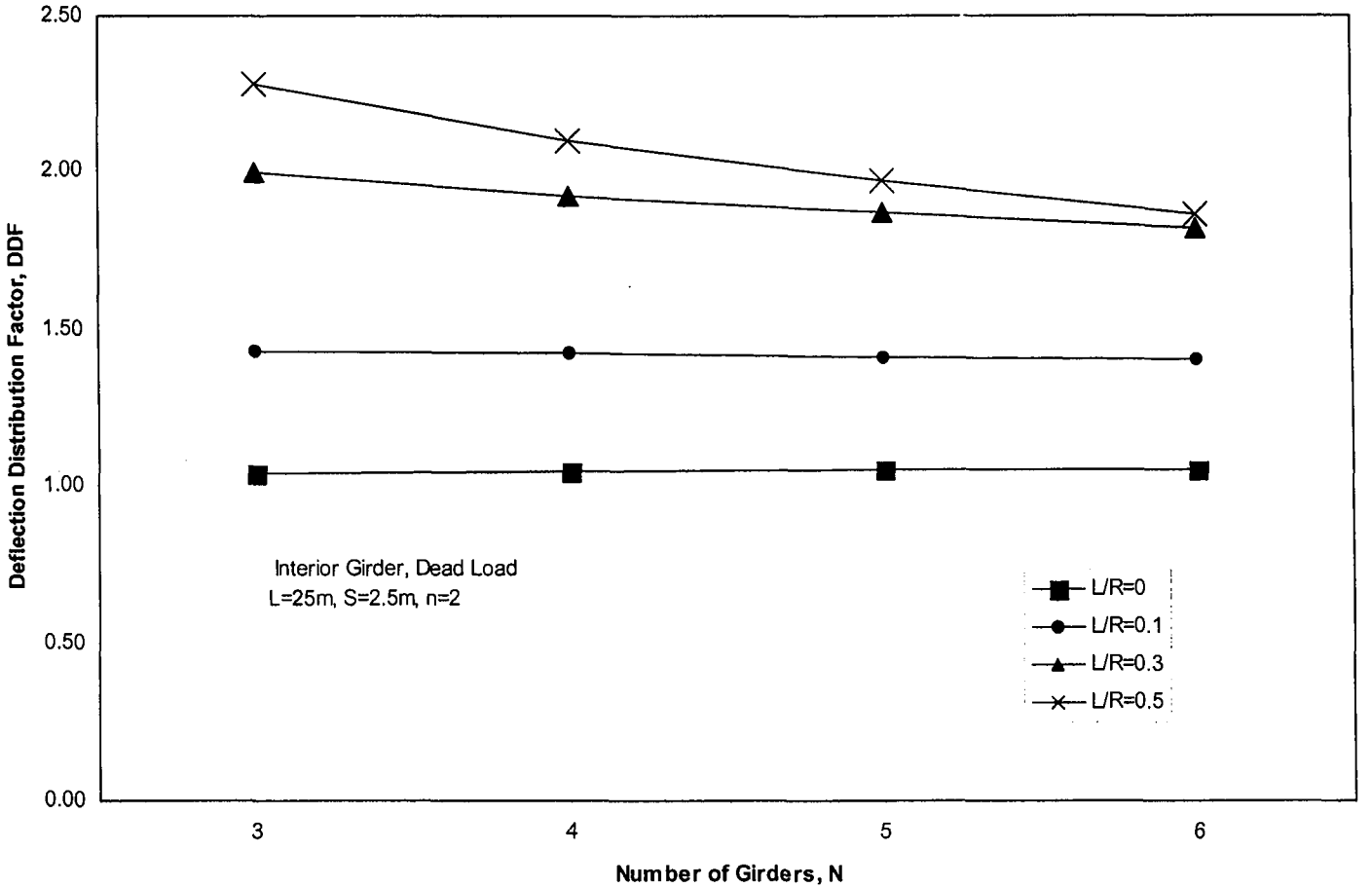

Figure 4.54 Effect of number of girders on the deflection distribution factor for the interior girder due to dead load

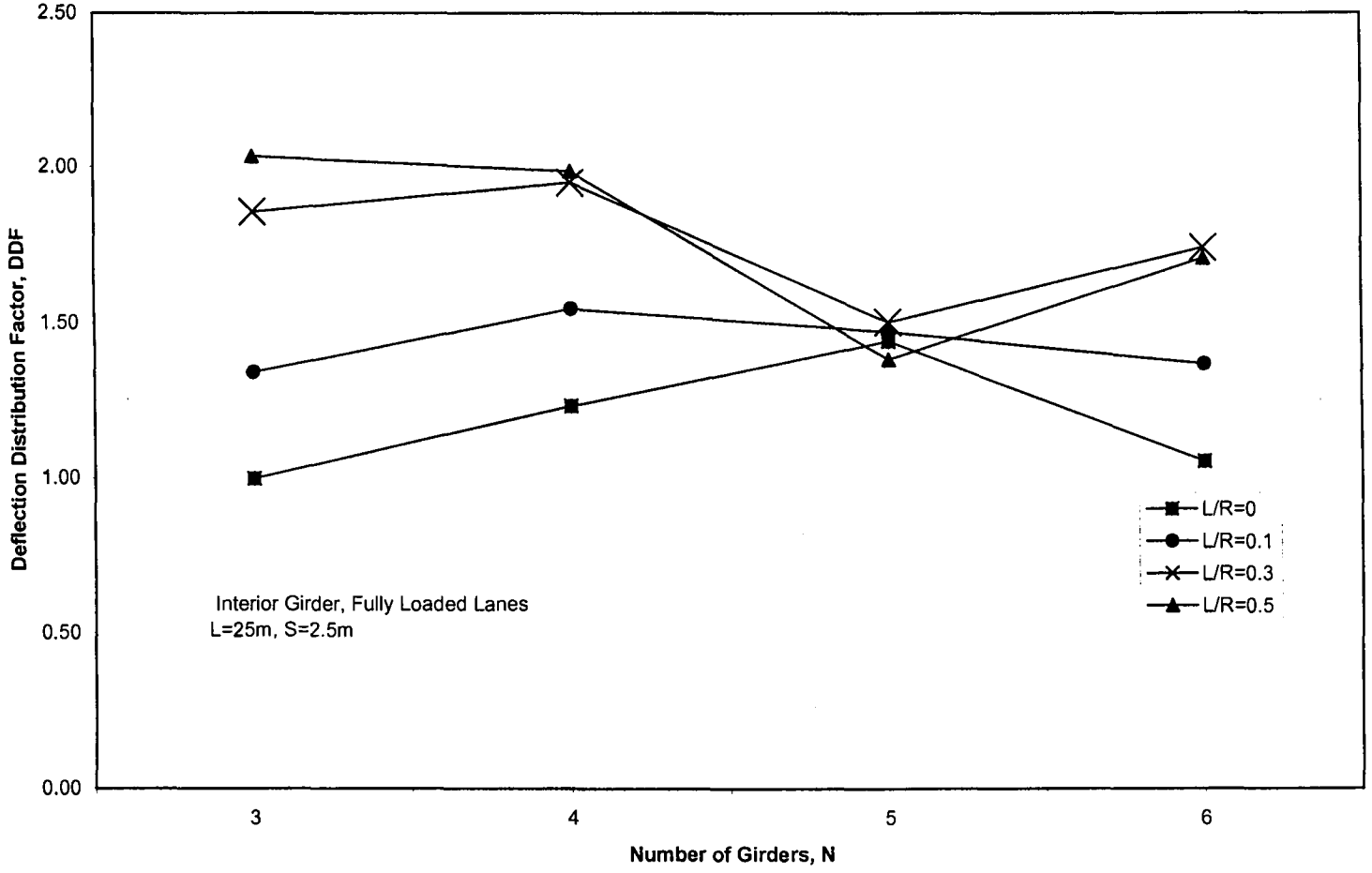

Figure 4.55 Effect of number of girders on the deflection distribution factor for the interior girder due to fully loaded lanes

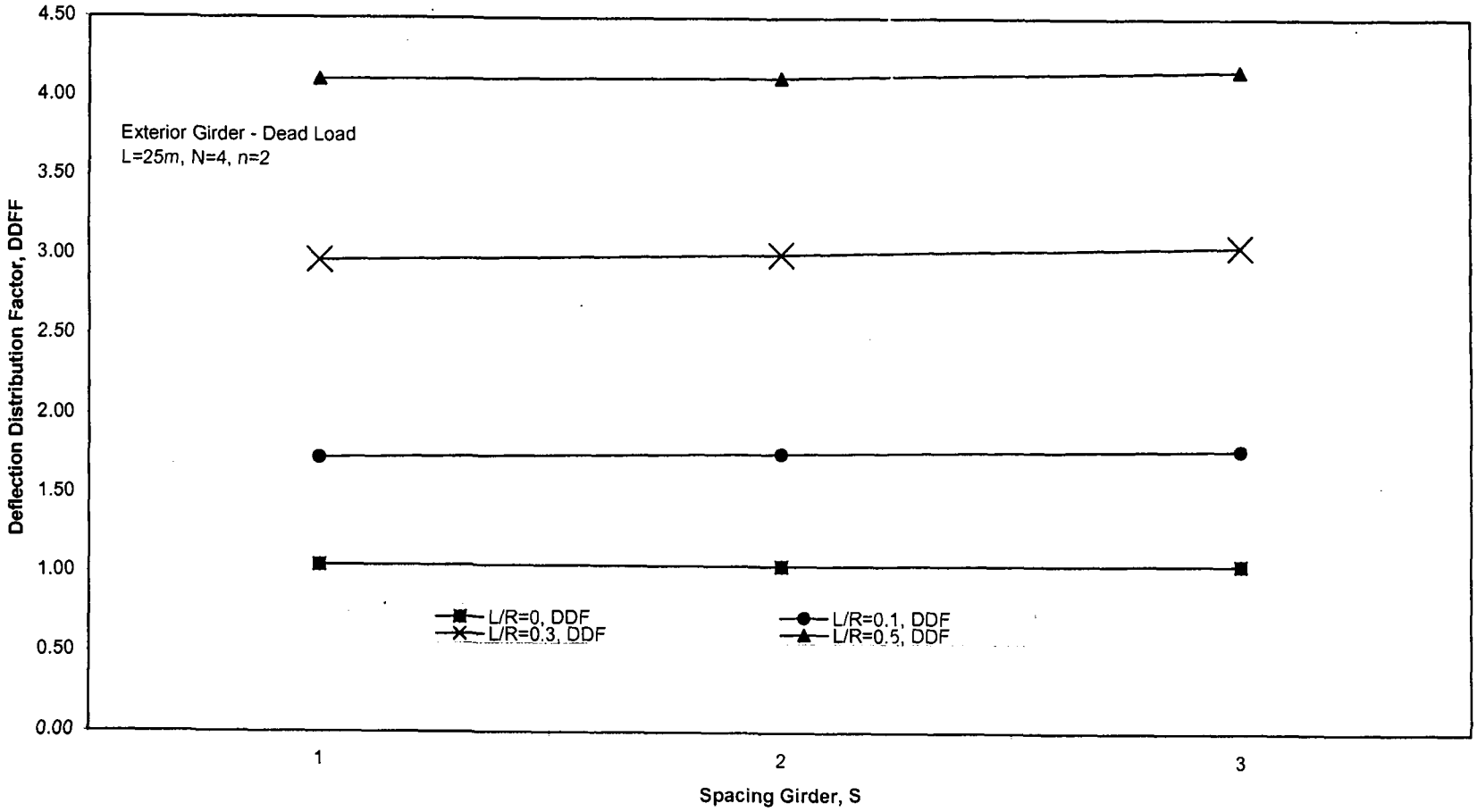

Figure 4.56 Effect of spacing on the deflection distribution factor for the exterior girder due to dead load

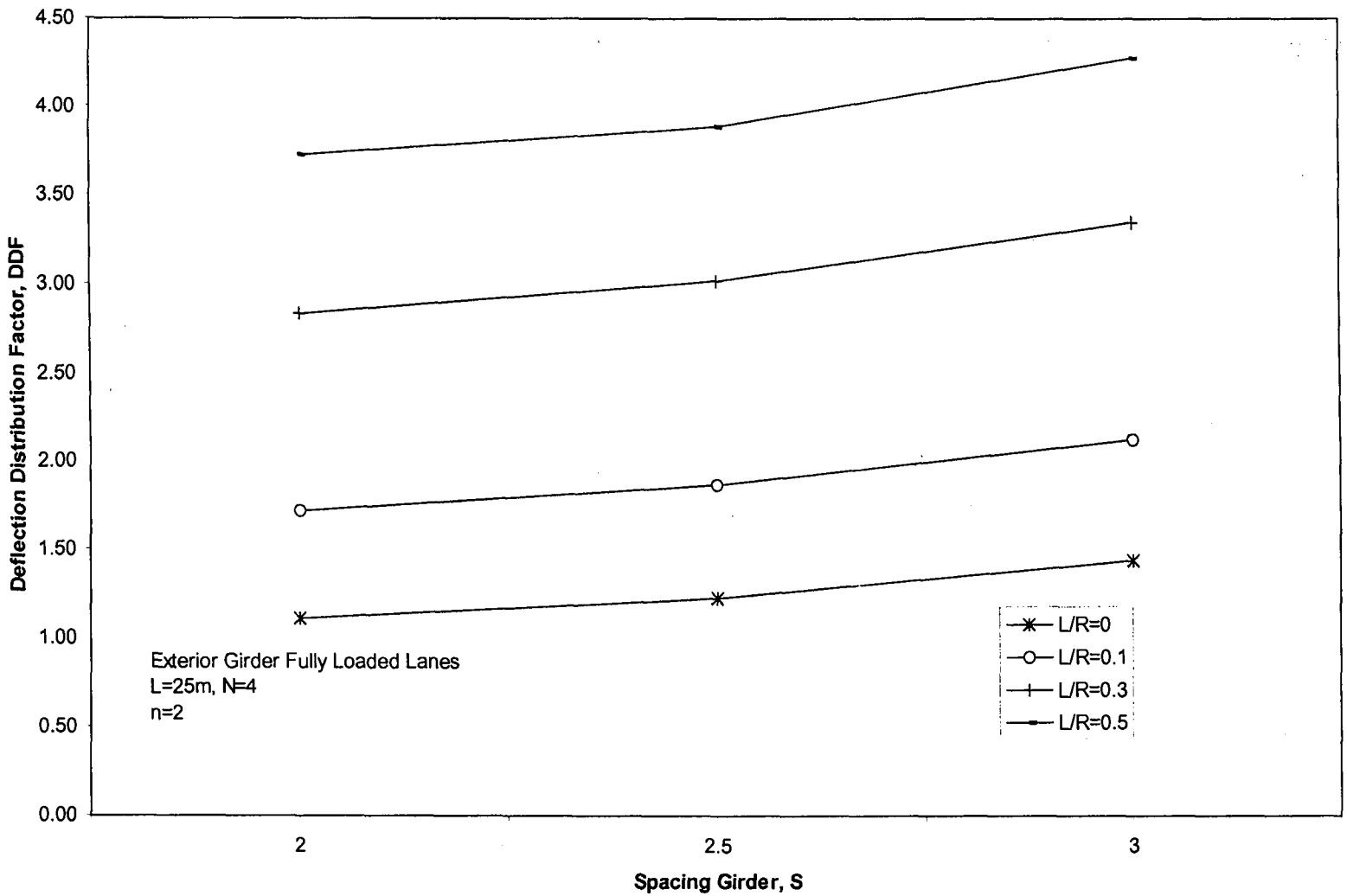

Figure 4.57 Effect of spacing on the deflection distribution factor for the exterior girder due to fully loaded lanes

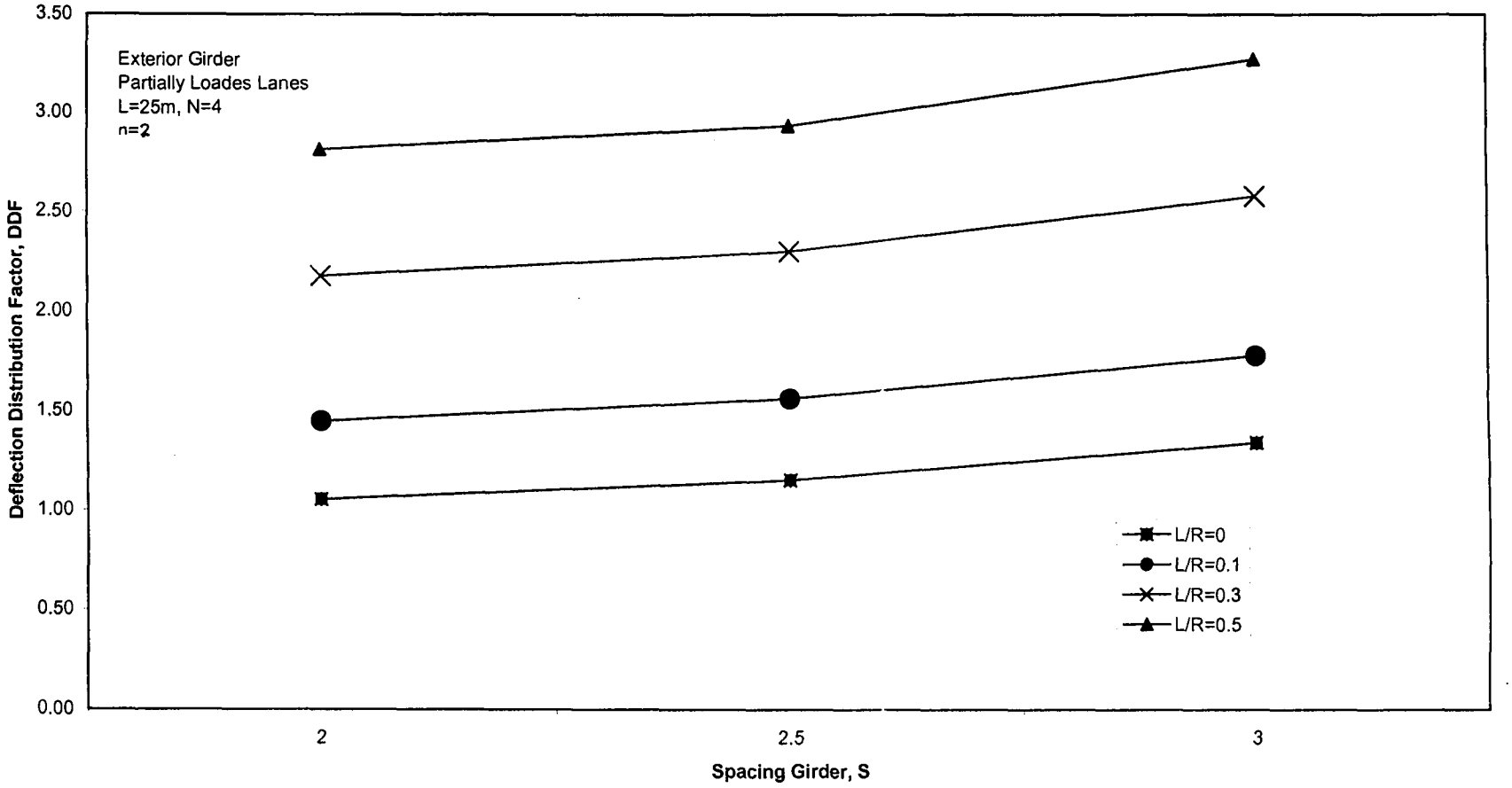

Figure 4.58 Effect of spacing on the deflection distribution factor for the exterior girder due to partially loaded lanes

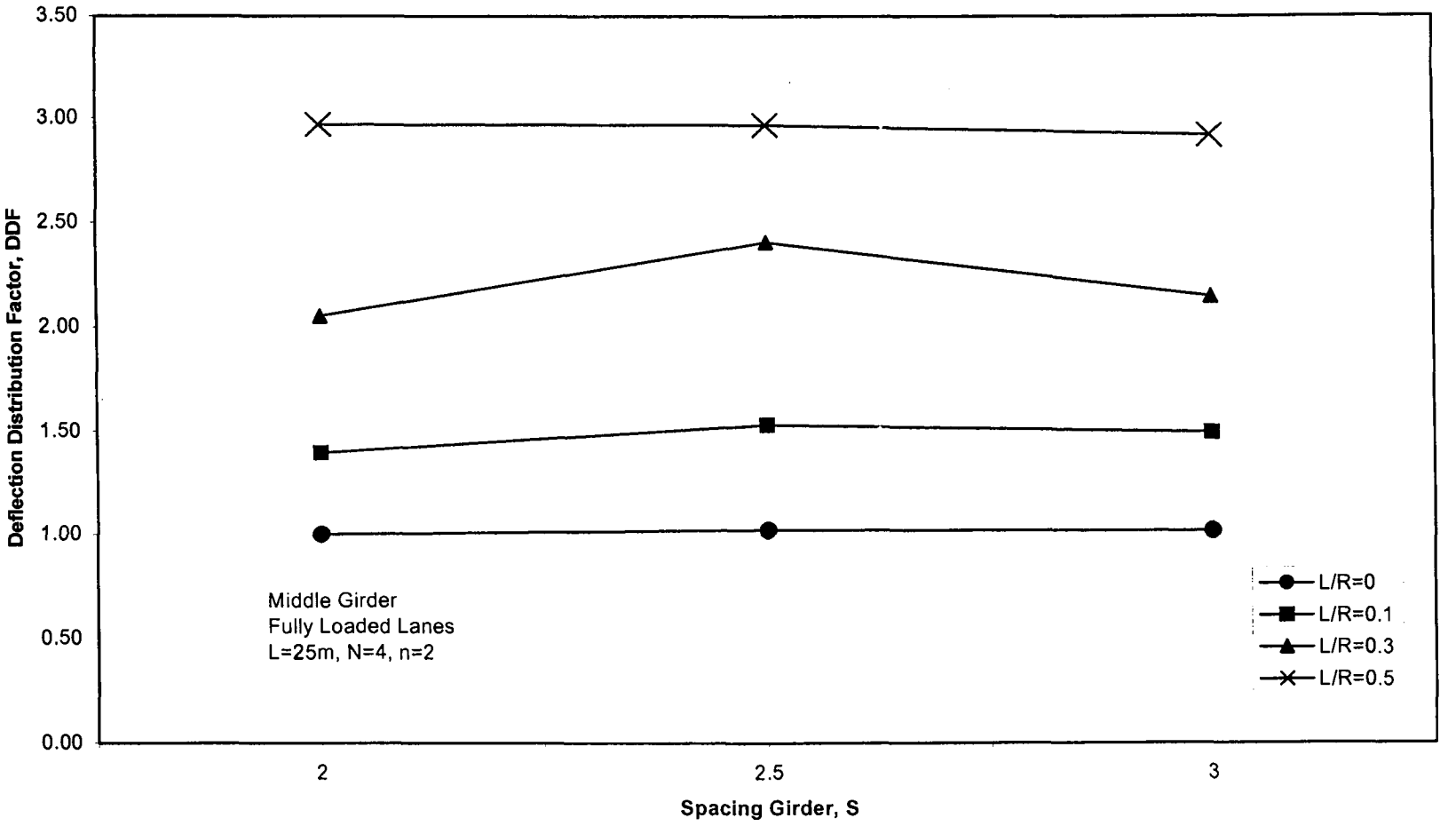

Figure 4.59 Effect of spacing on the deflection distribution factor for the middle girder due to fully loaded lanes

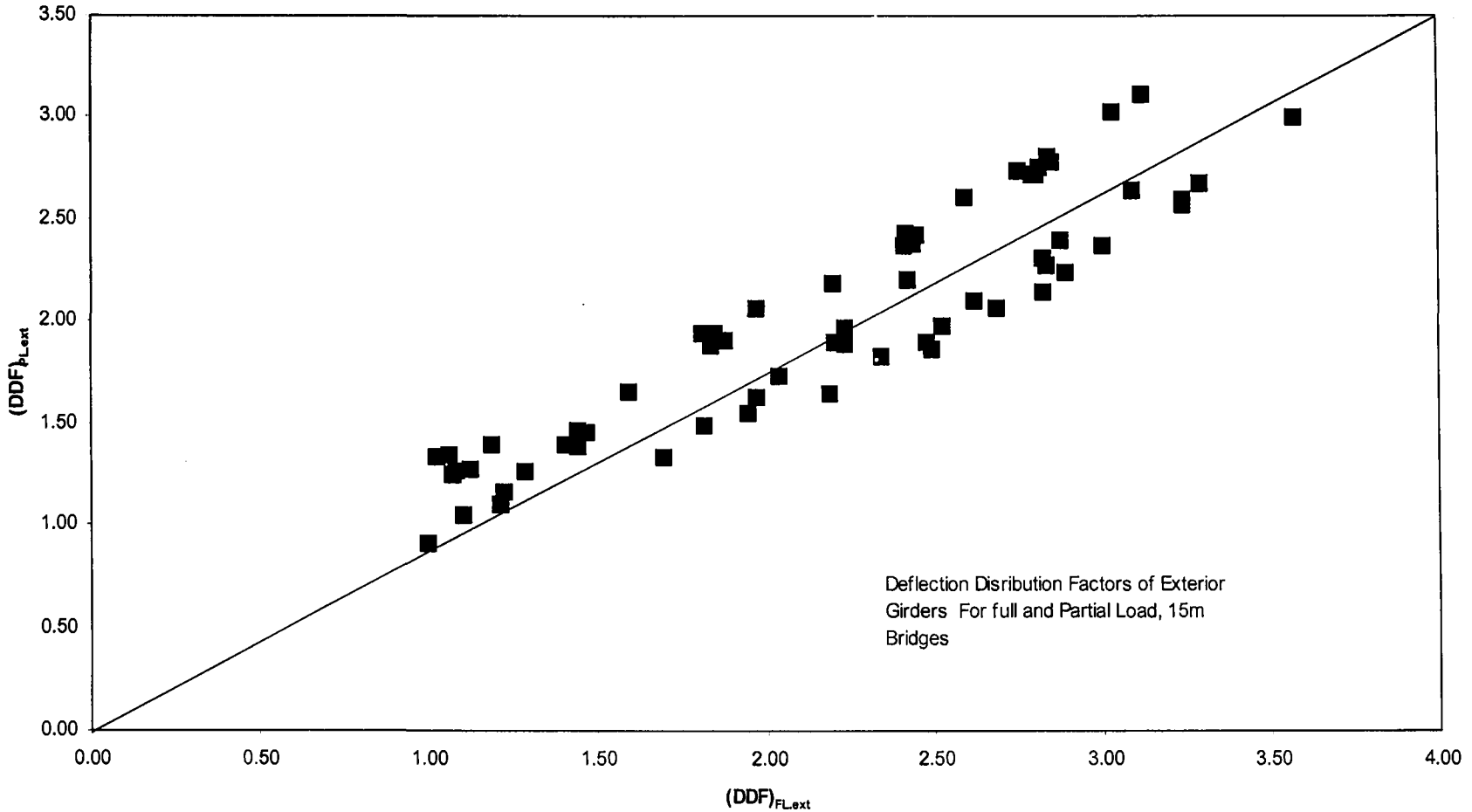

Figure 4.61 Effect of loading condition on the deflection distribution factor for the exterior girder of 15-m-span bridges

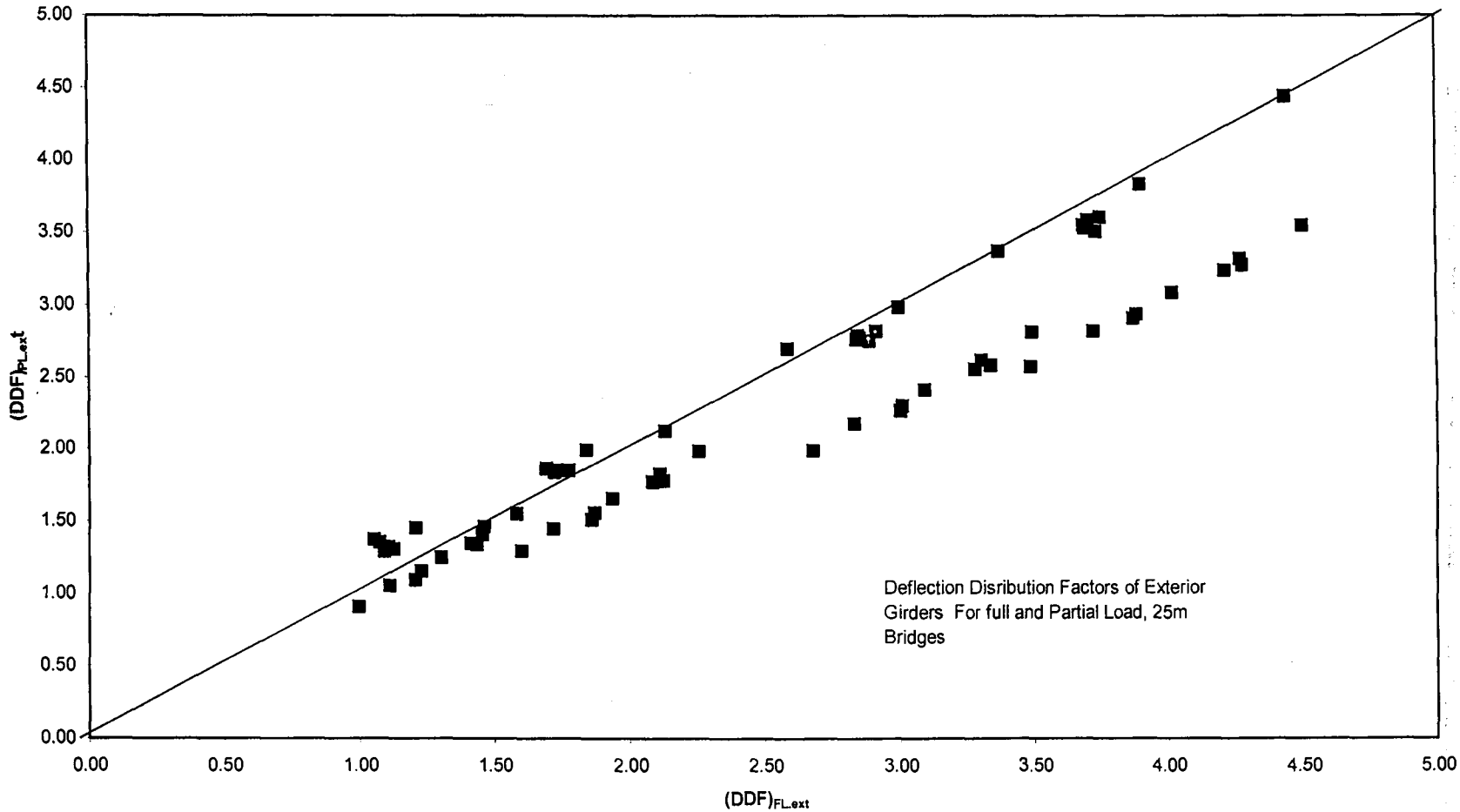

Figure 4.62 Effect of loading condition on the deflection distribution factor for the exterior girder of 25-m-span bridges

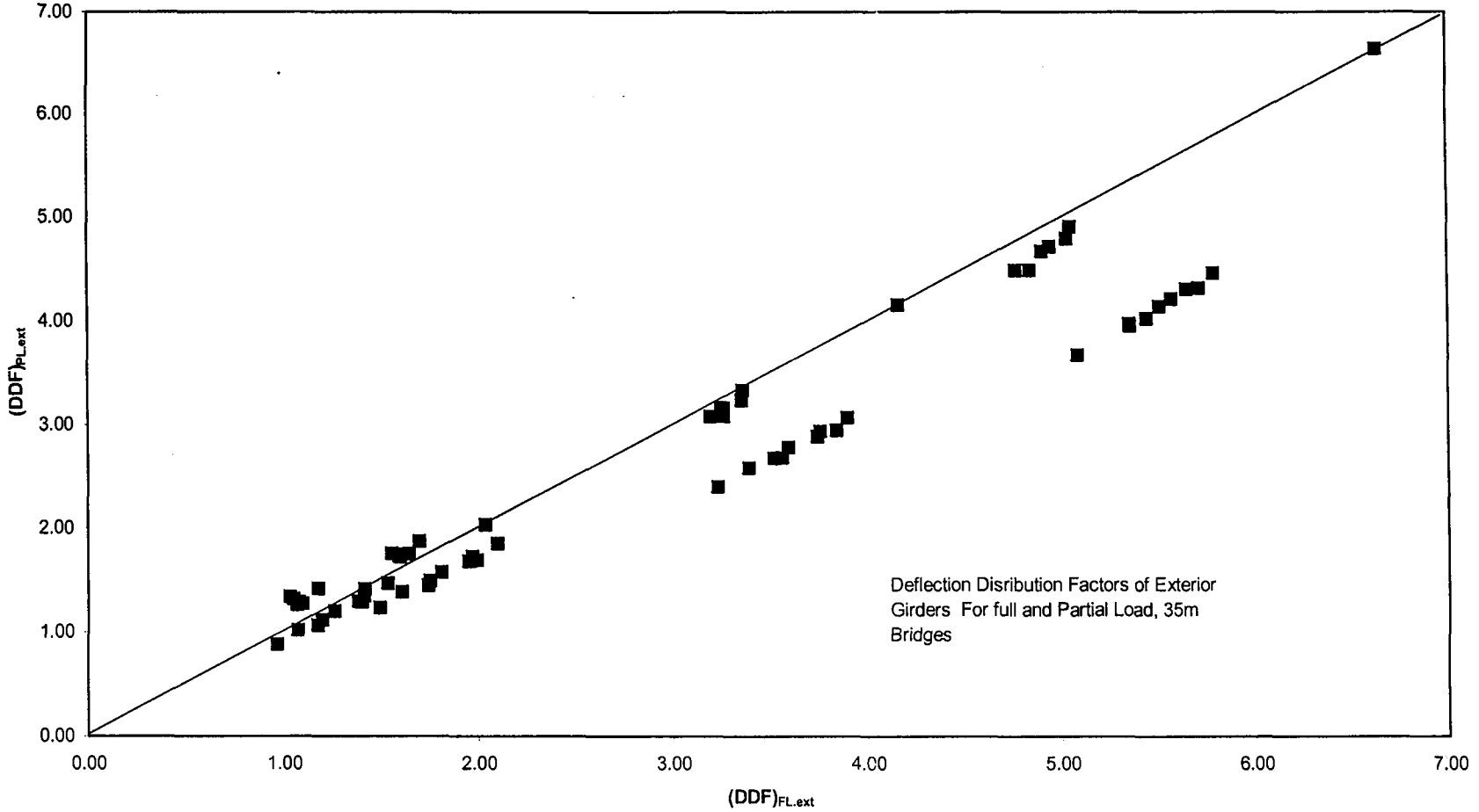

Figure 4.63 Effect of loading condition on the deflection distribution factor for the exterior girder of 35-m-span bridges

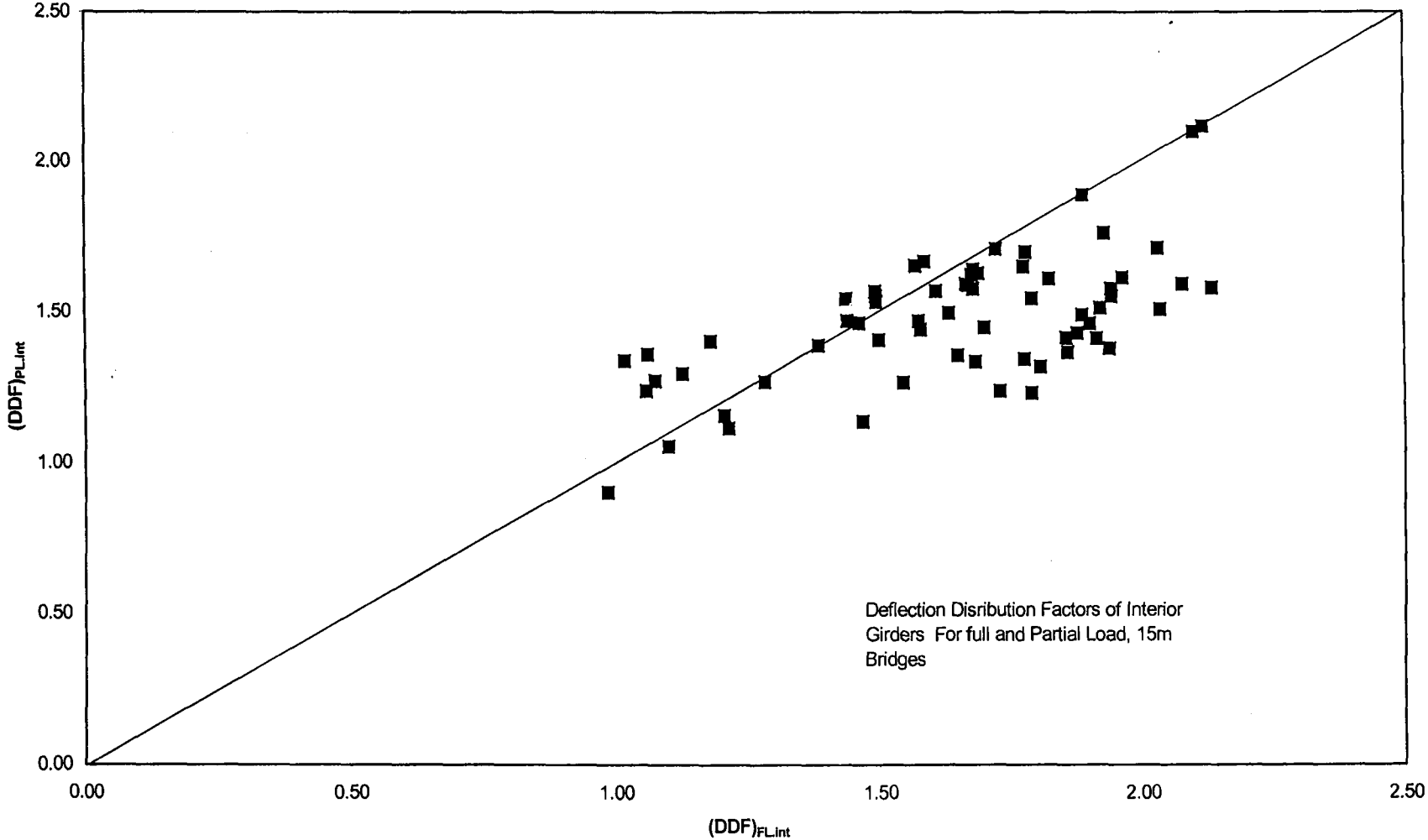

Figure 4.64 Effect of loading condition on the deflection distribution factor for the interior girder of 15-m-span bridges

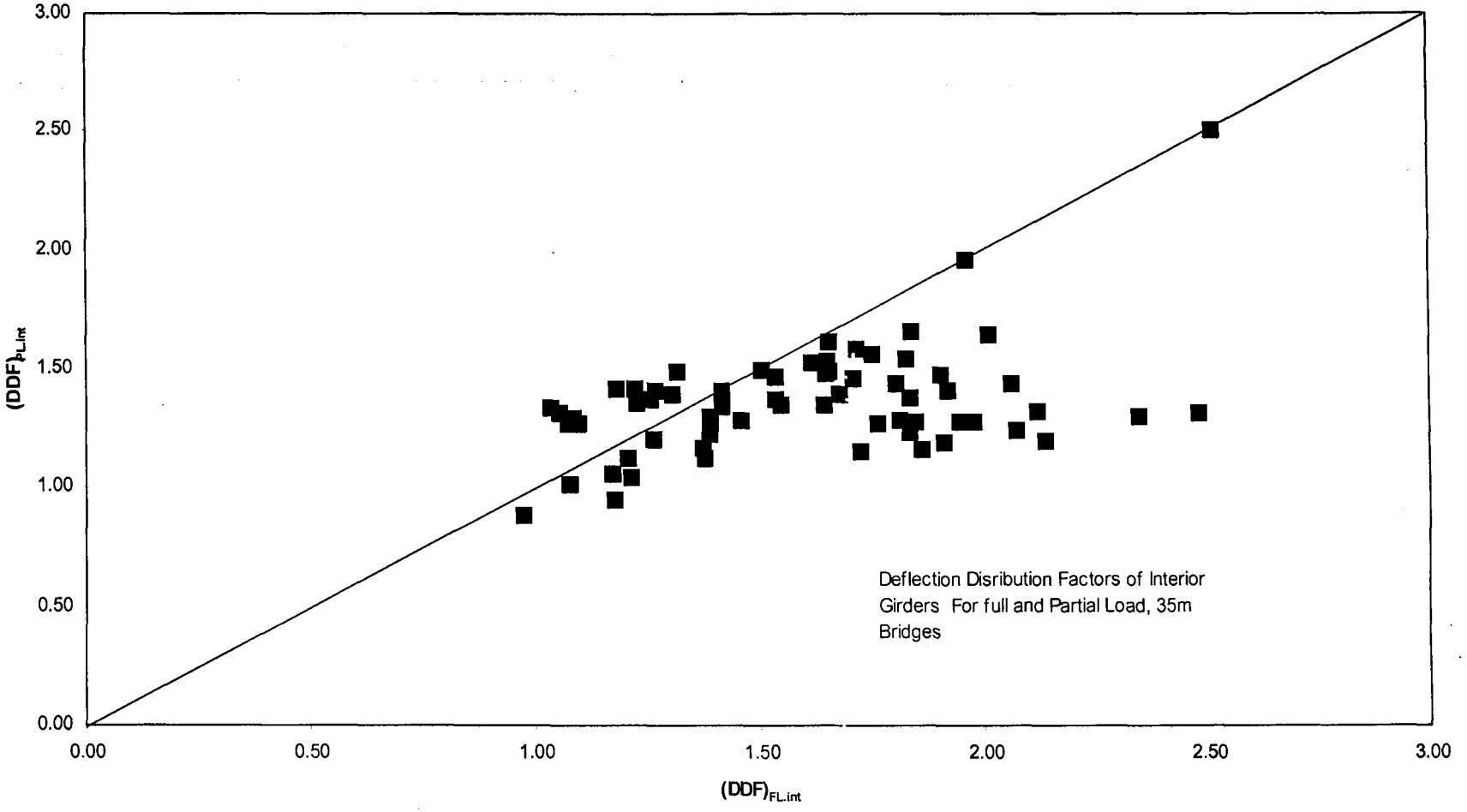

Figure 4.66 Effect of loading condition on the deflection distribution factor for the interior girder of 35-m-span bridges

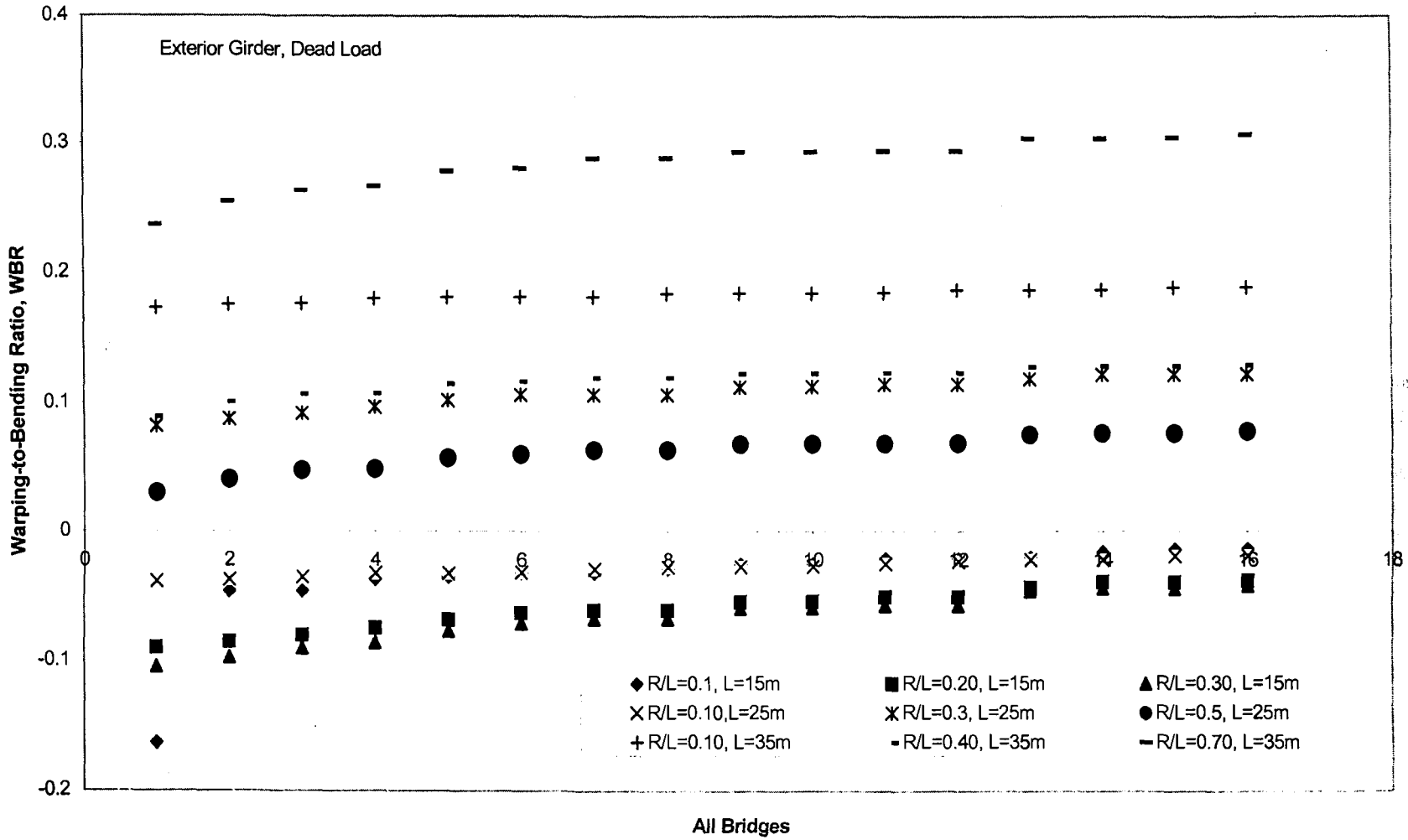

Figure 4.67 Effect of curvature on the warping –to- bending ratio for the exterior girder due to dead load

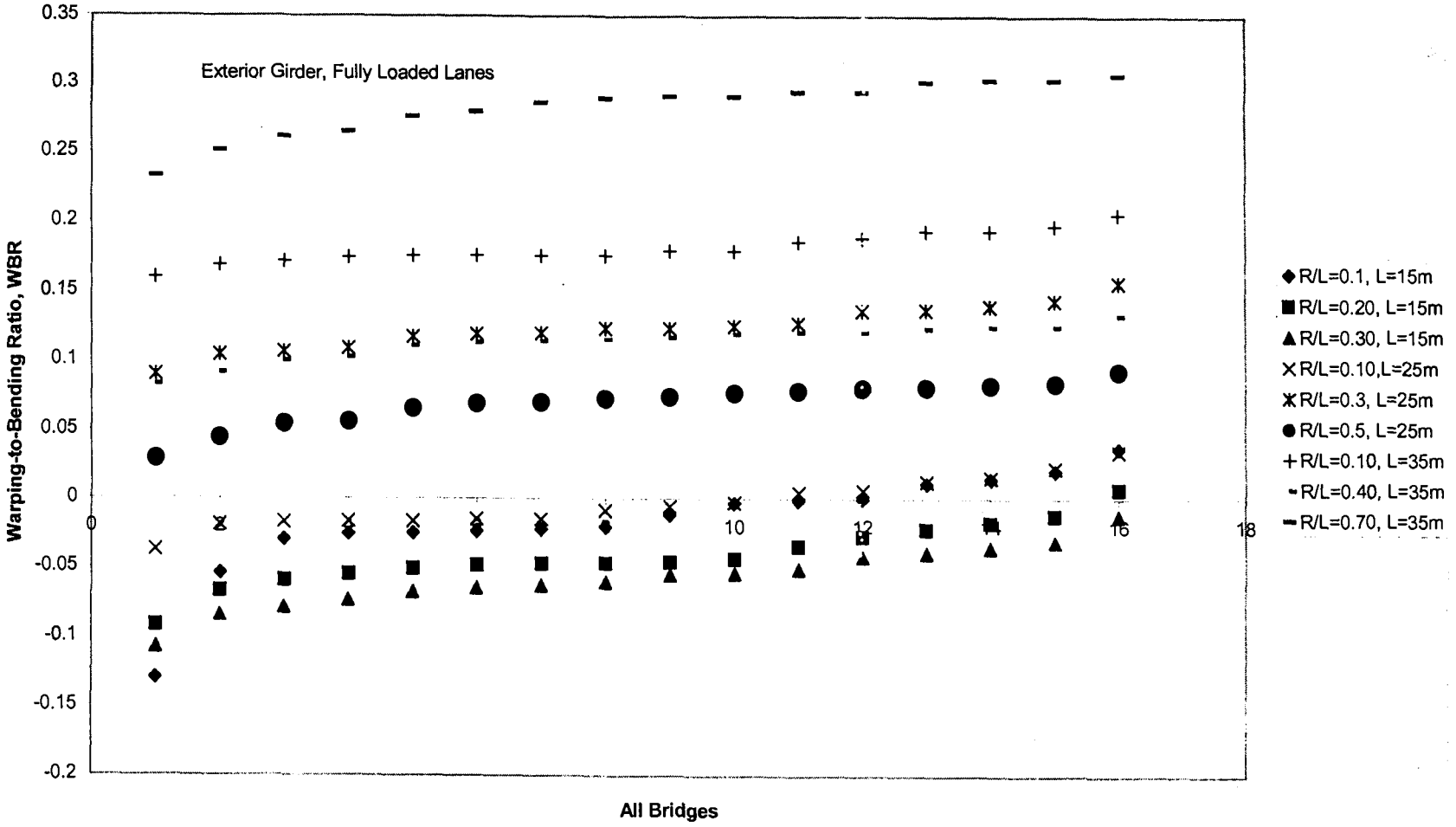

Figure 4.68 Effect of curvature on the warping –to- bending ratio for the exterior girder due to fully loaded lanes

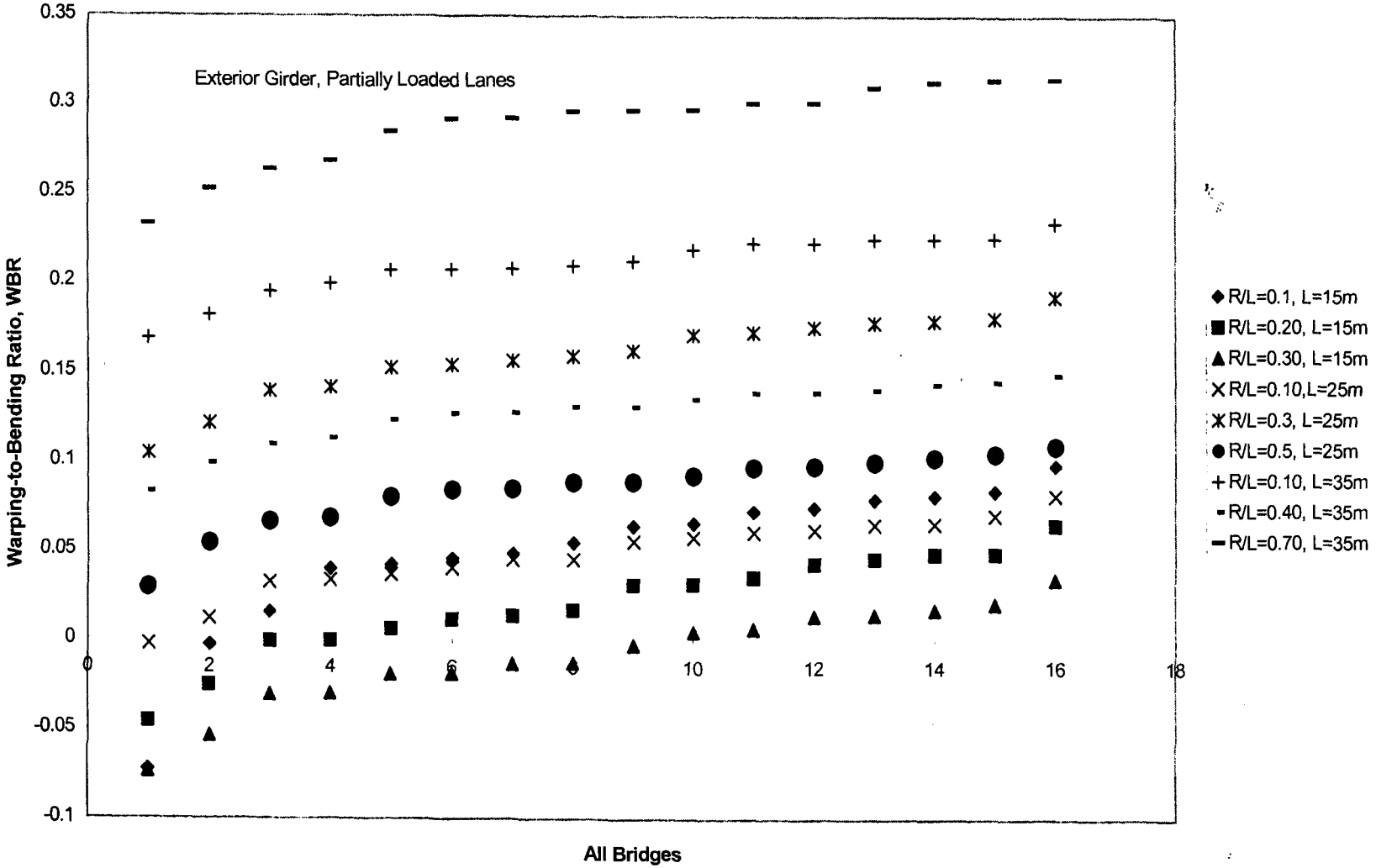

Figure 4.69 Effect of curvature on the warping –to- bending ratio for the exterior girder due to partially loaded lanes

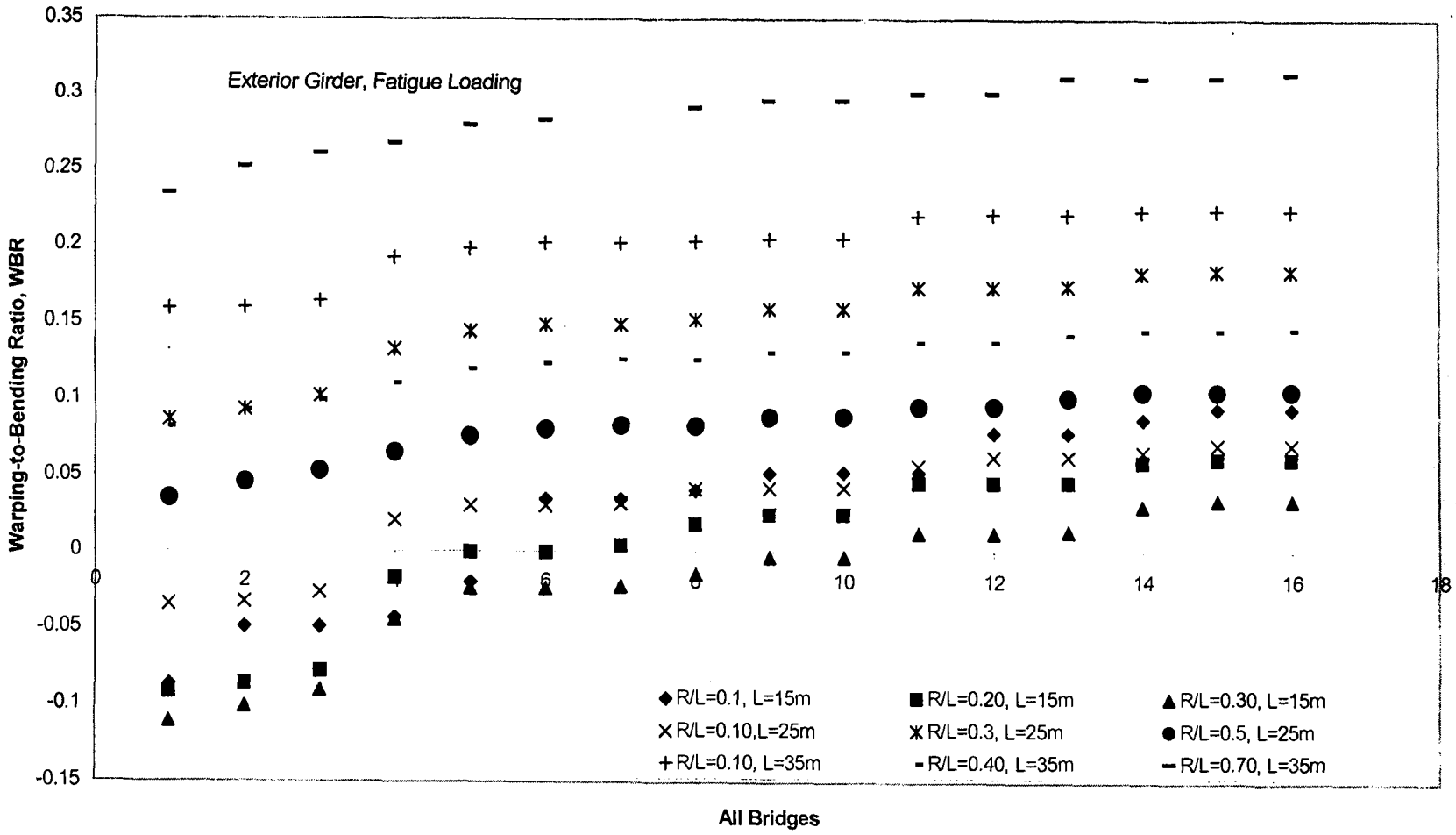

Figure 4.70 Effect of curvature on the warping –to- bending ratio for the exterior girder due to fatigue loading

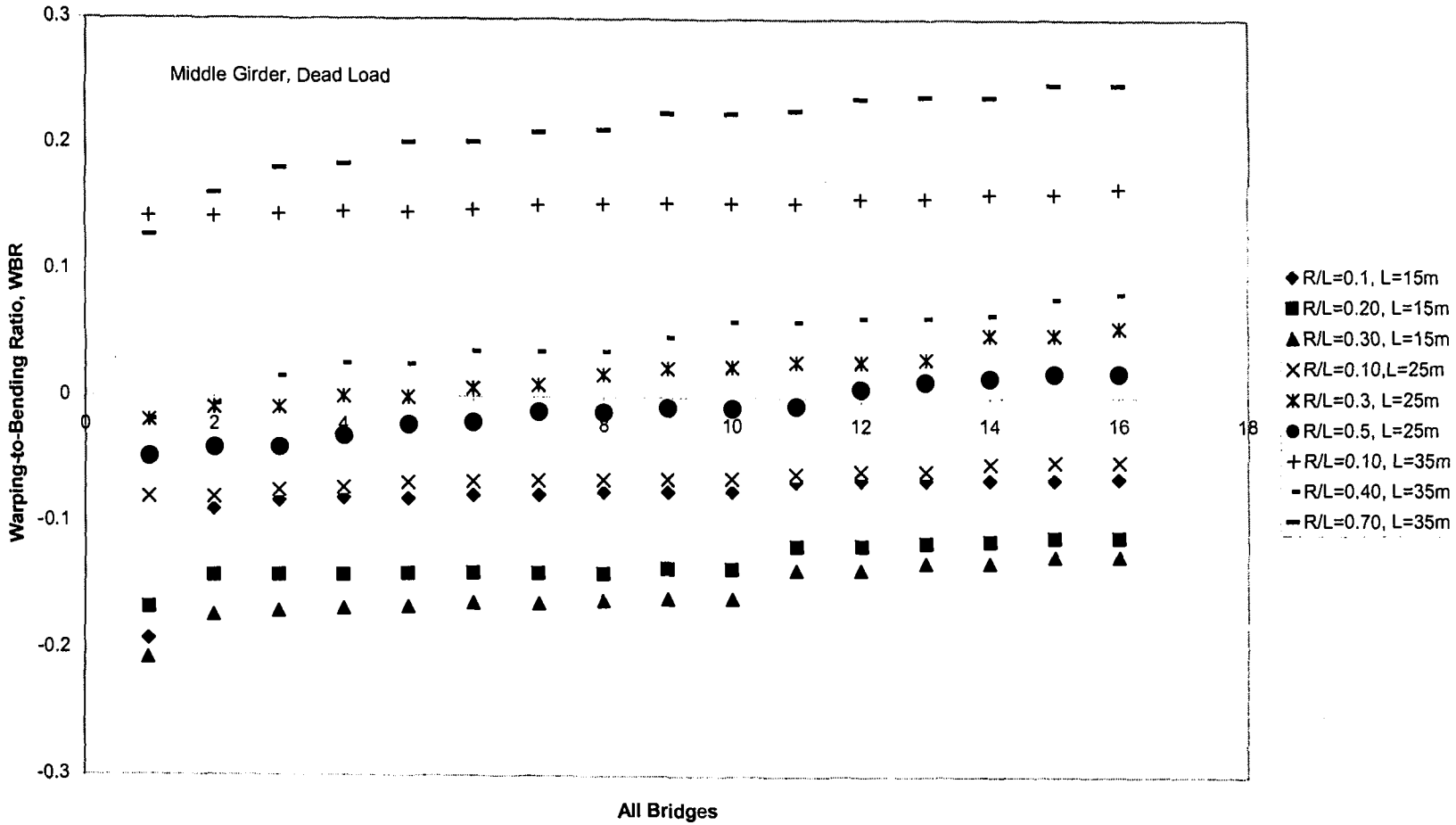

Figure 4.71 Effect of curvature on the warping –to- bending ratio for the middle girder due to dead load

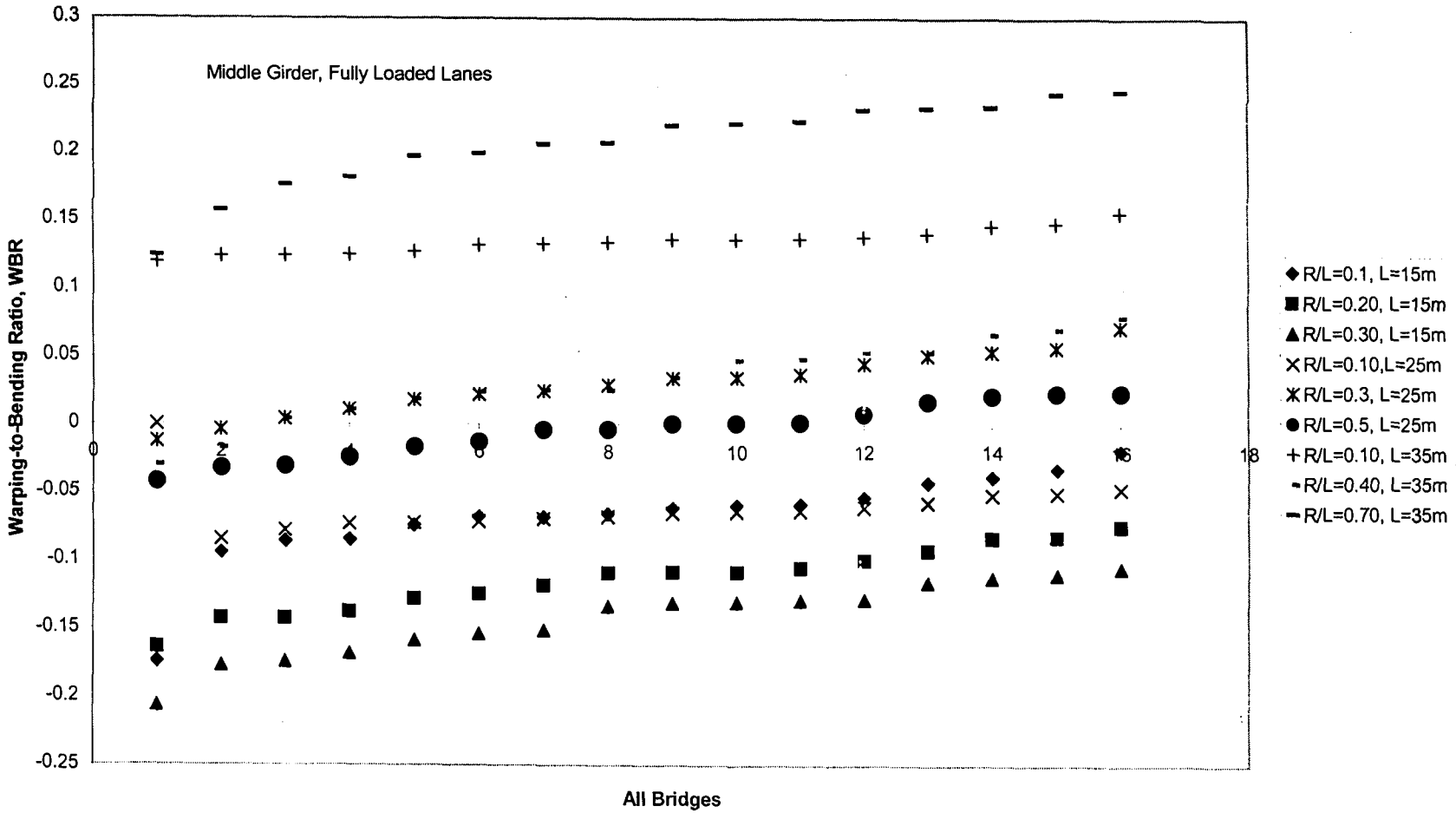

Figure 4.72 Effect of curvature on the warping –to- bending ratio for the middle girder due to fully loaded lanes

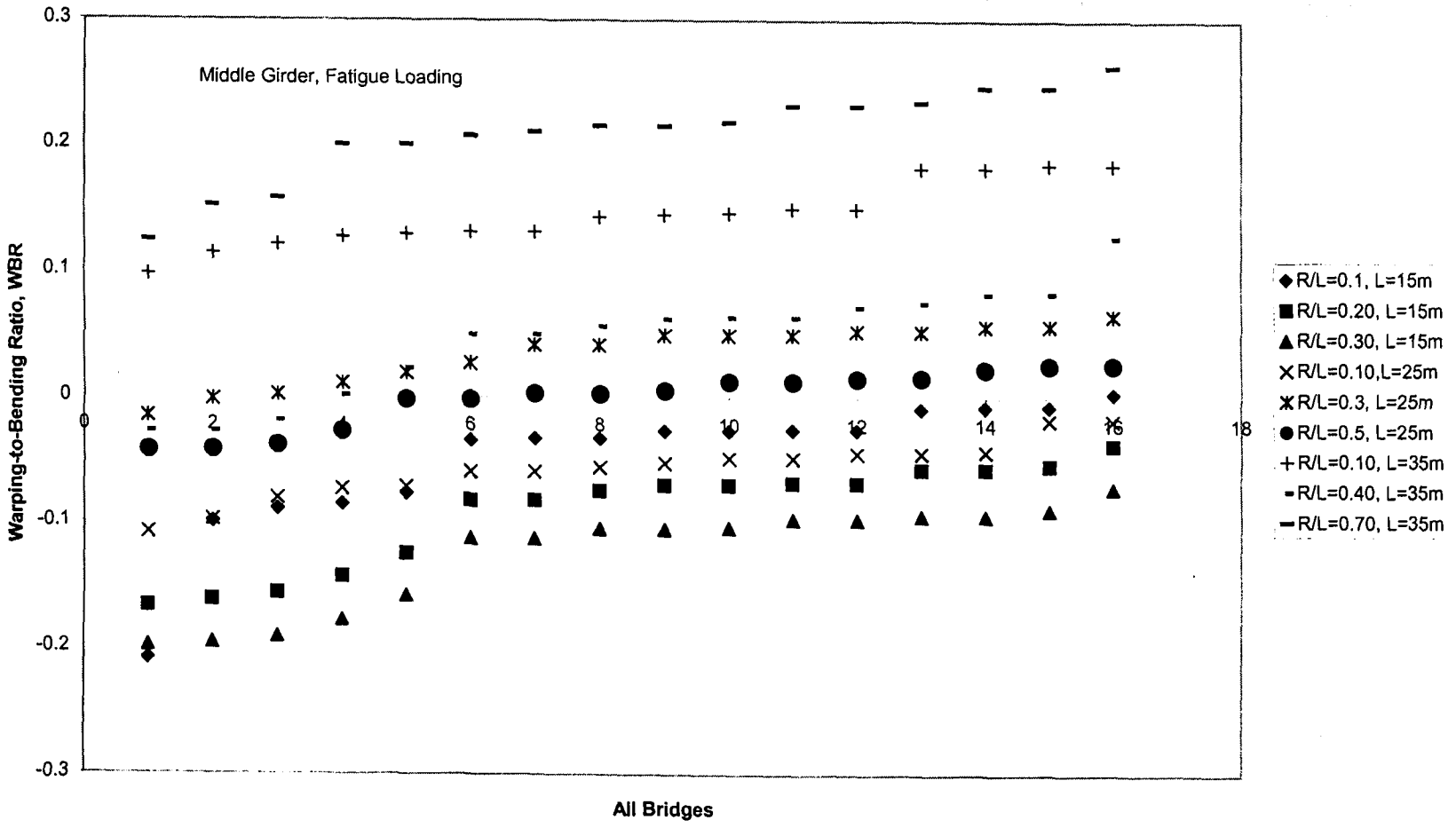

Figure 4.73 Effect of curvature on the warping –to- bending ratio for the middle girder due to fatigue loading

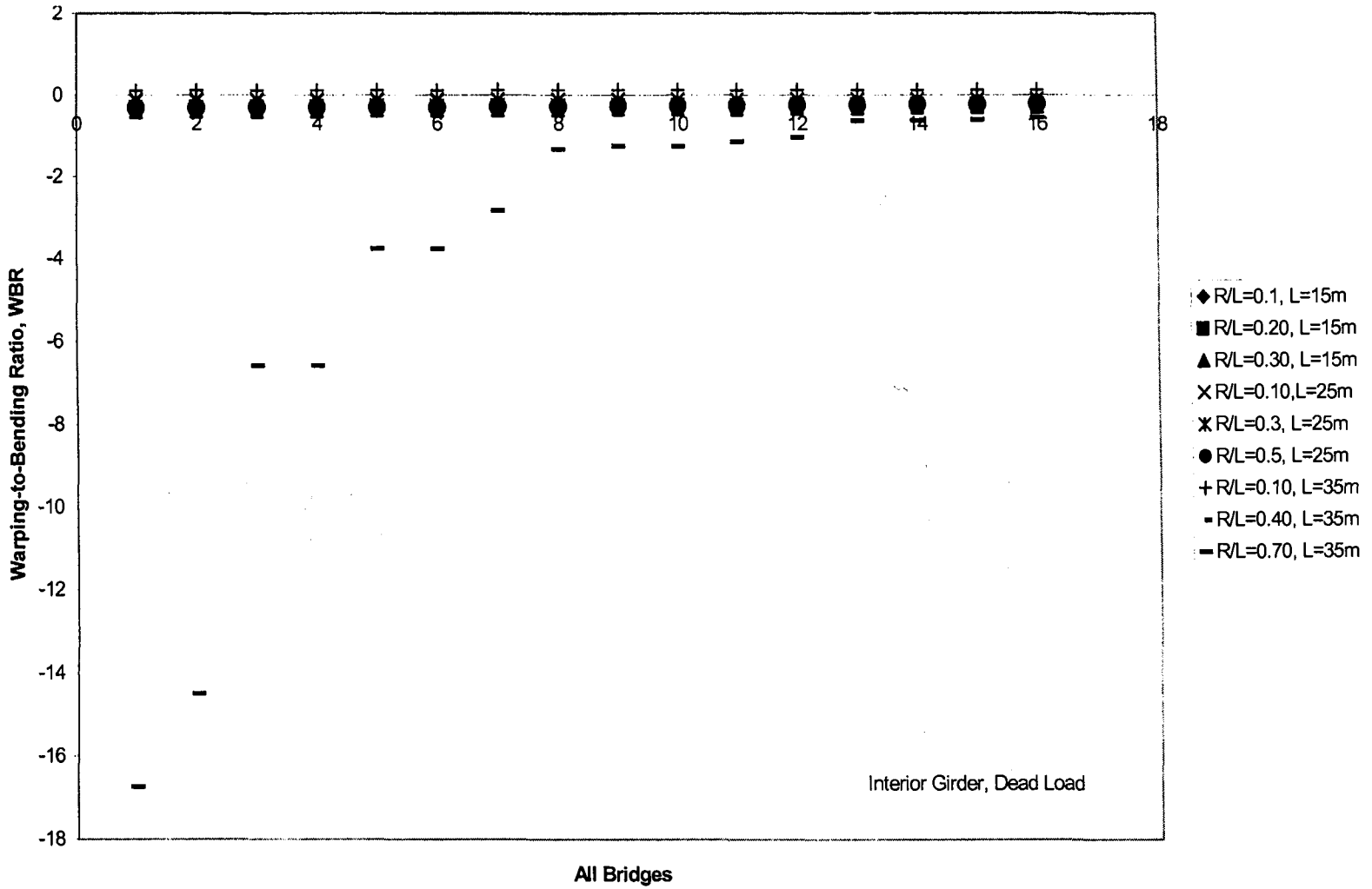

Figure 4.74 Effect of curvature on the warping –to- bending ratio for the interior girder due to dead load

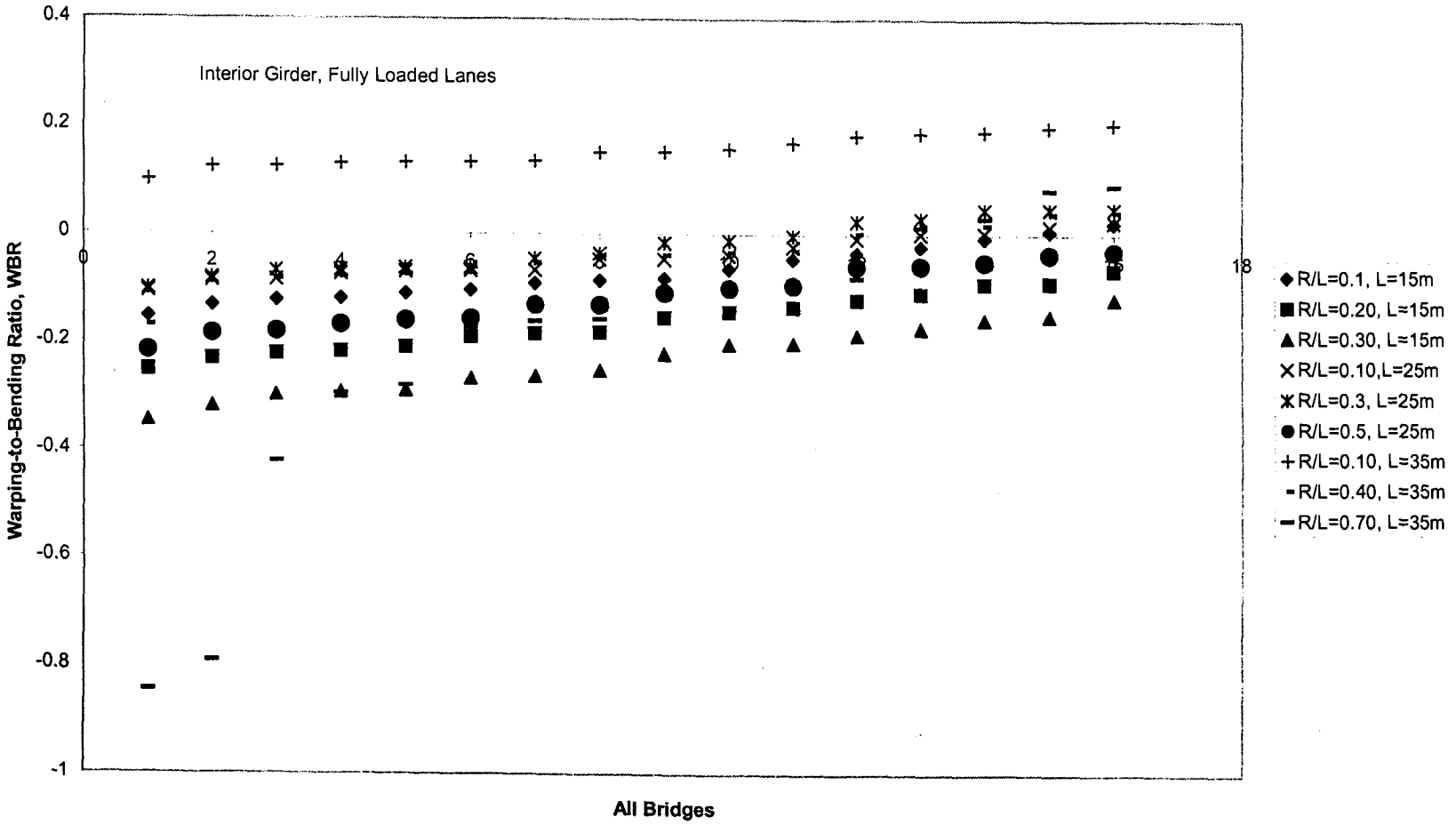

Figure 4.75 Effect of curvature on the warping –to- bending ratio for the interior girder due to fully loaded lanes

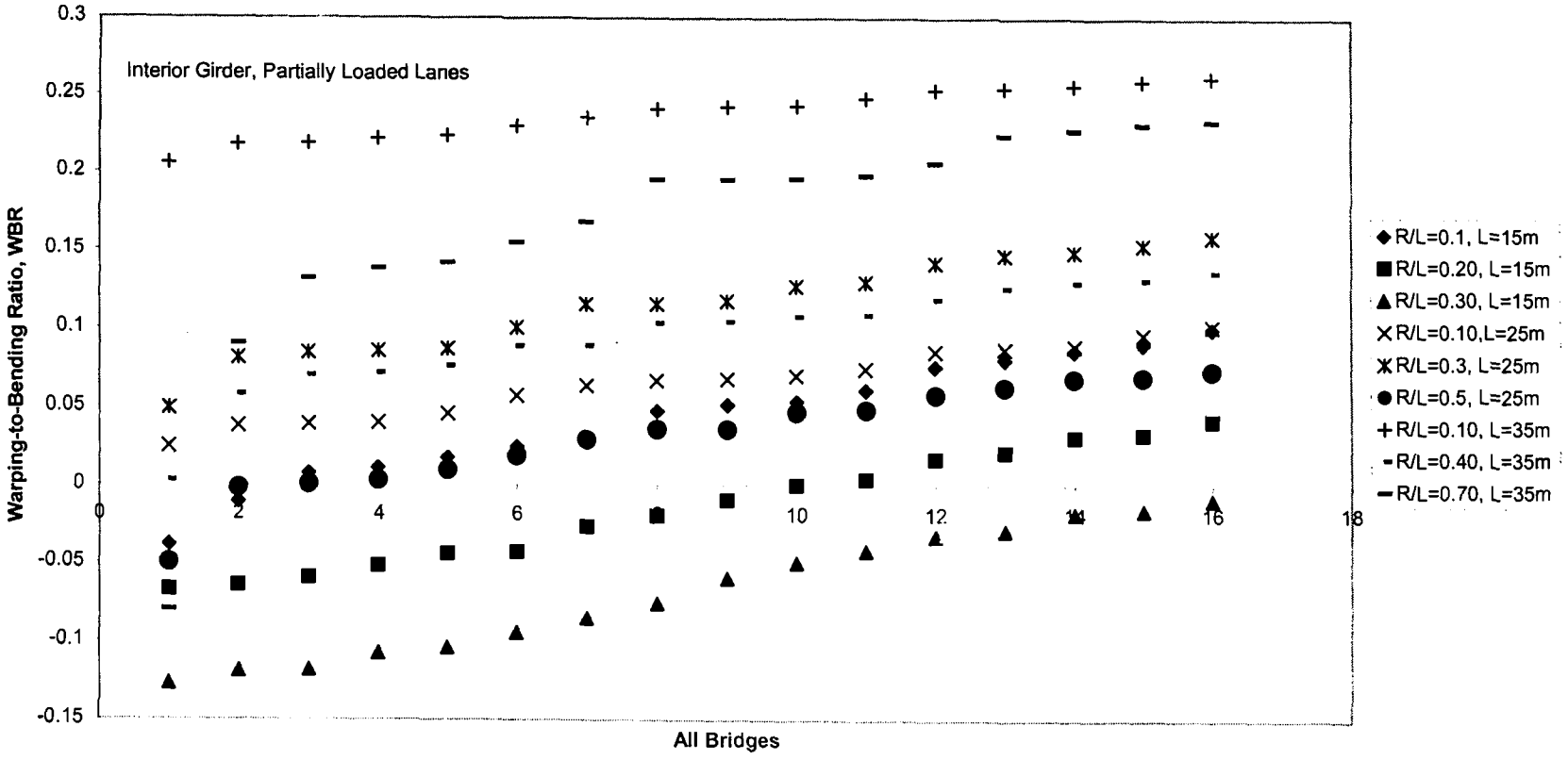

Figure 4.76 Effect of curvature on the warping –to- bending ratio for the interior girder due to partially loaded lanes

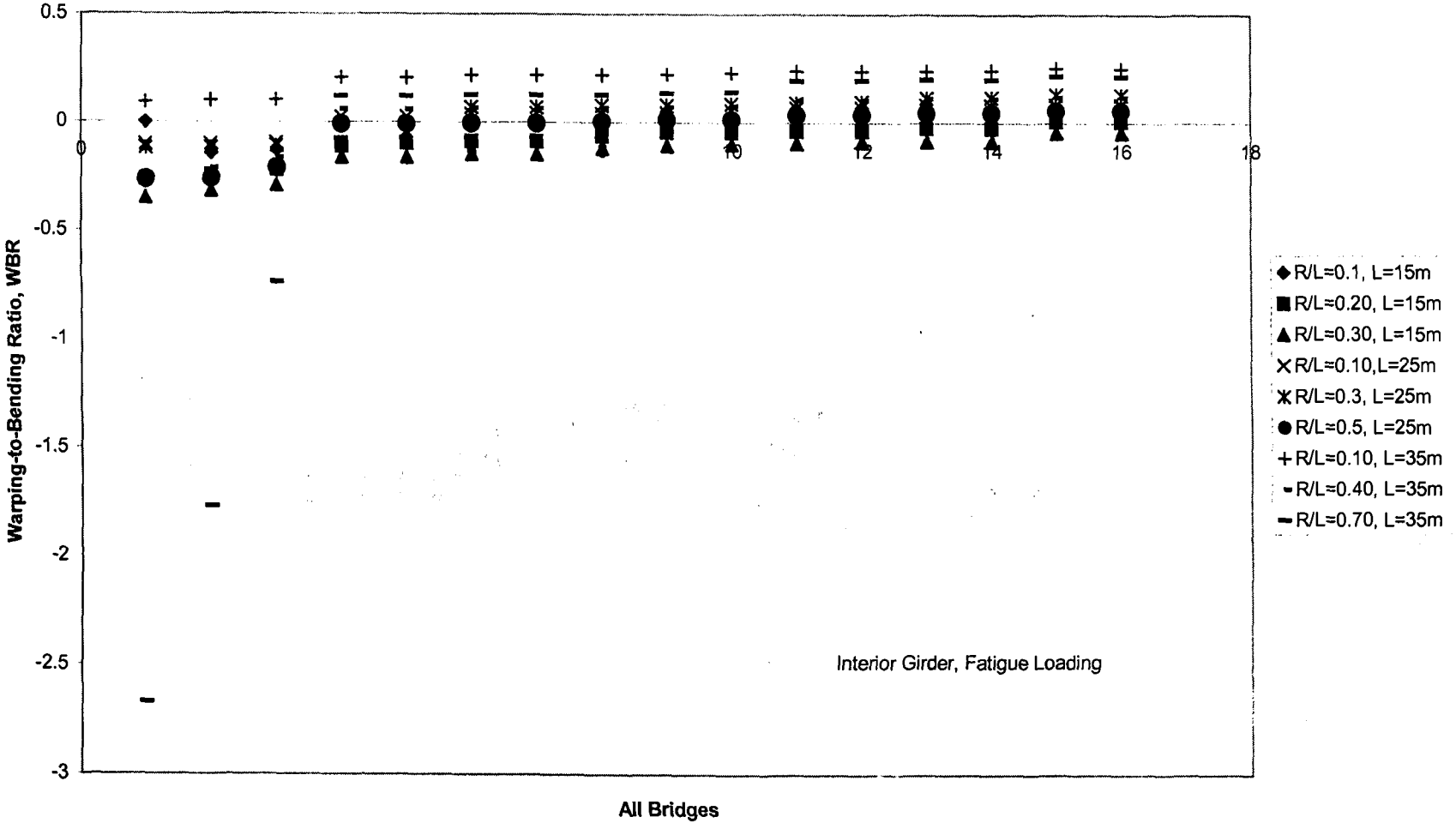

Figure 4.77 Effect of curvature on the warping –to- bending ratio for the interior girder due to fatigue loading

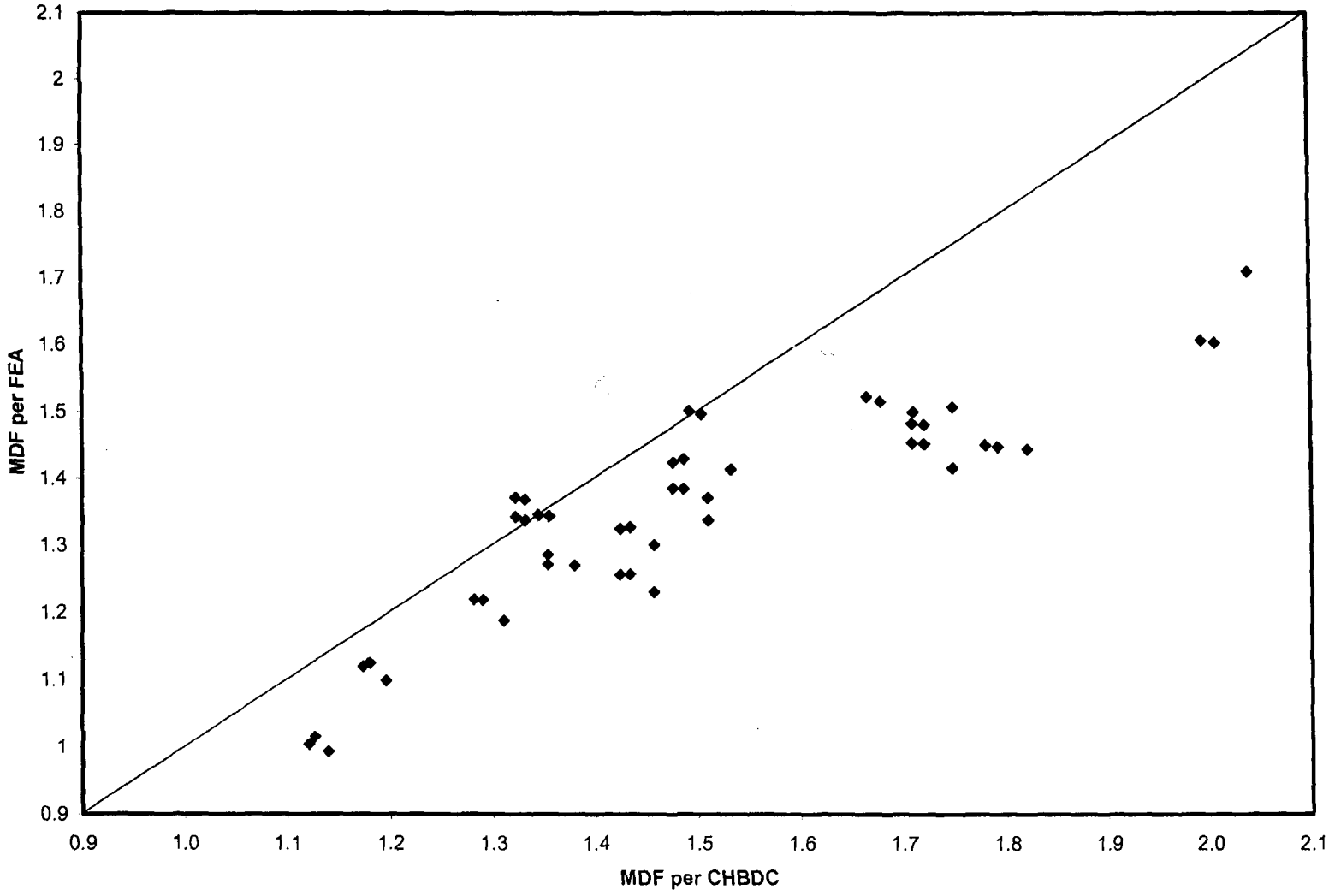

Figure 4.78 Comparison between the moment distribution factors of the exterior girder due to truck loading as specified in the CHBDC and from the present study

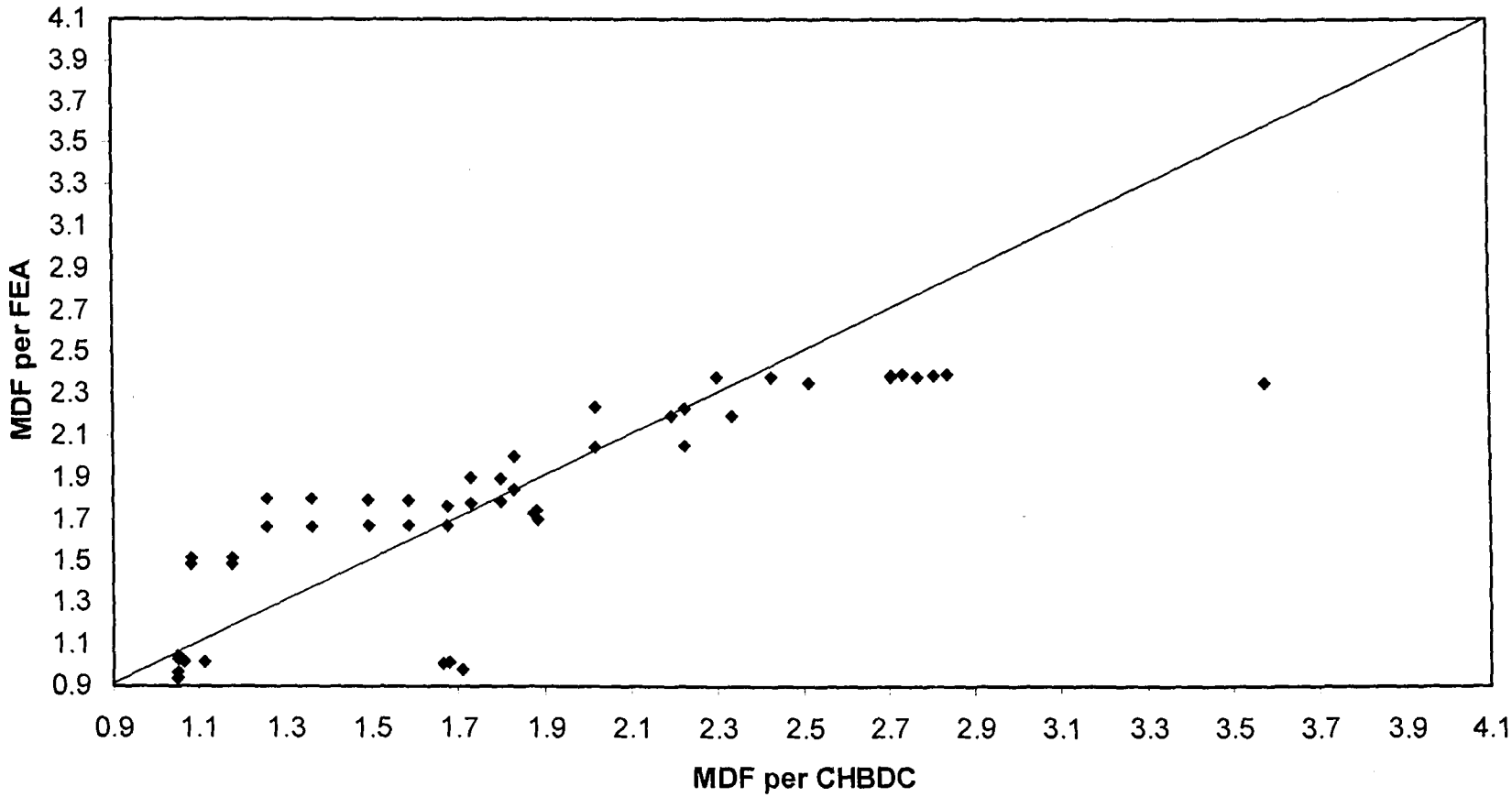

Figure 4.79 Comparison between the moment distribution factors of the exterior girder due to fatigue loading as specified in the CHBDC and from the present study

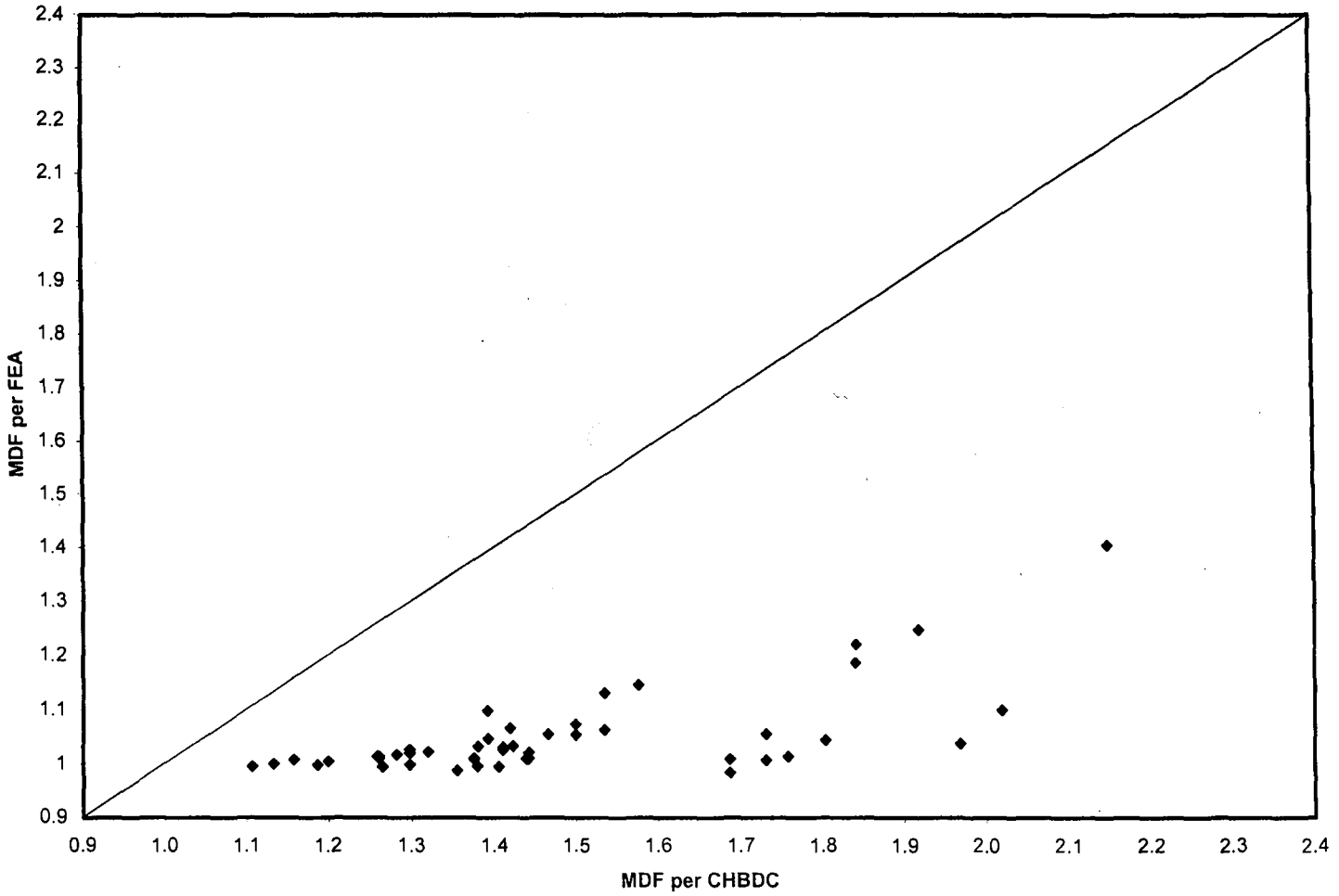

Figure 4.80 Comparison between the moment distribution factors of the middle girder due to truck loading as specified in the CHBDC and from the present study

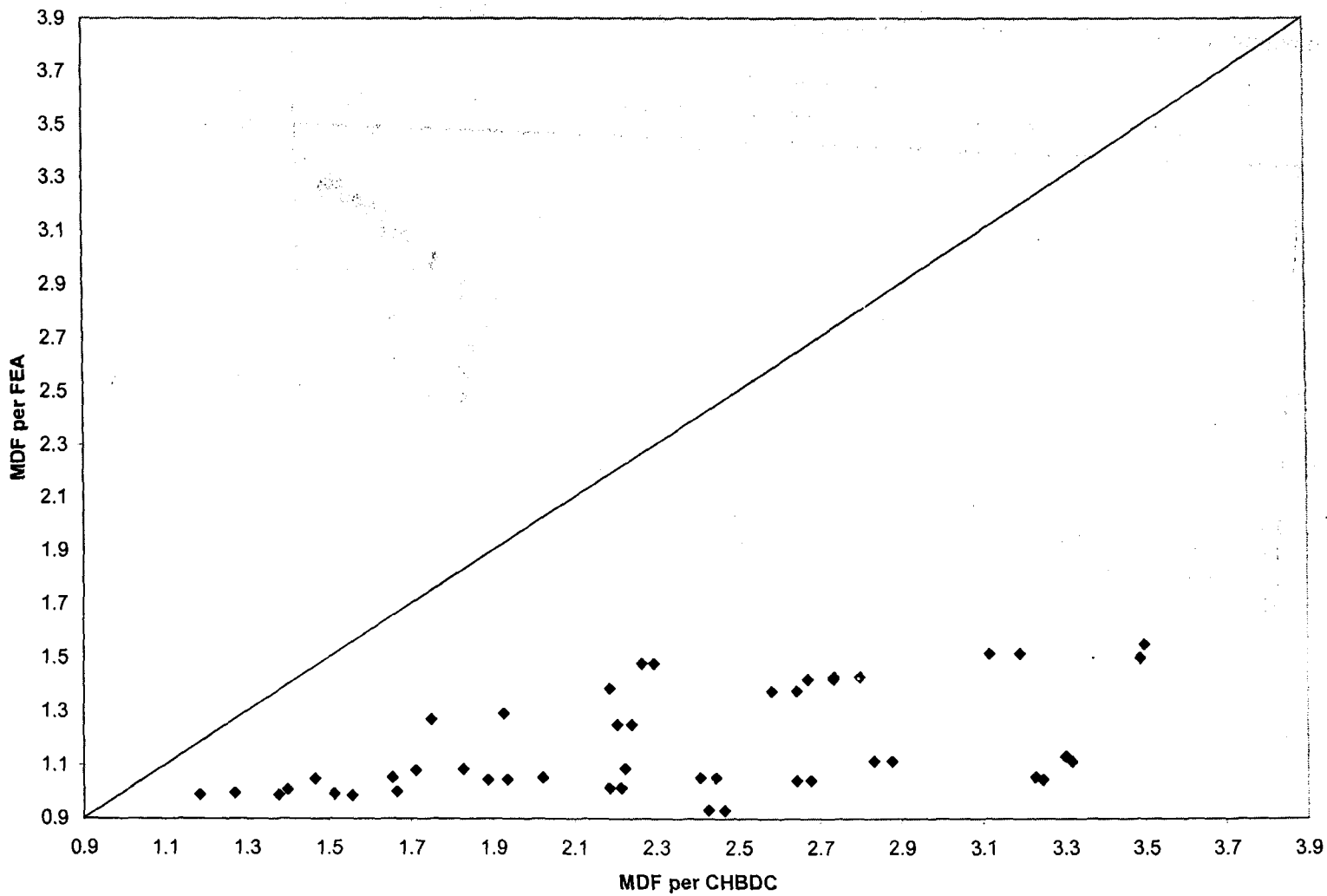

Figure 4.81 Comparison between the moment distribution factors of the middle girder due to fatigue due to truck loading as specified in the CHBDC and from the present study

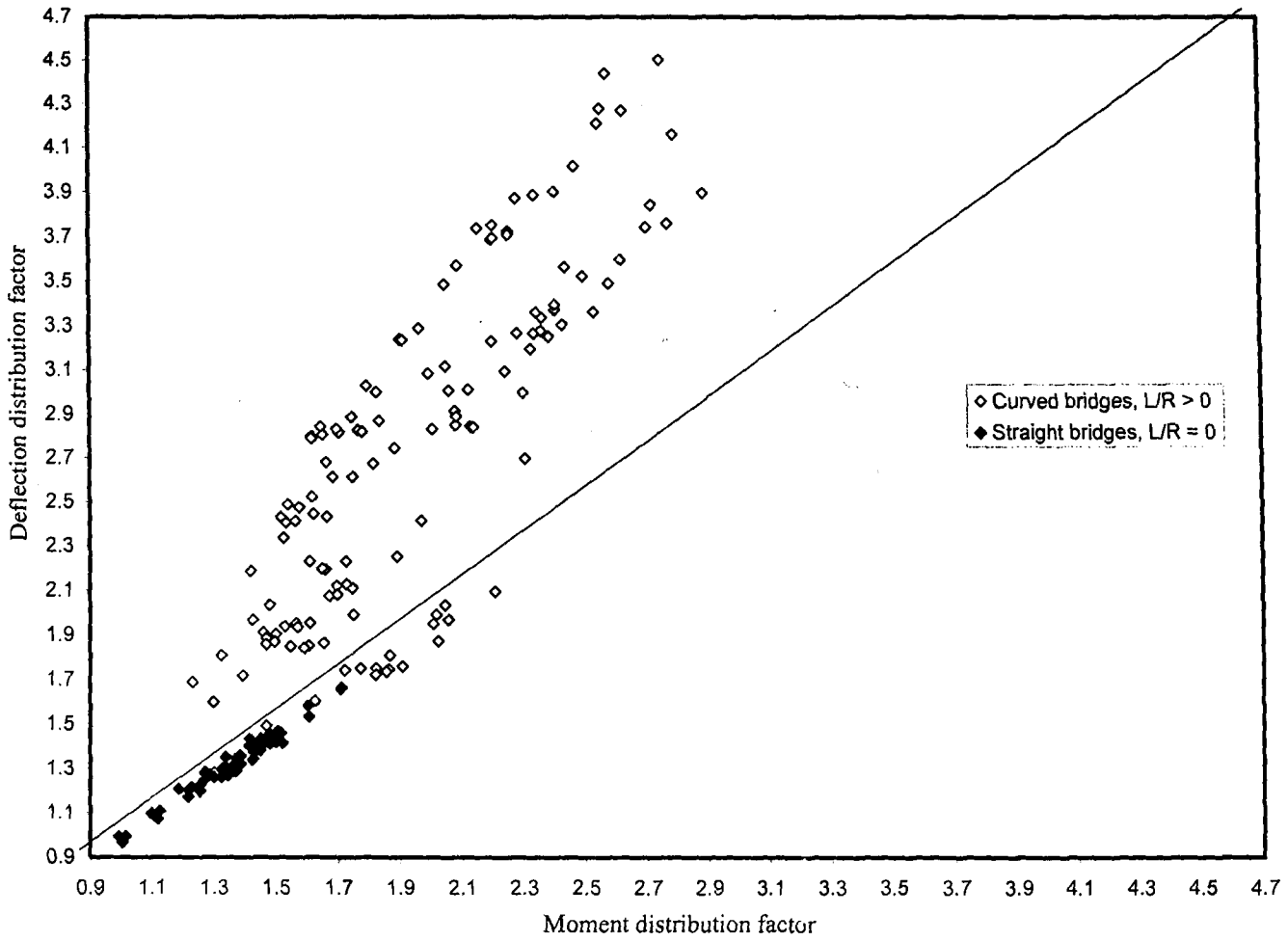

Figure 4. 82 Correlation between moment and deflection distribution factors for the exterior girder of the studied bridges due to truck loading

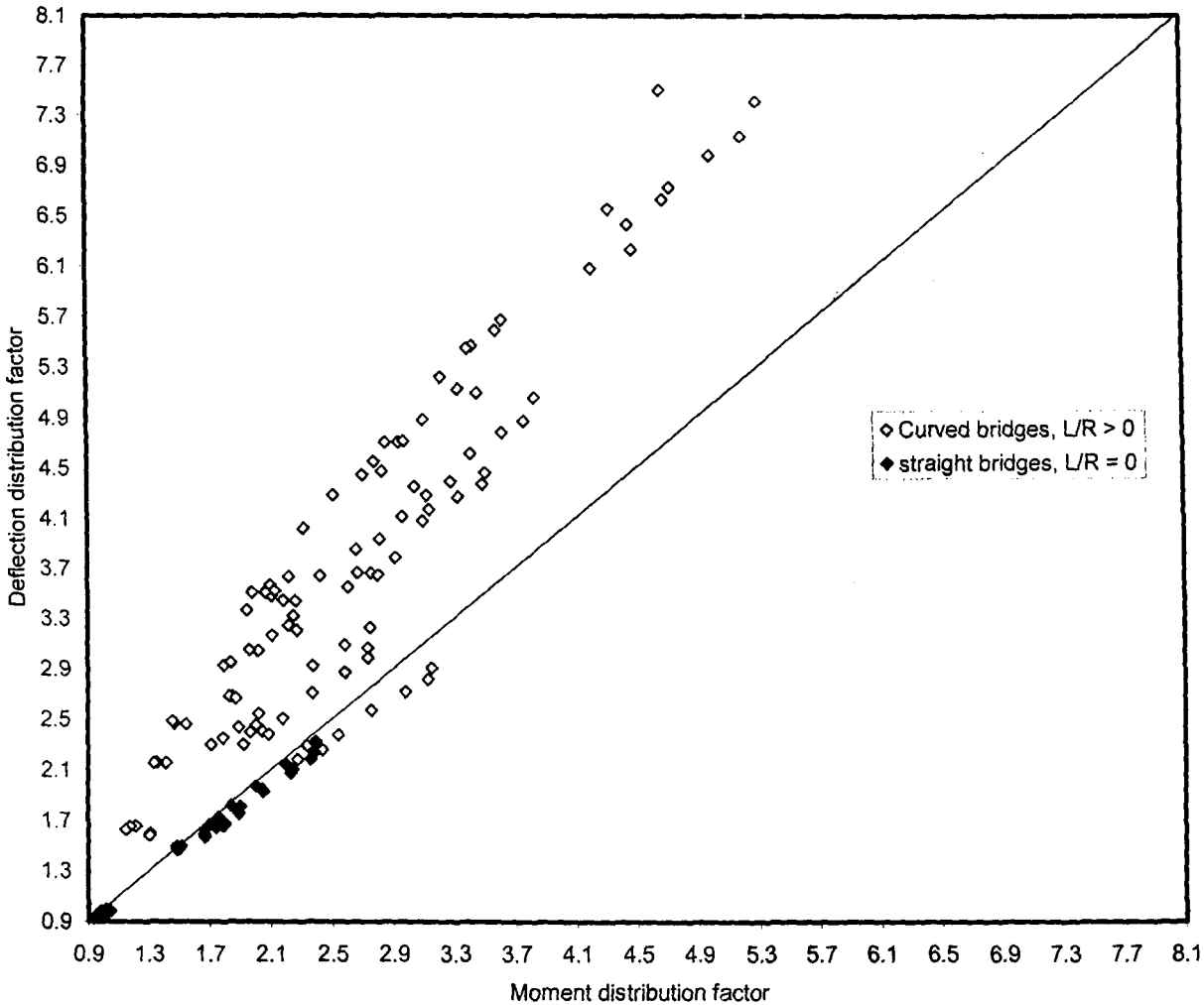

Figure 4.83 Correlation between moment and deflection distribution factors for the exterior girder of the studied bridges due to fatigue loading

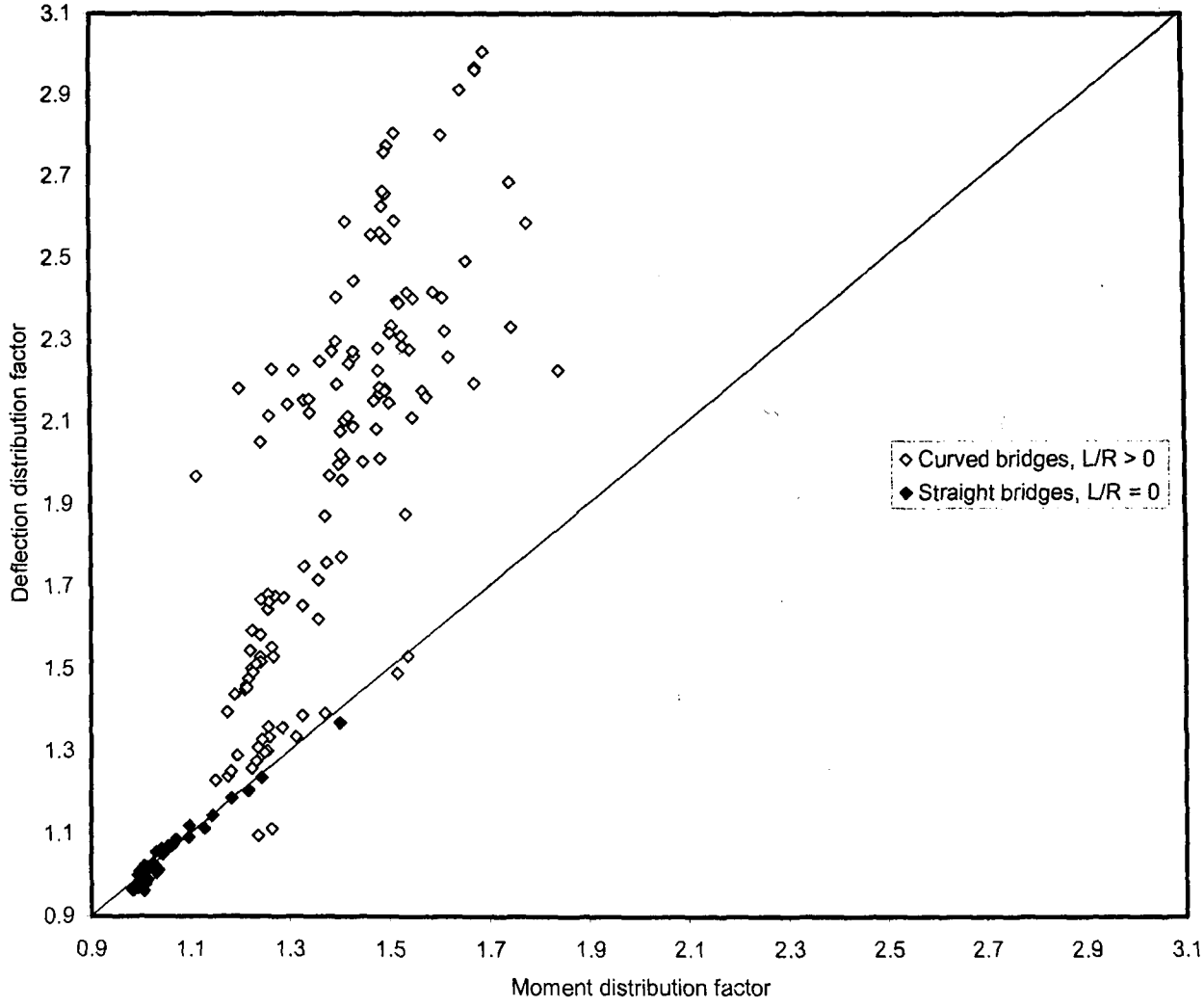

Figure 4.84 Correlation between moment and deflection distribution factors for the middle girder of the studied bridges due to truck loading

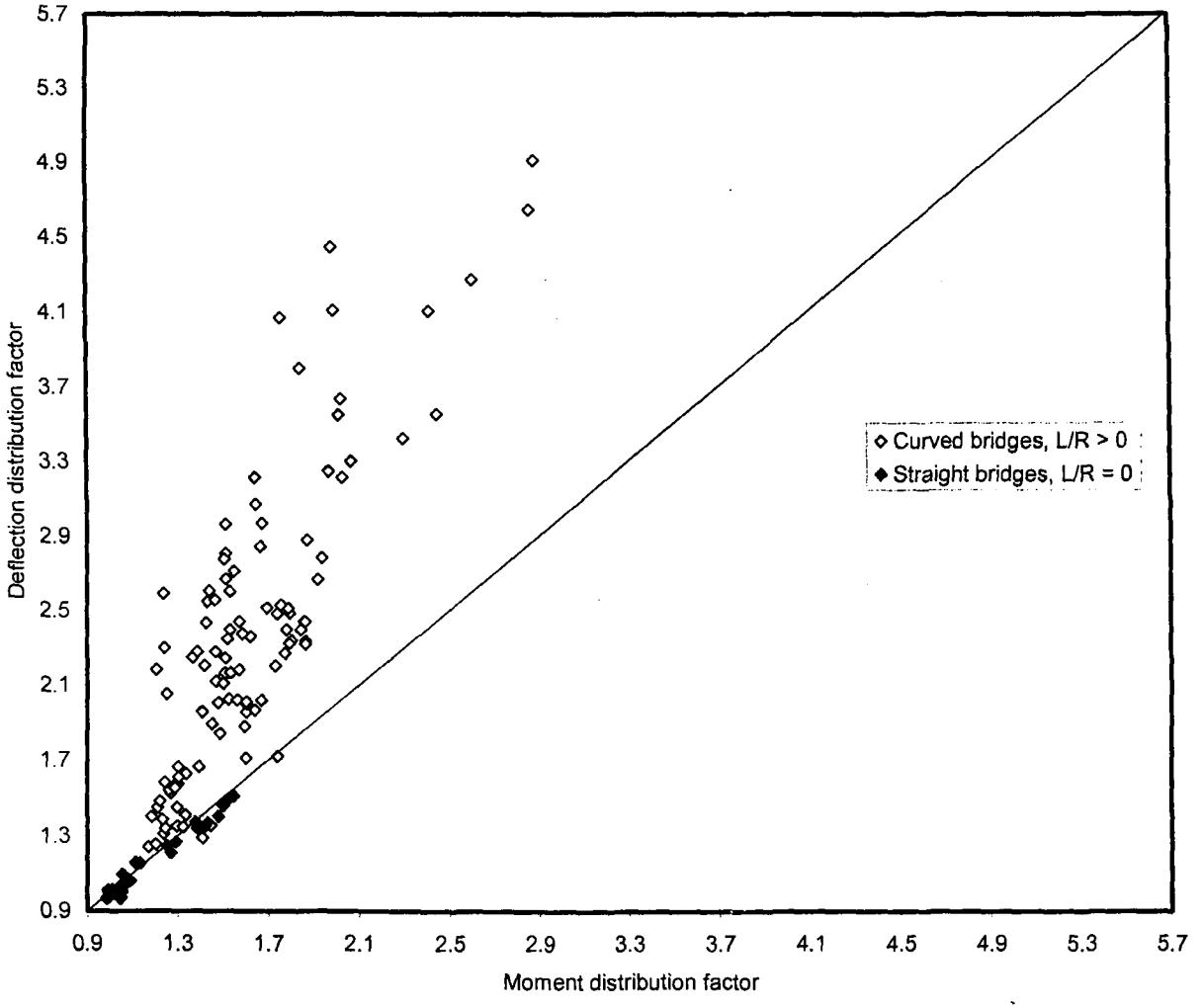

Figure 4.85 Correlation between moment and deflection distribution factors for the middle girder of the studied bridges due to fatigue loading

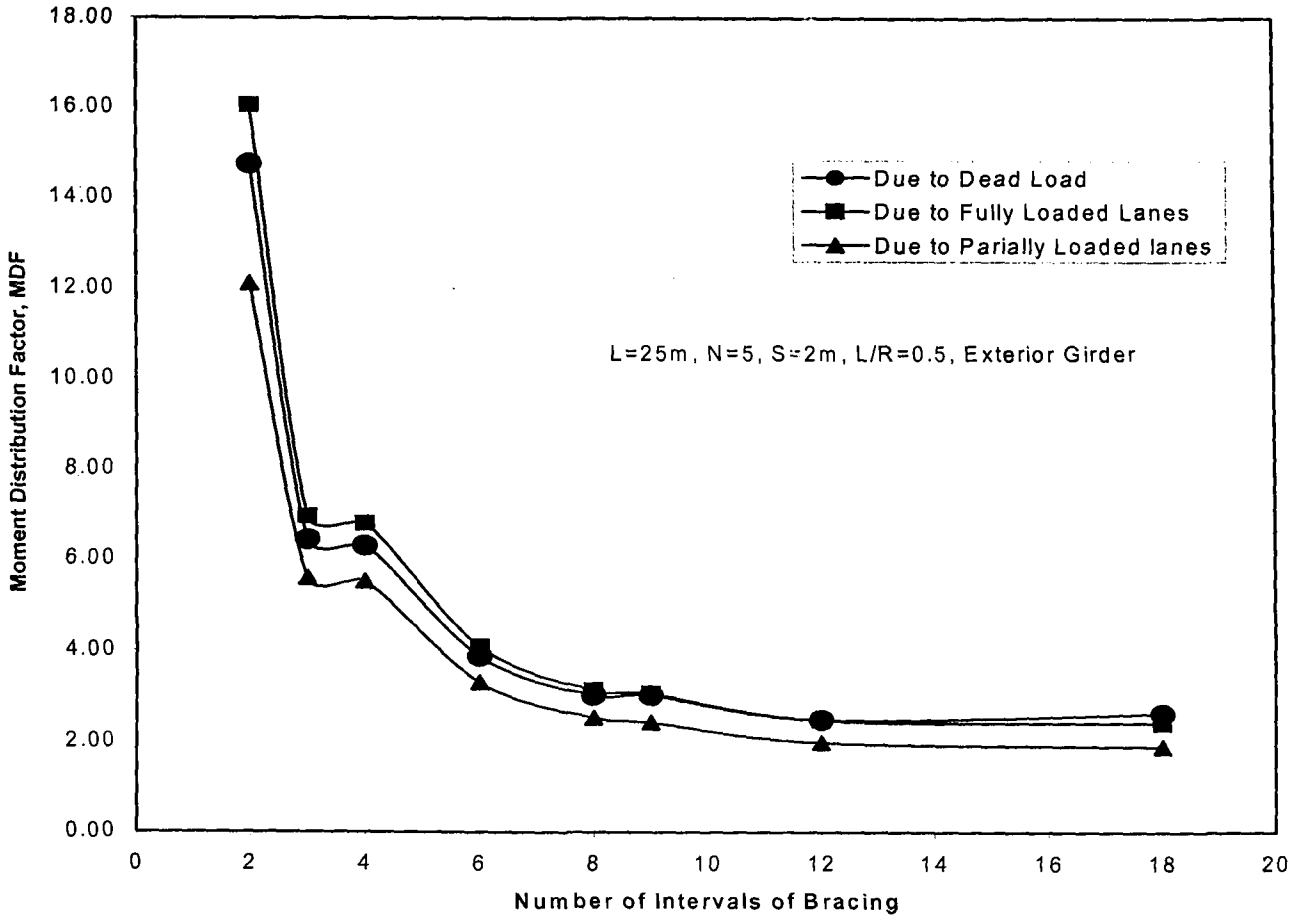

Figure 4.86 Effect of the number of cross-bracing intervals on the moment distribution factor for the exterior girder

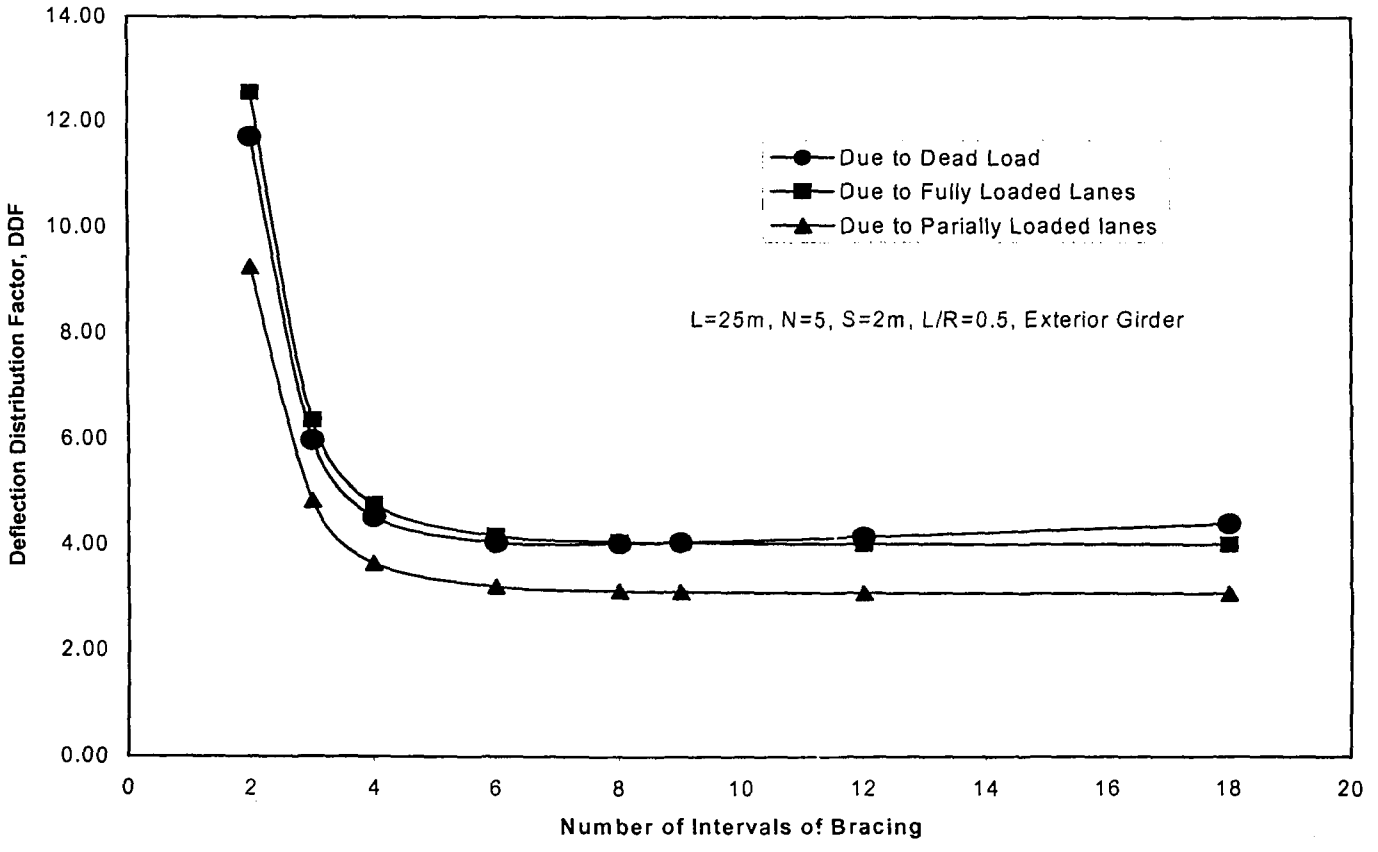

Figure 4.87 Effect of the number of cross-bracing intervals on the deflection distribution factor for the exterior girder

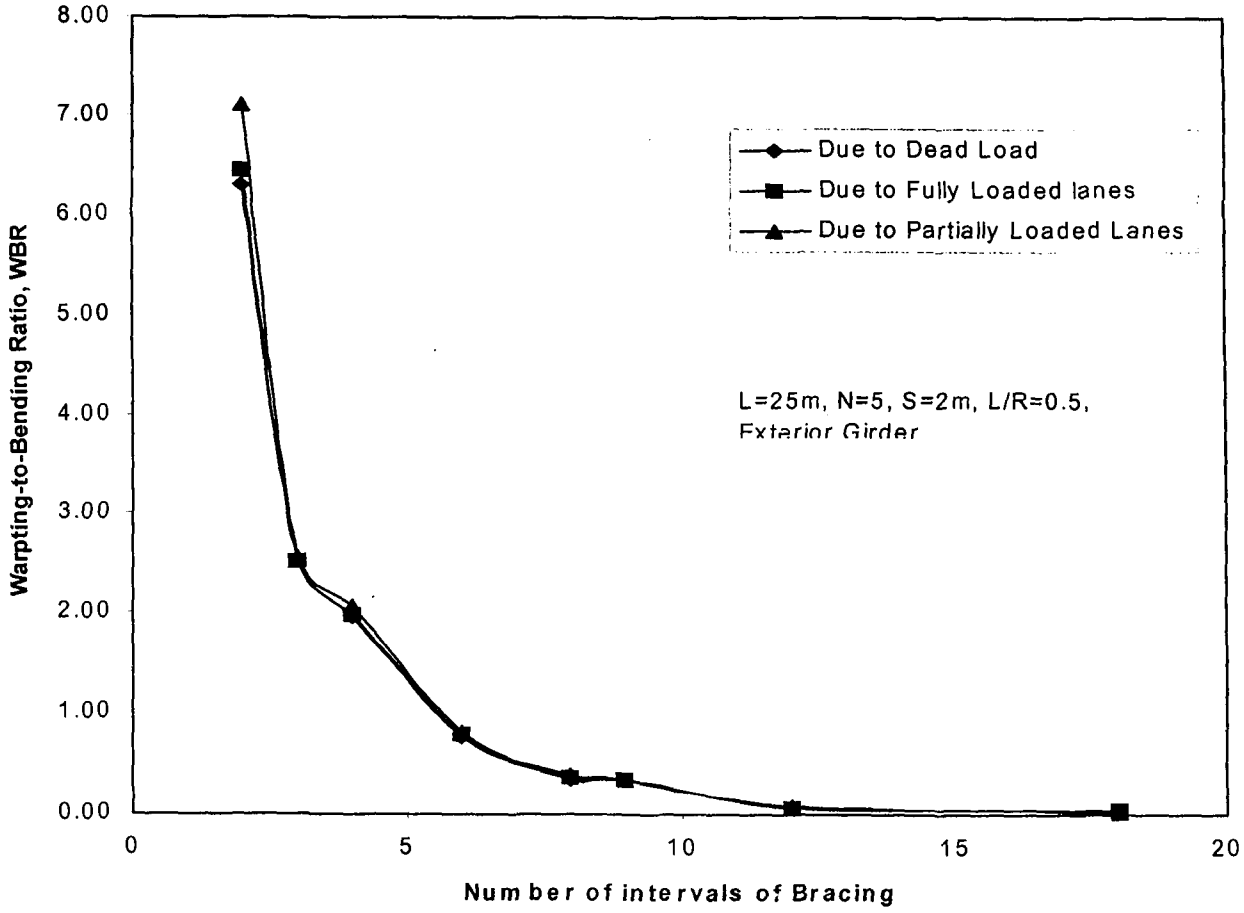

Figure 4.88 Effect of the number of cross-bracing intervals on the warping-to-bending stress ratio factor for the exterior girder

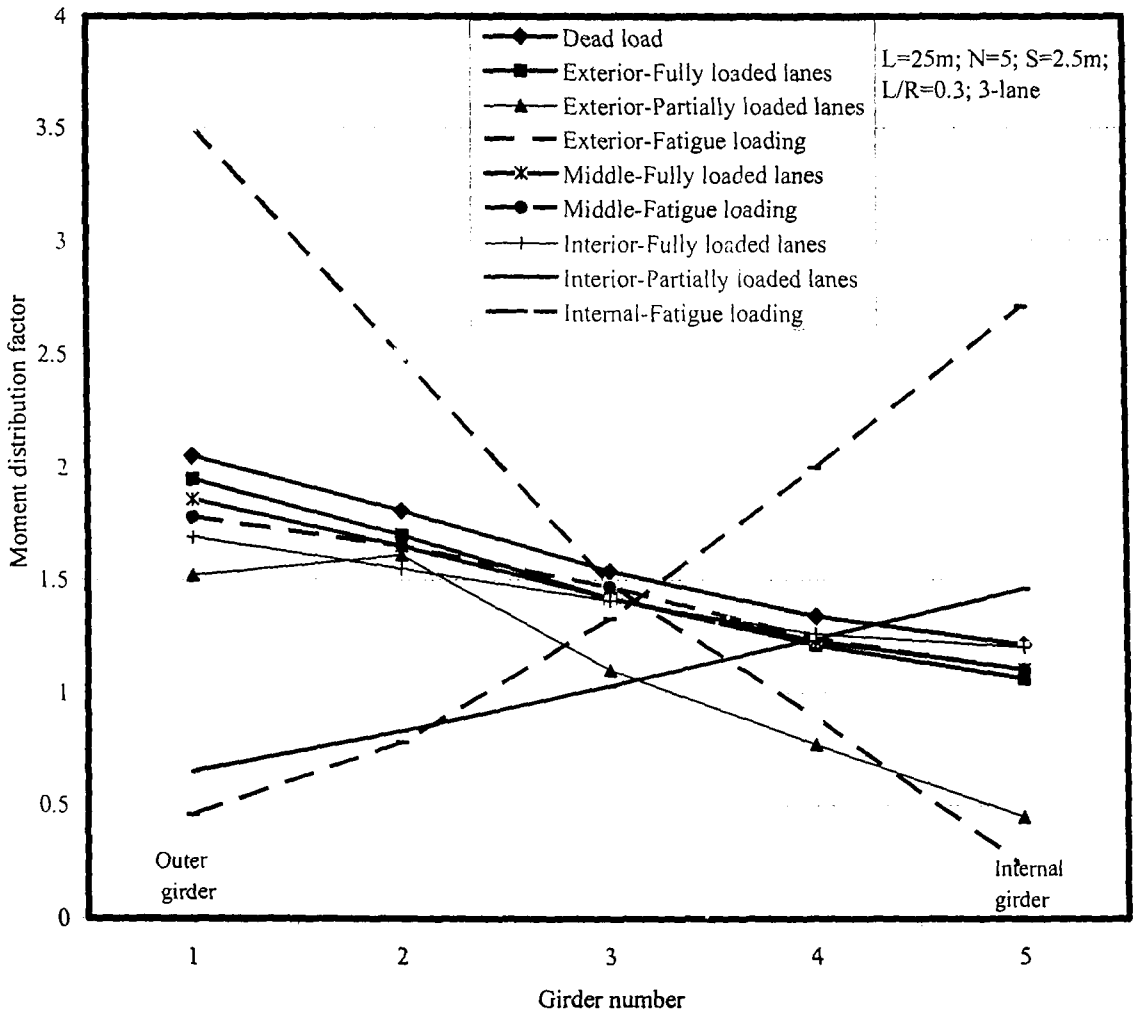

Figure 4.89 Moment distributions among girders

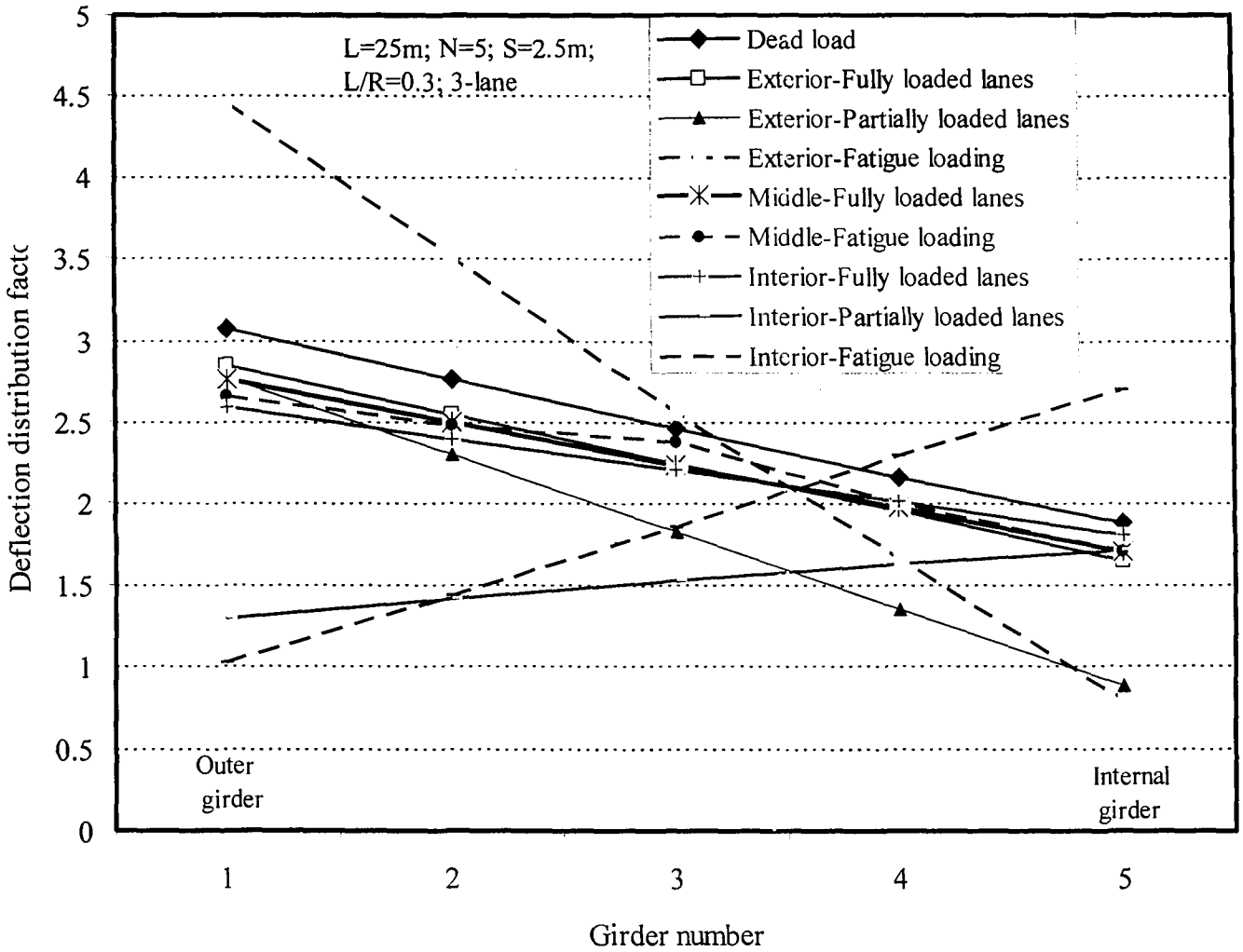

Figure 4.90 Deflection distributions among girders

APPENDEX (A): SAP 2000 Input file for a straight bridge

```
:CASE  L=15/STRAIGHT NB=3  NXBS=2  BS=2m  # OF ELEMENTS=72

SYSTEM
DOF=ALL     LENGTH=M  FORCE=KN

JOINTS
1       X=0             Y=0    Z=0.1225
73      X=0             Y=15   Z=0.1225
877     X=6             Y=0    Z=0.1225
949     X=6             Y=15   Z=0.1225       ;Deck
 Lgen=1,877,73,73,1
2500    X=0.85          Y=0    Z=0
2572    X=0.85          Y=15   Z=0
4500    X=4.85          Y=0    Z=0
4572    X=4.85          Y=15   Z=0    ;U. Flange
 Lgen=2500,4500,1000,2572,1
2700    X=1.15          Y=0    Z=0
2772    X=1.15          Y=15   Z=0
4700    X=5.15          Y=0    Z=0
4772    X=5.15          Y=15   Z=0    ;U. Flange
 Lgen=2700,4700,1000,2772,1
3100    X=0.85          Y=0    Z=-0.75
3172    X=0.85          Y=15   Z=-0.75
5100    X=4.85          Y=0    Z=-0.75
5172    X=4.85          Y=15   Z=-0.75        ;B. Flange
 Lgen=3100,5100,1000,3172,1
3300    X=1.15          Y=0    Z=-0.75
3372    X=1.15          Y=15   Z=-0.75
5300    X=5.15          Y=0    Z=-0.75
5372    X=5.15          Y=15   Z=-0.75        ;B. Flange
 Lgen=3300,5300,1000,3372,1
2600    X=1             Y=0    Z=0
2672    X=1             Y=15   Z=0
4600    X=5             Y=0    Z=0
4672    X=5             Y=15   Z=0    ;Top joint of Webs
 Lgen=2600,4600,1000,2672,1
2800    X=1             Y=0    Z=-0.1875
2872    X=1             Y=15   Z=-0.1875
4800    X=5             Y=0    Z=-0.1875
4872    X=5             Y=15   Z=-0.1875      ;middle joint of Webs

 Lgen=2800,4800,1000,2872,1
2900    X=1             Y=0    Z=-0.375
2972    X=1             Y=15   Z=-0.375
```

```
4900   X=5          Y=0   Z=-0.375
4972   X=5          Y=15  Z=-0.375      ;middle joint of Webs
 Lgen=2900,4900,1000,2972,1
3000   X=1          Y=0   Z=-0.5625
3072   X=1          Y=15  Z=-0.5625
5000   X=5          Y=0   Z=-0.5625
5072   X=5          Y=15  Z=-0.5625     ;lower joint of Webs
 Lgen=3000,5000,1000,3072,1
3200   X=1          Y=0   Z=-0.75
3272   X=1          Y=15  Z=-0.75
5200   X=5          Y=0   Z=-0.75
5272   X=5          Y=15  Z=-0.75       ;bottom joints of Webs
 Lgen=3200,5200,1000,3272,1

Pattern
 Name=Default

RESTRAINTS
 Add=4200,5200,1000        Dof=  Uy,Uz,
 Add=4272,5272,1000        Dof=    Uz,
 Add=3200                  Dof=Ux,Uy,Uz,
 Add=3272                  Dof=Ux,  Uz,

Material
Name=steel    W=78.5
        E=200000E3  U=0.3
 Name=concrete       W=24
        E=28000E3    U=0.2

Shell Section
 Name=slab          Type=Shell  Mat=concrete   Th=0.225
 Name=web           Type=Shell  Mat=steel          Th=1.6E-02
 Name=flange Type=Shell  Mat=steel          Th=2E-02
 Name=studs         Type=Shell  Mat=steel          Th=7.74E-04


SHELL
 Local=31  Pldir=0
1              J=1,2,74,75     Sec=slab ;DECK
 Gen=1 72 1 793 72  Jinc=1 73
2017   J=2600,2601,2800,2801       Sec=web ;WEB1
 Gen=2017 2088 1
2089   J=2800,2801,2900,2901       Sec=web ;WEB1
 Gen=2089 2160 1 2161 72  Jinc=1 100
```

```
2233   J=3000,3001,3200,3201        Sec=web ;WEB1
 Gen=2233 2304 1
2305   J=3600,3601,3800,3801        Sec=web ;WEB2
 Gen=2305 2376 1
2377   J=3800,3801,3900,3901        Sec=web ;WEB2
 Gen=2377 2448 1 2449 72  Jinc=1 100
2521   J=4000,4001,4200,4201        Sec=web ;WEB2
 Gen=2521 2592 1
2593   J=4600,4601,4800,4801        Sec=web ;WEB3
 Gen=2593 2664 1
2665   J=4800,4801,4900,4901        Sec=web ;WEB3
 Gen=2665 2736 1 2737 72  Jinc=1 100
2809   J=5000,5001,5200,5201        Sec=web ;WEB3
 Gen=2809 2880 1
4033  J=2500,2501,2600,2601         Sec=flange ;UPPER FLANGE1
 Gen=4033 4104 1 4105 72  Jinc=1 100
4177  J=3100,3101,3200,3201         Sec=flange ;LOWER FLANGE1
 Gen=4177 4248 1 4249 72  Jinc=1 100
4321  J=3500,3501,3600,3601         Sec=flange ;UPPER FLANGE2
 Gen=4321 4392 1 4393 72  Jinc=1 100
4465  J=4100,4101,4200,4201         Sec=flange ;LOWER FLANGE2
 Gen=4465 4536 1 4537 72  Jinc=1 100
4609  J=4500,4501,4600,4601         Sec=flange ;UPPER FLANGE3
 Gen=4609 4680 1 4681 72  Jinc=1 100
4753  J=5100,5101,5200,5201         Sec=flange ;LOWER FLANGE3
 Gen=4753 4824 1 4825 72  Jinc=1 100
6100  J=147,148,2600,2601    Sec=studs ;studs1
Gen=6100 6171 1
6200  J=439,440,3600,3601    Sec=studs ;studs2
Gen=6200 6271 1
6300  J=731,732,4600,4601    Sec=studs ;studs3
Gen=6300 6371 1

Frame Section
 Name=studs          Mat=steel      I=11922.9E-12 A=387E-6 AS=387E-6
 Name=dummy                Mat=steel      I=11922.9E-12 A=387E-6 AS=387E-6
 Name=bracing        Mat=steel      I=0                A=7500E-6


FRAME
 Local=13  Pldir=+Z +Y  ;  SAP90 default values
1  J=2600,3600          Sec=bracing   Irel=R3,R2  Jrel=R3,R2,R1  Nseg=4 ;Xbracing1
 Gen=1,9,4  Iinc=36  Jinc=36
2  J=2600,4200          Sec=bracing   Irel=R3,R2  Jrel=R3,R2,R1,;Xbracing1
```

```
 Gen=2,10,4  Iinc=36  Jinc=36
3  J=3200,3600          Sec=bracing   Irel=R3,R2  Jrel=R3,R2,R1,;Xbracing1
 Gen=3,11,4  Iinc=36  Jinc=36
4  J=3200,4200          Sec=bracing   Irel=R3,R2  Jrel=R3,R2,R1,;Xbracing1
 Gen=4,12,4  Iinc=36  Jinc=36
101  J=3600,4600        Sec=bracing   Irel=R3,R2  Jrel=R3,R2,R1,;Xbracing2
 Gen=101,109,4  Iinc=36  Jinc=36
102  J=3600,5200        Sec=bracing   Irel=R3,R2  Jrel=R3,R2,R1,;Xbracing2
 Gen=102,110,4  Iinc=36  Jinc=36
103  J=4200,4600        Sec=bracing   Irel=R3,R2  Jrel=R3,R2,R1,;Xbracing2
 Gen=103,111,4  Iinc=36  Jinc=36
104  J=4200,5200        Sec=bracing   Irel=R3,R2  Jrel=R3,R2,R1,;Xbracing2
 Gen=104,112,4  Iinc=36  Jinc=36
1300  J=147,148 Sec=dummy ;dummy
 Gen=1300,1371,1  Iinc=1  Jinc=1
1400  J=220,221 Sec=dummy ;dummy
 Gen=1400,1471,1  Iinc=1  Jinc=1
1500  J=293,294 Sec=dummy ;dummy
 Gen=1500,1571,1  Iinc=1  Jinc=1
1600  J=366,367 Sec=dummy ;dummy
 Gen=1600,1671,1  Iinc=1  Jinc=1
1700  J=439,440 Sec=dummy ;dummy
 Gen=1700,1771,1  Iinc=1  Jinc=1
1800  J=512,513 Sec=dummy ;dummy
 Gen=1800,1871,1  Iinc=1  Jinc=1
1900  J=585,586 Sec=dummy ;dummy
 Gen=1900,1971,1  Iinc=1  Jinc=1
2000  J=658,659 Sec=dummy ;dummy
 Gen=2000,2071,1  Iinc=1  Jinc=1
2100  J=731,732 Sec=dummy ;dummy
 Gen=2100,2171,1  Iinc=1  Jinc=1

Load
 Name=ow
  Type=Gravity  Elem=Frame
   Add=*  Uz=-1,
  Type=Gravity  Elem=Shell
   Add=*  Uz=-1


; EXTERIOR GIRDER
; 1 lanes, 1truck
        NAME=EXT1L1T    TYPE=CONCENTRATED  CSYS=0
        ADD=1704    D=0.056        UZ=-125.0/2  RX=-125.0/2*-0.10
```

```
        ADD=1736    D=0.000       UZ=-175.0/2  RX=-175.0/2*-0.10
        ADD=1767          D=0.152       UZ=-150.0/2  RX=-150.0/2*-0.10


        ADD=2104    D=0.056       UZ=-125.0/2  RX=-125.0/2*0.10
        ADD=2136          D=0.000       UZ=-175.0/2  RX=-175.0/2*0.10
        ADD=2167          D=0.152       UZ=-150.0/2  RX=-150.0/2*0.10


; MIDDLE GIRDER
; 1lanes
        NAME=MID+fat      TYPE=CONCENTRATED  CSYS=0
        ADD=1504          D=0.056       UZ=-125.0/2  RX=-125.0/2*-0.10
        ADD=1536          D=0.000       UZ=-175.0/2  RX=-175.0/2*-0.10
        ADD=1567          D=0.152       UZ=-150.0/2  RX=-150.0/2*-0.10


        ADD=1904          D=0.056       UZ=-125.0/2  RX=-125.0/2*0.10
        ADD=1936          D=0.000       UZ=-175.0/2  RX=-175.0/2*0.10
        ADD=1967          D=0.152       UZ=-150.0/2  RX=-150.0/2*0.10


; INTERIOR GIRDER
; 1 lanes
        NAME=INT1L1T      TYPE=CONCENTRATED  CSYS=0
        ADD=1304          D=0.056       UZ=-125.0/2  RX=-125.0/2*-0.10
        ADD=1336          D=0.000       UZ=-175.0/2  RX=-175.0/2*-0.10
        ADD=1367          D=0.152       UZ=-150.0/2  RX=-150.0/2*-0.10


        ADD=1704          D=0.056       UZ=-125.0/2  RX=-125.0/2*0.10
        ADD=1736          D=0.000       UZ=-175.0/2  RX=-175.0/2*0.10
        ADD=1767          D=0.152       UZ=-150.0/2  RX=-150.0/2*0.10

Output
ELEM=JOINT        TYPE=DISP,REAC LOAD=*
ELEM=SHELL TYPE=FORCE LOAD=*
ELEM=SHELL TYPE=STRESS LOAD=*
ELEM=FRAME TYPE=JOINTF LOAD=*

END
```

APPENDEX (B): SAP 2000 Input file for a curved bridge

```
:CASE  L=15 R=150 NB=3  NXBS=6 BS=2m  # OF ELEMENTS=72

SYSTEM
DOF=ALL     LENGTH=M  FORCE=KN

JOINTS
9998   X=-100          Y=0    Z=-5 ;Axis of Rotation
9999   X=-100          Y=0    Z=5 ;Axis of Rotation
1      X=47            Y=0    Z=0.1225       ;Deck
 Cgen=1,73,1  Da=0.080  Axvec=9998,9999,
74     X=47.5Y=0       Z=0.1225       ;Deck
 Cgen=74,146,1  Da=0.080  Axvec=9998,9999,
147    X=48            Y=0    Z=0.1225       ;Deck
 Cgen=147,219,1  Da=0.080  Axvec=9998,9999,
220    X=48.5Y=0       Z=0.1225       ;Deck
 Cgen=220,292,1  Da=0.080  Axvec=9998,9999,
293    X=49            Y=0    Z=0.1225       ;Deck
 Cgen=293,365,1  Da=0.080  Axvec=9998,9999,
366    X=49.5Y=0       Z=0.1225       ;Deck
 Cgen=366,438,1  Da=0.080  Axvec=9998,9999,
439    X=50            Y=0    Z=0.1225       ;Deck
 Cgen=439,511,1  Da=0.080  Axvec=9998,9999,
512    X=50.5Y=0       Z=0.1225       ;Deck
 Cgen=512,584,1  Da=0.080  Axvec=9998,9999,
585    X=51            Y=0    Z=0.1225       ;Deck
 Cgen=585,657,1  Da=0.080  Axvec=9998,9999,
658    X=51.5Y=0       Z=0.1225       ;Deck
 Cgen=658,730,1  Da=0.080  Axvec=9998,9999,
731    X=52            Y=0    Z=0.1225       ;Deck
 Cgen=731,803,1  Da=0.080  Axvec=9998,9999,
804    X=52.5Y=0       Z=0.1225       ;Deck
 Cgen=804,876,1  Da=0.080  Axvec=9998,9999,
877    X=53            Y=0    Z=0.1225       ;Deck
 Cgen=877,949,1  Da=0.080  Axvec=9998,9999,
2500   X=47.85         Y=0    Z=0    ;U.FLANG1
 Cgen=2500,2572,1  Da=0.080  Axvec=9998,9999,
2700   X=48.15         Y=0    Z=0    ;U.FLANG1
 Cgen=2700,2772,1  Da=0.080  Axvec=9998,9999,
3100   X=47.85         Y=0    Z=-0.75        ;L.FLANG1
 Cgen=3100,3172,1  Da=0.080  Axvec=9998,9999,
3300   X=48.15         Y=0    Z=-0.75        ;L.FLANG1
 Cgen=3300,3372,1  Da=0.080  Axvec=9998,9999,
3500   X=49.85         Y=0    Z=0    ;U.FLANG2
 Cgen=3500,3572,1  Da=0.080  Axvec=9998,9999,
```

```
3700  X=50.15       Y=0   Z=0    ;U.FLANG2
 Cgen=3700,3772,1 Da=0.080 Axvec=9998,9999,
4100  X=49.85       Y=0   Z=-0.75      ;L.FLANG2
 Cgen=4100,4172,1 Da=0.080 Axvec=9998,9999,
4300  X=50.15       Y=0   Z=-0.75      ;L.FLANG2
 Cgen=4300,4372,1 Da=0.080 Axvec=9998,9999,
4500  X=51.85       Y=0   Z=0    ;U.FLANG3
 Cgen=4500,4572,1 Da=0.080 Axvec=9998,9999,
4700  X=52.15       Y=0   Z=0    ;U.FLANG3
 Cgen=4700,4772,1 Da=0.080 Axvec=9998,9999,
5100  X=51.85       Y=0   Z=-0.75      ;L.FLANG3
 Cgen=5100,5172,1 Da=0.080 Axvec=9998,9999,
5300  X=52.15       Y=0   Z=-0.75      ;L.FLANG3
 Cgen=5300,5372,1 Da=0.080 Axvec=9998,9999,
2600  X=48         Y=0   Z=0    ;WEB1
 Cgen=2600,2672,1 Da=0.080 Axvec=9998,9999,
3600  X=50         Y=0   Z=0    ;WEB2
 Cgen=3600,3672,1 Da=0.080 Axvec=9998,9999,
4600  X=52         Y=0   Z=0    ;WEB3
 Cgen=4600,4672,1 Da=0.080 Axvec=9998,9999,
2800  X=48         Y=0   Z=-0.1875    ;WEB1
 Cgen=2800,2872,1 Da=0.080 Axvec=9998,9999,
3800  X=50         Y=0   Z=-0.1875    ;WEB2
 Cgen=3800,3872,1 Da=0.080 Axvec=9998,9999,
4800  X=52         Y=0   Z=-0.1875    ;WEB3
 Cgen=4800,4872,1 Da=0.080 Axvec=9998,9999,
2900  X=48         Y=0   Z=-0.375     ;WEB1
 Cgen=2900,2972,1 Da=0.080 Axvec=9998,9999,
3900  X=50         Y=0   Z=-0.375     ;WEB2
 Cgen=3900,3972,1 Da=0.080 Axvec=9998,9999,
4900  X=52         Y=0   Z=-0.375     ;WEB3
 Cgen=4900,4972,1 Da=0.080 Axvec=9998,9999,
3000  X=48         Y=0   Z=-0.5625    ;WEB1
 Cgen=3000,3072,1 Da=0.080 Axvec=9998,9999,
4000  X=50         Y=0   Z=-0.5625    ;WEB2
 Cgen=4000,4072,1 Da=0.080 Axvec=9998,9999,
5000  X=52         Y=0   Z=-0.5625    ;WEB3
 Cgen=5000,5072,1 Da=0.080 Axvec=9998,9999,
3200  X=48         Y=0   Z=-0.75      ;WEB1
 Cgen=3200,3272,1 Da=0.080 Axvec=9998,9999,
4200  X=50         Y=0   Z=-0.75      ;WEB2
 Cgen=4200,4272,1 Da=0.080 Axvec=9998,9999,
5200  X=52         Y=0   Z=-0.75      ;WEB3
 Cgen=5200,5272,1 Da=0.080 Axvec=9998,9999,
```

```
Pattern
 Name=Default

RESTRAINTS
 Add=4200,5200,1000 Dof=  Uy,Uz,
 Add=4272,5272,1000 Dof=   Uz,
 Add=3200                  Dof=Ux,Uy,Uz,
 Add=3272                  Dof=Ux,  Uz,

Material
Name=steel    W=78.5
        E=200000E3  U=0.3
 Name=concrete        W=24
        E=28000E3    U=0.2

Shell Section
 Name=slab           Type=Shell  Mat=concrete    Th=0.225
 Name=web            Type=Shell  Mat=steel           Th=1.6E-02
 Name=flange Type=Shell  Mat=steel               Th=2E-02
 Name=studs          Type=Shell  Mat=steel           Th=7.74E-04

SHELL
 Local=31  Pldir=0
1              J=1,2,74,75     Sec=slab ;DECK
 Gen=1 72 1 793 72  Jinc=1 73
2017   J=2600,2601,2800,2801        Sec=web ;WEB1
 Gen=2017 2088 1
2089   J=2800,2801,2900,2901        Sec=web ;WEB1
 Gen=2089 2160 1 2161 72  Jinc=1 100
2233   J=3000,3001,3200,3201        Sec=web ;WEB1
 Gen=2233 2304 1
2305   J=3600,3601,3800,3801        Sec=web ;WEB2
 Gen=2305 2376 1
2377   J=3800,3801,3900,3901        Sec=web ;WEB2
 Gen=2377 2448 1 2449 72  Jinc=1 100
2521   J=4000,4001,4200,4201        Sec=web ;WEB2
 Gen=2521 2592 1
2593   J=4600,4601,4800,4801        Sec=web ;WEB3
 Gen=2593 2664 1
2665   J=4800,4801,4900,4901        Sec=web ;WEB3
 Gen=2665 2736 1 2737 72  Jinc=1 100
2809   J=5000,5001,5200,5201        Sec=web ;WEB3
 Gen=2809 2880 1
```

```
4033  J=2500,2501,2600,2601  Sec=flange ;UPPER FLANGE1
 Gen=4033 4104 1 4105 72  Jinc=1 100
4177  J=3100,3101,3200,3201  Sec=flange ;LOWER FLANGE1
 Gen=4177 4248 1 4249 72  Jinc=1 100
4321  J=3500,3501,3600,3601  Sec=flange ;UPPER FLANGE2
 Gen=4321 4392 1 4393 72  Jinc=1 100
4465  J=4100,4101,4200,4201  Sec=flange ;LOWER FLANGE2
 Gen=4465 4536 1 4537 72  Jinc=1 100
4609  J=4500,4501,4600,4601  Sec=flange ;UPPER FLANGE3
 Gen=4609 4680 1 4681 72  Jinc=1 100
4753  J=5100,5101,5200,5201  Sec=flange ;LOWER FLANGE3
 Gen=4753 4824 1 4825 72  Jinc=1 100
6100  J=147,148,2600,2601     Sec=studs ;studs1
Gen=6100 6171 1
6200  J=439,440,3600,3601     Sec=studs ;studs2
Gen=6200 6271 1
6300  J=731,732,4600,4601     Sec=studs ;studs3
Gen=6300 6371 1

Frame Section
 Name=studs          Mat=steel      I=11922.9E-12 A=387E-6 AS=387E-6
 Name=dummy                Mat=steel      I=11922.9E-12 A=387E-6 AS=387E-6
 Name=bracing        Mat=steel      I=0            A=7500E-6

FRAME
Local=13  Pldir=+Z +Y  ;  SAP90 default values
1  J=2600,3600          Sec=bracing   Irel=R3,R2  Jrel=R3,R2,R1  Nseg=4 ;Xbracing1
 Gen=1,17,4  Iinc=18  Jinc=18
2  J=2600,4200          Sec=bracing   Irel=R3,R2  Jrel=R3,R2,R1,;Xbracing1
 Gen=2,18,4  Iinc=18  Jinc=18
3  J=3200,3600          Sec=bracing   Irel=R3,R2  Jrel=R3,R2,R1,;Xbracing1
 Gen=3,19,4  Iinc=18  Jinc=18
4  J=3200,4200          Sec=bracing   Irel=R3,R2  Jrel=R3,R2,R1,;Xbracing1
 Gen=4,20,4  Iinc=18  Jinc=18
101  J=3600,4600        Sec=bracing   Irel=R3,R2  Jrel=R3,R2,R1,;Xbracing2
 Gen=101,117,4  Iinc=18  Jinc=18
102  J=3600,5200        Sec=bracing   Irel=R3,R2  Jrel=R3,R2,R1,;Xbracing2
 Gen=102,118,4  Iinc=18  Jinc=18
103  J=4200,4600        Sec=bracing   Irel=R3,R2  Jrel=R3,R2,R1,;Xbracing2
 Gen=103,119,4  Iinc=18  Jinc=18
104  J=4200,5200        Sec=bracing   Irel=R3,R2  Jrel=R3,R2,R1,;Xbracing2
 Gen=104,120,4  Iinc=18  Jinc=18
1300  J=147,148 Sec=dummy ;dummy
```

```
 Gen=1300,1371,1 Iinc=1 Jinc=1
1400 J=220,221 Sec=dummy ;dummy
 Gen=1400,1471,1 Iinc=1 Jinc=1
1500 J=293,294 Sec=dummy ;dummy
 Gen=1500,1571,1 Iinc=1 Jinc=1
1600 J=366,367 Sec=dummy ;dummy
 Gen=1600,1671,1 Iinc=1 Jinc=1
1700 J=439,440 Sec=dummy ;dummy
 Gen=1700,1771,1 Iinc=1 Jinc=1
1800 J=512,513 Sec=dummy ;dummy
 Gen=1800,1871,1 Iinc=1 Jinc=1
1900 J=585,586 Sec=dummy ;dummy
 Gen=1900,1971,1 Iinc=1 Jinc=1
2000 J=658,659 Sec=dummy ;dummy
 Gen=2000,2071,1 Iinc=1 Jinc=1
2100 J=731,732 Sec=dummy ;dummy
 Gen=2100,2171,1 Iinc=1 Jinc=1

Load
 Name=ow
  Type=Gravity Elem=Frame
   Add=* Uz=-1,
  Type=Gravity Elem=Shell
   Add=* Uz=-1,

; EXTERIOR GIRDER
; 1 lanes, 1truck
        NAME=EXT1L1T    TYPE=CONCENTRATED  CSYS=0
        ADD=1704   D=0.056      UZ=-125.0/2  RX=-125.0/2*-0.10
        ADD=1736   D=0.000      UZ=-175.0/2  RX=-175.0/2*-0.10
        ADD=1767        D=0.152      UZ=-150.0/2  RX=-150.0/2*-0.10


        ADD=2104   D=0.056      UZ=-125.0/2  RX=-125.0/2*0.10
        ADD=2136        D=0.000      UZ=-175.0/2  RX=-175.0/2*0.10
        ADD=2167        D=0.152      UZ=-150.0/2  RX=-150.0/2*0.10


; MIDDLE GIRDER
; 1lanes
        NAME=MID+fat    TYPE=CONCENTRATED  CSYS=0
        ADD=1504        D=0.056      UZ=-125.0/2  RX=-125.0/2*-0.10
        ADD=1536        D=0.000      UZ=-175.0/2  RX=-175.0/2*-0.10
        ADD=1567        D=0.152      UZ=-150.0/2  RX=-150.0/2*-0.10
```

```
        ADD=1904        D=0.056     UZ=-125.0/2  RX=-125.0/2*0.10
        ADD=1936        D=0.000     UZ=-175.0/2  RX=-175.0/2*0.10
        ADD=1967        D=0.152     UZ=-150.0/2  RX=-150.0/2*0.10


; INTERIOR GIRDER
; 1 lanes
        NAME=INT1L1T    TYPE=CONCENTRATED  CSYS=0
        ADD=1304        D=0.056     UZ=-125.0/2  RX=-125.0/2*-0.10
        ADD=1336        D=0.000     UZ=-175.0/2  RX=-175.0/2*-0.10
        ADD=1367        D=0.152     UZ=-150.0/2  RX=-150.0/2*-0.10


        ADD=1704        D=0.056     UZ=-125.0/2  RX=-125.0/2*0.10
        ADD=1736        D=0.000     UZ=-175.0/2  RX=-175.0/2*0.10
        ADD=1767        D=0.152     UZ=-150.0/2  RX=-150.0/2*0.10


Output
ELEM=JOINTTYPE=DISP,REAC LOAD=*
ELEM=SHELL TYPE=FORCE LOAD=*
ELEM=SHELL TYPE=STRESS LOAD=*
ELEM=FRAME TYPE=JOINTF LOAD=*

END
```

APPENDEX (C): Excel data sheet for section and girder properties

The stresses and deflection of single girder for D.L,L.L

1)bridge 35m

1.1 spacing 2m

B	ts	n	Area(t)	Yi	A(t) X Yi	Y*(t)	Ys	I(t)	Is	Ie	w(kN/m3)	Wi(kN/m)	span	MT(D.L)	stress(D.L)	deflec(D.L)	MT(L.L)	stress(L.L)	12EIe	deflec(L.L)
2.28	0.225	7.14	0.063025	1.8825	0.11864	1.49712	0.885	0.00963			24	10.8								
0.3	0.02	1	0.006	1.76	0.01056	1.49712	0.885	0.00041	0.00459		78.5	0.471								
0.016	1.73	1	0.02768	0.885	0.0245	1.49712	0.885	0.01727	0.0069		78.5	2.17288								
0.3	0.02	1	0.006	0.01	0.00006	1.49712	0.885	0.01327	0.00459		78.5	0.471								
			0.102705		0.15376	1.49712		0.04059	0.01609	0.0369		13.91488	35	2130.716			3755.1		9E+07	6E+06	
values from FEA															78065.02	-3.58E-02		137649.8		-6.15E-02

1.2 spacing 2.5m

B	ts	n	Area(t)	Yi	A(t) X Yi	Y*(t)	Ys	I(t)	Is	Ie	w(kN/m3)	Wi(kN/m)	span	MT(D.L)	stress(D.L)	deflec(D.L)	MT(L.L)	stress(L.L)		deflec(L.L)
2.28	0.225	7.14	0.078782	1.8825	0.14831	1.54838	0.885	0.00913			24	13.5								
0.3	0.02	1	0.006	1.76	0.01056	1.54838	0.885	0.00027	0.00459		78.5	0.471								
0.016	1.73	1	0.02768	0.885	0.0245	1.54838	0.885	0.01908	0.0069		78.5	2.17288								
0.3	0.02	1	0.006	0.01	0.00006	1.54838	0.885	0.0142	0.00459		78.5	0.471								
			0.118462		0.18342	1.54838		0.04268	0.01609	0.0387		16.61488	35	2544.154			3755.1		9E+07	6E+06	
values from FEA															91753.65	-4.09E-02		135610.4		-5.89E-02

1.3 spacing 3.0m

B	ts	n	Area(t)	Yi	A(t) X Yi	Y*(t)	Ys	I(t)	Is	Ie	w(kN/m3)	Wi(kN/m)	span	MT(D.L)	stress(D.L)	deflec(D.L)	MT(L.L)	stress(L.L)		deflec(L.L)
2.28	0.225	7.14	0.094538	1.8825	0.17797	1.5876	0.885	0.00862			24	16.2								
0.3	0.02	1	0.006	1.76	0.01056	1.5876	0.885	0.00018	0.00459		78.5	0.471								
0.016	1.73	1	0.02768	0.885	0.0245	1.5876	0.885	0.02057	0.0069		78.5	2.17288								
0.3	0.02	1	0.006	0.01	0.00006	1.5876	0.885	0.01493	0.00459		78.5	0.471								
			0.134218		0.21308	1.5876		0.0443	0.01609	0.0401		19.31488	35	2957.591			3755.1		1E+08	6E+06	
values from FEA															105443.3	-4.60E-02		134128.9		-5.70E-02

2)bridge 25m

1.1 spacing 2m

B	ts	n	Area(t)	Yi	A(t) X Yi	Y*(t)	Ys	I(t)	Is	Ie	w(kN/m3)	Wi(kN/m)	span	MT(D.L)	stress(D.L)	deflec(D.L)	MT(L.L)	stress(L.L)	12EIc	deflec(L.L)
[illegible]	0.225	7.14	0.063025	1.3825	0.08713	1.13245	0.635	0.00421			24	10.8								
0.3	0.02	1	0.006	1.26	0.00756	1.13245	0.635	9.8E-05	0.00234		78.5	0.471								
0.016	1.23	1	0.01968	0.635	0.0125	1.13245	0.635	0.00735	0.00248		78.5	1.54488								
0.3	0.02	1	0.006	0.01	0.00006	1.13245	0.635	0.00756	0.00234		78.5	0.471								
			0.094705		0.10725	1.13245		0.01922	0.00717	0.0174		13.28688	25	1038.038	[illegible]	[illegible]	221.81	[illegible]	4E+07	2E+06	[illegible]
values from FEA															60768.43	-1.95E-02		128277.1		-4.12E-02

1.2 spacing 2.5m

B	ts	n	Area(t)	Yi	A(t) X Yi	Y*(t)	Ys	I(t)	Is	Ie	w(kN/m3)	Wi(kN/m)	span	MT(D.L)	stress(D.L)	deflec(D.L)	MT(L.L)	stress(L.L)		deflec(L.L)
[illegible]	0.225	7.14	0.078782	1.3825	0.10892	1.16812	0.635	0.00395			24	13.5								
0.3	0.02	1	0.006	1.26	0.00756	1.16812	0.635	5.1E-05	0.00234		78.5	0.471								
0.016	1.23	1	0.01968	0.635	0.0125	1.16812	0.635	0.00807	0.00248		78.5	1.54488								
0.3	0.02	1	0.006	0.01	0.00006	1.16812	0.635	0.00805	0.00234		78.5	0.471								
			0.110462		0.12903	1.16812		0.02013	0.00717	0.0182		15.98688	25	1248.975	[illegible]	[illegible]	221.81	[illegible]	4E+07	2E+06	[illegible]
values from FEA															72075.88	-2.25E-02		126543.1		-3.97E-02

1.3 spacing 3.0m

B	ts	n	Area(t)	Yi	A(t) X Yi	Y*(t)	Ys	I(t)	Is	Ie	w(kN/m3)	Wi(kN/m)	span	MT(D.L)	stress(D.L)	deflec(D.L)	MT(L.L)	stress(L.L)	12EIc	deflec(L.L)
[illegible]	0.225	7.14	0.094538	1.3825	0.1307	1.19488	0.635	0.00373			24	16.2								
0.3	0.02	1	0.006	1.26	0.00756	1.19488	0.635	2.6E-05	0.00234		78.5	0.471								
0.016	1.23	1	0.01968	0.635	0.0125	1.19488	0.635	0.00865	0.00248		78.5	1.54488								
0.3	0.02	1	0.006	0.01	0.00006	1.19488	0.635	0.00842	0.00234		78.5	0.471								
			0.126218		0.15082	1.19488		0.02083	0.00717	0.0188		18.68688	25	1459.913	[illegible]	[illegible]	221.81	[illegible]	5E+07	2E+06	[illegible]
values from FEA															83344.07	-2.56E-02		125227.1		-3.86E-02